EXAMINATION OF MARINE SEDIMENTS WITH A SUB-BOTTOM PROFILING SYSTEM

A

Thesis

submitted by

WEI NING LI

for the

Degree of Doctor of Philosophy

in the

Faculty of Science

University of London

August 1967

Geophysics Department
Imperial College
London, S.W.7.

ABSTRACT

The essential characteristics of the transmitting source and the receiving hydrophone of a sub-bottom profiling system were investigated during the process of the modifications to an existing commercial profiler. These together with the subsequent construction of a new system suitable for probing the continental shelf and slope are given in detail. A few geological findings in the Irish Sea deduced from a limited number of profiles are believed to be of some interest.

With a view to identifying the type of marine sediments by their acoustic properties trials of an approach using quantitative treatment of the acoustic data collected during sub-bottom profiling using a frequency analysis method are described. In conjunction with these the development of the associated instrumentation and the field and laboratory procedures are detailed. A facsimile weather chart recorder was successfully converted into a versatile profile recorder. Of particular significance are the development of a simple synchronization method for reproducing tape-recorded data for graphic display and a precision technique for isolating tape-stored pulses.

Preliminary results of the spectral analysis of the various bottom and sub-bottom reflections as well as some direct arrivals are given and discussed. It appears that the type of sea-floor materials could be closely related to the attenuation and frequency dependence characteristics obtained from reflection method. At the same time, intensity measurement coupled with a statistical treatment seems to give an indication of the relative roughness of a bottom or sub-bottom interface. The results suggest that the attenuation and its dependence on frequency and the relative roughness give an indication of the type of

sediment. It is considered that with the use of an improved sub-bottom profiling technique, it will be possible to measure a range of acoustic properties that will allow the diagnosis of the type of a marine sediment.

Three published papers in direct connection with the present research form the Appendices.

CONTENTS

CHAPTER I

INTRODUCTION

1.1. Continuous Reflection Sub-bottom Profiling

1.1.1. General

The emergence and the continued developments of various continuous seismic reflection profiling systems in recent years can certainly be regarded as a great stride forward in the advance of marine geophysical techniques. Being already one of the principal tools in the studies of marine geology and geomorphology, such equipment has also been widely used to assist off-shore petroleum and mineral exploration as well as marine engineering problems. As water-covered areas constitute approximately 72 per cent of the earth's surface, it may well be expected that increasing necessity will dictate more intensified geophysical efforts in this direction in the years to come.

The continuous seismic reflection profiling equipment, or simply the sub-bottom profiler, though varying in type and name, is essentially a special version of an echo-sounder. It utilizes pulses of various forms of sonic energy and a graphic recorder system that displays the acoustic data in the form of geological cross section. It can elucidate sub-bottom structures to varying depths and in varying degrees of details according to the specifications of the instrumental behaviour as well as the local geological conditions. The major difference in the various systems has been in the method of producing sonic energy which can be of either a single frequency or a broad spectrum.

Fig. 1-1 illustrates the basic functional elements and the operating principles of such a system. The sub-bottom profiler via the energy

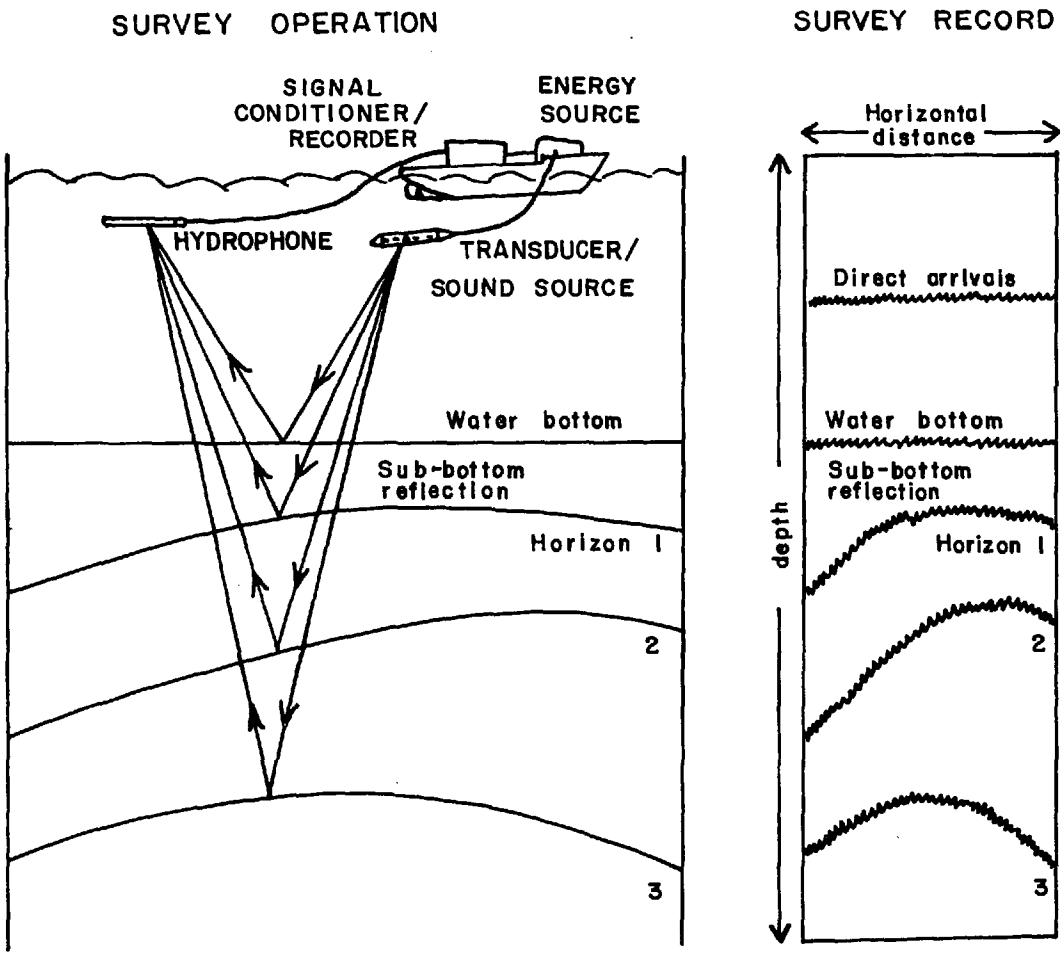

BASIC FUNCTIONAL ELEMENTS AND OPERATION PRINCIPLES OF A CONTINUOUS SEISMIC REFLECTION PROFILING SYSTEM

FIG. 1.1

source and transducer generates at precisely controlled regular intervals repetitive underwater acoustic pulses that are transmitted to and into the water bottom. Part of this energy is reflected from the water bottom and from sub-bottom reflecting interfaces of contrasting acoustic impedance. The reflections are received by the hydrophone and then converted into suitable electrical energy through a series of signal conditioning processes before being fed ultimately to a graphic recorder. Two-way travel times of the acoustic pulses are then continuously recorded across a moving strip of electro-sensitive paper to display the depths to reflecting layers graphically.

One great advantage concerning the use of the sub-bottom profiler is that it provides most rapid and economical coverage for any exploration projects where, within the penetration range of the instrument, high resolution and great sub-bottom detail are desired. Preliminary results are obtained immediately through straightforward interpretation of the distorted graphic presentation of geological sections. The operation is safe because explosives are not generally involved and hence the system can be used in many harbours and areas where explosives are forbidden. Admittedly, the reflection profiling using a sonar system also has some drawbacks when compared with conventional marine seismic shooting in aspects such as the comparatively lower source energy and the essentially single-trace recording which precludes the use of some seismic data processing methods. However, with a view to the continued improvement both in instrumentation and technique, nonexplosive continuous reflection profiling might be expected to be employed in an increasing proportion of marine seismic work in the future except, perhaps, for studies of mantle or inner earth.

1.1.2. Historical

Although the advance and development of the modern sub-bottom profiling system has been a rapid one, sub-bottom profiling with conventional echo-sounder began shortly after graphic recorders came into use for echo-sounding. Many observations were made in shallow-water areas where the sound pulse had penetrated the bottom to be reflected from a sub-bottom horizon below. Among the early observations made Murray (1947) reported the recording of dual-bottoms during a topographic investigation of the Gulf of Maine. During the Lake Meade Comprehensive Survey of 1947-1949 and subsequent underwater investigations in other shallow water areas, Smith (1958) established the characteristics of sound waves that can be used in shallow geophysical exploration by the echo-sounder method. A pulsed power sound source with a discrete frequency, ranging from 6 to 80 keps, was used during these investigations. It was observed that, as in seismic work, the lower frequencies were generally more satisfactory and penetrated with less attenuation. The Marine Sonoprobe system developed by McClure et al. (1958) is a modified version of the conventional echo-sounder. It is mainly a low-frequency sonar system which generates a pulse of sound energy with a dominant frequency of 3,800 cps from a directional magnetostrictive transducer.

The development of a broad-band sound source for sub-bottom profiling has followed somewhat different line. To study the frequency effect in a series of echo-sounding experiments, Knott and Hersey (1956) employed a sound source generated from an electric spark discharged under water together with the use of a graphic recorder. The spark sound source then used was found to have a broad spectrum over the range of 0.1 to 50 kcps. Comparison of graphic records, with

4-6 kcps and 400-500 cps respectively band-pass filtering, indicated that sub-bottom echoes appearing in the low band-pass records did not have any high-frequency counterparts. The feasibility of adapting the underwater electric spark as a repetitive broad-band sound source for sub-bottom profiling was then initially established.

The practical application of this system for marine geophysical work was reported by Beckman et al.(1959) at Lamont Geological Observatory. This sonar system, called the Sub-bottom Depth Recorder, utilized either an electrical spark discharge (Sparker) or a combustion chamber using mixture of propane and oxygen (RASS). Even with this early version of sub-bottom profiling equipment penetrations in excess of 600 ft. with Sparker and in excess of 1400 ft. with RASS in a certain shallow water area were claimed.

An electromagnetic sonar transducer, called the Boomer, or the Thumper, for producing underwater sound pulses was developed by Edgerton, Germeshausen and Grier, Inc. in conjunction with Woods Hole Oceanographic Institution (Hersey, Edgerton, et al. 1961). The Boomer transducer produces acoustic energy by a special electo-mechanical design using the eddy current effect. The transducer consists of a flat-wound coil mounted in an epoxy body and an aluminium plate spring-loaded against the face of the coil. The plate is violently repelled from the coil because of the interaction between the induced eddy currents in the plate and the primary current in the coil produced by the discharge of a condenser bank. This sudden movement of the plate against the water produces a precise, repeatable pulse which has a spectrum containing both high and low frequencies.

Another broad-band sound source for sub-bottom profiling is the pneumatic gun developed by Ewing et al.(1964). This device has proved

to be satisfactory with regard to reliability, energy output and safety of operation for continuous profiling both in shallow and deep ocean regions. The gun produces acoustic energy, releasing a volume of high-pressure air into the water through a pressure-actuated self-cycling piston action. Its effectiveness is a function of the amount of air released, the pressure of the air, and the rapidity with which it is released.

In general, relatively low power, high frequency sub-bottom profiling equipment gives high resolution for the upper few hundred feet, while higher power, low frequency gives as much as several seconds of penetration, but with loss of resolution. Each class of equipment has, therefore, an optimum objective, with detail of resolution balanced against depth of penetration.

Alongside the continuous development and improvement of various sub-bottom profiling equipment and techniques in recent years, there have been plenty of important applications too numerous to be cited here, amongst which may be included studies of facies delineation of the sea bottom, the sedimentary or structural framework of continental shelves, terraces and slopes, sub-marine ridges and canyons, and sediments and ocean basin structural history, etc. A better known applied geophysical work involving the intensive use of sub-bottom profiler was carried out by the Channel Tunnel Study Group in 1964-1965 in the English Channel area. In this instance, the results of the sub-bottom profiling surveys were thoroughly correlated with a considerable number of boreholes, which firmly established geological control usually lacking in such investigation. More recently, very wide use has been made of incorporating the sub-bottom profiler with conventional marine refraction method on seismic surveys to offer a solution to hidden layer problems, allowing both layer velocity and thickness to be computed rather than estimated.

1.2. The Marine Sediments

Sediments usually exist in one of the three states, namely, (a) unconsolidated sediments, (b) semi-consolidated sediments, and (c) consolidated sediments. The marine sediment is, in general, an unconsolidated sediment being an aggregate of particles with the interstices completely water-filled. The components of sediments are commonly grouped according to their origins: terrigenic (material derived from land), biogenic (the remains of marine organisms, principally carbonates and silicates) and authigenic (material precipitated directly from solution). Density, size, and size distribution are the controlling parameters in almost all the physical properties of sediments. Marine sediments are, therefore, frequently referred to as sand, silt, or clay according to size of the sediment particles and their distribution.

The size characteristics and physical properties of marine sediments are in fact very much mutually related. The size characteristics consist essentially of the median grain size, the sorting coefficient, and the percentage of gravel, sand, silt and clay. The physical properties of sediments consist of a great number of parameters amongst which there are compressional velocity, density, porosity and acoustic attenuation. Some general sediment-type classification according to particle size distribution and the empirical relationships connecting median diameter, density, velocity, acoustic impedance, and porosity are given in Tables I, II and III in Appendix C (Taylor-Smith & Li, 1966, Reprint pp. 357-359).

In the examination of marine sediments, the recoverable sediments of the topmost part of the sedimentary column can be studied in detail on samples. However, deep sediments or even the superficial

sediment *in situ* may differ widely in property from that obtained by measurements on samples in the laboratory. *In situ* acoustic measurements can therefore play a major role in any study of the dynamic physical properties of marine sediments.

1.3. The Particular Approach

Despite the great progress made in the use of marine continuous reflection profiling to elucidate sub-bottom features, very few known attempts have been made to treat the acoustic data so collected in a quantitative manner. The information extracted from acoustic analysis and its correlation with the physical properties of the submarine layers involved may lead to the possible identification of the sea-bottom sediment or rock type.

Kendall (1941) has reported the noticeable effect that on reflection records taken in many areas, the reflection from the deeper horizons have their energy concentrated in a frequency band definitely lower than that of the reflection from shallow horizons. Jakosky and Jakosky (1952) have carried out some frequency analyses of seismic waves by first recording the seismic wave energy on some reproducible media such as magnetic tape and then repetitively playing back this recording as the various circuit parameters were changed to accentuate the desired components under study. The results of their studies indicated that the instrumental technique of frequency discrimination could improve the signal-to-noise ratio. Bruckshaw (1956) has pointed out that the shape of the arrival, its frequency spectrum, etc. are obviously related to the absorption of energy in the ground and the dispersion of waves, and these in turn are related to the elastic properties and their imperfections. The study of the phenomenon of

differential attenuation of the various frequencies may yield valuable clues concerning the nature of the media through which the various waves have passed.

It was found by a number of workers (Hampton, 1966, Nolle, et al. 1963, & Shumway, 1960) from laboratory experiments that sediments on the sea floor acted as low-pass filters, the high frequency cut-off position being dependent to a certain extent upon the sediment type, or more correctly, the size and physical characteristics of the sediment. For instance, sand filters out the higher frequencies much more rapidly than clay. In water-saturated marine sediments, attenuation and its frequency dependence may well be regarded as two of the most revealing acoustic parameters concerning the general properties of the sediments. Li and Taylor-Smith (1966a, Appendix A) have proposed a method of the possible identification of sea-bottom sediments by a ship underway. By taking a sub-bottom reflection, and its associated multiples, and comparing each to the pulse reflected from the sea floor itself, and to their respective neighbours at some distance along the layer, it is possible to provide a reasonable analysis of the bulk properties of the sea-floor medium in terms of variations in the frequency spectrum. At the same time it is believed that by a suitable statistical treatment of the reflected energy fluctuations, the relative roughness of a bottom or sub-bottom interface can be determined.

With this particular approach in mind, existing equipment was modified, new instrumentation systems were designed and developed, appropriate techniques were introduced, various experiments were carried out, and the experimental results analysed and discussed. It is believed that a new angle has been opened for the examination of marine sediments with a sub-bottom profiling system.

CHAPTER II

THEORETICAL CONSIDERATIONS

2.1. The Nature of Underwater Sound

When a source is emitting sound in water, it is transforming electrical or mechanical energy into acoustical energy by generating an alternating pressure that is superimposed on the ambient static water pressure. The acoustic power involved is the time rate at which this energy is radiated.

To determine the numerical values of the velocity of propagation and other pertinent constants identified with an acoustic wave in water it is necessary to consider the density and the elasticity of the med ium through which the wave is propagated. The density (ρ) is defined simply as the mass per unit volume. The bulk modulus (K) is defined as the ratio of the stress (Δp) to the strain ($\Delta V/V$). The fundamental relation between the velocity c of propagation of the wave and the elasticity and density of the water is

$$c = \sqrt{\frac{K}{\rho}} \qquad (2 - 1)$$

For sea water, the velocity of propagation is dependent on the temperature, salinity, and the confining pressure. However, a velocity of 1,500 m/sec is commonly used as a standard velocity for making simple calculations rather than the more precise empirical formula.

Any system which responds to a sinusoidally varying stimulus in such manner that the response also varies sinusoidally, and at the same frequency is characterized by a property known as impedance.

The quantity ρc is the acoustic impedance of a given medium. The quantity can also be expressed as

$$\rho c = \sqrt{\rho K} \qquad (2 - 2)$$

The rate of flow of the energy of acoustic waves through some given surface is measured in terms of their acoustic intensity. For a plane, acoustic wave the relationship between the intensity I and the pressure p is

$$I = \frac{p^2}{\rho c} \quad \text{(Wood, 1955)} \qquad (2 - 3)$$

The source intensity is the acoustic intensity at a given distance along a given bearing from the source. This intensity is normally measured at a distance of 1 yard from the effective centre of the source.

2.2. The Direct Propagation of Underwater Sound

In underwater sound, ray paths are the routes along which the acoustic energy is propagated through the water with a minimum time. Points between which changes in acoustic intensity are to be studied will, in general, lie on some specific ray path.

Although the character of the radiation field of a typical sound source may vary with distance from the source in its immediate vicinity the particle velocity is not necessary in the direction of travel of the wave and an appreciable tangential velocity component may exist at any point. This is spoken of as the near field. The extent of the near field of a source depends amongst other factors on the frequency, on the characteristic source dimensions and on the relative phases of the radiating parts of the surface. It is

difficult to establish general limits for the near field of an arbitrary source with accuracy. Often the sound field must be explored experimentally.

In the far-radiation field the sound intensity is proportional to p^2. Most acoustic measurements are made in terms of effective sound pressure. Therefore, it is convenient to have a decibel scale for sound pressures. To define the decibel scale for sound pressure, logarithm of the ratio of mean-square sound pressure is used, i.e.

$$10 \log_{10} \frac{p^2}{p^2_{ref}} \qquad (2 - 4)$$

Thus the sound pressure level is

$$20 \log_{10} \frac{p}{p_{ref}} \qquad (2 - 5)$$

where p_{ref} is the reference sound pressure.

2.2.1. Spherical Spreading

Consider a point source emitting sound equally in all directions. The intensity of the acoustic wave decreases as the distance from the source increases, because the total power must spread over a larger spherical area. If I_o is the source intensity, then the intensity of sound at a greater distance is

$$I = \frac{I_o}{4 \pi r^2} \qquad (2 - 6)$$

or, in terms of pressure amplitude p,

$$\frac{p^2}{\rho c} = \frac{p_o^2}{\rho c \times 4\pi r^2}$$

or

$$p = \frac{p_o}{2r \times \pi^{\frac{1}{2}}} \qquad (2 - 7)$$

p_o being the pressure amplitude of the source. Hence in the far field, in the absence of other loss mechanisms, the sound-pressure level decreases 6 dB as the distance is doubled.

If the source intensity L is known, $L = 20 \log_{10} p_o$ (decibels), then the sound level L_1 at any range r from the source is determined by the inverse square law

$$L_1 = L - 20 \log_{10} r \qquad (2 - 8)$$

where L and L_1 are in decibels.

2.2.2. Attenuation

The decrease in sound energy per unit length of ray path is not entirely due to spherical spreading. Any loss mechanism will result in the conversion of acoustic energy into heat energy. If the loss mechanism is linear (e.g. the finite viscosity of the water) then the sound pressure amplitude decays exponentially with distance. This expression simply states that, for each unit of distance travelled, the sound wave suffers the same percentage reduction in amplitude. Energy losses associated with this phenomenon are said to be due to absorption. In actual practice viscosity does not account for all the absorption. Changes in the direction in which acoustic energy is

propagated caused by reflection from foreign bodies are said to be due to normal scattering. These foreign bodies in the medium may vary widely as to size and acoustic impedance and the existence of biological scatterers cannot be ignored. In some situations, practically all of the energy to reach certain regions of the sea does so because of scattering. The combined effect of absorption and normal scattering is referred to as attenuation. The attenuation of a medium through which radiant energy is propagated causes a reduction in the intensity of this energy which is characterized by the fact that, if the attenuation is constant, the fractional reduction per unit distance is also constant.

Normally the attenuation through sea water is nearly constant so the fractional reduction in intensity due to a single unit length of ray path is given by

$$\frac{I_{r+1}}{I_r} = k \qquad (2-9)$$

where k = constant less than unity, I_r the intensity at the beginning of the path of unit length and I_{r+1} the intensity at the end. The fractional reduction due to Δr unit lengths of ray path is then

$$\frac{I_{r+\Delta r}}{I_r} = k^{\Delta r} \qquad (2-10)$$

It is convenient to put $k = (10^{0.1})^{-\alpha}$, then considering attenuation only

$$\frac{I_2}{I_1} = (10^{0.1})^{-\alpha (r_2 - r_1)} \qquad (2-11)$$

where I_1 and I_2 are the intensities at the beginning and end of the specified path, r_1 and r_2 the distances along the ray from the source to the beginning and end of the ray path, and α is the attenuation coefficient.

The attenuation in dB from r_1 to r_2 is given by

$$10 \log \frac{I_2}{I_1} = -\alpha (r_2 - r_1) \qquad (2 - 12)$$

or expressed in acoustic pressure amplitude p

$$20 \log \frac{p_2}{p_1} = -\alpha (r_2 - r_1) \qquad (2 - 13)$$

The attenuation coefficient α for a particular frequency has been determined by Horton (1959) and its dependence on frequency is given by the expression

$$\alpha = 0.20f + 0.00015f^2 \text{ dB/kyd}, \qquad (2 - 14)$$

where f is the frequency in kilcycles per second. Fig. 2-1 shows the experimental results after Albers (1965).

The transmission losses in the passage of sound through the sea water or other attenuating medium are those incurred due to spherical spreading and attenuation. The total loss H between two points in the ray path is the sum of the individual losses expressed in dB which is given by

$$H = 20 \log \frac{r_2}{r_1} + \alpha (r_2 - r_1)$$

or $$H = 20 \log_{10} r_2 - 20 \log_{10} r_1 + \alpha (r_2 - r_1) \qquad (2 - 15)$$

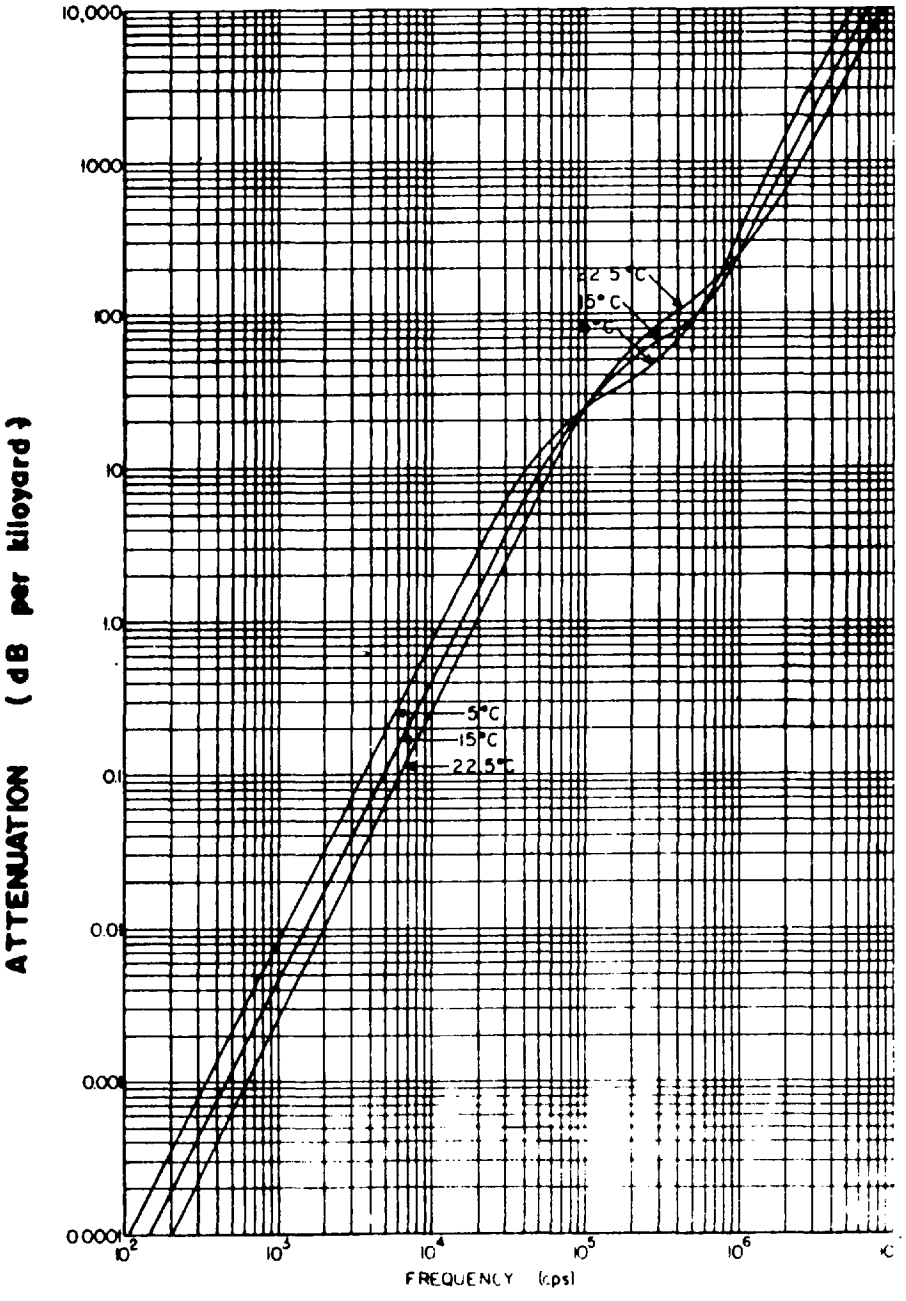

FIG. 2.1 Attenuation of sound in sea water. (after Albers)

2.3. The Effects of Reflection and Refraction

2.3.1. Reflection

The geometrical laws of reflection of sound waves at a boundary are the same as for light waves, the angles of incidence and reflection being equal and in the same plane. The amount of sound energy reflected at a boundary is quantitatively related to the acoustic impedance between the two media at the boundary. The reflection coefficient is generally defined as the ratio of the amplitude of the reflected wave to the amplitude of the incident wave. For nonrigid, compressible media the reflection coefficient for plane waves incident at an angle ϕ_n upon a boundary between two media with densities ρ_1 and ρ_2 and velocity c_1 and c_2 was shown by Rayleight to be

$$R = \frac{\frac{\rho_2 c_2}{\rho_1 c_1} - \left(1 + \tan^2 \phi_n \left(1 - \frac{c_2^2}{c_1^2}\right)\right)^{\frac{1}{2}}}{\frac{\rho_2 c_2}{\rho_1 c_1} + \left(1 + \tan^2 \phi_n \left(1 - \frac{c_2^2}{c_1^2}\right)\right)^{\frac{1}{2}}} \qquad (2 - 16)$$

This can also be expressed as

$$R = \frac{\rho_2 \cos \phi_n - \rho_1 (n^2 - \sin^2 \phi_n)^{\frac{1}{2}}}{\rho_2 \cos \phi_n + \rho_1 (n^2 - \sin^2 \phi_n)^{\frac{1}{2}}} \qquad (2 - 17)$$

where $n = c_1/c_2$ is the index of refraction. This is a measure of the transmission loss suffered by the acoustic wave, following a given ray path, on crossing the boundary between two media with different specific acoustic impedances. It is evident that this transmission loss is not independent of the direction of energy flow.

Reflection at a free surface however, is nearly perfect at all angles of incidence because of the marked contrast in acoustic impedance between the water and the air above. Reflections from the surface often exhibit a phenomenon similar to that known in optics as the image effect. It is only the presence of water waves, large compared to the lengths of acoustic waves, which prevents this surface from being an almost perfect reflecting surface. In fact, sea surface roughness causes scattering of the sound at the water-air interface so that reflection from the surface is far from ideal. The surface topography, in general, is highly irregular and does not easily lend itself to an exact mathematical treatment of sound reflection. The most significant feature of the surface-reflected signal is the rapidity and magnitude of its fluctuation.

2.3.2. Refraction

The change in direction in the transmitted part on reaching the boundary between two different media, or on reaching a point at which the wave velocity changes, is known as refraction. The relation between refraction and velocity in the case of sound waves in water is similar to that found in the case of light waves. The law of refraction, generally known as Snell's law, is given as

$$\frac{\sin \phi_1}{\sin \phi_2} = \frac{c_1}{c_2} \qquad (2 - 18)$$

where ϕ_1 and ϕ_2 are the angles between the normal to the boundary and the rays in the media with velocities c_1 and c_2 respectively. This relation is independent of the direction along the ray in which

the sound wave is travelling.

The critical angle, when $\phi_2 = 90^\circ$, is given by

$$\sin \phi_1 = \frac{c_1}{c_2} \qquad (2 - 19)$$

The wave refracted at the critical angle may be considered as a disturbance travelling along the interface of the velocity discontinuity, with the larger velocity. For angles greater than the critical angle there can be no refracted ray in the second medium and so no penetration into that medium, and all the incident energy is totally reflected.

Within a single medium the velocity of propagation may vary from place to place. Continuous changes in velocity within a single medium cause refraction which may have as great an effect upon the acoustic intensity as those accompanying the passage of a wave from one medium to another. Gradual changes in the velocity of propagation within a single medium are known as velocity gradients. In sea water, velocity gradients occur due to the combined effects of temperature gradients, the salinity gradients, density gradients and a pressure component of the velocity gradient. The continuous bending of a ray path may form shadow zones at sound channels, in addition to its effect on transmission time. Wherever there are velocity gradients in a medium the sound ray between two points will, in general, be longer than the straight line distance. For short range, however, errors due to the curvature of ray paths by refraction may generally be considered negligible compared to those due to other more dominating causes.

2.4. Bottom Reflection

Whereas for surface reflection a 180° phase reversal of the incident sound can be assumed because of the neglect of any transmission through the water-air interface, phase changes varying from 0° to 180° can be experienced upon reflection of sound from the bottom owing to the diversive character of the bottom properties. The sea floor is a sound-reflecting surface whose characteristics depend on the nature of the bottom and on the wavelength of the sound. Mud is apparently a poor reflector so transmission with a mud bottom in shallow water often closely resembles transmission through deeper water. A sand bottom behaves as a good reflector and as the particle size of the bottom increases, the reflectivity increases and less of the acoustic energy is transmitted.

2.4.1. Specular Reflection

For specular reflection, the reflectivity of the bottom can be described by the application of the Rayleigh reflection coefficient. Theoretical analysis and experimental results have been given by Arons and Yennie (1950) showing that phase shifts when sound waves are reflected from interfaces of higher sound velocity occur only at angles exceeding the critical angle and the phase shift depends only upon the acoustic parameters of the media involved and upon the angle of incidence, being independent of the frequency of the incident wave train.

The energy loss upon reflection from the bottom is in fact involved in the attenuation in the bottom because of the transmitted portion of the plane waves being closely related to the incident and reflected ones. Thus the reflectivity in itself depends upon several parameters which include the angle of incidence, attenuation in the bottom, the magnitude of the impedance ratio and the ratio of the sound velocities in the two media. Two examples from the work of Becken (1964) are shown in Fig. 2-2 where bottom reflected to incident pressure ratios are plotted as a function of the grazing angle measured from the horizontal, demonstrating the effect of velocity ratios greater than and less than unity. In these α is the attenuation coefficient in the bottom (α may itself be a function of frequency)

and $$\beta = \frac{\omega H}{c_1} = \frac{2\pi H}{\lambda},$$ a dimensionless variable

where H = the water depth, λ = the wave length, and c_1 = wave velocity in water.

The sound reflected from the bottom as a function of grazing angles often shows a multiplicity of maximum and minimum points from normal incidence out to grazing incidence. The peaks and troughs in the reflectivity can be attributed to interference effects from sound reflected from sub-bottom layering. At low frequencies the effective reflector is often a sub-surface layer rather than the water sediment interface. This has been mentioned by Taylor Smith and Li (1966, Appendix C) in a paper discussing thoroughly the received signal amplitude and the effect of frequency in terms of the parameters of sea floor sediments. They have indicated that among a number of variables influencing the reflection process at the sea-floor, sediment porosity is by far the most important property.

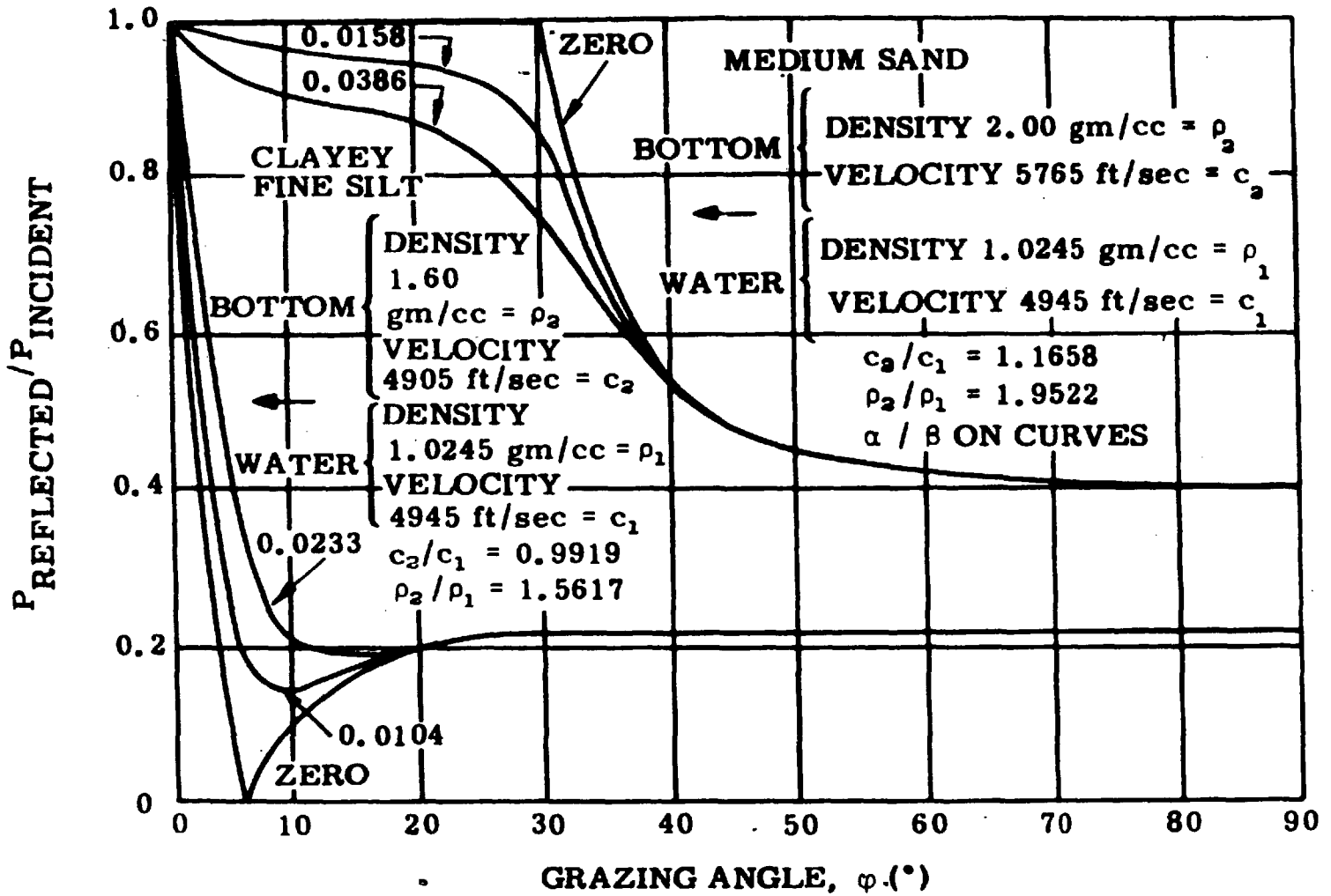

Fig. 2.2. Bottom reflected to incident pressure ratios versus grazing angle (after Becken).

Since the bottom reflecting properties depend a great deal on the acoustic impedance of the sediment and which is roughly related to the sediment type but more closely correlates with the porosity, the temperature effect on water-saturated sediments is approximately the same as for water alone. This similarity to water behaviour has been experimentally demonstrated by Shumway (1960) inasmuch as the compressibility of a water-sediment mixture is dominantly due to the relatively large water compressibility. Again porosity comes into the play.

2.4.2. Nonspecular Reflection

Bottom reflection, in general, consists of both specularly and non-specularly reflected sound the latter being analogous to diffusely reflected light. Energy returned by reflectors other than that which is desired to observe is known as reverberation. Reverberation levels are proportional to source level, also increase with pulse duration.

Often, it is not possible to make a distinction between specularly and non-specularly reflected sound. Scatterers are understood to have dimensions which are small as compared to the signal wave length. Each may be considered to act as a point source of secondary radiation.

Albers (1965) has made measurements in a model tank using media of different sizes as a reflector. With a the radius of the particles and λ the wavelength he found that for particle sizes such that $2\pi a/\lambda$ is greater than one, scattering is only slightly

influenced by the roughness of the surface. Rayleigh shows that the amplitude of scattering varies directly as the volume of the scattering particles and inversely as the square of the wave length λ of the incident sound, or

$$I_s \propto \frac{1}{\lambda^4} \qquad \text{(Wood, 1955)} \qquad (2\text{-}20)$$

Prediction of the reflection by a rough surface, the shape of which is neither periodic nor known, is one of the most difficult problems of reflection. Bottom scattering phenomena are not the same for all types of bottoms. Although wide variations are observed, in general, for a given frequency the highest reverberation levels are observed over rock bottom and smallest values over sand and mud. This dependence would seem to indicate that the properties of the bottom material control the amount of scattering.

Mackenzie (1961) has observed that bottom non-specular reflections also obeyed Lambert's law of diffuse reflection reasonably well. Lambert's law states that the intensity dI_r, at a unit distance from dA due to the energy scattered at any angle Q (not necessary in the plane of incidence) is given by

$$dI_r = \mu I_i \sin \phi \sin Q \, dA \qquad (2 - 21)$$

where the incident intensity at a grazing angle ϕ is I_i so that the effective area is $\sin \phi \, dA$ and μ is a constant of the surface. The reverberation level due to non-specular reflections was then analyzed to obtain the scattering constant of the bottom. A value of $10 \log \mu = -27$ dB was obtained for both a 530 cps and a 1030 cps sound. According to Mackenzie the returning sound essentially retraced its outgoing path so that $Q = \phi$, and Lambert's law predicts

a $\sin^2 \phi$ dependence of the reverberation, and the omnidirectional scattering a sine ϕ dependence, his experimental data fits nicely for grazing angles from 80° to 30°. His results, in comparison with published values of other investigators, indicates that for clay, muds, or fine grained sands, there appears to be no significant frequency dependence over a range of seven octaves. On the other hand, a well-controlled field study of reflection and scattering of sound by a flat and absorbing sea bottom (Bell 1964) is capable of explaining the dependence of bottom loss on frequency, location, and incident angle. Geological and acoustical reflectivity properties can be related by considering the bottom impedence as derived from the established correlation between the physical properties of the sediments and their fundamental velocity and absorption characteristics but the form of his field data has shown no evidence that scattering processes play a significant role in either adding to or subtracting from the sound reflected in the specular direction.

2.5. Signal Fluctuations

The basic physical concepts of the problem of transmission of sound are quite simple, but the problems relating to the study of the actual propagation of sound in water can be very complex because of the wide variability of the various properties of the medium and its surrounding environment. Environmental conditions are therefore important factors in underwater acoustic measurements. As a measurement problem, the signal reflected in the specular direction can be considered as the sum of a coherent component

reflected by an average plane surface and incoherent components scattered by the irregularities or caused by phase interference. A pulse of sound from the source will often produce a cluster of arrivals at the receiver at a time close to that corresponding to the specular path. For most bottoms, multiple arrivals are caused by reflection from the sea surface and from bottom and sub-bottom strata. Under many experimental conditions, interference effects are an important factor in signal fluctuations. This is particularly true in shallow water when observations are made from ships which are subject to sufficient motion to shift the transducer in the sound field pattern. There is also the complex relation existing between the grazing angle and inteference effect produced by the phase of a sub-layer reflection acting successively in concert with and in opposition to the phase of the reflection from the water-bottom interface as the incident angle is changed. In continuous reflection profiling work, the reflection angle, though normally very small, varies with the changing vertical distance to various reflecting interfaces. In deep water, volume reverberation levels predominate, while in shallow water, surface and bottom reverberations are predominant.

In theory, observations of the interference patterns may lead to significent information concerning the bottom layering if the bottom were probed with a sequence of pulses having suitably chosen frequencies. Each frequency would lead to a set of possible models, but in principle, only one model would be common to all sets. In practice, however, many unknown parameters make solutions to such complicated problems extremely difficult if not impossible.

Signal fluctuation due to the state of smoothness of a reflecting interface is another problem. Even in the specular direction, the reflectivity as a function of frequency and incident angle is dependent on the roughness of the bottom as well as on the acoustical velocity and density of the bottom and sub-bottom layers.

For reflection at an irregular interface, Tolstoy and Clay (1966) have worked out through rigorous mathematical derivations a frequency dependent term K, given by

$$K = (\omega / c) \sin \phi$$

where ϕ = grazing angle, c the velocity in water and ω the angular frequency of the sound. For a Gausian distribution function having a mean-square roughness σ^2, the mean signal differs from the mirror-reflected signal by the factor $e^{-2K^2\sigma^2}$ which is identified as being a measure of the coherence of the scattered radiation, being unity for coherent reflection and zero for incoherent reflection. The Rayleigh reflection coefficient R and the coherence factor can be combined to form a coherent reflection coefficient

$$(\bar{R}) = Re^{-2K^2 \sigma^2} \qquad (2 - 22)$$

The coherent reflection coefficient is dependent upon the distributio n of the surface roughness and independent of the general shape of the surface. Without change of other properties, it follows that roughness of the bottom decreases the coherent reflection coefficient.

In general fluctuations other than at the source appear to be

primarily due to the following mechanisms:

(1) Variation of ray path or paths owing to the roll and pitch of the vessel carrying the transmitter and receiver. Besides, additional paths or their removal may be brought about by a change of sound speed structure (refraction).

(2) Interference between and among directly transmitted, surface reflected, bottom reflected, and sub-bottom reflected sounds.

(3) Variation of reflectivity due to the lateral and vertical variability of the various acoustic properties of bottom and sub-bottom strata.

(4) Variation of the proportion between specular and non-specular reflections. This depends to a great extent on on the degree of roughness of various reflecting interfaces and thus the proportion between coherent and incoherent signals.

It is therefore self-evident that the study of the phenomena of fluctuation can only be conducted by statistical rather than deterministical means. Measurements and further considerations of fluctuations found in acoustic data collected during the present continuous sub-bottom profiling experiments will be given in a later chapter (Chapter VII).

2.6. Attenuation in Marine Sediments

Acoustic attenuation in a layer of marine sediment, like that in sea water, is the irreversible conversion of acoustic to thermal energy. The nature of viscous damping losses and solid friction

losses may cause sound waves to be attenuated as they travel through a physical medium.

Born (1941) has shown that solid friction losses are primarily responsible for the observed attenuation of seismic waves but his experimental data were obtained on small samples of consolidated earth material. Kendall's (1941) investigation on reflection records of several widely separated areas show, after correction for divergence, a number of amplitude-time curves in which the amplitudes decrease exponentially with time. The relative amplitude plotted as a function of frequency (0 - 120 cps) shows that the earth acts as a low-pass filter the high frequency components of a wide-band impulse will be rapidly attenuated as compared with the low frequency components. Biot (1956) expresses elastic wave attenuation in terms of permeability, fluid viscosity, frequency, and the elastic constants of the material. The validity of this theory, experimentally tested by Wyllie et al,(1962) seems only conditionally applicable to porous media.

Elastic wave attenuation in marine sediments, however, is due in part to the relative motion of the liquid and the solid involving both viscous damping and solid friction. In viscous damping, heat conducted during one period increases proportionally with frequency because the increased steepness of the temperature gradient. This part of the loss is based on the assumption that the energy lost is dissipated in viscous friction. It is found that although high degree of water saturation exists practically in all marine sediments, attenuation is also a function of solid friction because of the inter-granular pressure. For this the energy lost per cycle is independent of the frequency of the cyclic stress, and depends only

upon the nature of the material and the maximum strain amplitude. Both of these factors cause frequency dependent acoustic attenuation in marine sediment. Laughton (1957) has conducted some investidation in sound propagation in compacted marine sediments. His experiments have shown that the velocity is a function not only of the solid to liquid in the sediment but also of the intergranular pressure. Neither pressure nor void ratio alone can account for the velocity changes. Void ratio can be expressed as

$$\text{Void Ratio} = \frac{\rho_s - \rho}{\rho - \rho_w}, \qquad (2 - 23)$$

where ρ is the density of the saturated sediment, ρ_s that of the solid grains and ρ_w of the water.

It would seem that compaction and porosity in unconsolidated sediments may play a similar important role in attenuation and its associated frequency dependence. In addition, the scattering of elastic waves by the intrinsic small inhomogeneities of sediment grain surface areas and shapes found in the sorting of natural sediments should also contribute to the overall phenomenon of the attenuation process. Officer (1955) has reported that marine sediment is dispersive.

The nature of compressional wave attenuation in marine sediments is thus found to be complex. Frequency dependence of the attenuation does not simply follow the normal relaxation law but appears to have some correlation among the various physical properties of the sediments with porosity as probably the dominant factor. When invesitgating the acoustic properties of unconsolidated layers of marine sediments, the problem is rather difficult in the general case

of naturally occuring mixtures of sands and clays with various grain sizes where interaction between particles may lead to the effect of a homogeneous medium with properties intermediate between the two components. With the exception of the particular case of attenuation in the propagation of sound waves in highly irregularly stratified heterogeneous media, it is believed, however, that any values obtained of attenuation and frequency dependence might still be the two most revealing parameters in the diagnosis of the type of a whole layer of marine sediment in situ where, apart from the top few tens of feet, the layer is inaccessible for sampling except by boring.

2.6.1. Measurements Per Se

Empirical results on marine sediment attenuation have been obtained by a number of workers, over a wide range of frequencies. The laboratory investigations have been carried out on both artificial and natural samples.

In a laboratory study over the frequency range of 4-600 kcps Hampton (1966) has found that the frequency dependence of attenuation varies from $f^{1.37}$ for clay (Kaolinite) to $f^{0.5}$ for sand, and that there is a steady change between the two. Shumway (1960) has reported that on average α is proportional to $f^{1.79}$, with a standard deviation of 0.98, measured in the frequency range 20 to 37 kcps. Using a resonant technique, his data yeild attenuation values of 20 dB/m (30 - 37 kcps) for natural silt and fine sand and 0.5 dB/m for medium clay (28.4 kcps). He has found that

the relationship between attenuation and porosity exhibited an maximum for sediments of intermediate porosity, in range of 45% to 60% for dominant coarse silt samples. Nolle et al.(1963) has given an experimental figure of frequency dependence of well sorted sands of $f^{0.5}$, which is in good agreement with that given by Hampton.

2.6.2. In Situ Measurements

In field experiments, successful measurements were made by Wood and Weston (1964) in undisturbed mud over the frequency range 4 to 50 kcps. An absorption coefficient in dB/ft approximately equal to f/50 was found indicating a linear frequency dependence but being smaller by a factor of 20 [illegible] than their laboratory values. The cause of this discrepancy they attributed to the disturbance of the mud, and the air content of the samples taken. Cole (1965) has conducted some experiments on the attenuation of sound in marine sediments which he has shown to depend on the first power of the frequency for a range of 100 - 1,000 cps. McCann (1967) carried out an investigation measuring in situ the acoustic properties in water-saturated materials of various sedimentary types mainly in beaches by insertion probes. Over the frequency range 7.5-52 kcps, some representative values of attenuation coefficient amongst his findings give $0.10f^{1.05}$ dB/ft for coarse silts (mean diameter 4.4 phi), $0.09f^{1.17}$ dB/ft for very fine sand (m.d. 3.1 phi), and $0.043f^{1.26}$ dB/ft for fine sand (m.d. 2.5 phi), where f is in kcps.

2.7. A Theoretical Development

The theoretical basis of this particular approach is the differential attenuation characteristics of marine sediments between the bottom and sub-bottom reflectors when sonic waves are passing through the medium. Assumptions are made which simplify the problem but the limitation of the results are discussed. These limiting factors, however, are not considered unsurmountable as improved methods and instrumentation could be expected to be developed in the future.

The essential advantage of the present theoretical approach is that many of the parameters which affect the propagation of an underwater acoustic pulse are not required. Nevertheless, comparative results so obtained could be indicative of some physical properties of the sediments involved. In a sense, the method could be compared with many standard geophysical techniques in which relative values of the observed data is adequate for an applied geophysical purpose.

2.7.1. Simplifying assumptions

It is generally known that in interpreting continuous reflection sub-bottom profiling records, one point has to be kept in mind that the recording from a given reflecting horizon at depth does not appear as a single event on the record but as a short sequence of events. As a usual practice the sound source and receiving hydrophone are shallowly submerged beneath the sea surface. Thus, in addition to the ray path which goes from the source to the reflecting horizon and back to the receiver, there will be three adjacent ray paths

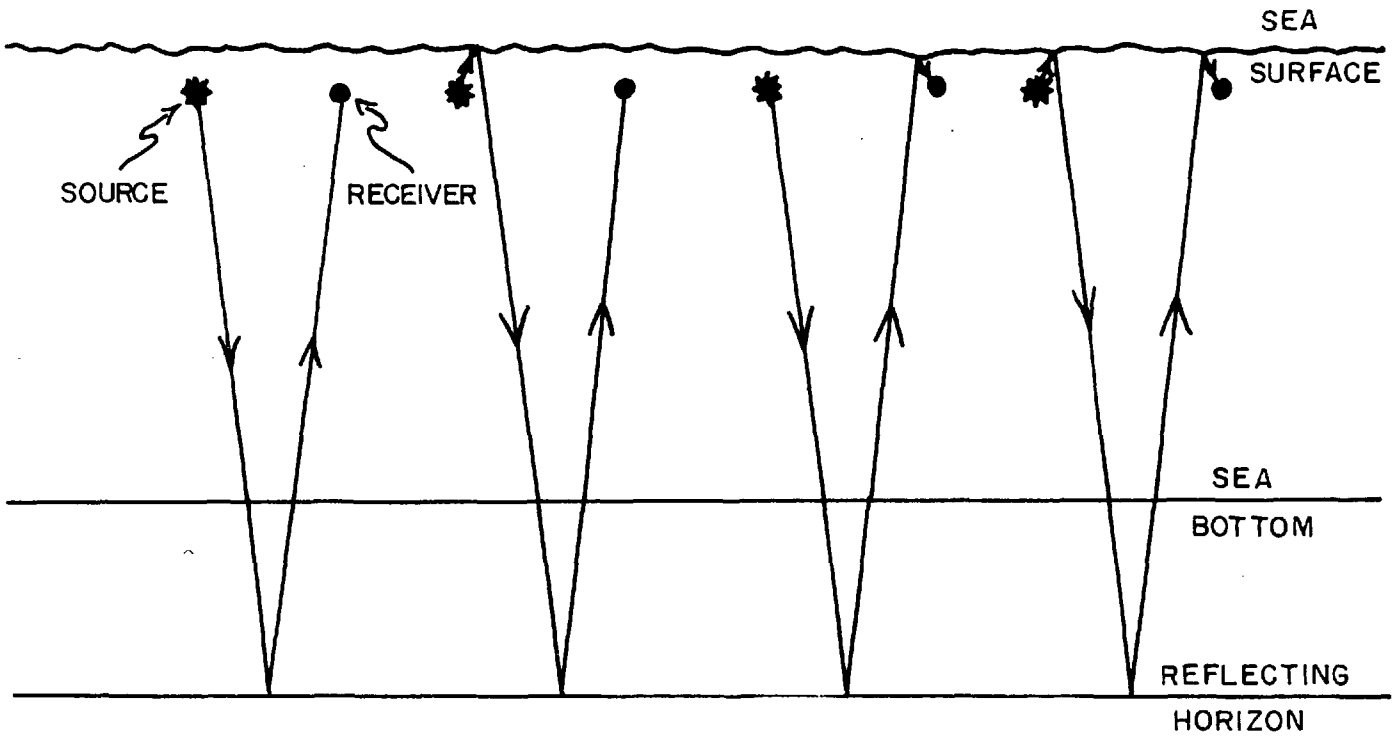

SURFACE REFLECTIONS

FIG. 2.3

illustrated in Fig. 2-3. However, the propagation of useful seismic energy can be considered adequately for most purposes to behave according to a grouped ray theory. A complex source point is the origin of ray paths which radiate in all directions. Along the tube defined by a series of adjacent rays a train of sound travels. For the four rays, of small path difference shown in Fig. 2-3, the energy of finite length will arrive at the receiver within a very short period of time and the lengths of the pulses will overlap. The output of the receiver will, accordingly, depend upon the interference between these pulses. In the analysis it will be assumed that all the recorded pulses followed the simple path shown at the left.

The reflection process of the present experiments is approximated by a fluid-topped three-layer model, with attenuation in the second layer which is wedge-shaped due to either a sloping upper or lower boundary. The third layer is assumed to be of infinite depth with a very high positive acoustic impedance contrast. The sites chosen for acoustic analysis of the sediment approximate closely to one or other of the situations illustrated in Fig. 2-4 (See also Chapter VII).

A wave originating at the source, travelling downward to a reflecting horizon and then back to the receiver will be influenced in amplitude by three primary factors, namely

(i) the spherical spreading

(ii) the partial reflection at the boundaries

and (iii) the attenuation within the layers.

The first factor can be accurately determined. The third factor gives rise to an exponential decrease of amplitude with distance, and the second reduced the amplitudes by a constant factor. Hence

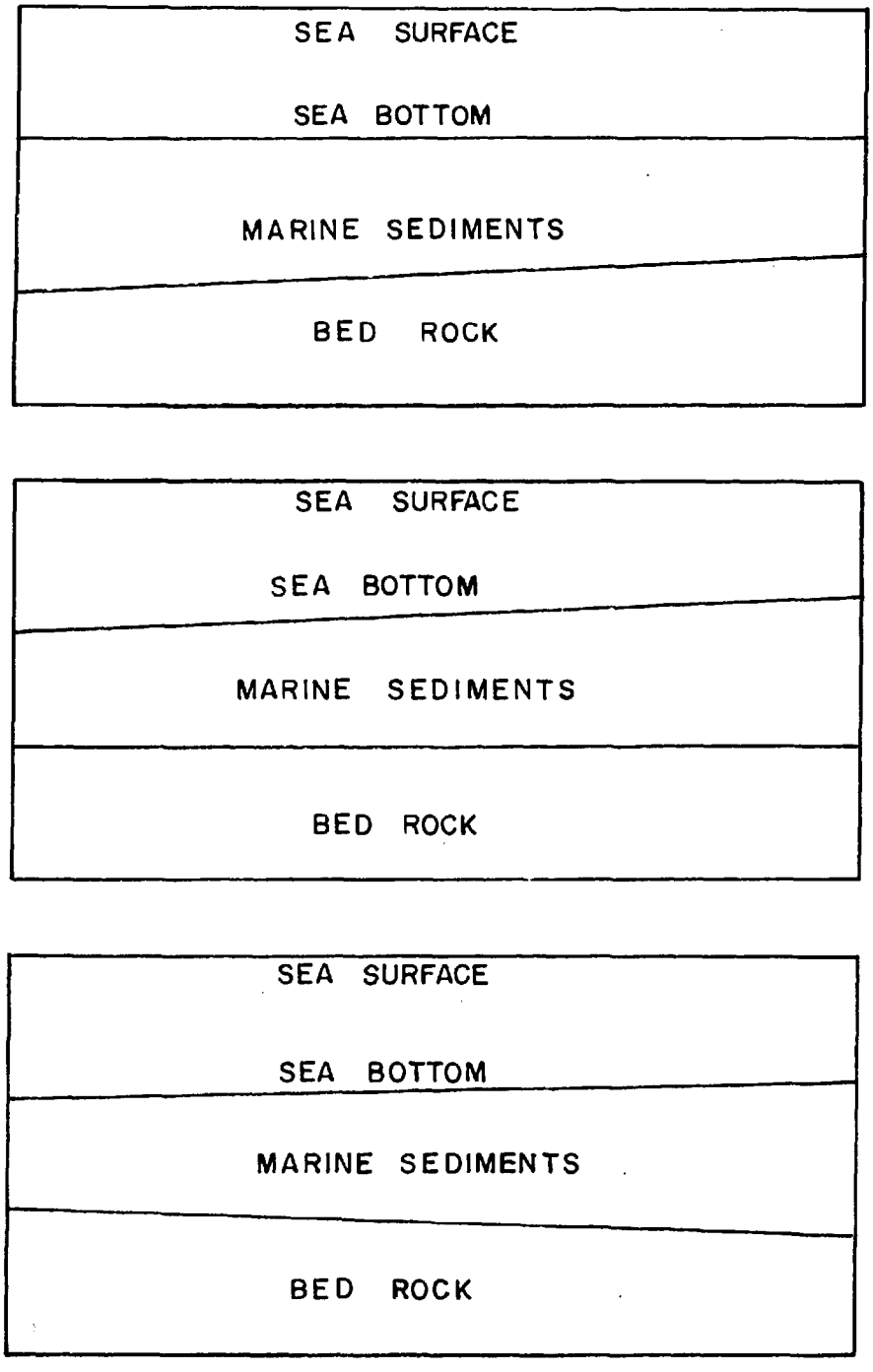

THE SIMPLIFIED MODELS

FIG. 2.4

one can be determined only if the other is known. Due to scattering and other effects at the boundary, when a ray penetrates a reflecting horizon and returns by further reflection, the reflection coefficient must be replaced by the proper combination of reflection and transmission coefficients in an obvious manner. For instance it is found in laboratory measurements that gas bubbles in the sand medium may increase the incoherent scattering by more than 10 dB. Bubbles would be expected also to decrease the reflection loss and to increase the transmission loss. The transmitted part of the ray, after bending due to refraction, goes through a similar process when a second reflecting horizon is penetrated. The number of variables necessary to formulate such coefficients involves a large number of parameters which must be taken into account. The form of this function is seldom known and it is difficult to isolate individual effect. Nevertheless a way of avoiding these difficulties was found and the results yield effective attenuation characteristics, at least comparatively, of marine sediments in situ.

The geometry of reflection from a dipping horizon is shown in an exaggerated form in Fig. 2-5 (a). A correction for migration of dip is usually made for reflection from steeply dipping horizons, but in the present case this correction will be small. Neglecting this effect, the models illustrated in Fig. 2-4 reduced to the simple three layer model shown in Fig. 2-5 (b).

2.7.2. The Working Model and Equations

The following assumptions were made.

(1) The sea water is non-attenuating at the frequencies employed and for the transmission paths at the sites analysed (Fig. 2-1).

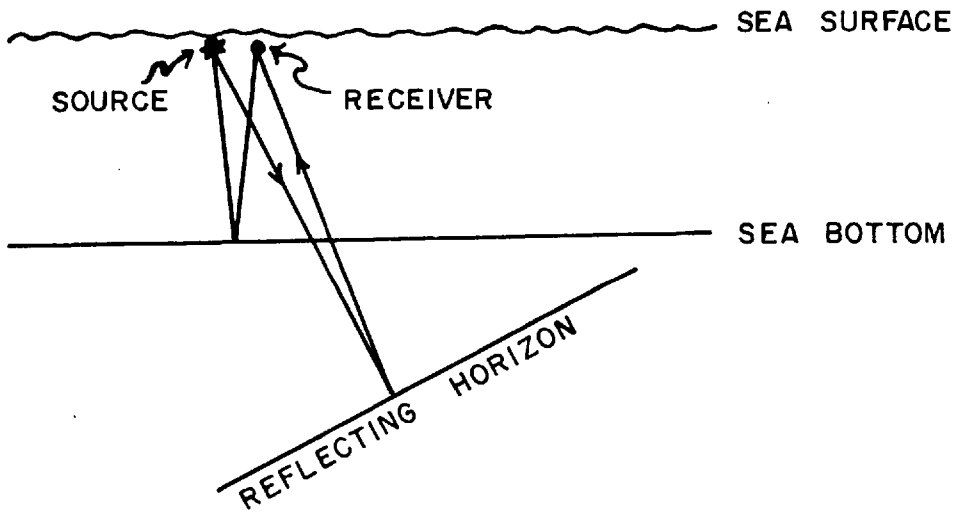

(a)

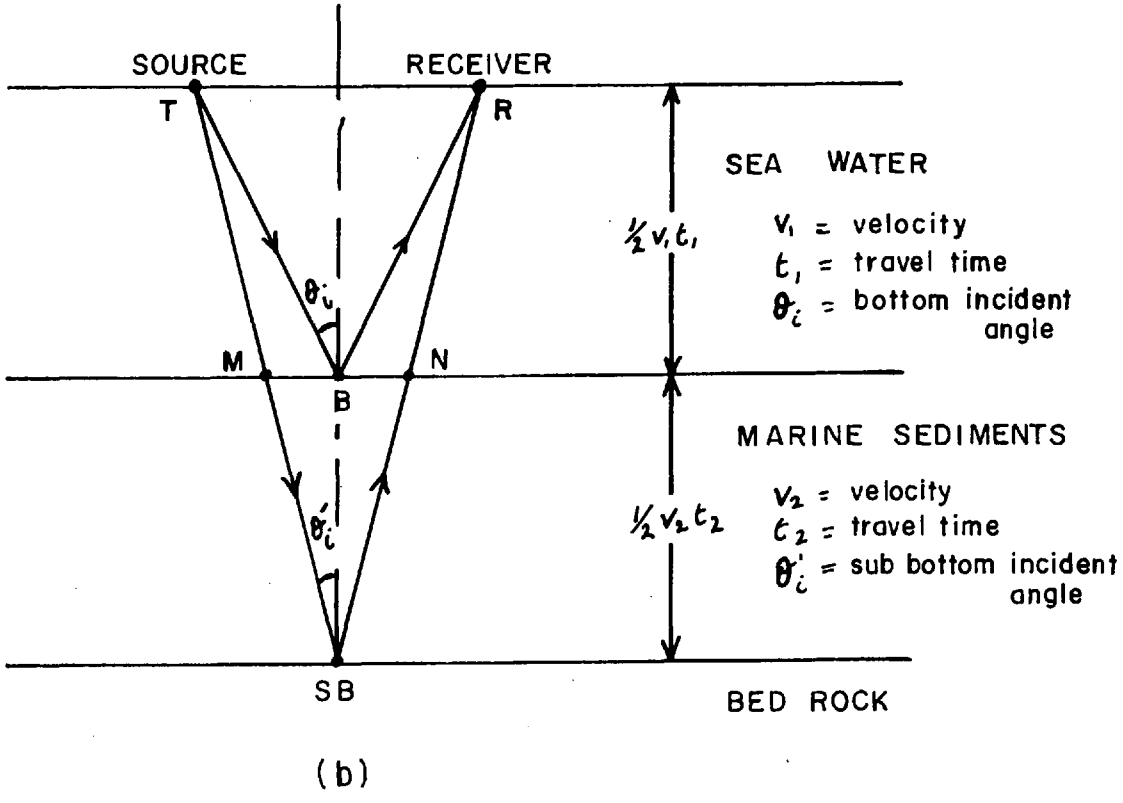

(b)

OBLIQUE AND HORIZONTAL SUB BOTTOM REFLECTIONS

FIG. 2.5

(2) At small incident angles, a boundary reflection is neither angle dependent nor frequency dependent. The results of Becken (Fig. 2-2) indicate such independence up to at least 18° from normal. In the present experiments, this angle was never exceeded even in the shallowest reflection area.

(3) At near normal incidence, path lengths of the bottom and the sub-bottom reflections are treated as incident normally, i.e. TM is assumed equal to TB.

Referring to Fig. 2-5 (b), the equations (2-8) and (2-15) the pressure level of the bottom echo at the receiver, and that of the sub-bottom echo at the receiver for a given frequency, can be related to the source level by

$$E_{bf} = S_f - B - 20 \log_{10} v_1 t_1, \qquad (2\text{-}24)$$

and $$E_{sbf} = S_f - (M + SB + N) - 20 \log_{10}(v_1 t_1 + v_2 t_2) - \alpha_f v_2 t_2, \qquad (2\text{-}25)$$

where E_{bf} = the pressure of bottom reflection in dB,

E_{sbf} = the pressure of sub-bottom reflection in dB,

and S_f = source pressure in dB,

B is the bottom reflection loss in dB,

M = incipient loss at the water/sediment interface in dB,

SB = sub-bottom reflection loss at the sediment/bedrock interface in dB,

N = emergent loss at the sediment/water interface in dB,

and α_f is the effective attenuation coefficient of the sediment.

The values of v_1 and v_2 and t_1 and t_2 are defined in Fig. 2-5 (b).

Assuming that the spectrum analysis, carried out on the pressure amplitude of the returned echos in dB from bottom and sub-bottom reflections is made with reference to an arbitrarily normalized decibel level, equations (2-24) and (2-25) can then be expressed as

$$E_{bf} = S_f - K_1 - 20 \log_{10} (v_1 t_1) \qquad \ldots\ldots\ldots\ldots\ldots\ldots (2 - 26)$$

$$Esbf = S_f - K_2 - 20 \log_{10} (v_1 t_1 + v_2 t_2) - \alpha_f v_2 t_2 \ldots\ldots\ldots (2 - 27)$$

where K_1 and K_2 are related to the losses at the interfaces.

Hence $$E_{bf} - E_{sbf} = K + 20 \log_{10}(v_1 t_1 + v_2 t_2) - 20 \log (v_1 t_1) + \alpha_f v_2 t_2 \ldots\ldots (2 - 28)$$

where $K = K_2 - K_1$

If the velocity of sound in the sediment is known or can be measured the evaluation of $(E_{bf} - E_{sbf})$ as a function of frequency and sediment thickness by spectral analysis of bottom and sub-bottom echos enables ~~particular frequency or spectral range~~ α_f to be computed from equation (2 - 28).

CHAPTER III

SOME MODIFICATIONS AND EXPERIMENTS CARRIED OUT ON A COMMERCIAL SUB-BOTTOM PROFILER

A commercial continuous seismic profiler, the Sparker manufactured by Alpine Geophysical Associates Inc., had been procurred by the Geophysics Department for carrying out work in various marine areas. This equipment was effectively used during an exploratory expedition to the Persian Gulf in 1962 and in the geophysical investigations of Mount's Bay and St. Ives Bay in 1963, work in the latter areas being reported in detail by Marke (1965) and Lee (1966) respectively. The performance of this profiler was found to be satisfactory only in limited situations because of its inherent design characteristics among which are the energy level of the source, the predominant frequency of the source, the directivity of the hydrophone, and the sensitivity of the receiving system. Primary attention was given to these factors in trying to improve this profiler with a view to achieving deeper bottom penetration, better record definition, and greater versatility of the system as a whole. Modifications on the Alpine Sparker were then carried out first in the laboratory and evaluated through a subsequent series of field experiments in Cornwall. The improvements were largely the result of experiments as all of the modifications in the above characteristics did not consistently produce improved results. However, some useful knowledge and experience obtained during this period contributed substantially to the design and the eventual development of a much improved new system, the more powerful and complex record/reproduce sub-bottom profiler eminently suitable for continental shelf and slope investigations as well as for carrying out the acoustic analysis approach in the identification of marine sediments.

3. 1. The Description of the Alpine Continuous Seismic Profiler

The equipment consists of a receiving and recording unit and a source unit. It is a dual channel system for Sparker and Gas Exploder operation. The receiving and recording system consists of one or two magnetostrictive hydrophones attached to a cable approximately 200 ft. long towed astern of the survey vessel, two preamplifiers, two variable bandpass filters, two signal amplifiers, a control chassis, and two recording sections on a single drum. A block diagram of the recording set-up is shown in Fig. 3-1. The dual channel system offers various possible recording schemes. The one that is actually used will, of course, depend on the particular survey problem and the information that is desired.

3. 1. 1. The Source

Sound is transmitted from the source on a regular or timed schedule controlled by triggering contacts within the recorder. In the Sparker the sound pulse is generated in this particular model by discharging a capacitor bank, with a potential difference variable up to 12, 000 volts, in an underwater spark. The source energy is about equivalent to a small blasting cap fired underwater. In the gas exploder a mixture of oxygen and propane is ignited in a combustion chamber. This source should have a much higher energy than the sparker, and a lower frequency range. The two sources might be used to supplement each other, the sparker giving good resolution at shallow depths, while the gas exploder permitting greater penetration. However, actual experience by several workers with the gas exploder part of this Alpine equipment proved to be disappointingly unsuccessful. Due possibly to some constructional fault existing in the ignition chamber there appeared to be a continuous burning of the gas mixture, rendering any sustained profiling work impossible and the records thus obtained,

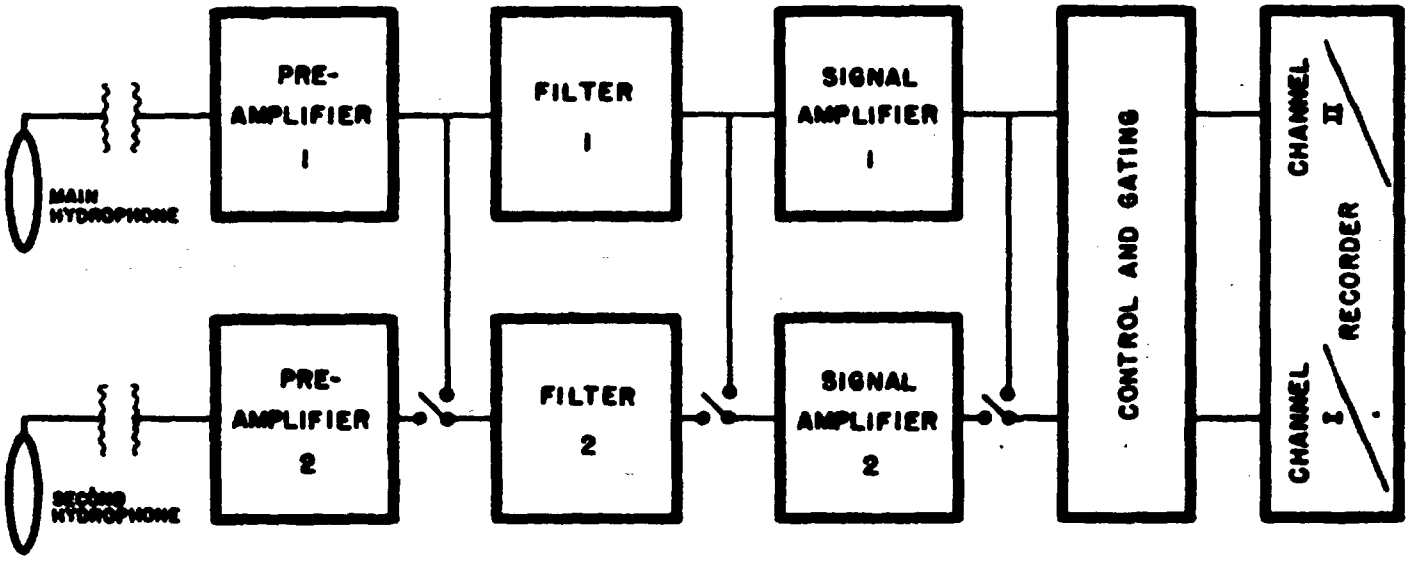

Fig. 3.1. DUAL CHANNEL SPARKER RECEIVING AND RECORDING SYSTEM

uninterpretable. Owing to all the fruitless tests and field results the gas exploder part of the system will not be further discussed.

Fig. 3-2 is a diagram of the spark trigger source and power source. The potential for the underwater spark is stored in two 1 mfd 15, 000 volts condensers connected in parallel. The energy is passed to the water spark electrode by an air gap switch designed to conduct when the gap is ionized by a small trigger spark. The trigger is a high voltage low power spark such as used in automotive ignition. The trigger gap of the air gap switch is formed between the water earth side of the air switch and a small pointed "tickler" electrode. The small amount of ignition from the tickler spark provides sufficient breakdown in the air gap to pass the main potential. The water spark electrode is connected to the end of the central conductor of a long length (approximately 250 ft. including the inboard part) of coaxial cable which leads from the other side of the circuit at the condensers. A second length of cable is used to connect the air gap switch to the water earth electrode. Basically the water spark electrode is a piece of insulation material such as polythylene with the 1/8 in. diameter central electrode showing at the end flush with the insulation or protruding 1/16 - 3/16 in. The water earth electrode can exist in the form of a copper ring around the insulation, or just a piece of copper strap or shielding braid.

3.1.2. The Hydrophone

The detector in the water is a magnetostriction hydrophone. The hydrophone cable is a two-conductor shielded cable of small diameter with sufficient strength to tow the hydrophone. The cable is floated with oval fish-net floats except at its far end where the hydrophone is weighted and towed at a depth of from five to ten feet beneath the surface.

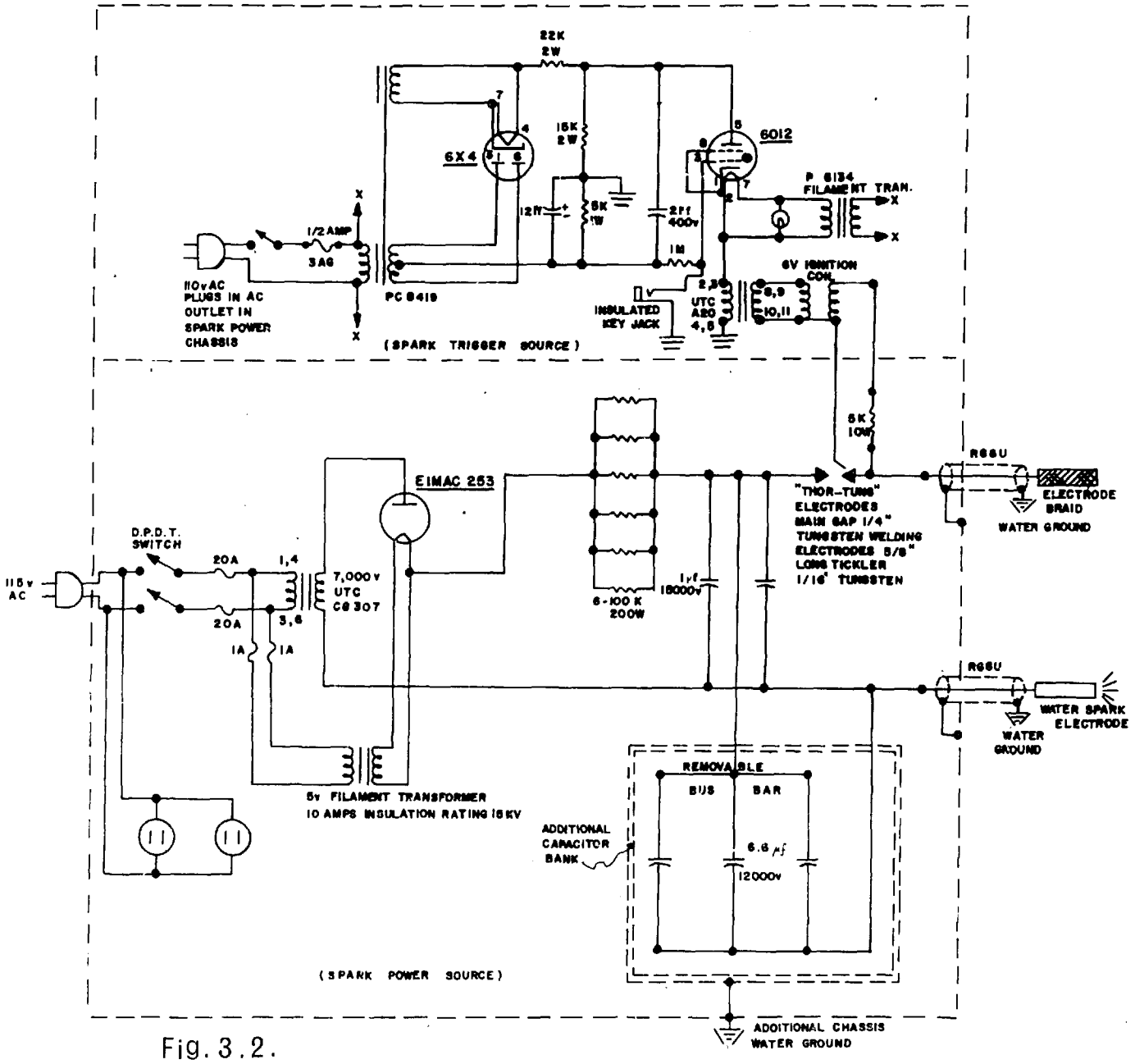

Fig. 3.2.

DIAGRAM OF SPARK TRIGGER SOURCE AND SPARK POWER SOURCE

3.1.3. Various Signal Conditioners

The preamplifier is a two stage, fixed gain amplifier with flat frequency response from 20 cps to 10, 000 cps. The filter is a variable band-pass filter which can be set at any band-pass from 0 to 9,600 cps.

The signal amplifier raises the output from the filter to an appropriate level for recording and contains all the amplifier controls for the signal. These include an input attenuator and an interstage attenuator to control the gain of the signal. There is also an output limit control which provides a bias cutoff for signals above a certain level, and is used to prevent arcing on the recorder paper from a particulary strong signal, such as the initial pulse or the bottom reflection in very shallow water. In addition there is a compression switch which is generally left off but when switched on, imposes on the signal an automatic gain control. The final control on the amplifier is the rectifier switch, a two position switch, one for full-wave retification and the other for half-wave rectification.

3.1.4. The Recorder

The recorder is an Alden dual-channel facsimile recorder. The equipment consists of a recorder drum with two helical wires attached to the drum in a 370^{o} arc. The helix wire forms one of the electrical contacts of the recorder. The other contact is a knife blade located above the paper. When a current is passed from the helix wire to the knife blade, it makes a mark on damp electro-sensitive paper. The amount of discolouration on the paper is proportional to the strength of the electrical signal passed from the helix wire to the helix blade. About 20 dB of shading can be observed on the record. For the horizontal movement of the paper there is a paper transport system with a gear train which moves the recorder paper past the knife blade at a constant rate.

Before the output signal from the amplifier goes to the recorder itself, it passes through a fairly complicated gating system. This system is incorporated in the control chassis and in the commutator sections of the recorder. The program control determines whether a spark is initiated for every 1, 2, 3 or 4 revolutions of the helix drum and also whether the signals from the amplifier are recorded during any one of these revolutions. The phase control determines in which cycle of drum revolutions after the spark has been initiated, that a record will be made. For instance, on a programme setting of 1 : 2, which means to pulse every second revolution of the drum, there is a choice of recording either on the same revolution that the pulse was initiated or on the following revolution. For a phase setting of 1 a recording would be made on the same revolution that the spark was initiated. There is also a four position sweep time switch which controls the revolution period of the recorder drum, to either 1/16, 1/8, 1/4 or 1/2 seconds. A photograph of the Alpine profiling equipment installed inside the cabin of a survey boat is shown in Fig. 3-3, (a) being the receiving system mounted on top of the recorder (b), while the source unit including the trigger unit is indicated by (c).

3.2. Methods of Improving the Spark Source

The acoustic level, the pulse length, and the pulse shape, or frequency content, of the source are the governing factors for obtaining penetration and resolution in a seismic record. The pulse length, being in the time domain, occupies a definite portion of the record along the time axis and hence gives a limitation to the resolution of various events though signal processing methods can be employed to improve it. The pulse shape, or frequency content of the source has effects on both the penetration and resolution as attenuation versus frequency and noise spectrum etc. have to be taken into account.

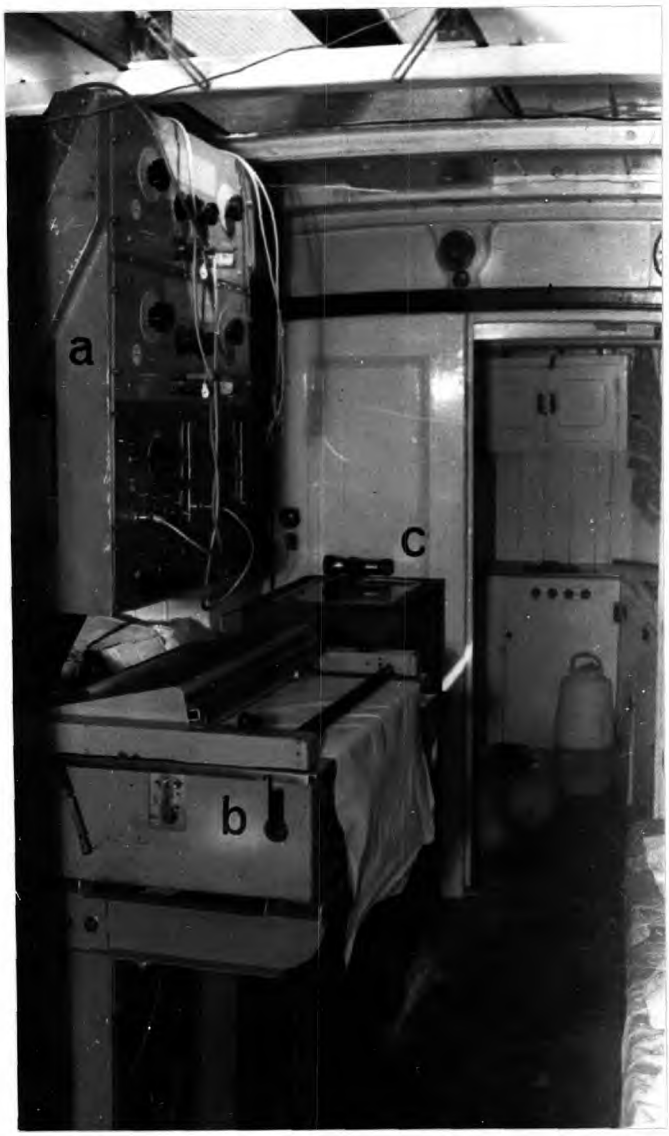

Fig. 3.3. The Alpine Continous Seismic Profiler installed on board a survey boat.

For the Alpine Sparker system, an underwater spark is used as the seismic source; its pulse is essentially constant in its character providing no versatility of the spark source. Along with the modification in giving extra energy to the existing system, a versatile spark source was also developed and tried out on an experimental basis. Results obtained indicate that it is feasible to adapt an adjustable gap spark electrode for field geophysical applications.

3.2.1. The Increase of Source Energy.

The total source energy is, though not necessarily solely, the paramount factor in obtaining greater penetration in any seismic system. This is obvious because the reflected and refracted signal strength is determined largely by the available source energy. In order to increase the penetration range of the existing Alpine sparker, primary consideration was given to increasing the energy of the source.

An extra capacitor bank was connected in parallel with the original 2 mfd condensers, drawing charging current from the same rectified high voltage supply. The capacitors used to form this extra bank consisted of 3 paper dielectric 6.6 mfd capacitors manufactured by the Telegraph Condenser Co. Ltd., designed with a 12 KV discharge rating to sustain one discharge per second plus 25% overswing. A bank of these capacitors connected in parallel, each contained in a rectangular steel case fitted with two insulated terminals, provided 1,000 joules at 10 KV. A special steel cabinet was built to house this extra capacitor bank with a front panel safety latch installed so that a linked leverage would place a shorting bar across the terminals of the condenser should the front panel be opened, a system used in the original Alpine equipment. A circuit diagram of this modified source can be seen in Fig. 3-2 where the extra capacitor bank is shown inside the double-dashed line block.

Combinations of these capacitors were achieved by detachable busbars so that 1/3, 2/3 or full capacity of this extra bank could be selected. An actual photograph of this unit is shown in Fig. 3-4.

3.2.2. Some Considerations on the Essential Characteristics of the Underwater Spark Discharge.

Capacitor discharges are determined by the resistance (R), inductance (L), and capacitance (C) of the discharge circuit. The discharge is either underdamped, overdamped, or critically damped depending on whether R is greater, less or equal to $2\sqrt{\frac{L}{C}}$.

In the case of a critically damped circuit, the voltage decays practically exponentially from its peak value. Because of the exact nature of the resistance, critical damping seldom occurs in practice, and most circuits are either over-damped or underdamped.

In the case of an over-damped circuit, R is greater than $2\sqrt{\frac{L}{C}}$. The voltage decays continuously similar to that in a critically-damped circuit, but that the peak current is reduced and the time of decay is increased.

In the case of under-damped circuits, R is smaller than Rc, the critical damping resistance. Voltage and current reversals occur resulting in an oscillation of frequency depending mostly on the total circuit inductance and capacitance. The oscillations diminish only as a function of the total circuit resistance.

The storage capacitors, the air gap or in some cases ignitron switching systems, transmission line, electrodes and spark can be represented by a simplified equivalent RCL series circuit for which the general equations are known. The current may be oscillatory, critically damped, or over-damped depending on the circuit constants.

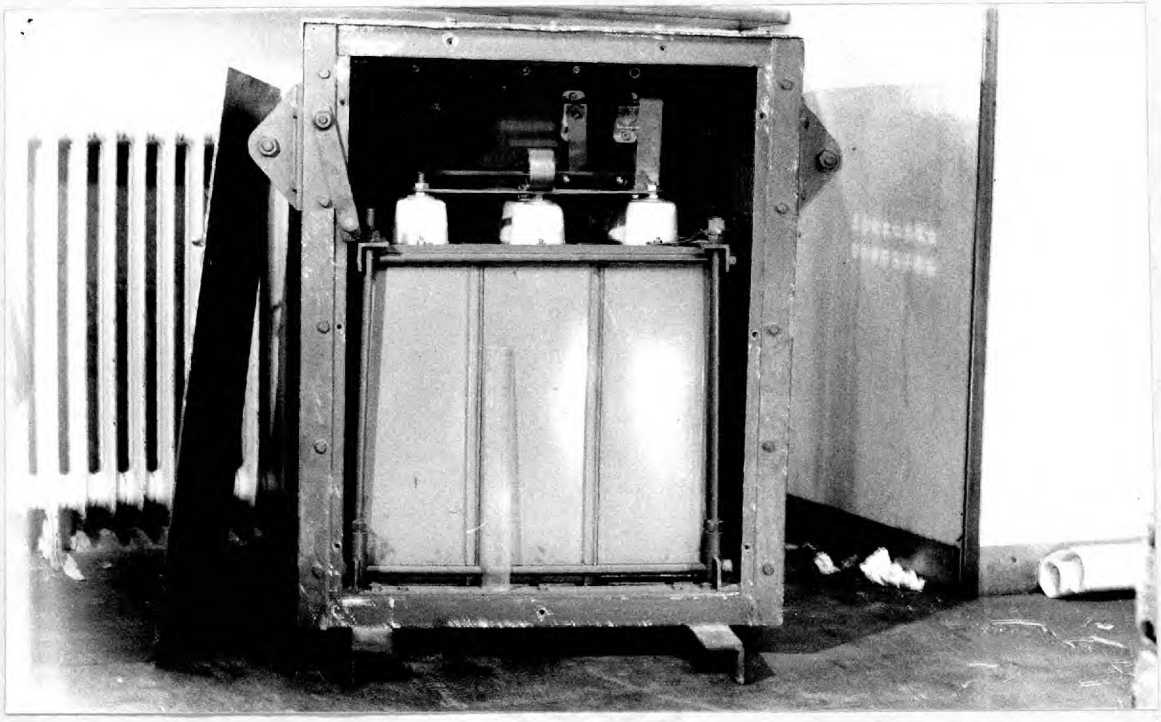

Fig. 3.4. The extra 1,000 joule capacitor bank.

With these simplified assumptions, the capacitance is largely controlled by the storage capacitors, and the inductance by the transmission line, thus remaining fairly constant. The internal resistance of the ignition switch may be neglected in comparison with the resistance of the rest of the system while the spark plays a most important role in determining the total resistance in the series circuit.

Caulfield (1962) made some measurements of the acoustic pressure of a spark discharge at a shallow depth (10 ft.) for various voltages and for various electrode surface areas, and found that the peak acoustic pressure observed was proportional to the peak current. Among his experimental results, there is, however, a very debatable point about the effect of the polarity of the discharge electrode on the acoustic output in peak pressure and energy. He states that the peak pressure in the water and the energy transfer are larger, the increase being by a factor of 2, with the spark electrode positive, attributing that this is due to hydrogen formation at the central electrode. This may well be an erroneous result both in phenomenon and reasoning as compared to the theoretical and experimental findings from the present research. It can be proved that electrolysis plays only a very limited part except in creating resistance in the underwater spark gap and larger transfer of energy occurs, contrary to his conclusion, with the spark electrode negative.

When conventional dynamite for seismic investigations is detonated underwater the detonation wave propagates through it and is converted to gas at a high pressure. A spherically symmetrical shock wave is radiated into the water. The pressure rise in the shock wave is practically instantaneous, and is followed by a decay which is initially exponential with a time constant typically a fraction of a millisecond. By the time the gas bubble has expanded to its maximum radius the gas pressure has

become slightly negative relative to the hydrostatic pressure. Thus the bubble overshoots its equilibrium radius and then contracts and thus undergoes a damped radial oscillation. The bubble pulse has an impulse comparable with that of the shock wave. Similarly a powerful electric underwater spark also produces a single intense pressure pulse. A bubble pulse also occurs as in the case of explosives, and is related to the amount of energy in the initial disturbance. The pressure effects are possibly due to the large fluctuations of temperature and density of the medium in the path of the spark, the corresponding expansions and rarefractions spread as spherical sound waves which may be sonic or ultrasonic according to the frequency of the electrical oscillation in the spark discharge, as well as the oscillation of the bubble or bubbles created. In other respects the spark bubble pulses deviate from those of explosives, because there are no residual foreign gases.

The actual phenomenon of an underwater spark is undoubtedly very complex. However, some basic considerations can be given to the contributions from the gas and vapour derived from electrolysis and that due to heating in the formation of the bubble. Examples are presented in a simplified manner to demonstrate these effects.

According to Faraday's laws of electrolysis, for any given substance, the mass liberated, removed, or deposited at an electrode is proportional to the quantity of electricity which passes, and the mass of any substance liberated, removed, or deposited by a given quantity of electricity is proportional to the electro-chemical equivalent of the substance.

This can be expressed as

$$w \propto Q \quad \text{or} \quad w = ZQ$$

where w = mass of substance electrolysed in grams

Q = quantity of electricity which passes in coulombs

Z = a constant = the electro-chemical equivalent

The electro-chemical equivalent of hydrogen, i.e. the mass liberated when 1 coulomb passes is 1.04×10^{-5} grams, hence that of water is approximately $(1 + 8) \times 1.04 \times 10^{-5}$ because of the bivalent oxygen contained in the H_2O molecule. Therefore, for 1 coulomb of electricity passing through the sea water electrolyte, the total amount of hydrogen and oxygen liberated is equal to $9 \times 1.04 \times 10^{-5} = 9.36 \times 10^{-5}$ grams.

For the improved source of the Alpine profiling system, the following results were calculated for the dissipation due to electrolysis when other effects in the discharging circuit are ignored:

Energy available = $\frac{1}{2}CV^2 = \frac{1}{2} \times 22 \times 10^{-6} \times (10 \times 10^3)^2 = 1,100$ joules.

Electrical charge stored, $Q = CV = 22 \times 10^{-6} \times 10^3 = 0.022$ coulombs.

Weight of water electrolysed = $Q \times 9 \times Z = 0.022 \times 9.36 \times 10^{-5} =$ 2.06×10^{-6} grams.

To produce 1 gram of water by burning H_2 in 0 liberates 3,800 cals., or $3.8 \times 10^3 \times 4.18 \times 10^7$ ergs $= 15.8 \times 10^3$ joules, where 1 cal. $= 4.18 \times 10^7$ ergs (mechanical equivalent of heat).

The energy required for electrolysis in the spark discharge $= 15.8 \times 10^3 \times 2.06 \times 10^{-6} = 32.5 \times 10^{-3} = 0.0325$ joules.

The percentage of energy used up in the spark of electrolysis is therefore $(0.0325/1,100) \times 100 = 0.003\%$.

For another system developed later with a capacitive bank of 160 mfd when charged up to 4 KV:

Energy available = $\frac{1}{2} CV^2 = \frac{1}{2} \times 160 \times 10^{-6} \times (4 \times 10^3)^2 = 1,280$ joules.

Electrical charge stored = $CV = 160 \times 10^{-6} \times 4 \times 10^3 = 0.64$ coulombs.

Weight of water electrolysed = $Q \times 9 \times Z = 0.64 \times 9 \times 1.04 \times 10^{-5}$ grams = 6×10^{-5} grams.

The energy required for electrolysis thus found in the spark discharge is equal to 0.95 joules, being 0.07% of the total.

Assuming the spark phenomenon occurs at approximately atmospheric pressure, the volume of the bubble produced for a passage of 1 coulomb can be computed as follows:

The density of H_2 at N. T. P. is 9.06×10^{-5} grams/c.c.

Volume of hydrogen and oxygen liberated by 1 coulomb at N. T. P. = $1\frac{1}{2}$ volume of $H_2 = 1\frac{1}{2} \times \frac{1.04 \times 10^{-5}}{9.06 \times 10^{-5}} = 1.72$ c.c.

The volumes of the gas produced due to electrolysis in the spark discharge in the above cited two examples are therefore respectively equal to:

(i) $2.2 \times 10^{-2} \times 1.72 = 0.038$ c.c.

(ii) $64 \times 10^{-2} \times 1.72 = 1.1$ c.c.

These figures of the volume of the gas, even under the simplified assumption of being at atmospheric pressure, certainly look incredibly small although heating might play a small role in expanding them but the extent of which must be a very limited one. There is, therefore, very good reason to believe that the heat generated due to the resistance of the water and of polarization in the path of the high density current, which in turn converts the surrounding water into steam vapour plays the all dominant part in the formation of underwater spark bubbles.

Suppose that all the resistance in the discharge circuit is in the underwater spark, then all the heat dissipated in the spark from a 1,000 joule system will be in the form of $I^2 R_s t$, I being the average discharge current and R_s the average resistance of the spark during the brief discharge period of t. For 1,000 joules, the heat available is $\frac{10^3}{4.18} =$ 240 cals. To turn 1 gram of water at 0° C to 100° C steam at atmospheric pressure, 100 cals + 540 cals = 640 cals are needed. Hence the 240 cals.

of heat from the 1,000-joule source can turn 0.375 grams of water at 0° C into 100° C vapour at atmospheric pressure, occupying a volume of $\frac{0.375}{0.6 \times 10^{-3}} = 6.25$ c.c., where 0.6×10^{-3} is the density of water vapour at 100° C under atmospheric pressure in grams/c.c. Neglecting the effect of hydrostatic pressure, an underwater bubble thus formed has a diameter of approximately 10.6 cm. or 4.17 in. A single bubble with diameter of this order was actually visually observed when the Alpine 1,100 joule source was discharged in an underwater spark at a depth of about 2 ft. below the water surface during field tests conducted in Cornwall.

In the Alpine sparker, the spark electrode is arranged in such a way that the discharging electrode (the inner central electrode) is connected to the negative side of the capacitors. During a laboratory experiment with simulated sea water contained in a transparent tank, the original 2 mfd storage capacitors charged to various voltages were used to observe the spark discharge. The polarity of the spark electrodes was also reversed to compare sparking from negative and positive discharge. For a negative electrode discharge, a distinct underwater spark explosion commenced when the capacitors' voltage was charged to 2.8 KV. While for the same voltage with a positive electrode discharge a barely visible glow was observed at the inner electrode, with practically no explosion at all. Further acoustic measurements were made using various types of electrodes, including a specially developed adjustable-gap system and as pressure transducer a small barium-titanate crystal disk placed some 3 ft. distant. With applied voltages to the condensers varying from 4 KV to 12 KV, 9 sets of data were obtained from the output of the detector in the form of oscilloscopic photographs. Each set of data consisted of five peak-pressure amplitude recordings of the positive spark using arbitrary amplitude units which were

then compared under the same conditions with those of the negative spark. The five ratios of the negative to the positive spark pressure amplitudes were averaged to obtain 9 ratios which varied from 1 to 3.5 giving an average ratio of 2.2. These experiments, carried out with Maranzana (1966), indicate that the peak pressure in the water, and hence the energy transfer, is larger with the spark electrode negative, in contradiction to Caulfield (1962). Contrary to Caulfield's reasoning, with the spark electrode negative, since double the amount of hydrogen is liberated by electrolysis than of oxygen when the spark electrode is positive the hydrogen will initially cover, possibly in the form of a thin film, the exposed area of the inner electrode, thus creating a larger resistance due to polarization, increasing the heat generating function or energy transfer of the underwater spark as a whole.

3.2.3. The Development of New Electrodes

For a larger capacitor bank providing up to 1,100 joules per discharge, the construction of larger electrodes was necessary. In fact, one of the original Alpine electrodes was subjected to a 1,100 joule discharge test and was instantly destroyed by the excessive arcing and the explosive force. Proportionately larger electrodes, designed more on an experimental than a theoretical basis, were constructed. Tungsten steel rods $\frac{1}{4}$ in. diameter were used for the inner discharging electrodes with outer copper rings of 1.5 in. and 2 in. diameter respectively for sea water earthing. The insulating material between these used finally was canvas base tufnol with both the inner rod and outer sheathing ring protruding about 1/8 in. These electrodes were found to be satisfactory during tests. It was found that the electrode with the larger earthing ring appeared to give more energetic sparks. The larger open type electrode was subsequently used throughout most of the field work. At the same time an adjustable-gap

2 in. outer diameter electrode was designed and built. In Fig. 3-5 (a), on the left is the original 100 joule Alpine electrode, the middle two electrodes are the open type with 1.5 in. and 2 in. outer diameters respectively and on the right is the adjustable-gap electrode specially developed for experiments on source versatility. Above these four electrodes is shown a standard electrode holder which terminates the power transmission line and which contains a brass adaptor with a rubber "0" ring inside the polythene housing which in turn can be screwed on to the individual electrodes, making the connection water-tight.

Roi and Frolov (1958) have performed laboratory model tank experiments to measure the acoustic pressure waves generated by an electric spark discharge in water. By varying the length of the spark gap in addition to changing the capacitance and voltage of the capacitor bank, they found that the transfer of energy from an electrical form into an acoustical one occurs most effectively in the case of long-spark discharges, where the electro-acoustic efficiency can amount to 30%. Based on the concept of these findings, it was decided that it would be worth while to design and construct a rugged adjustable-gap electrode of appropriate size for field experiments. It was believed that a change in gap length would produce an associated change in the characteristics of the acoustic pulse, because the arcing phenomenon, the effective resistance in particular of the spark, and the size of the bubble created are bound to undergo some changes with varying spark gap length in the conducting sea water.

The adjustable-gap electrode (Fig. 3-5 (b)) was designed using the basic dimensions of the 2 in. outer diameter open type electrode. The sea-earthing sheathing copper ring was extended another $1\frac{3}{4}$ in. enclosing a cylindrical brass section at the other end with a central hole to hold a second $\frac{1}{4}$ in. tungsten steel rod which could in turn be fixed

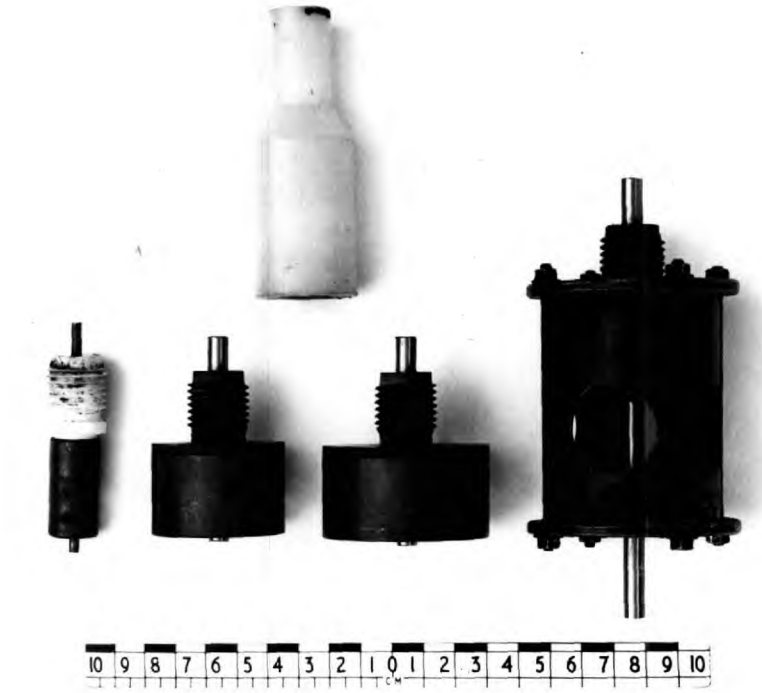

a

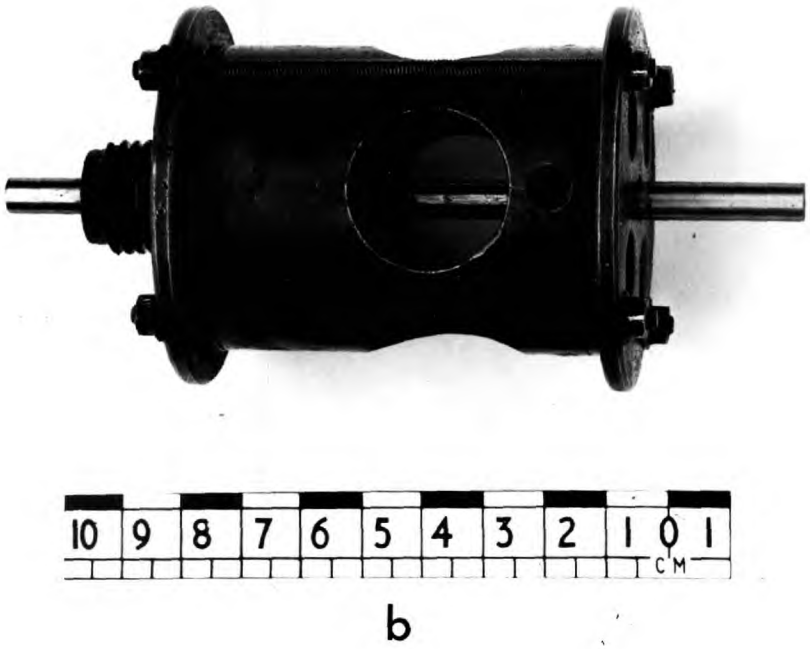

b

Fig. 3.5. The various spark electrodes.

rigidly by two side screws 90° apart, thus making the gap width between the two opposite electrodes adjustable. In the middle portion of the sheathing four 1 in. diameter side holes were drilled to facilitate the propagation of the acoustic pressure. Another four ½ in. diameter holes were also drilled in the end block of the adjustable rod for the same purpose. Two end plates clamped by four threaded rods were used to reinforce the spark chamber against the explosive force of the spark. It was expected that the confined space with limited outlets would restrict the acoustic output of the spark formed between the gap. However, the rugged construction was primarily designed in an initial attempt to establish some working characteristics of a device for continuous field use.

3.2.4. Results of Field Tests

3.2.4.1. The Increased Energy Source

Field tests of the Alpine equipment with the added storage capacitors for increasing the source energy were conducted in St. Ives Bay, Cornwall, using the larger open type electrode. Trial tracks were run mostly inside St. Ives Bay where water depth seldom exceeds 80ft. and where the bottom geology primarily consists of patches of sand over "killas" or granite bedrock. The shallow water region extends a great distance both seaward and towards and beyond Land's End. Records obtained with 2/3 of the increased source energy in one traverse near the "Island" at the southern end of the Bay revealed unconsolidate material, probably coarse sand, forming pockets up to more than 60 ft. in thickness. However, a comparison of the present records with those of other workers in the area failed to show the increased penetration which should have resulted from the greater power. The difference in acoustic impedance between the "killas" and the granites in the area might well be too small to produce any appreciable interface reflection observable on the records, should these

boundaries indeed exist. Marke (1965) has claimed that they do from his interpretation of sparker records using 100 joule source. It must be pointed out that the lengthening of the acoustic pulses due to the increased source energy would tend to lessen clarity and resolution of any reflected events on a small scale record. Furthermore the masking effect due to strong reverberation in this shallow region would add more uncertainty to the interpretation of the record. Thus the test results obtained with the increased source were not considered satisfactory.

Among the drawbacks in using the Alpine system with the 1,100 joule source was the fact that the firing rate was necessarily reduced to allow the charging current sufficient time to charge the condensers fully before each transmission commenced. The Alpine power source has a high voltage single-phase half-wave rectifier which can deliver at most 0.3A. It should be noted that the efficiency of retification of such a circuit is only 40 per cent. This efficiency is defined as the ratio of the d.c. output power to the plate circuit power (Millman, 1958). Actually, the overall efficiency of the system, which is obtained by considering the power supplied to the entire system, is considerably less than this. In addition, the ripple voltage exceeds the d.c. output voltage. The single-phase half-wave rectifier is therefore a relatively poor device for converting alternating into direct current. In the present application a fast firing rate with the high energy discharge was impossible to achieve. For the Alpine system, the slowest transmission rate is once every two seconds using a programme setting of 1 : 4 with the maximum sweep rate of $\frac{1}{2}$ second. At this 2-second transmission rate, when only 2/3 of the extra capacitance bank was connected, the capacitors could be charged up to the full voltage of 10 KV while approximately 3 seconds was required for charging up the full bank. Consequently, only

1/3 or 2/3 of the extra capacitance bank was connected during all the survey trials. At the 2-second transmission setting, record presentation suffered additional adverse effects due to both the scale contraction and the slow paper-feed motion which in turn caused some degree of the drying-out of the electro-sensitive paper, resulting in poor signal marking.

3.2.4.2. The Adjustable-gap Spark Electrode

Experiments attempting to find out the electrical and acoustical features as well as the field applicability of the adjustable-gap spark electrode were also carried out at sea around north-western Cornwall in conjunction with other instrumental trials on the modifications of the Alpine equipment. Investigations on the electrical and acoustical aspects of the adjustable-gap spark were conducted on board the fishing boat "Cape Cornwall" while anchored in the shallow St. Ives Bay. Oscilloscope photographs were taken to record the results. In this field environment, there was difficulty in isolating the direct pulse from various interface reflections. However, the experimental results obtained can still be regarded as qualitatively valid. A quantitative analysis of the acoustic characteristics of spark pulses produced with varying electrode gap-width is given in Chapter VII.

In Fig. 3-6 (a), (b), (c) and (d) are shown the dual beam oscilloscope photographs indicating some transient phenomena in the discharge circuit when the adjustable-gap spark electrode was used. All the upper traces indicate the discharging voltages tapped from a small capacitance chain across the terminals of the main condensers while the lower traces give those tapped from a high resistance chain across the power ends of the two transmission lines. The total length of each trace is 1 millisec., or 0.1 millisec. per graticule division. The vertical scale values were suitably but arbitrarily chosen so that direct comparison between them could be

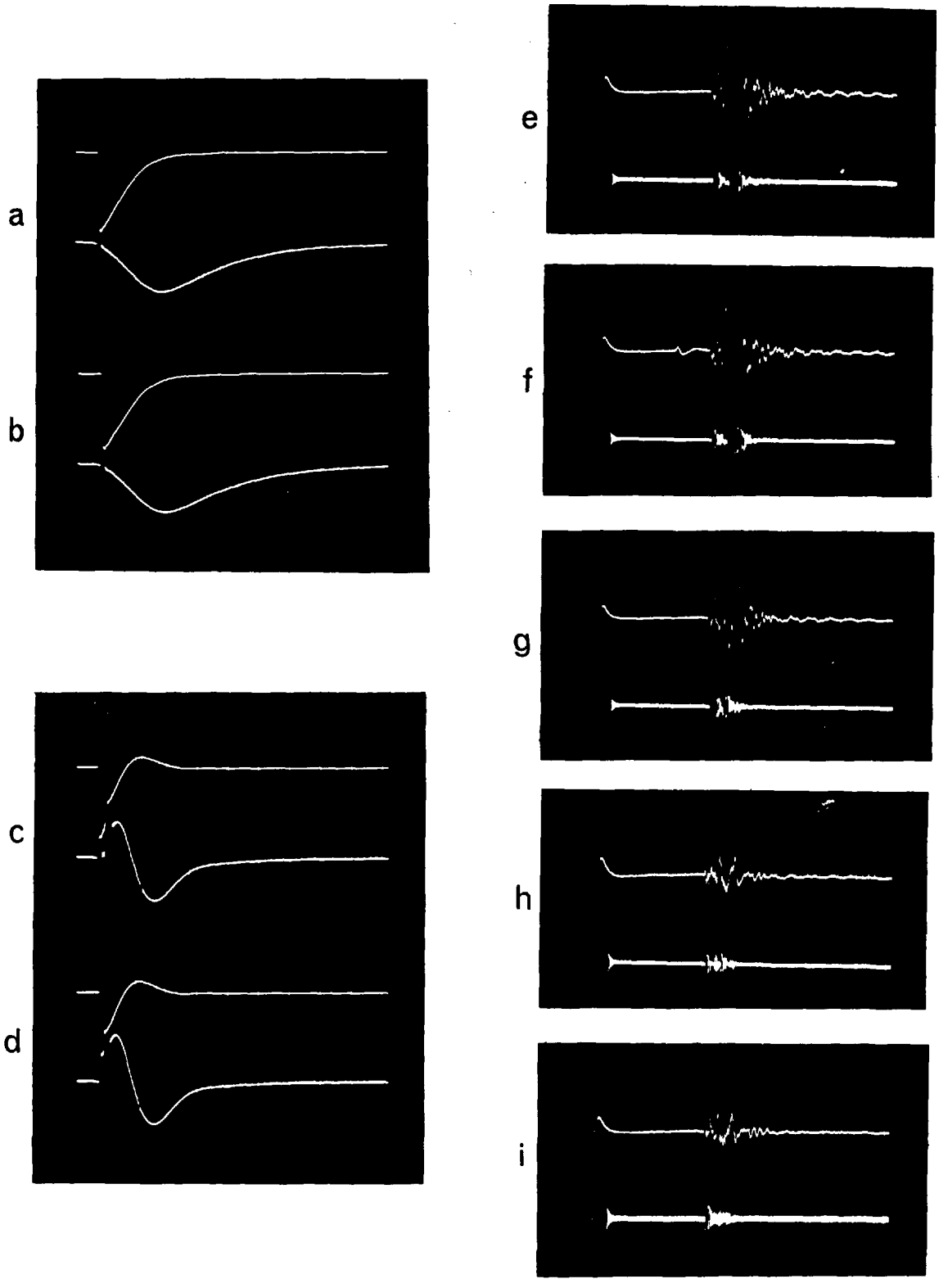

Fig. 3.6. The electrical and acoustical characteristics of the adjustable-gap spark.

made. The gap-width settings of the electrode were $\frac{3}{4}$ in., $\frac{1}{2}$ in., $\frac{1}{4}$ in. and 1/8 in. corresponding to (a), (b), (c) and (d) respectively. It can be seen that both the tapped signals begin to oscillate when the electrode gap-width was narrowed down to $\frac{1}{4}$ in. The magnitude of the voltage reversal increased slightly as the gap-width was further shortened to 1/8 in. This would seem to be a further proof that the resistance of the spark is the dominant resistance in the RCL series discharge circuit. One thing difficult to explain in (c) and (d) is the phase difference between the lower and upper traces; the former appears to lag behind the latter. As the measurements made involved a circuit of high voltage and large current and the technique employed on board was relatively crude, the results presented here may well involve some electromagnetic pickup masking the true shapes of the voltage or current during the discharge. However, this should in no way invalidate the evidence of the oscillatory nature of a narrow gap spark discharge.

Fig. 3-6 (e), (f), (g), (h) and (i) show the acoustic patterns detected by two types of hydrophones, the upper traces were recorded by the 10-element array hydrophone which had very poor definition while the lower traces were detected by the Alpine magnetrostrictive hydrophone. The distance between the adjustable-gap source and the receivers was some 150 ft. each division on the horizontal scale being 10 millisec. The gap-width settings for the spark were 1 in., $\frac{1}{2}$ in., 3/8 in., $\frac{1}{4}$ in. and 1/8 in. corresponding to (e), (f), (g), (h) and (i) respectively. It can be seen that the peak acoustic pressure decreases with decreasing spark gap-width, indicating a decreasing ratio of electro-mechanical energy transfer. A second pressure peak immediately following the first peak can also be seen in all the lower traces. These are believed to be due to the associated bubble pulses. It is of interest to note that at the 1/8 in. gap setting (i), the

much diminished bubble pulse can be only just recognised. This is in agreement with the small spark resistance and the oscillatory nature of the underwater discharge.

The Field survey test record shown in Fig. 3-7 (a) was obtained with the use of the open type electrode and the record, Fig. 3-7 (b) was obtained with the adjustable-gap type set at 1/8 in. gap-width. This test was conducted on a short track between Land's End and Seven Stones Lightship over a water depth averaging 220 ft. each profile representing a distance of 2/3 of a nautical mile. First bottom multiples are obvious in both profiles though no distinct sub-bottom structures are indicated. The energy discharge into the spark circuit in each case was the original Alpine 100 joules plus 2/3 of the added bank, totalling approximately 800 joules. The filter band-pass (150-600 cps) and gain settings were made identical for both recordings. A difference can be noted in the predominant frequency content by comparing the resolution of the water/bottom interface and the ringing pattern in the two records; Fig. 3-7 (b) being the better of the two. However, Fig. 3-7 (a), on the basis of record intensity, indicates that the effective energy transfer is greater for the open type electrode.

From these experimental results, it appeared that there was sufficient qualitative information to indicate the feasibility of adapting an adjustable-gap spark electrode to a sparker profiling system to provide source versatility.

3.3. Methods of Improving the Hydrophone

3.3.1. Some Considerations on Receiving Hydrophones

Piezoelectricity, magnetrostriction and electrostriction are the most widely used phenomena in underwater acoustic transducers. Based on these, hydrophones are built to convert acoustic energy into electrical energy, and vice versa, in the case of transmitters.

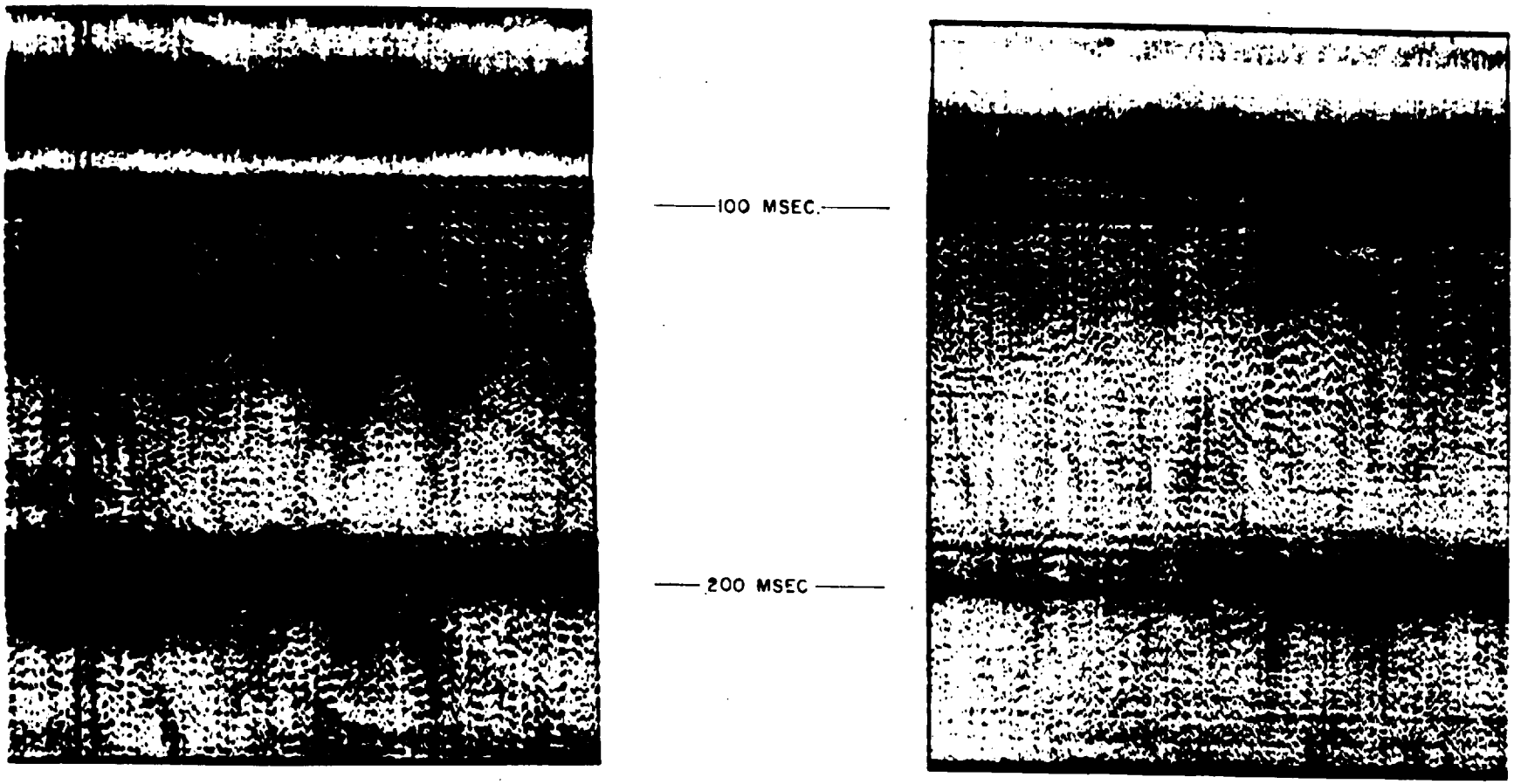

Fig. 3.7. Field test records, open and adjustable-gap sparks.

In the case of piezoelectricity, if a force is applied to a solid crystalline dielectric, it will produce stress within the crystal and a deformation of the crystal lattice. In certain crystals with asymmetrical charge distribution, the lattice deformation is, in effect, a relative displacement of the positive and negative charges within the lattice. The displacement of the internal charges will produce equal external charges of opposite polarity on opposite sides of the crystal (piezo-electric effect). The charges can be measured by applying electrodes to the surfaces and measuring the potential difference between them. The magnitude and polarity of the induced surface charges are proportional to the magnitude and direction of the applied force. In the case of magnetrostriction, when a body is magnetized, its dimensions are changed slightly, usually by not more than a few parts per million, and such changes are referred to as magnetostriction. The magnetic permeability of ferromagnetic materials changes in general when the material is subjected to machanical stress. The permeability can increase or decrease (negative magnetostriction), depending upon the material, the type of stress (compression, tension, or torsion) and the magnetic flux density in the sample. The elastic deformation of a dielectric under the forces exerted by an electrostatic field is called electrostriction. In solids the effect is small and easily masked by deformations arising from extraneous causes. The attractive forces between metal electrodes in contact with the dielectric may bring about deformations within the volume of the dielectric which have nothing to do with electrostriction.

Magnetostrictive transducers essentially consist of a probe of magnetoelastic material around which a coil is wound. If a force is applied causing a stress in the probe, the permeability of the probe and thus the inductance of the coil will change. These transducers are used

extensively for underwater acoustics. A magnetostrictive transducer often serves as both sound source and receiver. It sometimes is operated at its natural resonant frequency and it has an effective bandwidth of one-third octave or less, being then considered a special purpose device. The chief advantages of magnetostrictive transducers are low impedance and rugged construction.

The analytical evaluation of the properties of crystal cuts used in piezoelectric transducers is complicated because of the mechanical and electrical anisotropy of the crystals and because of the variation of the crystal constants with varying mechanical load. However, piezoelectric elements made from barium titanate ceramics ($BaTiO_3$) are free from limitations imposed by the crystal structure. They can be molded in different sizes and shapes, and the electrical axis can be artifically created in the production process. The single barium titanate crystal is ferroelectric, i.e., if exposed to an electric field it becomes polarized and maintains its polarization after the field is removed. The effects of compression along and across the axis of polarisation are opposite in sign but not equal in magnitude. A volume change produced by subjecting the transducer to pressure from all sides (hydrostatic pressure) causes an output voltage. The voltage-output versus applied stress characteristic is not linear, except over a limited operating range.

In most underwater acoustic experiments, it is important that the hydrophone does not introduce any changes in the waveform and this dictates the use of the linear portion of the electroacoustic conversion effect. Compensation for any variation in response with frequency can usually be made in the electronics. The cable and preamplifier which are connected to the output of the hydrophone can limit seriously the effective performance of the hydrophone. They usually increase noise output from

noise generation in the cable or preamplifier. The cable and preamplifier also may load the hydrophone sufficiently to reduce its output, and thereby reduce the effective signal-to-noise ratio.

Linear array hydrophones possess certain distinct advantages over single-element hydrophones in many sonar system applications. The linear additive system, in which the outputs from the elements of the array are added, provides a directional sensitivity in a two dimensional pattern due to the forming of a broadside main lobe with minor side lobes, as well as giving an enhanced signal-to-noise ratio. Higher directionality can be achieved with the use of long array hydrophones but the practical size of an array must also be considered. Methods such as superdirectivity, multiplicative processing, and multifrequency operation in sonar systems have been reported by Tucker (1961) to have achieved varying degrees of success. In spite of this, the normal additive simple linear array hydrophones are comparatively easier to construct and are in general more reliable.

3.3.2. Construction of Array Hydrophones

The hydrophones used in the Alpine receiving system are Harris MP-510-C magnetostrictive type instruments manufactured by General Instrument Corporation. Although the housing of each of these hydrophones is 40 in. long but the effective length is only about 10 in. and is composed of 4 cylindrical magnetostrictive elements of 2 in. diameter aligned end to end on a common core and embedded in resin. Its frequency response is not flat but rises gradually from -120 dB at 100 cps to -78 dB at 11, 000 cps where resonance occurs, dB values being in reference to 1 volt/μ bar. With a view to improving the performance of the receiving system of the Alpine equipment, it was decided to build a comparatively long plain additive multi-element array hydrophone so as to possess the desirable

features of directivity and increased sensitivity.

This multi-element array was a modified version of a basic design used by N. I. O. (Bower, 1963). It was made up of 10 barium titanate spheres connected in parallel with a sensitivity minimum on the axis. The barium titanate spheres were manufactured by Plessey Ltd. each being $1\frac{1}{4}$ in. o. d. with a $\frac{1}{4}$ in. wall thickness and having a resonant frequency of 104 kcps. The spheres were roughly uniformly spaced at intervals of 19 in. and forming an effective array approximately 14 ft. long housed in a 16 ft. oil-filled polythene tube of 2 in. o. d.

Also mounted in the hydrophone tubing in the castor oil was a transistor preamplifier consisting of a cascade emitter follower input stage, amplifier, phase splitter, and push-pull emitter output. The preamplifier had a total amplification of about 40 dB or a power amplification factor of 10, 000, with input impedance of 100 K ohms and output impedance of 1.5 K ohms tested at 50 cps.

For the computation of the directivity of an array made up of a number of equally spaced elements, a general formula may be used to express the ratio of the resultant voltage for any value of the angle β to the voltage when $\beta = 0$, β being the deviation angle measured between the normal to the array and the specified bearing of the sound source. This is given by Horton (1959) as:

$$\frac{e_d}{e_{do}} = \frac{\sin n \phi}{n \sin \phi} \qquad (3\text{-}1)$$

where

e_d = the voltage generated by a distant sound source located on a specified bearing

e_{do} = the voltage generated by the same sound when at the same distance along the normal to the array

$2\phi = (2\pi s/\lambda) \sin\beta$

= the phase difference in radians between outputs of adjacent hydrophones

s = the separation between adjacent elements

λ = the wave length of the signal used

n = the number of individual elements in the array.

From equation (3-1), it can be seen that the first zero in the directivity pattern of a linear array occurs when $n\phi = \pi$, so long as $\sin\phi \neq 0$. For this point ϕ can be expressed as

$$\phi = \frac{\pi}{n} = \frac{\pi s}{\lambda} \sin\beta$$

or $$\sin\beta_o = \frac{\lambda}{ns}$$

where β_o being the specific deviation angle at this point. This shows that, for any frequency, the width of the primary lobe identified with a given number of elements may be reduced by increasing their separation. For a given array the width of this lobe decreases with increasing frequency.

It was therefore thought that by utilizing these characteristics the directivity as well as the sensitivity of the array could be made more versatile by having a variable connection arrangement on the ship. This was done by using an 8-core shielded cable for the array and by the building of a shipboard control box. Fig. 3-8 (a) shows the 10-element hydrophone array in a coiled position and (b) the inside view of the control box. Fig. 3-9 is a diagram of the wiring connections for the hydrophone array whose features of versatility are clearly illustrated, i. e. the number of element connected (down to 1), the effective length, and even the spacings between elements can be readily changed.

It should be noted that when an element of transducer material is used, the tuned bandwidth is dependent upon the electromechanical coupling

a

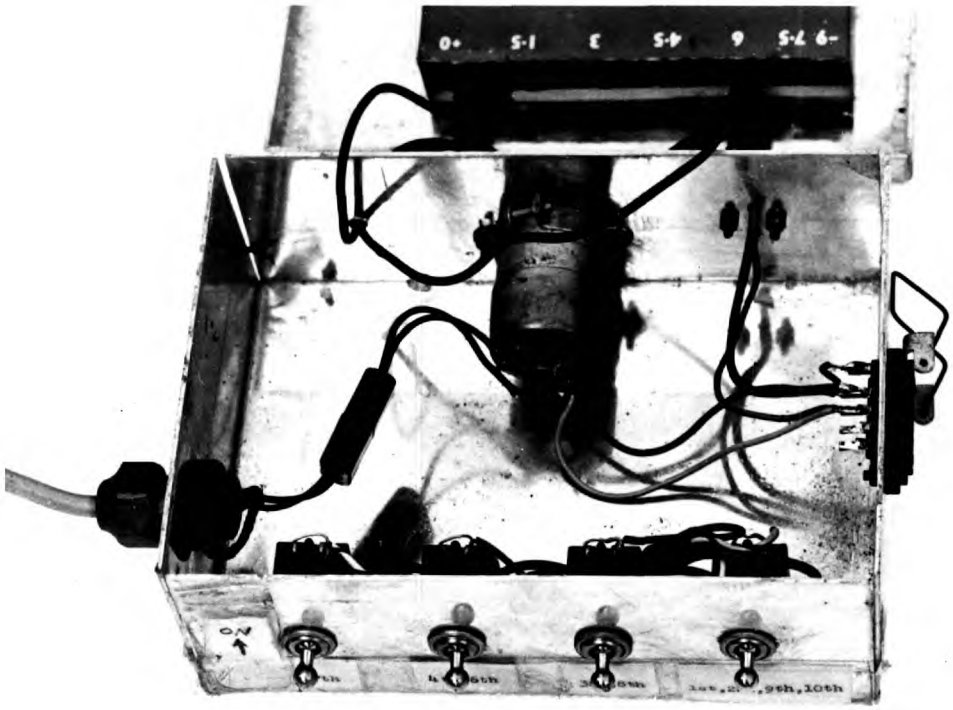

b

Fig. 3.8. The hydrophone array and the control box.

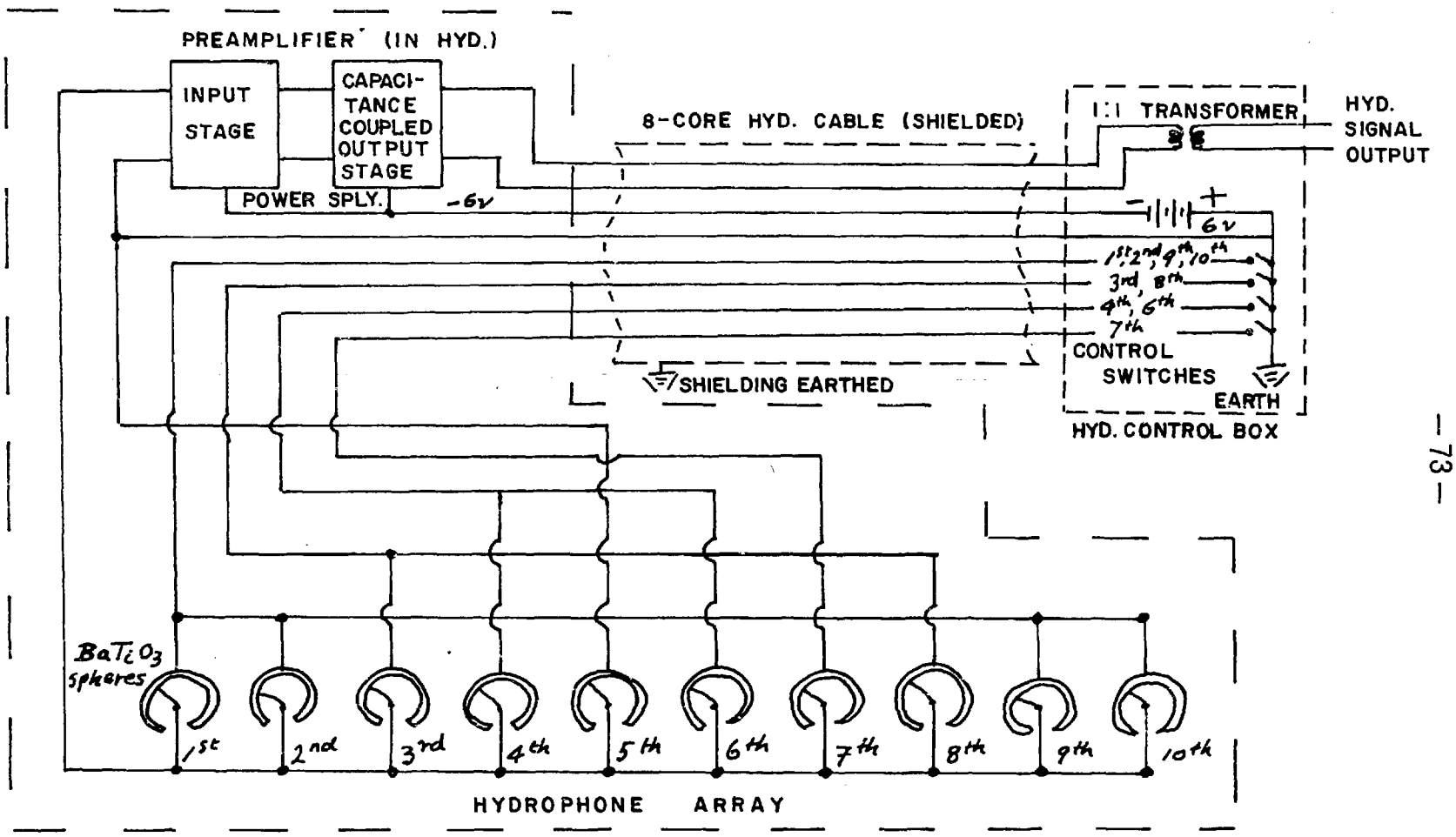

FIG. 3.9 SIMPLIFIED CONNECTION DIAGRAM OF THE CONTROLLABLE MULTI-ELEMENT HYDROPHONE ARRAY.

factor which is a maximum when the two factors in the transducers, $Q_m \simeq Q_e$ where Q_m is the mechanical Q and Q_e the electrical Q. Q_m can be calculated from the equation

$$Q_m = \frac{\omega_o M_e}{\rho_o c_o A} \qquad \text{(Schofield, 1961)}$$

where M_e is the effective mass of the element, $\rho_o c_o$ is the characteristic impedance of the loading liquid, A is the effective radiating area, and ω_o is the resonant angular frequency.

The versatile control system required extra cores in the hydrophone cable. When the capacitance of the cable equals the capacitance of the transducer, the sensitivity of the transducer is divided by two. Thus, the effective tranducer sensitivity is reduced by increasing the cable length between the transducer and the preamplifier. Loss of optimum electrical coupling and a relative reduction in sensitivity due to cable loss were therefore expected in the new array system. It should be pointed out, however, that electrical noise generated in the cable itself is often a serious problem for ceramic transducers. Twisting or flexing a coaxial cable discharges electrons in the cable dielectric to both the centre conductor and the shield. This produces a broad-band noise signal output in parallel with the transducer output. Such noise output is usually proportional to the effective length of the cable used even when the cable is a low-noise one.

3.3.3. Results of Field Tests

The equations of motion, conservation of mass and energy can be simplified by suitable approximations and converted to equivalent circuits from which the desired properties of resonant frequency, band-width, coupling coefficient and power conversion efficiency could be predicted. Actual measurement of an element whose design is based upon such simplified analysis seldom produces parameters which agree exactly with theory. This applies to a degree to the directivity of a hydrophone array.

There was, therefore, a plan to measure the general characteristics of the array hydrophones constructed utilising the calibration facilities then available at the Admiralty Underwater Weapon Establishment at Weymouth. A special rig-up would need to be made to adapt the 16 ft. long flexible array. However, due to the tight schedule at the Portland Dockyard, this plan was never matured. Field tests on the array were, nevertheless, conducted using the Alpine equipment in conjunction with some oscilloscope observations. These again were done in St. Ives Bay, Cornwall.

The Alpine receiving system was set at the dual-channel operation mode and the push-pull outputsfrom the array were transformer-coupled to the second preamplifier. The graphic profiling records thus obtained provided a direct comparison in quality between the acoustic signals received by the Alpine magnetostrictive hydrophone and the array respectively. The array was towed on the 8-core shielded cable some 20 ft. ahead of the spark. This put it between the boat and the source and as it was in line with both it should pick up very little noise from either. Both the array and the cable were negatively buoyant. Instead of using oval fish-net floats, sections of 1 in. o.d. polythene tube with water-tight rubber bungs plugged at both ends were attached by strings along a great part of the cable as well as along the array, enabling the array to be only slightly negatively buoyant to remain at a submersion level about 6 ft. below the water surface when being towed at a survey speed of $3\frac{1}{2}$ knots. The proper floating attachments went through a series of experimental trials. It appeared that the use of long sections of floating tube created less flow noise when compared with the use of a large number of fish-net floats. Accordingly the former proved a better floating method.

It was found, rather disappointingly, that the output from the array was very unstable and often oscillated persistently at a low frequency

(60-300 cps) to mask completely the graphic profile. This instability seemed to be closely related to a range of hydrophone element combinations. When all the ten elements were connected in parallel, it was noted that the profile quality thus obtained indicated increased sensitivity but decreased definition when compared with the other channel obtained with the magneto-strictive hydrophone. These oscillation phenomena were puzzling. Only after repeated trials was it realized that these were most probably caused by the regnerative feed-back due to the noise pick-up from the generator mains, the ship's engine, and possibly the profiling signal itself because of the interaction effects between the low-level signal leads and those with the output from the preamplifier.

Although the individual element control was a very desirable arrangement for providing a high degree of versatility to a hydrophone array, it must be admitted that this possible interference between high-level and low-level signals was not expected. Armoured cable consisting of individually-shielded cores would be a better choice but even using such a cable there would still exist the danger of having noise contamination when making low-level connections on board the boat. A better design would be to have a built-in preamplifier for each hydrophone element within the array. Any combinations of elements made would then be of relatively high signal strength. The effects of regenerative feed-back or low-level noise pick-up would then be completely eliminated.

A later check in the field on the 8-core shielded cable manufactured by Radiospares Ltd. revealed that the outer dielectric had been punctured resulting in sea water leaking into contact with the inner cores. A good quality 6-core armoured cable originally used for a sea-borne magnetometer was then the only alternative cable available. The practical remedy left to be done in the field then was to re-connect the inside wirings of the array

hydrophones making a permanent connection of the 10 elements in parallel. Only 4 cores of this substitute cable were used, two for power supplies into the preamplifier and two for the signal outputs from the push-pull stage. The control box, with most of the variable connections wiring removed, thus became a simple connection box.

During subsequent survey tests of the array no further oscillation occurred but record obtained generally indicated a poor resolution when compared with that simultaneously obtained with the magnetostrictive hydrophone. This could be attributed to the general shallowness in the testing area and excessive reverberations due to strong bottom reflections from the sandy or rocky bed. When the 14 ft. hydrophone array was towed 20 ft. ahead of the spark source over water of 40 ft. deep, differential path length between the bottom reflection to the first element and the last element could amount to more than 4 ft. thus effectively lengthening the overall reflection signals. The effect of reverberation in shallow water would act in a more diffused manner, further complicating the profile pattern. In the St. Ives Bay area, where the water depth is generally very shallow, no satisfactory profile records were obtained with the array.

The over-all pulse length and definition from the output of the hydrophone array as compared with those of the magnetostrictive hydrophone can best be seen in (e), (f), (g), (h) and (i) of Fig. 3-6 in a series of measurements of the adjustable-gap spark pulses mentioned previously in Section 3.2.4.2. In another set-up for finding the directivity of the hydrophone array, the array was fixed to a long oar which was immersed horizontally at 3 ft. below the water surface on one side of a dinghy while, on the other side of the dinghy, the Alpine hydrophone was similarly fixed. Fig. 3-10 gives a comparison between the outputs of the magnetostrictive elements (lower trace, total length 10 millisec.) and the hydrophone array

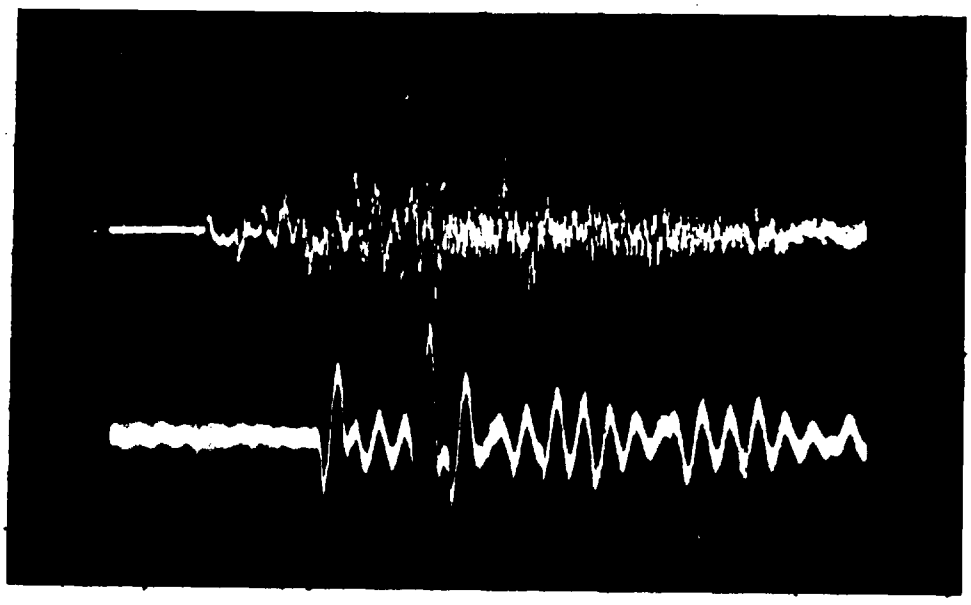

a

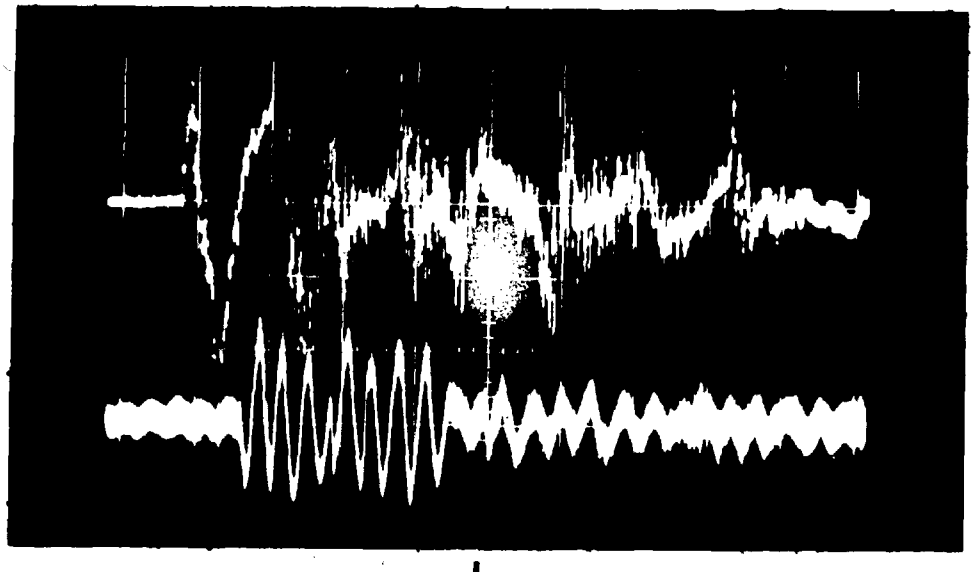

b

Fig. 3.10. Comparison of directivity between two hydrophones.

(upper trace). In 3-10 (a) the sparker source was on a line along the hydrophone chain and in 3-10 (b) the source was broadside on. Evidence of the highly directional characteristic of the array hydrophones can certainly be seen here.

CHAPTER IV

DEVELOPMENT OF A SYNCHRONIZED RECORD/ REPRODUCE SUB-BOTTOM PROFILING SYSTEM

For an improved version of a sub-bottom profiling system for use over the continental shelf and slope, it was decided to develop an apparatus with a generally higher performance. As has already been discussed in previous chapters, resolution is inversely proportional to pulse length while penetration is directly proportional to source energy. In general, an increase of energy decreases the frequency and resolution but increases the depth of penetration. However, it is obvious that an apparatus with a higher source energy is essential for continental shelf and slope investigations. A new sub-bottom profiling system was built for this purpose giving a facsimile record and a record on magnetic tape. Associated with this was a play-back system which proved to be invaluable. The components of this system will be described item by item.

4.1. The Acoustic Source

4.1.1. The Central Capacitor Bank

The central capacitor bank consisted of ten 16- mfd 4,000-volt capacitors capable of storing a maximum of 1,280 joules. The peak d.c. voltage rating was chosen in order to facilitate convenient matchings with several standard transducers, in particular the Boomer and the Pinger, manufactured by E.G. & G. Inc. The capacitors used were Sprague Electric Type 5-3-3-426B with an energy density of 0.81 joules per cubic inch. These had a very compact design and

at the same time were much lighter in weight when compared with most other similar products available. These capacitors were clamped together in two rows of five each and were inter-connected in parallel to form a central energy storage bank. A pair of easily disconnected busbars between the two rows was installed so that full or half-power operation could readily be selected. Further sub-division of the stored energy presented no difficulty as the connection made of short brass strips between the individual components could easily be altered. The entire bank was bolted firmly to the base of a steel-framed aluminium case 18 in. x 24 in. x 16 in. which had a polythene transparent top and a removable front panel to facilitate observation and to allow adjustment of the trigger discharging unit, which was being housed in the same case.

4.1.2. The Charging Unit

Unlike the Alpine charging unit described previously in Chapter III, a single-phase full-wave rectifying circuit was designed to be used with the new system. The average direct current supplied to the load in the case of the full-wave rectification circuit is twice that for the half-wave circuit. Hence the power delivered to the load is larger by a factor of 4 in the full-wave rectifying circuit. In addition to a far better efficiency of rectification, the full-wave circuit has a ripple factor of 0.472, being less than 40% of that of the half-wave rectifier (Millman, 1958). However, the power depends upon the circuit constants and parameters in the same way as for the half-wave circuit.

Two Mullard RR3-1250B Xenon valves were used for the present design as the rectifiers and were capable of providing ample safety

margin. Two prototype transformers were specially acquired, one for stepping up the a.c. supply voltage from a mains generator while the other serving as the filament transformer for the rectifying valves. Both were manufactured by Partridge Trnasformers Ltd. The high voltage transformer was a light construction intermittent-duty transformer with the following characteristics:-

> Primary: 115 v single phase 50/60 cps
> Secondary: 5,400 v (rms) center-tapped capable of supplying, with full-wave rectification, a peak charging current of more than 2A, and an average current of more than 1A at the rate of at least 1,000 joules per second.

To limit the current during each charging surge, sixteen 20-K ohm resistors in parallel were inserted in the charging circuit, forming a resitance bank having an effective value of 1.25 K ohms. These were vitreous enamelled resistances, size R7 type C each rated at 180 watts, manufactured by Resistance Ltd. Thus the total heat dissipating capacity of the resistance bank was as high as 2,880 watts, providing an adequate margin for what is essentially a 1,000 watt system. If the comparative low values of the resistance of the rectifying valves and of high voltage transformer are neglected, the time constant of this full-wave rectifying circuit is approximately RC = 0.2 sec. Thus, in a time of 0.8 sec. (4 RC) the whole capacitor bank was charged up to practically the maximum d.c. voltage (3,800 v), with a storage energy of 1,170 joules. The system can therefore be operated very satisfactorily on a one-second cycle with full-bank energy discharge or on a $\frac{1}{2}$ second cycle with half-bank energy discharge. It should be noted here that the mains supply for

this source during all field work was a 5-KW Onan petrol driven alternator (60 cps) used only for this purpose. As a result the effects of the intermittent load on the mains would not affect the receiving system and a second similar alternator was used exclusively for this.

All the components of the charging unit were suitably housed in a second steel-framed aluminium container (18in x 18in x 16in). In order to ensure proper cooling for longer component life, a Vent-Axia 6 in window type blower with reversible three-speed control was installed on one side of the case near the Xenon valves. The volume of air per hour moved by this unit could be as high as 12,000 cubic feet. A number of louvres were made at suitable positions on the side plates, producing an effective forced air flow. No overheating or breakdown of the component parts in the source system occurred throughout the present experiments.

4.1.3. The Discharging Unit

The circuit of the trigger unit for initiating the discharge in the new system was essentially similar to that of the Alpine system but some slight modifications were incorporated to meet the new requirements. The trigger charge for the ignition spark was stored in a small 2-mfd condenser. Instead of being controlled by a mechanical switch which earthed the grid bias, the bias of the grid-controlled thyratron was removed through a capacitance coupling. A negative voltage pulse of sufficient amplitude was furnished by the output of the Solartron Pulse Generator. This in turn was triggered electronically by a photocell activated by the recorder.

The main discharge switch, an open air gap, was also similar to that in the Alpine equipment. It was found necessary, however, to insulate thermally the electrodes from the tufnol-polythene mounting by a layer of asbestos compound. This insulating layer prevented distortion of the holder by overheating. The surface of the thorium-tungsten electrodes were found to tend to be excessively pitted when the new system was used for a prolonged full-power survey. At half power, however, this problem did not usually arise. The trigger spark unit together with the main air gap was enclosed in the box containing the capacitor bank. Natural air ventilation, provided by louvres in the walls of the case, was found satisfactory here.

4.1.4. Safety Features

Although the reduction in size and weight of units obtained by installing the charging and discharging units in separate cases proved a great convenience during handling and installation, it complicated the most important and essential safety precaution.

The high voltage energy source was unearthed and was insulated from its surrounding case, resulting in a floating system for the main high voltage. In the case of the underwater spark discharge, the water electrode was earthed to the sea. All high tension power cables were shielded cables with their sheaths earthed to the sea water as well as to the appropriate chassis. These were also adequately earthed by separate leads to the sea when installed for operation. These arrangements were employed to provide definite protection to the operator from the high potential if an insulation breakdown occurred, and to shield to some extent the leads.

The interior of the charging unit in its closed case was usually inaccessible while access to the discharging unit, incorporated with the capacitor bank, could be made only though the operation of a mechanical safety device which shorted the two central charging terminals of the storage capacitors whenever the bottom-hinged front panel was unlocked. However, the capacitor and discharge unit could be accidentally opened while the charging unit was in operation. The shorting of the condenser terminal would result in heavy continuous arcing across the shorting contacts with possible permanent damage to the charging transformer and rectifiers due to the overloading. To reduce the possibilities of this, an illuminated sign reading "Danger - do not touch" comes into operation whenever the mains switch to the charging unit is on. In addition, the first step for shutting down the entire profiling system is to disengage the leads to the charging transformer while the by-passed mains continue to energize the trigger spark circuit. Any residual energy build-up in the capacitors tends to be discharged in the normal manner by the following trigger signal originating from the recorder which is left operating. This avoids excessive wearing due to high energy arcing between the shorting points at the dropping of the safety shorting bar. As an extra precautionary practice, a large size well insulated screwdriver was always placed across the busbars of the capacitors before any component inside the discharging unit was touched.

Fig. 4-1 shows the front view of the discharging unit on top of the charging unit with both the front panels removed. Fig. 4-2 is the simplified schematic circuit of the charging and discharging units with the details of the trigger circuit omitted.

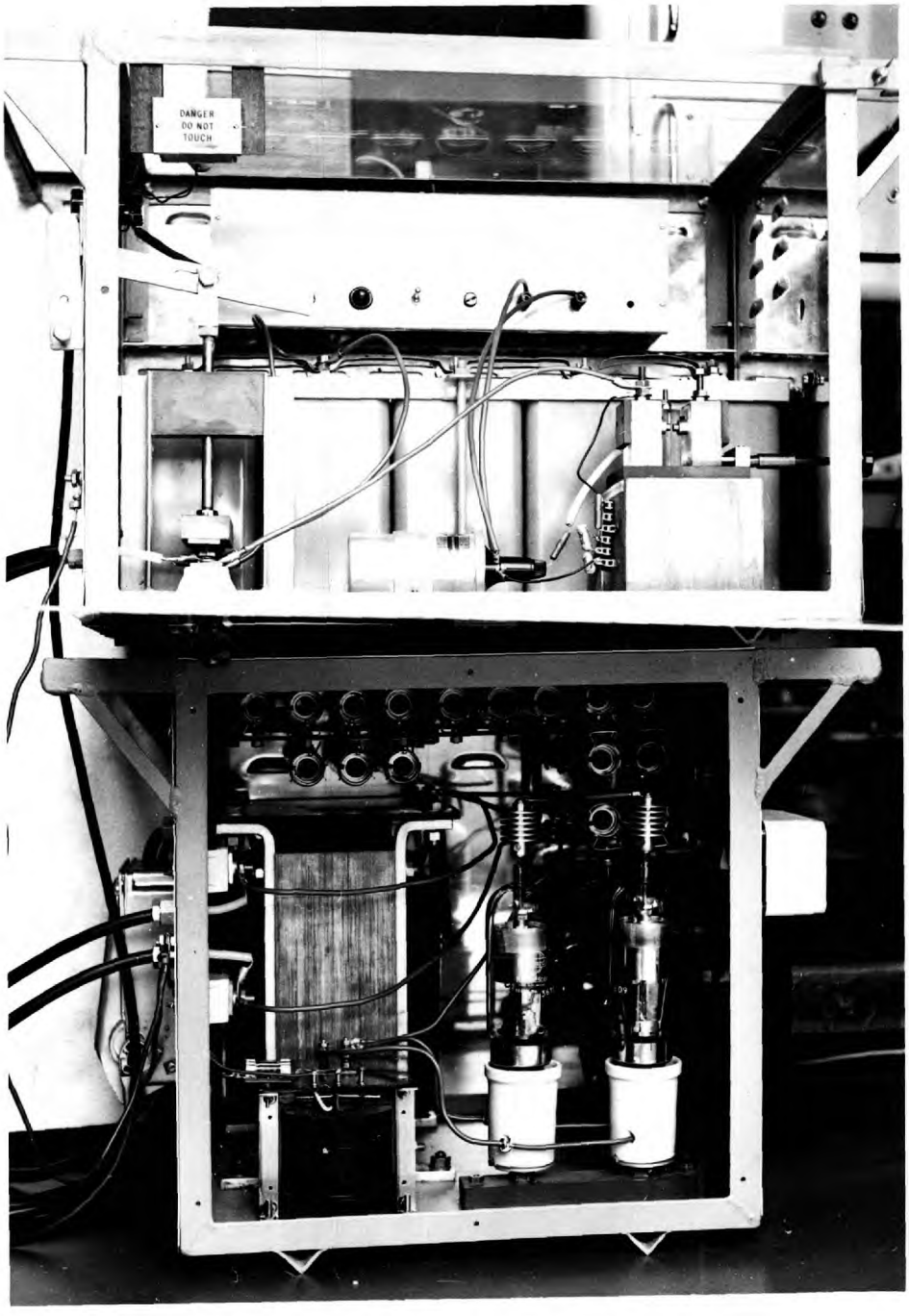

Fig. 4.1. The charging and discharging units.

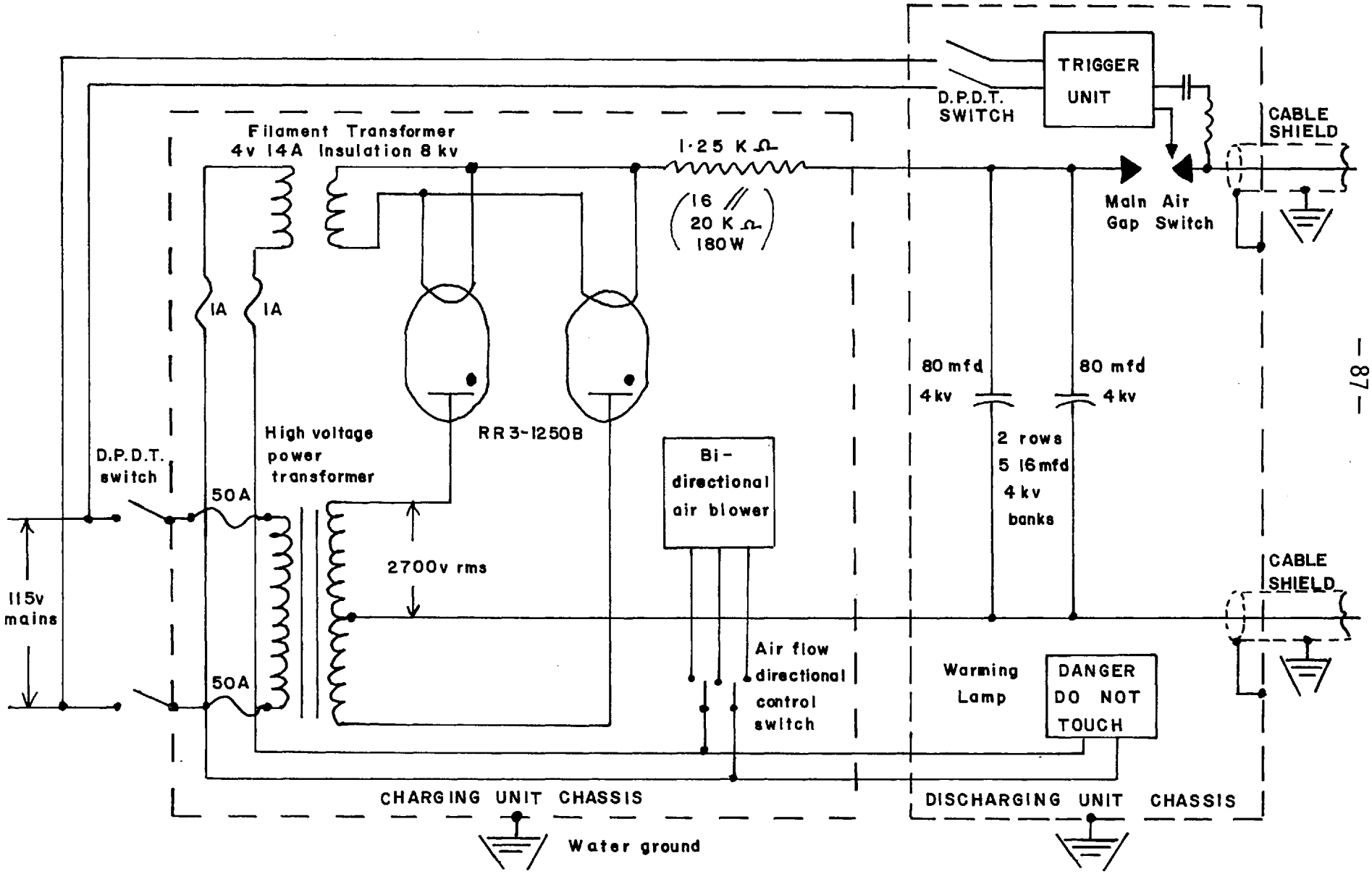

SCHEMATIC CIRCUITS OF THE CHARGING AND DISCHARGING UNITS

FIG. 4.2

4.1.5. The Multi-transducer Carrier

As found from the preliminary results obtained in Cornwall with the Alpine system, the conventional spark source can be made to be more versatile by the use of an adjustable spark gap. It is believed that the maximum amount of information from the area under investigation can be obtained with the proper choice of the acoustic source used. The ideal source system would be one which possesses various choices of energy output, pulse lengths, and frequency content. In practice this is nearly impossible to achieve due to the parameters inherent in a single type of transducer and the necessarily limited number of transducers readily available. On practical ground, however, a few effective acoustic source types with different output characteristics can be made readily available for rapid shipboard selection if they are mounted in a single carrier and can be easily matched to a common energy source.

With a Boomer installed in the bottom of a fiberglass dinghy and towed well astern of the survey ship, N.I.O. (Bower, 1963) has been able to obtain the shortest possible output pulse at a particular energy level. This arrangement has the principal advantage of eliminating the reflected pulse from the sea surface as well as the possible reflections from the surface and ships hull when towing alongside, and the absence of these interfering pulses will tend to give a shorter event. A project was therefore contemplated using a specially designed and properly ballasted float accommodating several types of transducers, including the Boomer.

This project was, in fact, started but its continuation had to be deferred owing to the fact that proper handling facilities of such a float requires the use of vessels with special equipment. During the present experiments, the boat time used was mainly

in collaboration with other research projects so that such facilities were not available.

In Fig. 4-3, (a) shows the oblique view of this boat-like transducer float and (b) is the bottom section near the stern where a Boomer transducer has been installed. Copper plating, serving as an effective earth return has also been mounted near the stern where three specially-designed spark electrodes will be installed at the corners of a triangle. Amongst these will be an adjustable gap system in which the electrode distance from the earth plate can be varied. Forward of the Boomer, a 6 kcps Pinger will be installed.

Each of these transducers will be joined to the shipboard installation by individual power cables leading from the central compartment of the float. Versatility among the source parameters to suit a particular requirement will therefore be obtained with great ease.

4.1.6. The Sparkarray

In autumn 1964 at the invitation of the Channel Tunnel Study Group, several commercial firms were selected to demonstrate the capabilities of their sub-bottom profiling equipment competitively over a small, well-surveyed area between Dover and Calais during a one-week evaluation exercise. Using a patented "Sparkarray" and "Rocket" hydrophone, the firm E.G. & G. Inc. demonstrated a slightly improved overall effectiveness in their instrumental performance and their equipment was thus chosen to perform the principal survey over a large area.

It is commonly known in acoustics that small intensity sources of a large area have a better transmission efficiency than point sources

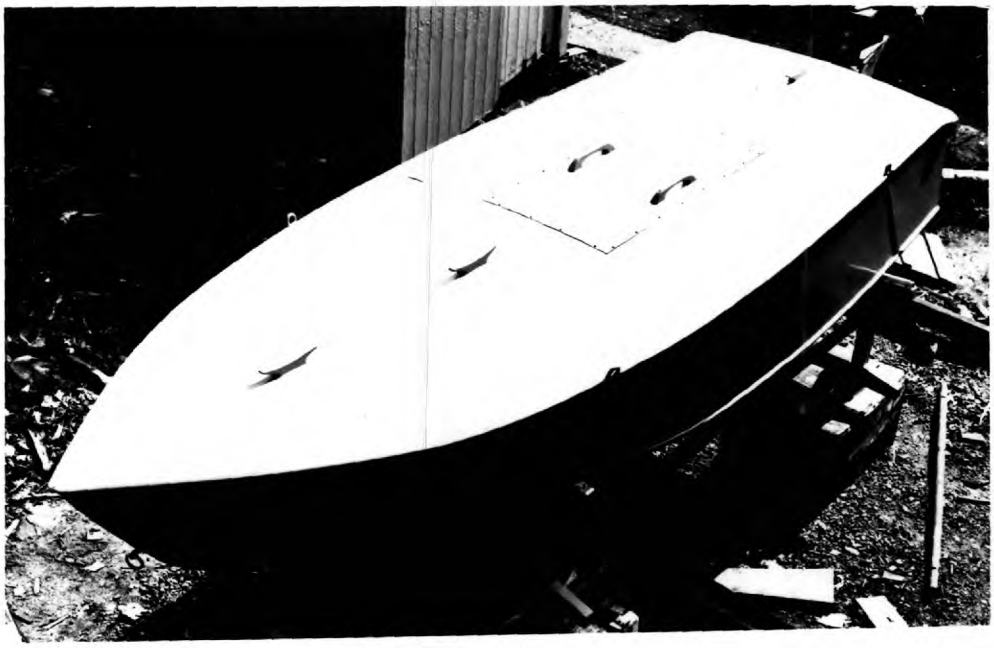

a

b

Fig. 4.3. The multi-transducer carrier.

of larger intensity. The basic E.G. & G. Model 267 Sparkarray was designed for 3 electrodes installed at equal distance along the centre line of a frame of triangular section (9 in. x 9 in. x 9 in) and of length $7\frac{1}{2}$ ft. and which formed the earth. The welded stainless steel frame with three female electrode holders was carefully constructed to provide a constant anode-cathode distance as the male plug-in electrode eroded through use. The use of multiple electrodes was dictated by an improved efficiency and a longer electrode life. The end of the electrode was in contact with sea water. When an electrical pulse from the capacitor bank (4 kv) was discharged through the Sparkarray electrodes, the rapid discharge of electrical energy between the electrodes and the frame quickly heated and vapourized the sea water, generating a rapidly expanding plasma bubble which in turn caused an acoustic pulse. According to tests conducted by the manufacturer, when viewed with a spectroscope, the spark thus created showed a strong yellow light indicative of sodium ionization. This "yellow spark" formed between the electrode and the earthing frame spaced several inches away (5" approx.) in the conducting medium had an electrical resistance of several ohms compared with the common "blue spark" resistance of a fraction of an ohm. They also pointed out that for seismic profiling, the longer acoustic pulse length characterized by lower frequencies of the Sparkarray transducer enabled deep penetration but less resolution than the Boomer manufactured by the same firm.

As the E.G. & G. Sparkarray and Rocket Hydrophone were readily available and more reliable than any of the experimental types, they were used in conjunction with other components during all the practical surveys of this investigation. Fig. 4-4(b) shows the actual

a

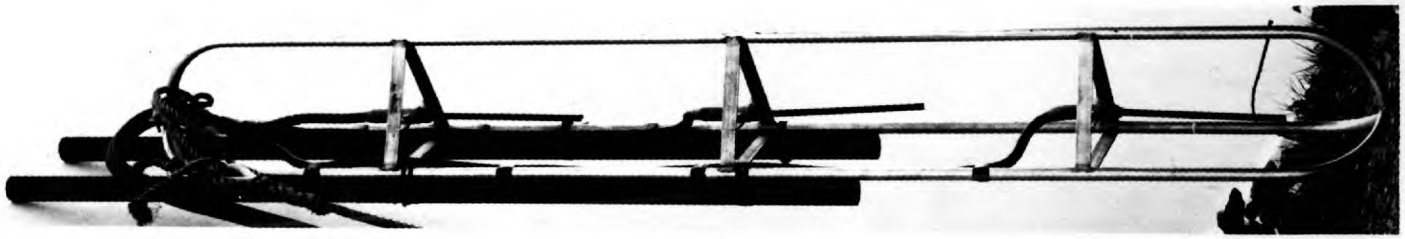

b

Fig. 4.4. The E.G.& G. hydrophone and Sparkarray.

Sparkarray with two rods each of 50 lbs attached for underwater balance when towing at the usual surveying speed of 6 knots.

4.2. The Receiving System

The various acoustic signals are detected by a hydrophone. After preamplification the output of the hydrophone is used to operate a tape recorder and in parallel with this, and after filtering and further amplification, a precision graphic recorder.

4.2.1. Hydrophone

An experimental receiving system consisting of multiple hydrophones proved to be unsatisfactory in its general performance and a piesoelectric crystal type hydrophone shown in Fig. 4-4(a) (Manufactured by E.G. & G. Inc.) was used. This submersible, omni-directional, towed hydrophone was pressure sensitive, and had a substantially flat response in the portion of the acoustic spectrum 100-2000 cps which are mainly involved in continuous reflection marine geological and geophysical investigations. Mounted in a rugged, streamlined, stainless steel fish, this Model 262B "Rocket" hydrophone was comparatively quiet, even when towed at speed of 6 knots. It also had 45 feet of towing line and 70 feet of hydrophone cable. The last 20 feet of both were covered by a fairing to minimize towing noise. The sensitivity of this hydrophone, specified by the manufacturer, was 90 dB referred to 1 volt per microbar. In practice, this hydrophone was used throughout the Cardigan Bay survey because the sub-bottom profiles it produced

were very satisfactory. The details of its electrical and acoustic performance will be given in the chapter on data analysis (Chapter VII).

4.4.2. Pre-Amplifier

The pre-amplifier chosen was a solid state low noise unit with a high input impedance (1 megohm shunted by 25 pf), made by Hewlett-Packard (Model 466A). It was a portable, transistorized amplifier with a wide frequency range (± 0.5 dB, 10 cps to 1 Mcps) and high stability. A stable gain of either 20 or 40 dB might be selected with a panel switch so that the sensitivity could be increased by a factor of 10 or 100 as desired. The amplifier was designed to be non-blocking with the output voltage clipped at 2.1 volts peak to peak, thus ensuring quick recovery from overloads.

4.2.3. Continuously Variable Passive Filters

The filters employed were Allison Model 2AB passive units. A passive unit has the basic advantage over the electronic filters in that it does not generate any appreciable noise. Their ability to analyze transients is enhanced by a minimum ringing effect. A change of impedance with frequency forms the filtering action. It was very important that the source impedance and the load impedance be 600 ohms to match these particular filters. The impedance of the filter will change radically outside the pass-band. The Allison 2AB was composed of two separate filter networks, a low cut-off K section filter, and a high cut-off double K section filter. Tuning was accomplished by a variable inductor. Its passive nature and

shielding construction allowed its operation with low level signals over a wide dynamic range. The attenuation of these filters was at least 30 dB per octave. The low cut-off and high cut-off sections were isolated from each other and from the case, but busbars were provided to connect the two in series making the two into a band-pass filter. Each filter was provided with two controls, an octave band switch, and a multiplier dial. The multiplier dial tuned the cutoff frequency over one octave. The multiplication factor on the dial timed the octave band setting and gave the cutoff frequency. The cutoff frequency is defined as that frequency at which the filter attenuates approcimately 3dB from the minimum insertion loss. Two impedance matching transformers were also used when necessary to provide flexibility to match impedances of 600 ohms. The input transformer was an auto-transformer designed to work from approximately 10,000 ohms to the 600 ohm circuit of the filter, while the output transformer also an auto-transformer was designed to match the 600 ohm impedance of the filter into the grid of a vacuum tube. Each transformer was enclosed in a mu-metal case and an earthed steel case.

4.2.4. Power Amplifier

A Vortexion Super 50-watt audio-amplifier was selected to be used in this new sub-bottom profiling system for its general reliable performance. This amplifier was designed for a long life without trouble. The 807 output valves employed can handle 80 watts, but were deliberately underrun to give a longer life. Tertiary feedback was used; the distortion is less than .15%, and

the amplifier was stable with all types of load. The final stage could supply 50 watts within the frequency range 30-20,000 cps, or 30 watts at 20-50,000 cps, and the total hum and noise was better than -85 dB referred to the 30-watt level.

In the original design of this amplifier, which was made to drive speakers, two inputs for microphones and gramophone respectively were used for electronic mixing, .15 volt on a 1/4 megohm line being required for the gramophone and 0.1 millivolt on a 15 ohm line for microphone. In the present application, certain alterations were made. Both the input impedances were converted to 600 ohms. For the high level input, the saturation on voltage was set at 1.5 volts rms, while the low level one was set at 7.5 mv rms. The bass and treble control parts of the circuit were eliminated in order to maintain true signal fidelity. However, a test conducted on its frequency response was flat with a fall of 1.5 dB at 50 cps and at 10,000 cps on the high level input, and a fall of 2.5 dB at the same frequencies on the low level input. These variations would have a negligible effect on the quality of the record produced by the graphic recorder.

4.3. The Graphic Display

4.3.1. The Mufax Chart Recorder

As the continuous reflection profiling method depends critically on the automatic correlation of successive recordings provided by the graphic recorder, it is essential that the recorder used should be of the precision type for accurate display of coherent information.

A Mufax 18-inch Chart Recorder Type D-649 was found eminently suitable for use as a multi-purpose precision graphic recorder in sub-bottom profiling. This is because of the chart recorder's two important features, namely the rotating helix writing system and the 1,000 cps tuning-fork motor drive. It was specially designed for the reception of meteorological weather maps transmitted either by radio or by land-line. The electro-sensitive paper was drawn at a constant speed between the stainless steel writing edge and a rotating helix. Current was passed through the paper at the point of contact, causing a chemical reaction which produced black discoloration. The density of discoloration depended upon the current, which was controlled by the signal received. The staining ranged from the natural colour of the paper to a deep brown. Any increase above this level would lead to burning of the paper. The input current rating could vary through a range as great as 25 dB. The rotation of the helix, and the movement of the paper together caused the point of contact to traverse the paper in a series of parallel lines. A graphical picture formed out of successive lines of correlated signals was therefore built up. The paper, which had an effective recording width of $18\frac{1}{2}$ inches, was advanced at 96 or 48 lines/inch, and each line sweep would take $\frac{1}{2}$, 2/3 or 1 second according to its original design as a weather chart recorder.

As the chart recorder was an expensive piece of facsimile communication equipment, most useful for receiving existing radio transmissions of meteorological maps, it was considered worth while to let its weather chart receiving functions remain essentially intact in the process of modification, so that the converted instrument could be used for one more purpose. As the performance

of most geophysical work is, to a varying extent, dictated by weather conditions, the extra facility of being able to receive first hand meteorological maps on board a surveying vessel is certainly a desirable feature.

Fig. 4-5 shows the front (a), back (c), and side (b) and (d) views of the modified Mufax recorder with its original and extra controls. A simplified schematic diagram of the final version of the profile recorder is shown in Fig. 4-6 indicating most of the additional features added to the instrument. The weather chart receiver had three modes for receiving meteorological signals. For line working, it was designed to operate from an amplitude-modulated signal which had maximum amplitude when a black portion of the chart was being produced, and a minimum amplitude when white was being produced. When receiving over a radio link the recorder could be arranged to operate from a frequency-modulated sub-carrier transmission (s.c.f.m.), or a carrier-shift transmission (c.s.). In Fig. 4-6 only the a.m. portion of the original Mufax is indicated as only that part was useful in the modification.

4.3.2. The Modifications

4.3.2.1. The Programming Controls, etc.

In the upper part of Fig. 4-6 a signal fed to the profile input passes through a programme control, a phase control, a recording mode control, and a limiting control to the writing edge of the recorder. The programme switch selects the transmission as well as the reception rate, at a ratio of either once per one helix revolution, or once per two helix revolutions. At the setting 1/1 an acoustic

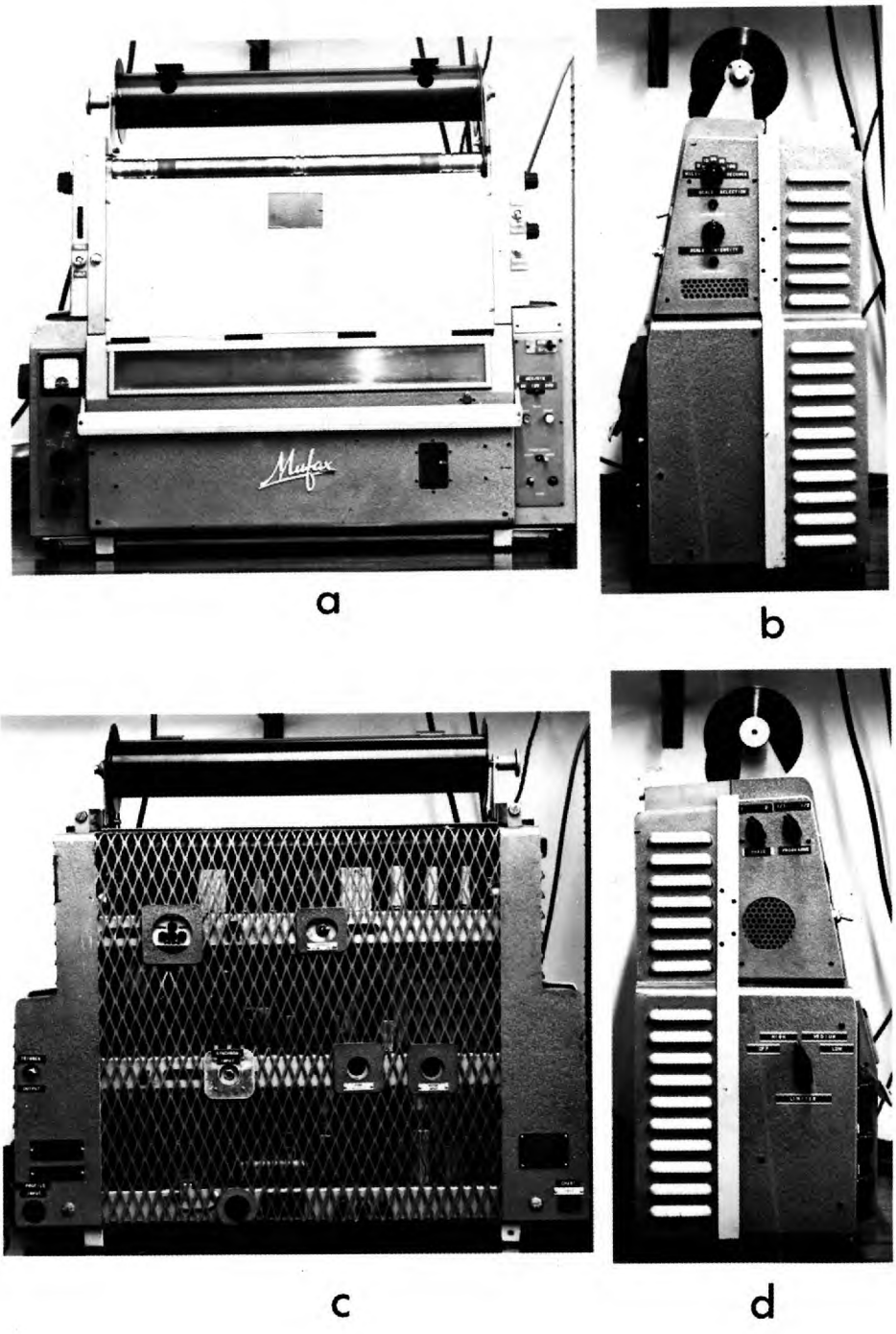

Fig. 4.5. The modified Mufax recorder.

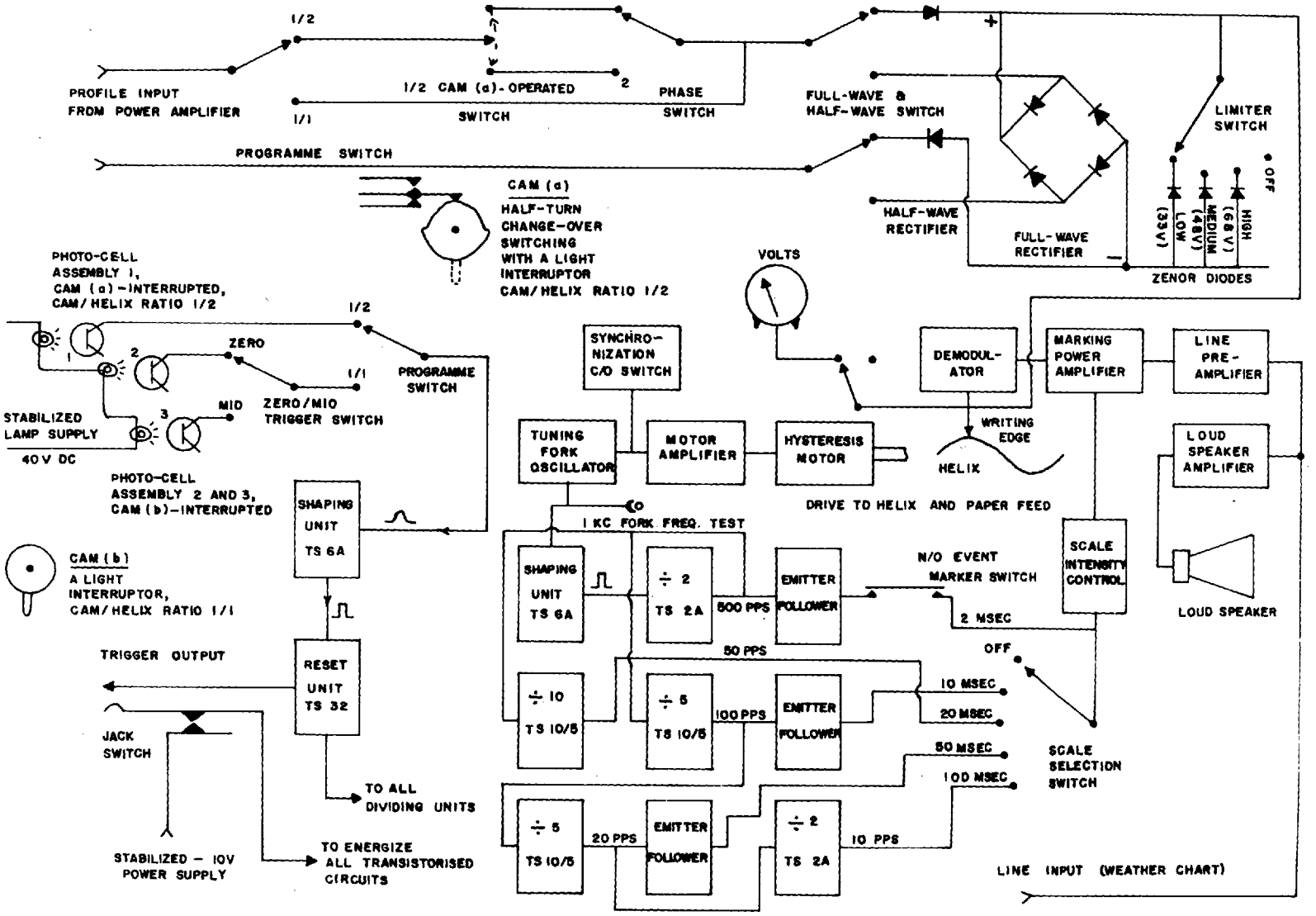

Fig. 4.6. SIMPLIFIED FUNCTIONAL SCHEMATIC DIAGRAM OF THE SUB-BOTTOM PROFILING RECORDER

signal is being continuously recorded, or every sweep is a recording sweep. At the setting 1/2 the input passes through a cam-operated change-overswitching device. The cam (a) has a cam/helix speed ratio of 1/2, and is so constructed that, because of the differential diameter, it will almost instantly alter the connections of a change-over switch every half turn of the cam, or one turn of the helix. The phase switch then selects the desired portion of the signal to be recorded every other sweep.

The full-wave/half-wave switch selects the desired mode of recording, letting the signal pass through either a full-wave rectifier or a half-wave rectifier. The rectified signal then goes through the limiter switch which consists of a set of Zener diodes of different voltage values. The selected portion of signal, after rectification and limiting (when used) is connected parallel with the Mufax demodulator which is basically a full-wave rectifier. A graphic profile will therefore be printed out on the electro- sensitive paper by the direct current going through it from the writing edge to the helix. At the same time, a d.c. voltmeter can be connected to indicate the marking level, i.e. the available voltage across the recording paper.

4.3.2.2. Photocell Assemblies

In the lower left portion of Fig. 4-6 the programmed electronic triggering system employed three photocell assemblies as shown. Each photocell assembly consisted essentially of a light sourse from a tiny lamp and a photo-transistor. A pulse is generated whenever the constant light ray on the photocell is obscured by a revolving

interruptor attached to the mechanical cam(a) or cam(b). The same programme switch mentioned previously selects the transmission ratio of either 1/2 or 1/1. When the programme switch is set at 1/1, trigger signal will come from either photocell assembly 2 or 3. These two assemblies are mounted opposite each other around cam(b), sharing the single light interruptor. The sloping-edged pulse inherent in the light interruption of a photo-transistor is converted to a square pulse by passing it through a transistorized pulse-shaping unit. The trigger pulse is led out from the following stage, a reset unit, to obtain exact synchronization of the resetting of the time scale, to be described below.

4.3.2.3. The Scales and Event Marks

Besides forming the basis of the very accurate helix shaft drive and transmissiin timing, the 1 kcps signal from the tuning fork was used to generate calibration marks for the graphic recorder. This system is shown in the centre of the lower portion of Fig. 4-6. The 1 kcps signal, after being converted into pulses, is passed through a frequency divider giving 500 pulses/sec., the time interval between these being two milliseconds. Similar treatment of the pulse by other frequency dividing units produces signals of 100, 50, 20, and 10 pulses/sec at various stages, with pulse intervals of 10, 20, 50, and 100 millisecs. respectively. One of these signals of small amplitude, when selected by a switch, passes through the scale intensity control, to the first stage of the marking power amplifier for recording together with the acoustic signals. The two-millisecond pulses by-pass the scale selection switch, and

are used solely for printing lines across the record. The marker switch used for this is of the push-button type, being normally open. These lines, usually printed at intervals of about 5 minutes, can be used to correlate the record with position determined by the navigation of the vessel.

Most of the transistorized units used are standard ones, manufactured by Venner Electronics Ltd. These units have compact dimensions, and are rugged in construction. The pulse shaping unit (TS 6A) is basically a two transistor Schmitt trigger circuit. The operation is such that the state of the circuit depends on the d.c. input level. When the input is below the trigger level, the circuit remains in the 'rest' condition, i.e. there is no voltage output. When the input rises above this level, the circuit becomes conducting and it will remain in this condition until the input once more falls below the critical level, when it will reset to initial condition. Thus an input signal is shaped into a square pulse output. The stages which divide the frequency by 2 employ binary units (TS 2A) which are essentially electronic gates. After resetting, the first pulse received at the input causes the gate to be opened, and the second causes it to shut. The succeeding pulses will actuate the gate in the same manner. The Venner decade unit (TS 10/5), which divides by ten, consists of four binary stages with feedback incorporated to reduce the natural count of sixteen to ten. It may also be used to divide by five. The reset unit (TS 32) has been designed to enable binary and decade counter units to be reset electronically. The application of a pulse wave-form to the input of the device will cause the d.c. potential at the output to rise momentarily towards the H.T. level. This raises the potential on the reset line connected to the binary and decade units, thus giving sharp and clean trigger and reset operations.

When the time scale signals are led out between binary and decade units, emitter followers are used as an impedance converter or 'buffer' stage. Proper selection of the input impedance of the emitter follower allows the appropriate input level to the following dividing stage to remain unaffected. A differentiating circuit employing a capacitor, a resistor, and a diode, is used as the final stage of each time calibration output. This is because of the necessity to convert square wave into single-sided pips such as those produced by a time mark generator. The scale intensity control is basically a variable resistance cathode connection coupled to the first stage of the marking power amplifier of the Mufax.

A 50 V. a.c. secondary output of the Mufax mains transformer is available for use in supplying stabilized d.c. to the 3 lamps in series (40 v) in the photocell assemblies, and the the H.T. (-10V) for all transistorized circuits. This modification has involved the insertion of a full-wave rectifier, two smoothing condensers, and a 10 V Zener diode. A jack type panel switch is installed for the trigger output from the reset unit. The construction of the switch is such that only when a plug is inserted is the power supply connected to the transistorized circuits.

The line input for weather chart signal can be fed to a loud-speaker amplifier and then to a loud speaker in the Mufax for audio monitoring. This feature was found just as useful during recording and playback of profiling signal. The low level acoustic signal could be connected to the line input and be heard on the loud speaker which has a volume control.

4.3.2.4. Some Internal Views of wiring and components

All modifications to the Mufax were either electrical or mechanical, both requiring suitable space to accomodate the extra parts. It is believed that best advantage was taken to utilize effectively the original functions and available space while the weather chart receiving ability of the Mufax was preserved.

Fig. 4-7 shows the additional component parts and wiring installed in the helix chamber with the helix removed. The scale calibration assembly together with part of the transmission trigger system is indicated by (a), the full-wave bridge rectifier and the half-wave diode rectifier respectively by (b) and (c). In Fig. 4-8, (a) indicates the upper cam and its surrounding phase changeover switch and the 1/2 programme photocell assembly. Cam (a) has a cam/helix turn ratio of 1/2. Because no such gear ratio existed in the original gear train, special driving, idle and driven gears had to be made to match the appropriate number of teeth and diametric pitch in order to obtain the 1/2 shaft revolution output. (b) indicates the zero/mid position trigger with two photocell assemblies located opposite each other across the lower cam. The relative position of both the cam and the photocell assembly to the camshaft (or helix shaft) can be adjusted readily by mechanical means. Black adhesive tapes were used to wrap around the lamps and photo-transistors to provide constant narrow light beams with sharp interruptions and, at the same time, to prevent ambient interference effects. The trigger output jack switch is shown at (c) with the profile input connector at (d). Fig. 4-9 shows the lower part of the right hand side of the Mufax recorder. The turning fork unit can be seen in the middle background in front of which are the limiter assembly consisting of three Zener diodes and a junction assembly of some of the extra wiring.

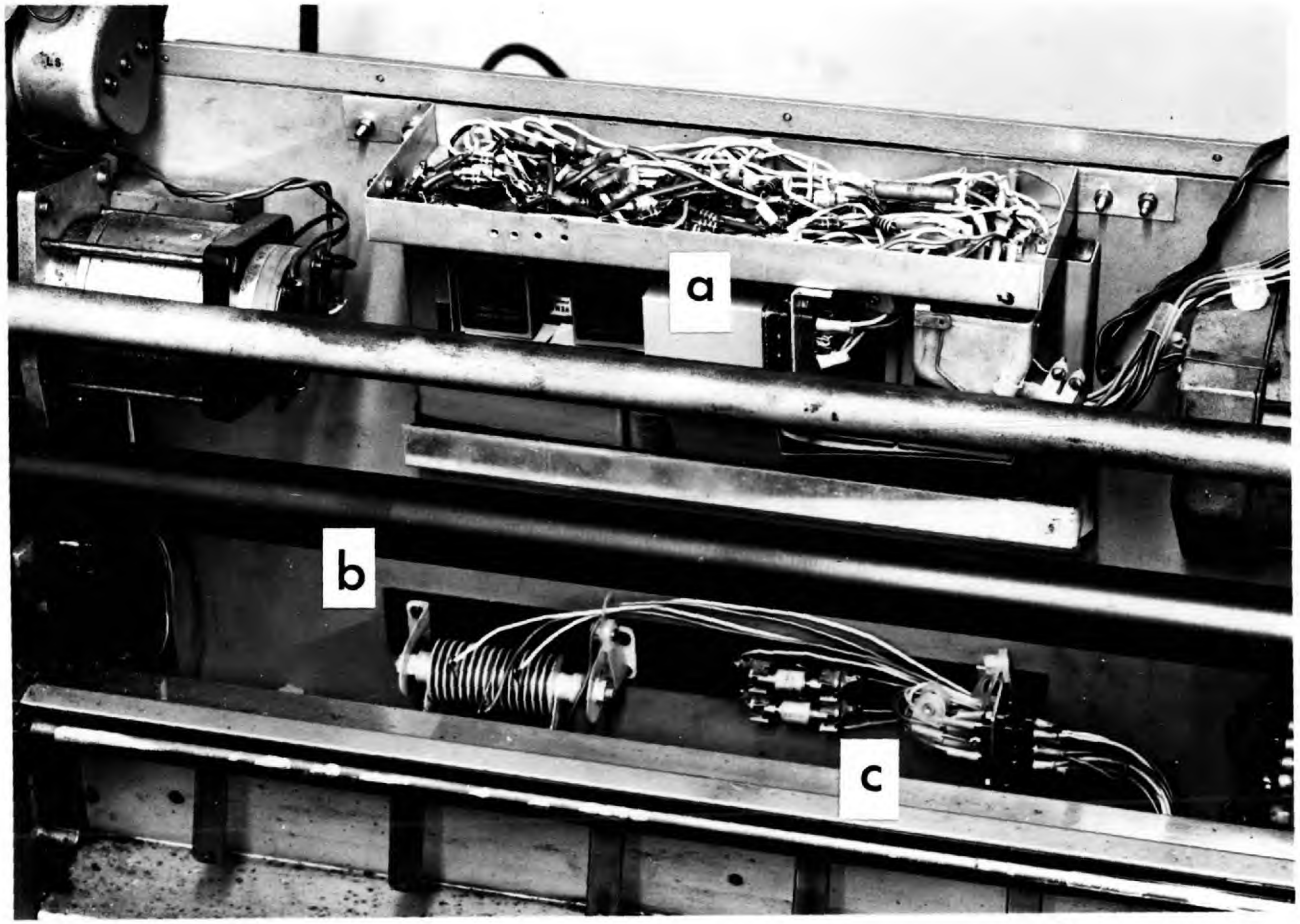

Fig. 4.7. New components installed in the helix chamber.

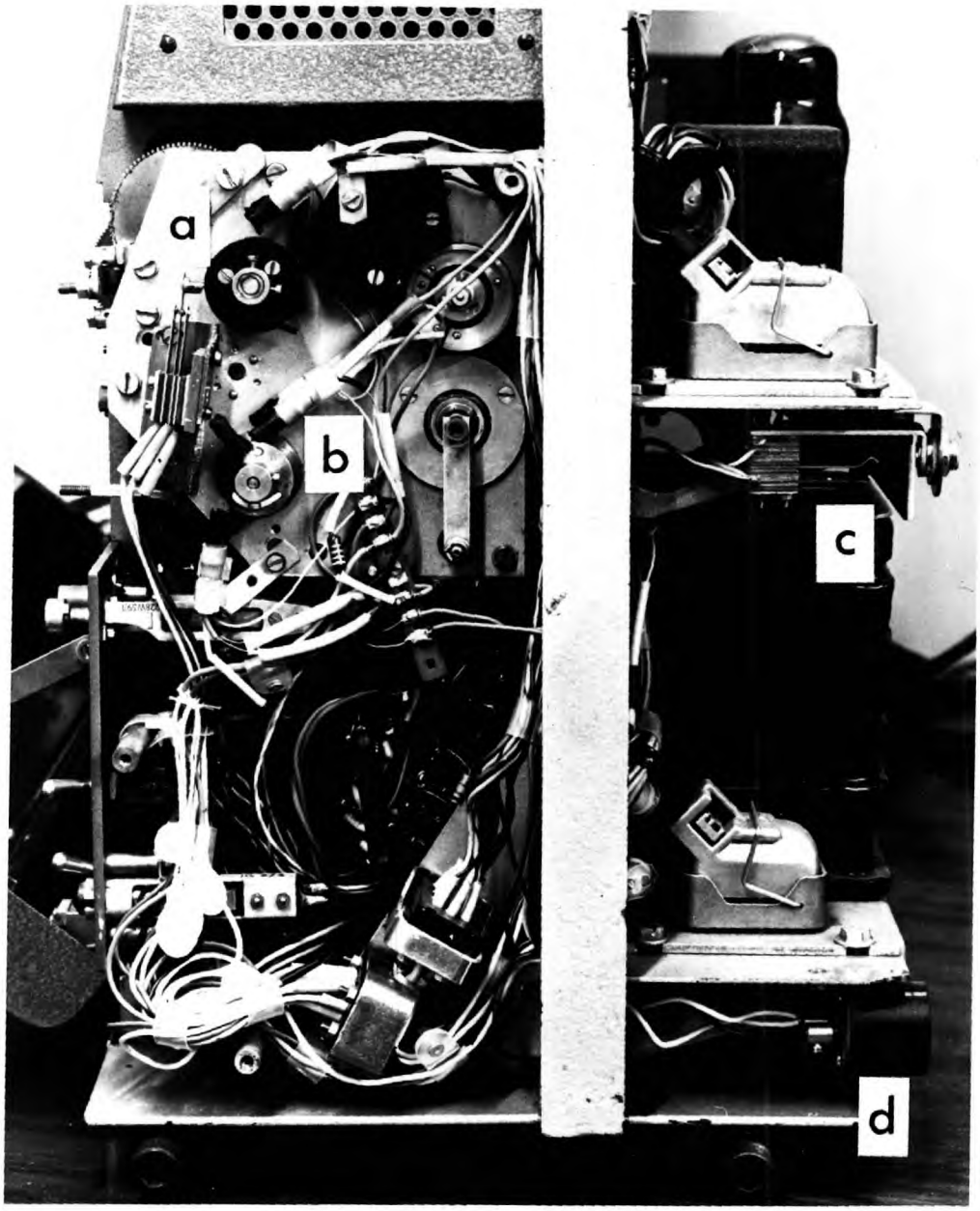

Fig. 4.8. The cams and the photo-cell assemblies, etc.

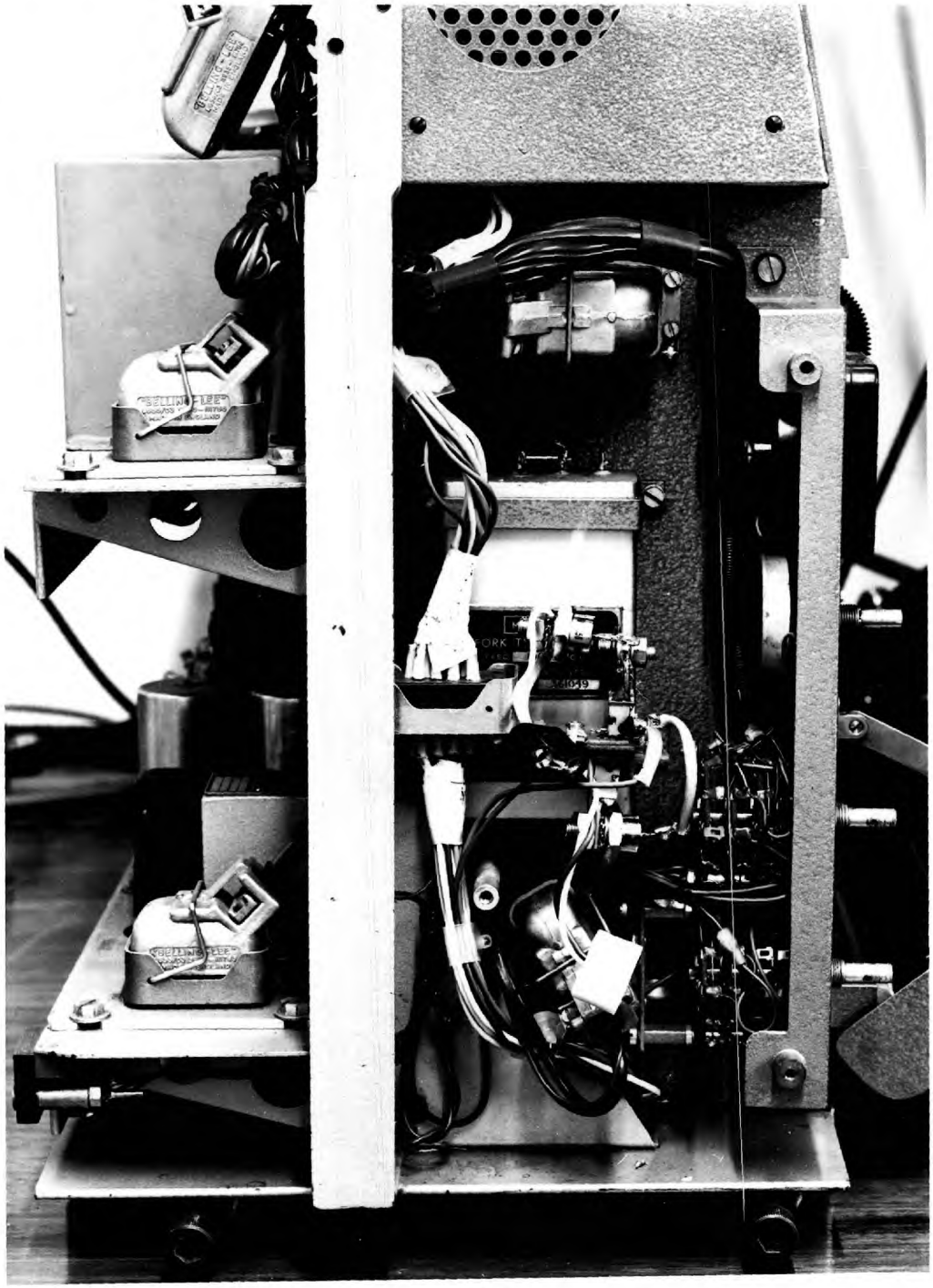

Fig. 4.9. The tuning fork unit, the limiter, and the extra wiring.

4.3.2.5. Change of Rotation Speeds

The original Mufax had three turning speeds: 60, 90 and 120 revolutions per minute. A gear lever was used to select one of three pairs of gears between the driving hysteresis motor and the helix clutch thus changing the speed of the helix. A special pair of gears was cut and fitted into the machine to replace that giving 90 r.p.m., resulting in modified machine speeds of 240, 120 and 60 r.p.m. This modification was carried out with the idea that the profiler might be effectively used in shallow areas with sufficient graphic resolution. On the other hand, this pair of gears, could be readily replaced by another one so that the helix speed could be 120, 60 and 30 r.p.m.

The paper feed drive had a positive linkage with the helix gear and had a separate gear lever for changing the paper feeding motion between normal speed (96 lines/inch) and fast speed (48 lines/inch). Again a change of speed selection into normal (96 lines/inch) and slow (192 lines/inch) is desirable for profile recording. This was accomplished in the same manner as with the helix gear train by altering the ratio of a set of gear in the paper-feed drive system.

A very useful feature of the Mufax chart recorder is the picture shift control. Pressing the picture shift button moves the graphic picture slowly to the left. When this button is pressed, a commutator is connected to the motor amplifier circuit causing an intermittent power flow to the motor. Its average speed is therefore reduced and successive lines of the chart are displaced across the paper as a result of loss of synchronism as long as the switch is operated. During laboratory playback of the profiling signal for the isolation of the various pulses, this feature was valuable because it allowed the feature of interest to be correctly positioned.

4.4. The Synchronized Record/Reproduce System

4.4.1. A Simple Synchronization Method

Li and Taylor Smith (1966 b, Appendix B) have described the general advantage of recording on magnetic tape acoustic data, acquired by continuous reflection profiling. A simple method can be used to obtain synchronism in its reproduction for graphic display free from any distortion caused by tape speed deviation. A reference signal from a precision graphic recorder can be simultaneously recorded on tape with the acoustic data by the use of a 2-channel recording technique. This reference signal can then be used to govern the speed of the graphic recorder during playback. This technique can be applied to any continuous data recording system which employs a precision graphic recorder or similar device. Relatively inexpensive tape recorders can therefore be used to broaden at low cost the scope of any sub-bottom profiling system which employs a precision graphic recorder.

For the present research, this undistorted graphic reproduction facility from tape-stored data is most essential. It is only through simultaneously graphic monitoring that isolation of data of interest can be ascertained in the laboratory. The reason is obvious because the sub-bottom profiling data are collected on a continuous basis. The correction technique and instrumentation of such a synchronized sub-bottom profiling recording and reproducing is described in Appendix B.

4.4.2. The Tape Recorder

A Tandberg model 62 2-track stereo-tape recorder was used throughout for both the collection of data in the field and the reproduction of selected data in the laboratory. This is a direct recording audio recorder with its important technical specifications listed below:

Motor: Hysteresis synchronous motor

Tape speeds: $7\frac{1}{2}$, $3\frac{3}{4}$ and 1 7/8 inches per second. The amplifiers are equalized.

Speed accuracy: Relative accuracy, repeated playback: $\mp$ 0.2%

Frequency response: $7\frac{1}{2}$ ips 30 - 20,000 cps ($\pm$ 3dB)
$3\frac{3}{4}$ ips 30 - 14,000 cps ($\pm$ 3dB)
1 7/8 ips 50 - 7,000 cps ($\pm$ 3dB)

Distortion: The distortion from the record amplifiers at maximum recording level is less than 0.5%
The distortion from the tape recorded with a 400 cps signal at 10 dB below maximum recording level is less than 0.5%, when played back.

Noise level: 58 dB below maximum recording level. Maximum recording level corresponds to 3% distortion.

Crosstalk: The crosstalk rejection is better than 60 dB at 400 cps

Wow and flutter: 0.15% rms, $7\frac{1}{2}$ ips
0.2% rms, $3\frac{3}{4}$ ips
0.3% rms, 1 7/8 ips

For practical purposes this type of Tandberg recorder has a performance standard approaching that required by audio engineers. It must be noted that in all direct recording processes there are two basic limitations, namely the inability to record very low frequencies and the amplitude instability caused by tape drop-outs. However,

the advantages are the ability to record signals having a wide continuous frequency spectrum using practical tape speeds and a wide dynamic range. One of the major applications for the direct-record process is the recording of signals where the significant information is contained in the relation between frequency and amplitude on a logarithmic basis such as in the measurement and subsequent spectrum analysis of noise and underwater-sound signals. Nevertheless, it should be pointed out that there is danger in using an audio recorder as a precision instrument since the signals do not, in general, have the particular spectral energy distribution characteristic of speech or music. The result is that the pre-emphasis in the record amplifier could result in serious distortion of the high and low frequencies. This could only be overcome by reducing the recording level by a considerable amount with resulting deterioration of the signal-to-noise ratio of the recording.

4.4.3. Constant Frequency Unit

The Tandberg tape recorder was not supplied with an internal constant frequency source for the capstan motor. To counter the adverse effects of excessive tape speed variation due to shipboard conditions, the use of an external precision frequency power supply is desirable in order to maintain data quality. For this, a constant frequency power supply unit was assembled.

The constant frequency unit consisted primarily of a 50 cps precision oscillator, and a 200-watt power amplifier. The output and input circuits of these commercial units were modified for

proper matching and a moving-coil meter, indicating the output voltage, was incorporated.

4.4.3.1. The 50 cps Precision Oscillator

A Racend Omega Timer, Type 1001A/1 (manufactured by Dawe Instruments Ltd. to specifications prepared by The Race Finish Recording Company Limited) was selected. It was a 50 cps frequency standard with 330 volt a.c. output which feeded an amplifier capable of delivering 5-6 watts in a 20 Kohm resistive load.

The frequency was controlled through a series of tuned divider stages from a 100 kcps crystal with an accuracy of 0.01%. The stages gave frequency divisions of 5, 4, 5, 5 and 4 respectively.

A self-contained power supply was included, and due to the high stability of the divider stages, neither the H.T. nor L.T. supply was stabilized.

As the original low power of the output was meant to drive an electric clock only, modifications were necessary to match the output to the input of the 200-watt amplifier. A low-level output from the final divider stage was brought directly out through a 470 Kohm resistor. The original power amplifier stage was entirely cut off. Normally 15 minutes were found to be sufficient for the valve characteristics to warm up and to stabilize.

4.4.3.2. The 200-watt Amplifier

This power amplifier was another Vortexion unit which would supply over 200 watts of an audio, or over 120 watts of a continuous, signal with a distortion of 0.2% and a noise level of -95 dB. The

output was 200/240 volt. The input was normally for 1 m.w. on a 600 ohm line, and the unit had a heater, and separate H.T. switches for easy control. This amplifier was arranged for continuous use and, in spite of its power, it remained quite cool. It, complete on its 12 1/4 in. rack panel, was mounted on a console cabinet which had ample lower space to incorporate the 50 cps precision oscillator, and an output voltage meter. To match the output from the timer, the original 600 ohm input impedance transformer was bypassed, feeding the input signal direct to a resistor of 100 Kohm.

4.4.3.3. The Output Voltage Meter.

To monitor the output voltage from the power amplifier in order to protect the tape recorder, a Radiospares Ltd. moving-coil d.c. meter Type MR31 was used together with a meter rectifier for a.c. voltmeter operation. A suitable resistor was chosen to give a full-scale deflection for 300 volts. The properly calibrated voltmeter was then connected across the 200-watt amplifier output terminals, but mounted alongside the oscillator on the lower rack of the console cabinet because of the availability of space. The complete constant frequency unit had a single mains lead, and could supply continuous power at variable voltages through the gain control of the amplifier. A male socket was also installed to replace the original panel jack type output terminals at the centre of the lower front of the console. A picture of this composit e precision power supply unit, together with the Tandberg tape recorder, is shown in Fig. 4-10.

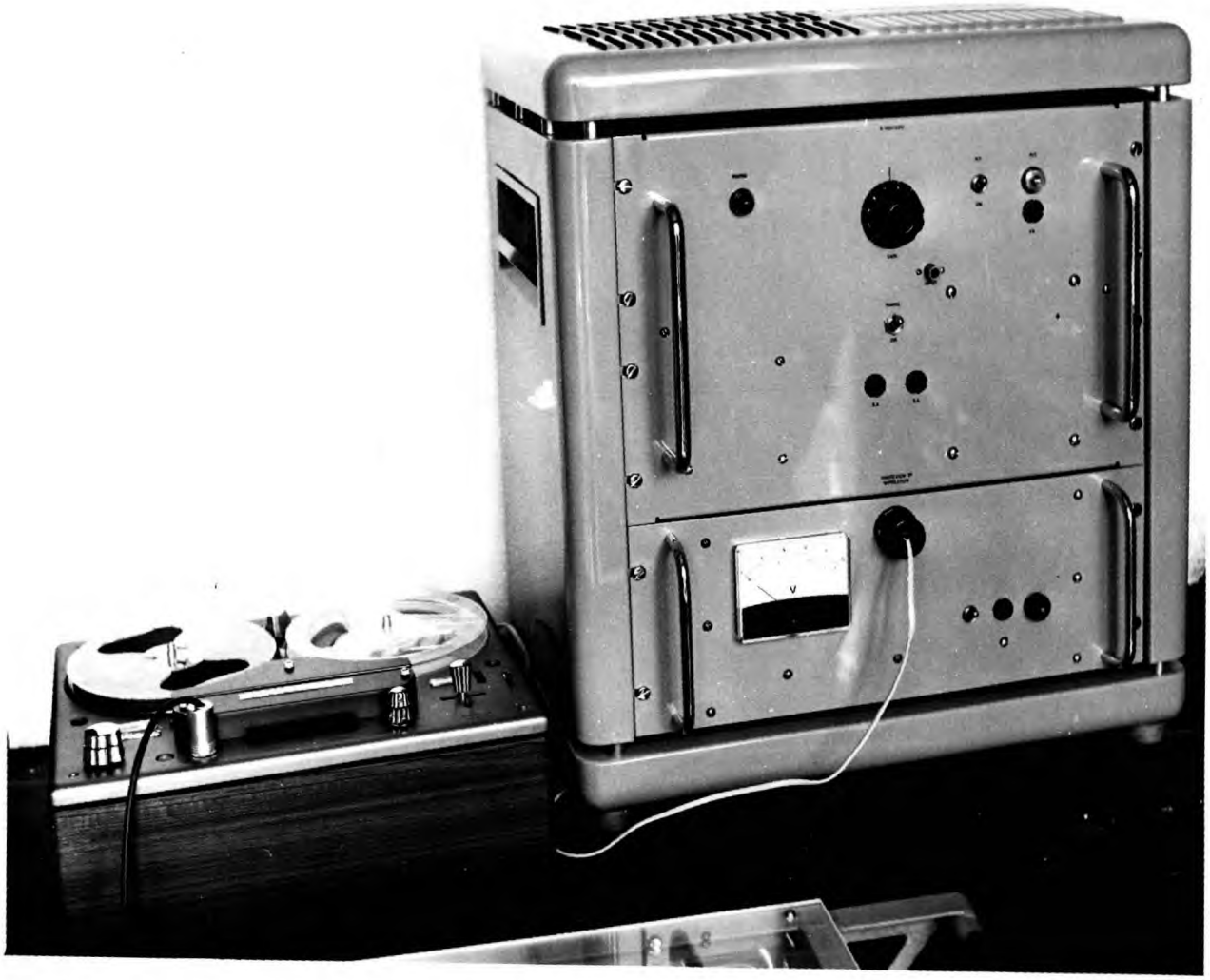

Fig. 4.10. The Tandberg tape recorder with the constant frequency power supply unit.

4.4.4. Additional Advantages

Some of the advantages of the developed system described in this work lies in the inherent characteristics of the modified Mufax recorder. Trigger output for acoustic transmission can be continued during change of recording paper or of the expendable writing blade, resulting in an uninterrupted survey tape recording which can later be played back to fill the gap produced by the interruption. It will, of course, still be necessary to observe that the recording tape and paper do not run out at the same time. This can easily be prevented by changing one of them a little in advance. As for qualitative examinations by reproducing the tape recorded data for graphic display, proper selection of speeds of the helix and of paper feed of the modified Mufax, different from that originally used, can expand or contract the graphic profile either horizontally or vertically, producing the desired degree of signal resolution and correlation.

CHAPTER V

EXPERIMENTAL WORK IN THE IRISH SEA

Work done in the Irish Sea consisted essentially of two parts: (a) instrumentation sea trials, exploratory excursions and reconnaisance west of Holyhead and the Isle of Man, and (b) cooperative seismic investigations in Cardigan Bay with Birmingham University. Of the former, approximately 80 nautical miles of sparker traverses were run, 60 miles west of Holyhead, and 20 miles west of the Isle of Man. Of the latter, more than 360 miles were covered in the 1965 season alone. In addition to these 28 acoustic stations were occupied in selected areas, plus some shipboard conducted instrumental experiments. All positions were fixed by Decca Navigator.

5.1. Features of Sediments in the Irish Sea

The Irish Sea is a shallow tidal sea. Mitchell (1965) has mentioned that the basin of the Irish Sea was formed in the Tertiary epoch and there is some evidence that the final details of the basin were only formed in the Lower Pleistocene. The Irish Sea and the North Sea, as well as some of the larger features of their margins are therefore believed to have been in existence at the beginning of the Ice Age. During the central part of the Gipping Glaciation, ice from Scotland advanced down the Irish Sea, resulting in a sea bed formed of glacial deposits which include wide-spread accumulations of bolder clay, loam, gravel and sand. The matrix of boulder clay of an essentially clayey or loamy nature is derived very largely from the Triassic portion of the bed of the Irish Sea which contains angular and subangular fragments of rocks. The boulder clay may in places contain a few stones or boulders and at some places may be made up almost entirely

of them. Later deposits of Würm age on the sea bed, including that of Cardigan Bay, consisted of shelly calcareous till together with erratics transported from a considerable distance. A number of ridges crossing the floor of the sea are described as moraines of the last glaciation.

There is little quantitative information about the sedimentation processes operative on continental shelves or shelf seas, although it has been possible to show that around the British Isles small differences between the peak speeds of ebb and flood tidal currents determine the direction of bed transport (Stride, 1963). It is believed that no appreciable deposition has occurred over large shelf areas from the end of the post-glacial transgression. Variations in sediment type usually occur due to differences in the conditions of transportation and deposition of the contributing material in different localities. The distribution of recent sediments in the Irish Sea by tidal currents which, due to changing sea level and basin dimensions, is probably in a state of gradual modification, indicates that the recent sedimentary history is complex. It is also possible, that late-glacial to post-glacial fine grained lacustrine deposits interpose between the glacial floor and the upper marine muds. A number of workers have taken grab or dredge bottom samples. A general result of these dredgings and grabbings on the sea bed is that the surface sediments are often Pleistocene deposits consisting largely of reworked boulder clay. The glacial deposits which blanket much of the rock floor of the Irish Sea now either lie buried beneath possible younger sediments or beneath a thin layer of residual reworked glacial material. Belderson (1964) describes the sediments in the western half of the northern end of St. George's Channel as coarse sand and gravel, and in the eastern half as gravels mixed with sand or muddy sand, consisting largely of residual reworked glacial deposits. He has also claimed that Holocene mud up to 100 ft. thick surrounded by

muddy sands and with a belt of sand to the south, has accumulated southwest of the Isle of Man. A chart indicating the distribution of sea floor surface material is shown in Fig. 5-1 (after Belderson). The Holocene sediments of the western Irish Sea occur as a lens shaped body occupying a basin overlying Pleistocence material. Using cores, echograms and oblique asdic records, together with British Admiralty survey charts his investigations also reveal the limits of the extensive belt of large sand waves situated at the northern end of St. George's Channel.

An earlier seismic reflection and refraction survey in the northern part of Cardigan Bay conducted by Blundell et al. (1964) indicates that the top layer is composed of material with seismic velocities in the range of 5,000 ft/sec to 6,000 ft/sec of presumed Pleistocene to Recent origin. Caston (1966) has reported that the correlation of known sedimentary deposits with their characteristic acoustic reflection has enabled an oblique asdic equipment to be used as a means of broadly identifying the bottom material. His findings on the extent and boundary of mud, sand, and undifferentiated gravels in part of Cardigan Bay has confirmed and supplemented the information he gained by bottom sampling. It must be pointed out here that the reliability of his oblique echo-sounding 'calibration' method is debatable (Taylor Smith & Li, 1966, Appendix C) and that his sample analysis results are confined to the very superficial part of the sea floor.

5.2. Field Procedures

5.2.1. Instrumental Trials and Reconnaissance Surveys

During and after the development of the new record/reproduce sub-bottom profiling system, instrumental trials and exploratory sub-bottom surveys were carried out in the motor boat "Insula" chartered by the Marine Science Laboratories, University College of North Wales, mainly

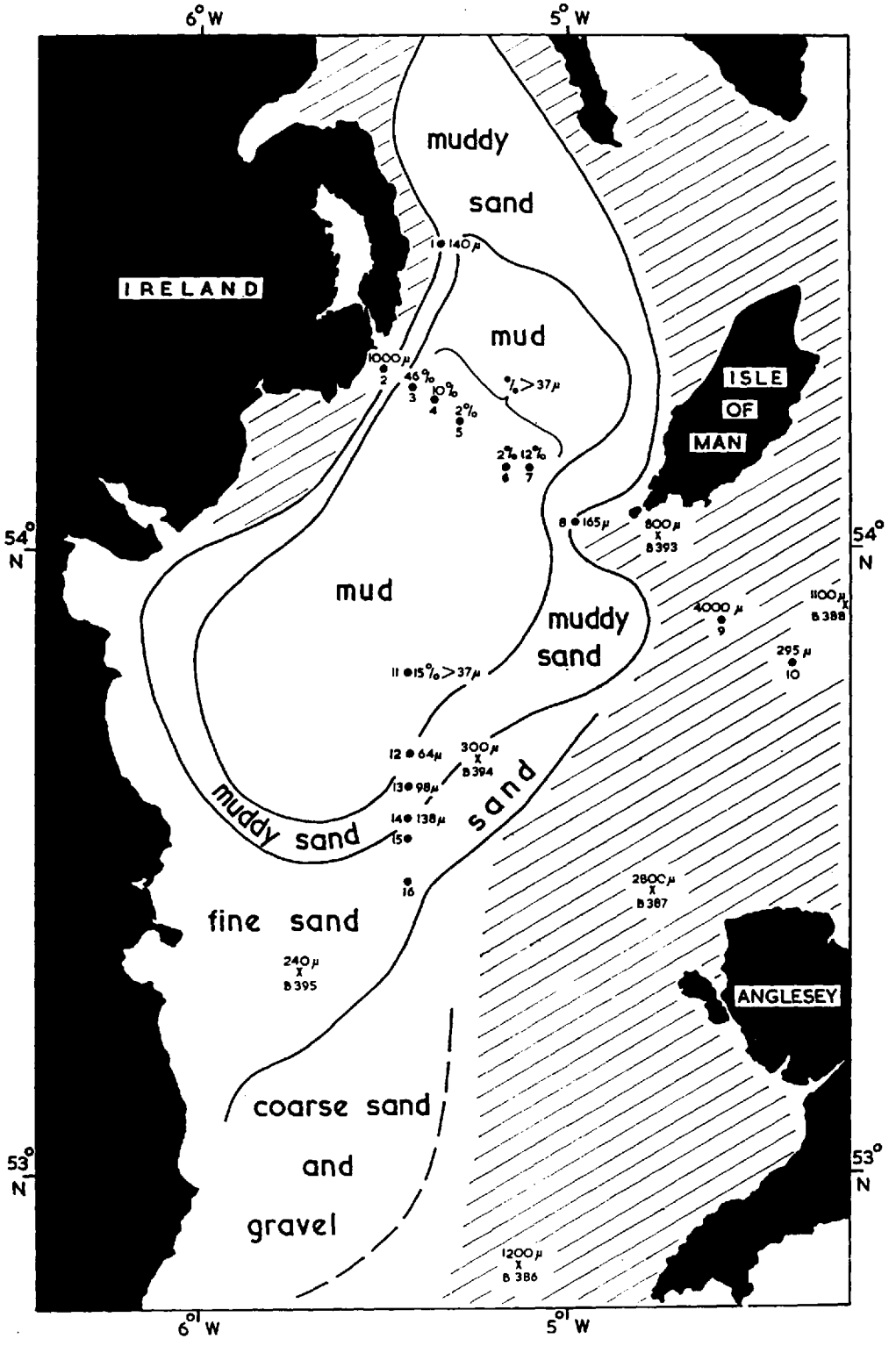

Fig. 5.1. Distribution of sea-floor surface material, the western half of the Irish Sea (after Belderson).

for carrying out a benthic fauna investigation project in the Irish Sea. "Insula" is 65 ft. long, with a net tonnage of 20.4 originally built as a motor fishing boat. Owing to a projected voyage planned by the owner of two and a half years with the Commonwealth Islands Expedition her fish-hold was converted into a combination of sleeping berths and laboratory space. This conversion has produced a small ocean research vessel whose engine is capable of making $7\frac{1}{2}$ knots. During the present experiments, an extra echo-sounder and a Decca Navigator were installed.

In the initial period when the various parts of the new profiling system were separately tested, reconnaissance surveys with a view to locating good sub-bottom reflectors were made mostly around the Holyhead Deep west of the Holy Island. Bottom samples using a bucket dredge were collected in various locations in conjunction with the bottom fauna investigation programme. The Alpine sparker low-power equipment was used at the same time. The outcrop of rock from loose overlying material of varying types and layer depths in the western part of the Holyhead Deep was clearly detected from the graphic profiles obtained. On one occasion when the sub-bottom traverse was extended into the central part of the Irish Sea, the sub-bottom reflecting horizon beneath large sand waves in a trench area was observed. For all these excursions, the boat was based at Holyhead and trips were made on a day-return basis.

After the instrumentation trials of the developed record/reproduce profiling system proved to be successful, an exploratory continuous sub-bottom profiling survey from Menai Bridge to Howth in Ireland, and from there to Peel in the Isle of Man, then back to Holyhead was contemplated. However, continuous bad weather prevented this plan from being carried out and an alternative shorter route had to be taken.

South of the Isle of Man, Jones (1951) has distinguished four types of deposit, the limits of which are believed to be mainly fixed by wave

action and the strength of the tidal current, namely: coarse sands, gravel including shell, and stony ground, (b) fine sand, (c) muddy sand, and (d) mud, all within a radius of 15 miles from Port St. Mary. Based on these findings a track was then chosen passing near the Calf of Man heading NNW, going well into Belderson's Holocene mud area, then turning east into Peel.

Eventually, unfortunately, rough seas marred the early part of this reconnaissance survey and the final acoustic stations during the return trip. In fact, the research vessel was held up in the port of Peel for four days because of the duration of a severe gale.

Due to the generally unfavourable state of the sea and the instability of the boat during this latter survey, excessive pitching and rolling made the towing abeam of the Sparkarray source and Rocket hydrophone unfeasible. Instead the Sparkarray was towed some 70 ft. astern with the Alpine magnetostrictive hydrophone further astern. This arrangement proved to be quite satisfactory, achieving an effective surveying speed of more than 6 knots even in a moderate sea. The layout of some of the instrumentation of the receiving side of the new system inside the shipboard laboratory is shown in Fig. 5-2.

5.2.2. The Combined Surveys in Cardigan Bay

In 1965 in continuation of their seismic investigations of the rocks beneath Cardigan Bay, the Birmingham Geology Department required a comprehensive continuous sub-bottom profiling survey over the entire Bay to obtain more precise thicknesses for the uppermost layer (Blundell et al, 1964) in order to supplement their seismic refraction and reflection velocity survey. The successful development of the record/reproduce sub-bottom profiling system could best serve this purpose giving more exact layer boundaries. This was the first combined Sparker and seismic refraction

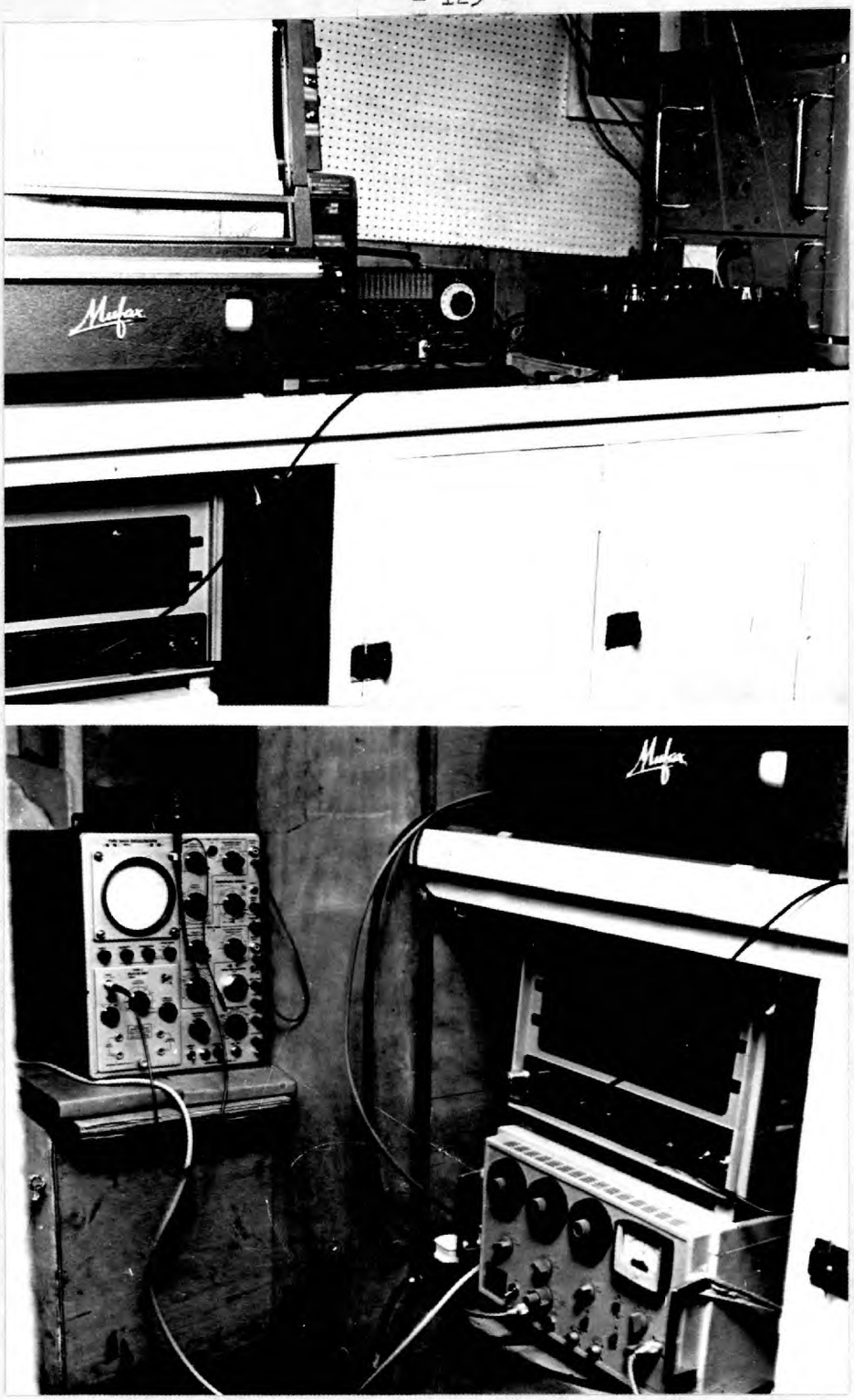

Fig. 5.2. Some sub-bottom profiling equipment on board M.V. "Insula".

and reflection survey in Cardigan Bay.

A coaster vessel, M. V. 'Jonrix'was chartered for 35 days starting in the latter part of August, 1965. "Jonrix" is a boat designed for home trade 188 ft. long with a net tonnage of 599 tons. Two main cargo holds forward of the navigation bridge were emptied for this period and equipped for the survey. In order to provide extra safety, the forward hold was used exclusively for the storage of dynamite for the seismic survey while temporary benches were set up on the two sides of the aft hold, one for the sonobuoy signal recording system and the other for the sub-bottom profiling system. Field work at sea consisted of a series of weekly cruises from Fishguard Harbour.

When sonobuoy work was not carried out, the sub-bottom profiler was operated day and night on a watch system by members of the scientific party whenever weather permitted. Despite adverse weather conditions which cut short the available boat-time for work, sparker traverses of varying separation effectively covered the entire Bay, including the occupation of a number of acoustic stations solely for the present experiments.

Both the hydrophone (E. G. & G. Rocket type) and the Sparkarray were mounted on one side of the ship 4 - 6 ft. beneath the water surface depending on the ship's speed. The hydrophone was guided outward at an angle from the ship's bow by a supporting rod and towed just slightly away from the bow wash turbulence to reduce noise. The Sparkarray, with its two steel rods attached, was suspended by one of the ship's cargo booms some 35 ft. aft of the hydrophone. The actual arrangement of these transmitting and receiving elements when the vessel was underway is illustrated in Fig. 5-3 showing the front part of the port side of the ship. Here H indicates the hydrophone rigging and S the suspension of the Sparkarray, with both the elements being immersed beneath the surface.

Fig. 5.3. Sub-bottom profiling arrangements alongside M.V. "Jonrix".

In the summer season of 1966, another similar survey in continuance of the seismic project was again conducted by the Birmingham team, chartering this time a sister ship of "Jonrix" the M. V. "Kenrix" for the work. The members of the scientific party, being familiar with the operation of this new profiling system, extended the profiling beyond Cardigan Bay into St. George's Channel. During this second season only a few deep-water transmission-and-reception experiments for measuring the direct arrivals from various kinds of spark sources were conducted in direct connection with this investigation.

5.3. Tracks Covered

The tracks covered in the three areas mentioned in the previous section are best illustrated with the actual traverses recorded in situ from the Decca Navigator and replotted on charts. The event marker was impressed on the profile produced by the graphic recorder whenever a reading of position, usually every five minutes, was taken. In the case of simultaneous recording by magnetic tape when the record/reproduce system was used, the indication of the tape reel revolution counter was also noted down to facilitate the selection of tape-recorded data for later reproduction. Liason between the instrumental control and the navigation bridge for time marking was either by the use of synchronized chronometers or by means of a small intercommunication system.

Fig. 5-4 is a chart showing the reconnaissance tracks covered with the use of the Alpine profiler west of Holy Island and Fig. 5-5 shows the tracks of the exploratory survey west of the Isle of Man, using the developed record/reproduce system. Ten acoustic station sites are also indicated in Fig. 5-5, the short straight line being the drift of the boat during the periods of station acoustic recording and which varied from some 7 to 20 minutes.

Fig. 5-6 is a comprehensive seismic traverse chart of Cardigan Bay

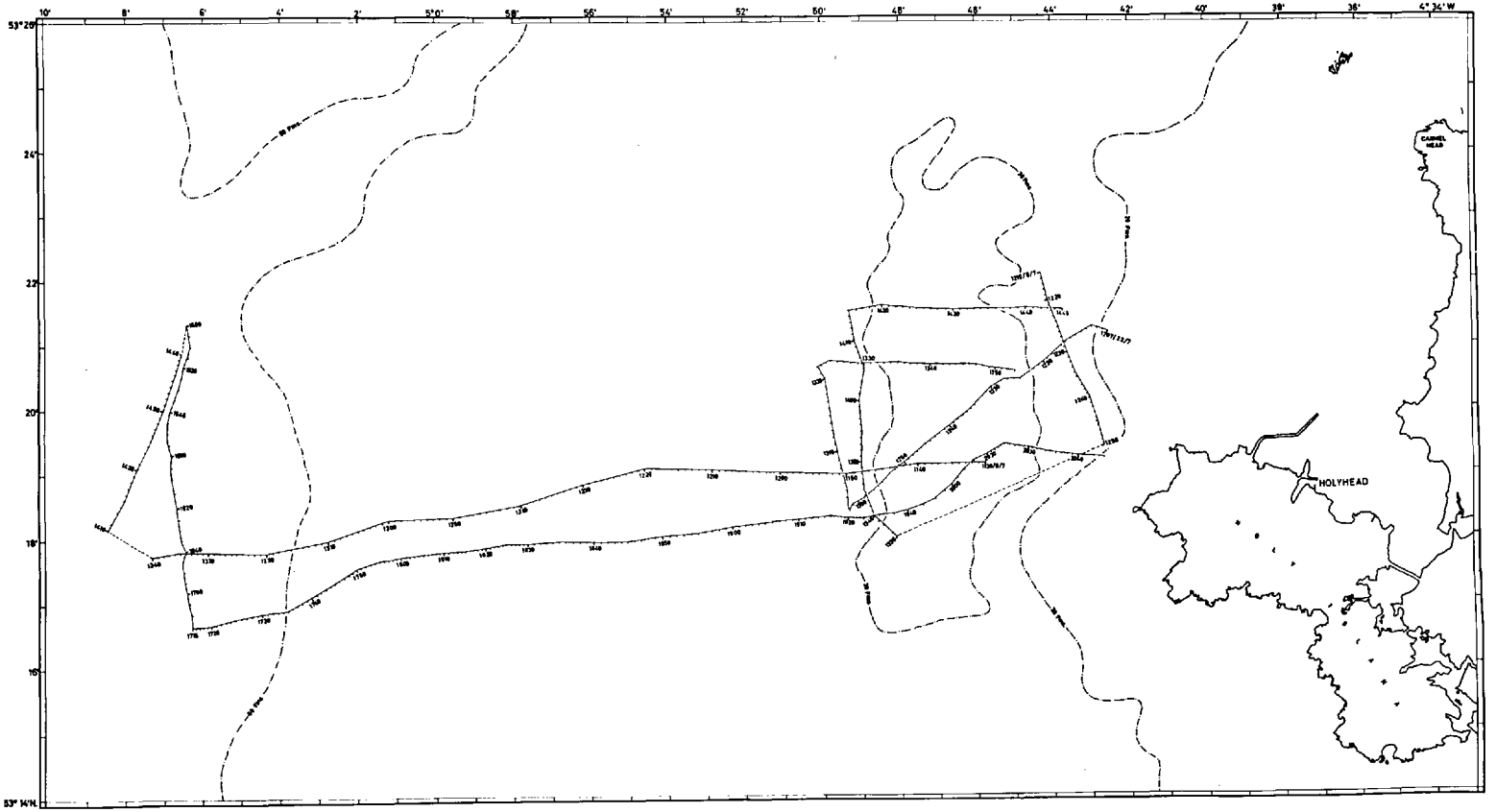

Fig. 5.4. Sparker traverses, west of the Holy Island.

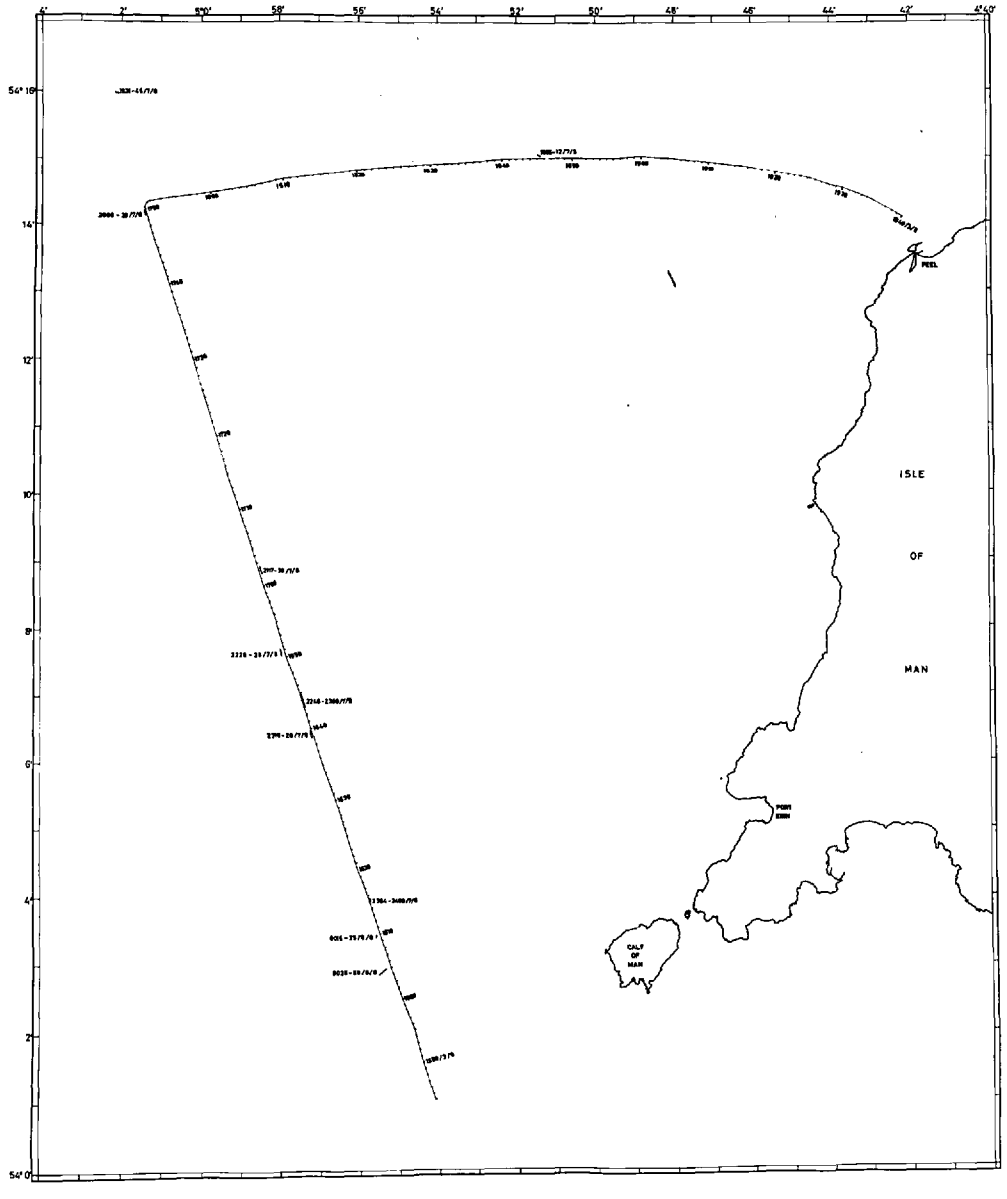

Fig. 5.5. Sparker traverse, west of the Isle of Man.

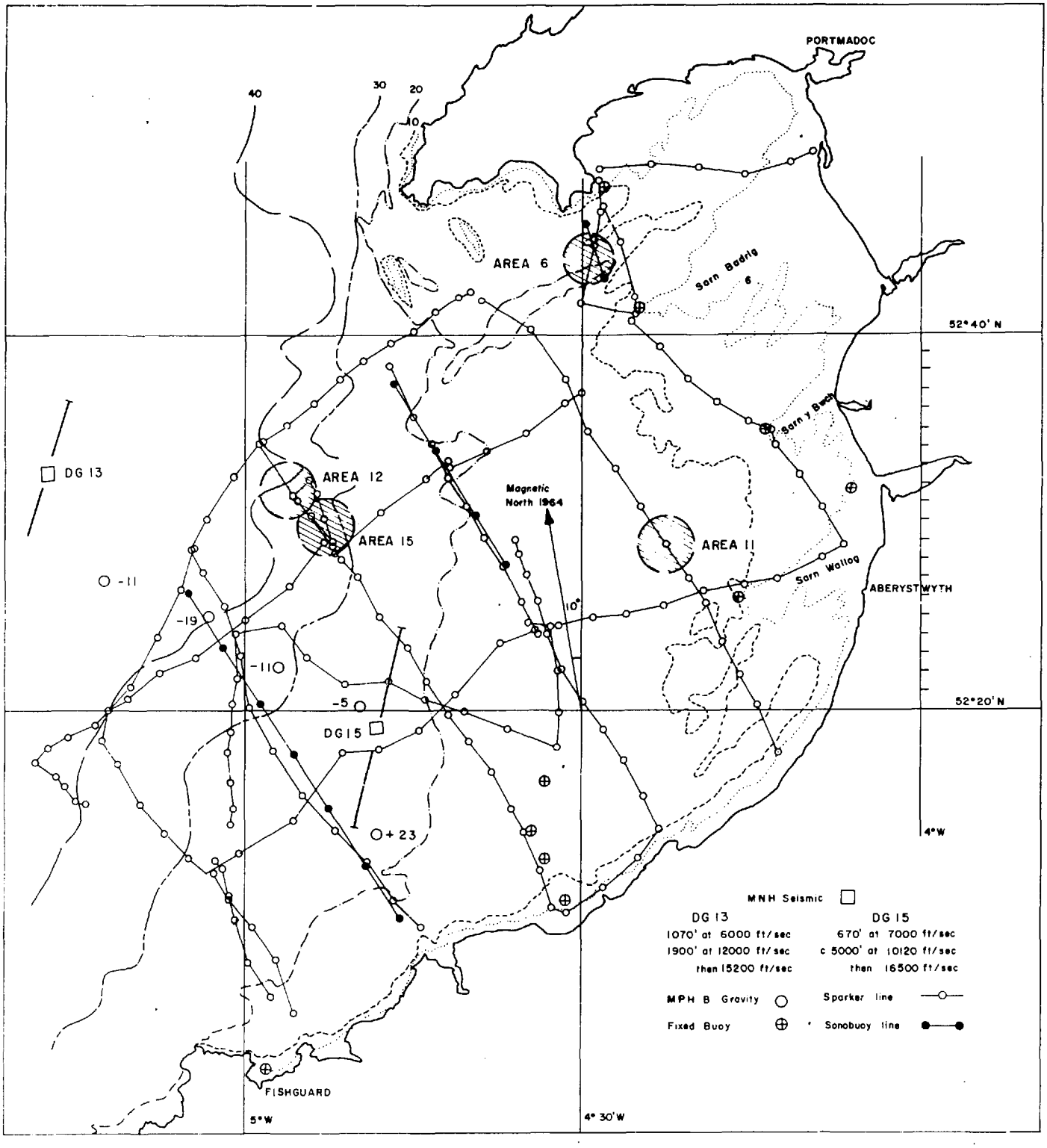

Map of Comprehensive Marine Geophysical Surveys in Cardigan Bay up to the Season of 1965 (after the University of Birmingham). Fig. 5.6.

up to the season of 1965 prepared by the Geophysics Section of the University of Birmingham. The positions of acoustic stations are not indicated in the chart but the four areas chosen, Area (15), Area (12), Area (11) and Area (6) for subsequent data analysis are enclosed in circled marks.

Small inaccuracies exist in all the positionings because of the errors inherent in the general Decca chains navigation system despite the choice of the best lane combinations in any investigated particular area. However, this small error does not have any significant bearing on the results of the present investigations.

5.4. Discussion of Some Sub-bottom Profiles

5.4.1. The Processing of Sub-bottom Profile

Much of the interpretation of the continuous sub-bottom profiling records was straight forward. The records are essentially a vertically exaggerated profile of the geological structure underlying the survey ship's track. The horizontal scale is a linear time scale whose linearity in horizontal distance depends on the constancy of the survey ship's speed; while the vertical scale is essentially a vertical reflection time scale except when the depth of the reflector becomes comparable with the source-receiver separation, a situation which occurs with shallow reflection events and a correction has then to be made. Except for the more steeply sloping reflectors, the correction for migration of dip will be small.

As mentioned previously (Chap. II, Sec. 2.7.1.) signals received from a given reflecting horizon at depth do not appear as a single event on the profile record but as a short sequence of events whose total length depends on the length of the initial pulse from the source plus the lengthening effect of the various paths involving reflection at the free surface. Also, there is a single bubble pulse following each spark. The sound energy of the

bubble pulse is comparable with that of the initial spark shock. In terms of reflection events, the bubble pulse reflection from a given horizon occurs adjacent to but later than the initial reflection by an amount approximately proportional to the spark source energy.

The recorder may be adjusted to show either half-wave or full-wave rectification of the incoming signal. The effect is illustrated in Fig. 5-7. With full-wave rectification the half cycles are dark bands and with half-wave rectification the dark bands are followed by white bands thus resembling the recordings made with the conventional variable density seismic recording system. Half-wave rectification is generally found to be more appropriate for exploration purposes and has been used throughout. On half-wave rectified records, the phenomena of surface reflections and the bubble pulse will, therefore, usually consist of several recognizable events following the initial reflection. When the corresponding time intervals are long and the signal-to-noise ratio of the deep-reflected arrivals is small then the use of the automatic gain control amplifiers, because of the automatic adjustment of sensivity, tends to smooth out the density contrast and results in poor resolution. Automatic gain control was never used during the profiling; instead the limiting function of the recorder was found most useful in examining weak signals.

It is generally known that optimum filtering has a profound effect in revealing any particular structures of interest. Good examples of this are shown in Figs. 3 and 4 of Appendix C published by Taylor Smith and Li, (1966) where the effect of frequency in accustic sounding is discussed in some details. However, it should be pointed out here that the use of half-wave rectification without any previous filtering is in effect a sort of high frequency cut off filtering process in itself. Referring to Fig. 5-7, any high frequency components of relatively small amplitude superimposed as

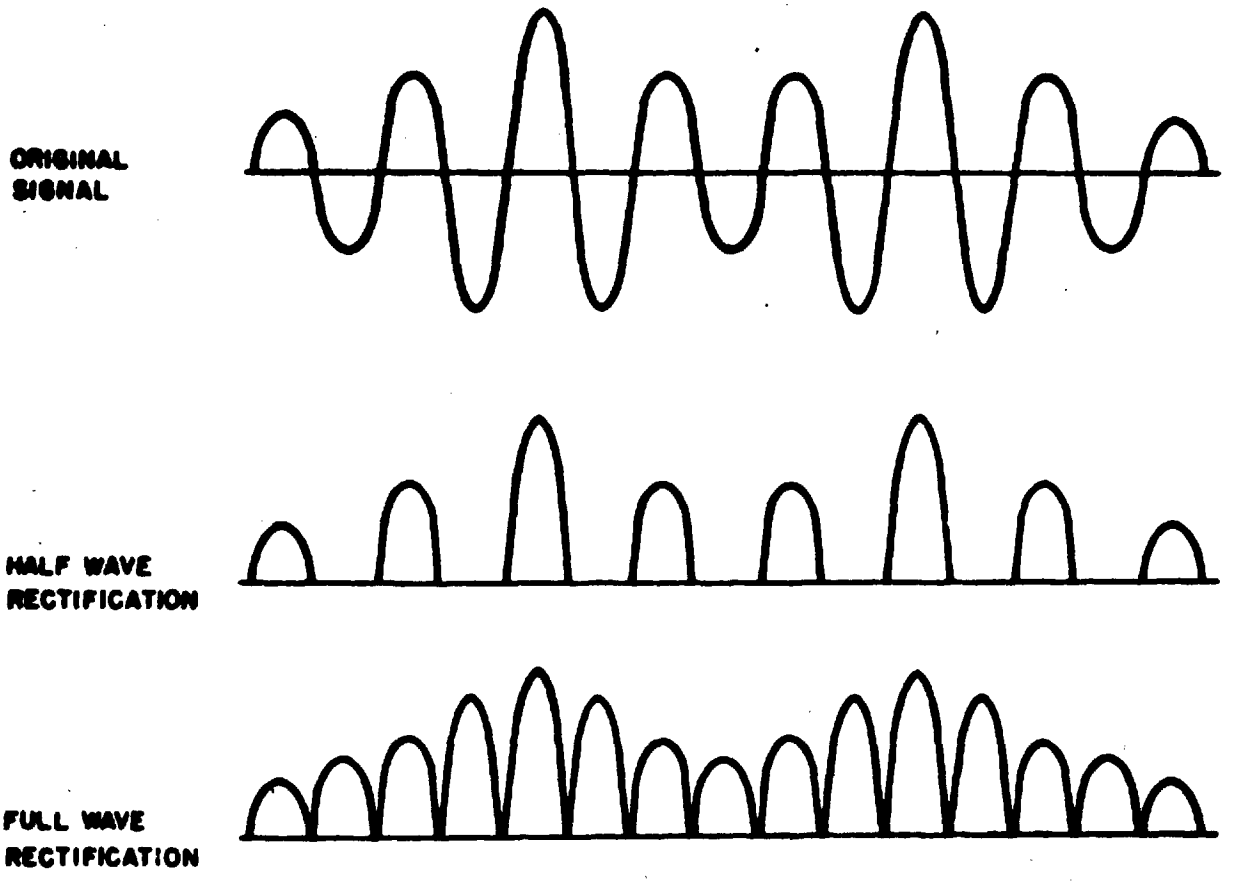

Fig. 5.7. SIGNAL RECTIFICATION

a ripple on the low frequency signal will be printed out combined with the low frequency signal as dark bands as though the high frequency were not there at all. On the other hand, a certain amount of ringing can never be entirely eliminated whenever a band-pass filter is used to process transient pulses. This is why in some instances the unfiltered reflection signal with half-wave rectification will produce an overall better quality sub-bottom profile record. Good demonstrations on this particular feature can be observed in Fig. 7-11 and Fig. 7-14 in Chapter VII where further discussions and comparisons will be made.

5.4.2. Incidental Geological Findings.

As indicated earlier in Chapter I,the aim of the present study is the development of the sonar instrumentation system to make the equipment more versatile in describing the sea-floor conditions. The study involves an assessment of the feasibility of combining a spectral analysis and a statistical treatment of reflected energy fluctuations for this purpose. Except in the sub-bottom profiling surveys carried out in Cardigan Bay and forming a part of Birmingham University comprehensive geophysical investigations of that and other related areas, the geological findings during the instrumental trial and reconnaissance profiling runs were more incidental than intentional. No attempt will be made to relate this incidental information in detail with the known regional marine geology. Nevertheless, this incidental information is described as it may be of value in other studies.

5.4.2.1. West of Holy Island, Anglesey

Of the three, day-return exploratory excursions west of Holyhead, Holy Island, (see Fig. 5-4) two of these were made to seek the unconsolidated sediment layers in the Holyhead Deep region. As a result, inside the Holyhead

Deep a boundary of some 5 miles between loose sediments to the west and rocky bottom to the east was delineated. The boundary line was located approximately along the north-south centre line of the Deep, the western portion being covered by a varying thin layer grading from shelly sand to very fine clay. This layer extends continuously westward with increasing thickness into the central part of the Irish Sea. But the sub-bottom reflection obtained by the Alpine equipment was not always satisfactory in following or distinguishing the sub-bottom horizons. Patterns of internal structure of the presumed loose sediments were also generally observed.

In one of the surveys into the extreme northern end of St. George's Channel a series of ridges were located in a north-south run over a depression of more than 75 fathoms deep. From bottom samples obtained these were composed predominantly of coarse sand. Harvey (1966) interpreted these ridges as large sand waves, typically some 45 ft. high from trough to crest. The significant finding on this profile was the discovery of a roughly horizontal sub-bottom interface at a depth, on average, of some 90 ft. below the mean elevation of the ridges. The information on the sub-bottom basement, should it be further extended, would certainly shed more light on the factors responsible for these sand waves.

5.4.3.2. The Traverse West of The Isle of Man

During the single long profiling traverse to the west of the Isle of Man (see Fig. 5-5) using the record/reproduce system, a few interesting features were indicated in the records. In the southernmost portion of this track passing through the bottom sampling area investigated by Jones (1951), no distinct layering in the superficial deposits was observed. But again the samples collected were at the very top of the superficial material. Instead

very contorted and interesting deeper layering was observed such as that shown in Fig. 5-8. This represents a typical sub-bottom profile and may possibly be an indication of the highly irregular successive glacial erosions and boulder clay depositions generally related to this area.

In that part of the traverse west of Port Errin, a profile reproduced from tape is shown in Fig. 5-9. Eastwood (1963) has reported that there is a considerable variety of intrusions of basic dykes distributed generally but not uniformly over the Manx slate tract. Also mentioned are the existence of a few Tertiary dykes near the south western part of the island coast running in a NW - SE direction. It has been suggested that the last connection of the Isle of Man with the mainland was during Glacial times. It may well be that the profile shown in Fig. 5-9 could be interpreted as an intrusion of a dyke swarm or of faulting either as local features or extending off-shore from the island.

Fig. 5-10 is a section near the eastward turn of the traverse on the NNW part. Accumulated unconsolidated sediments can be seen overlying a more or less horizontal but unevenly reflected sub-bottom structure. This is inside the Holocene mud area described by Belderson. A sample by dredging collected at an outlying station north of this part has indicated the muddy nature of the surface sediment. However, deeper internal stratification both contorted and uncontorted, not mentioned by Belderson, can still be observed in this top layer. Contention about this point concerning instrumentation capabilities, especially regarding frequencies used, has been put forward by Taylor Smith and Li (1966, Appendix C).

5.5. Selection of Sites for Investigation

The ideal place for carrying out this type of research would be where the marine geology is firmly established by sedimentary colum bore-hole

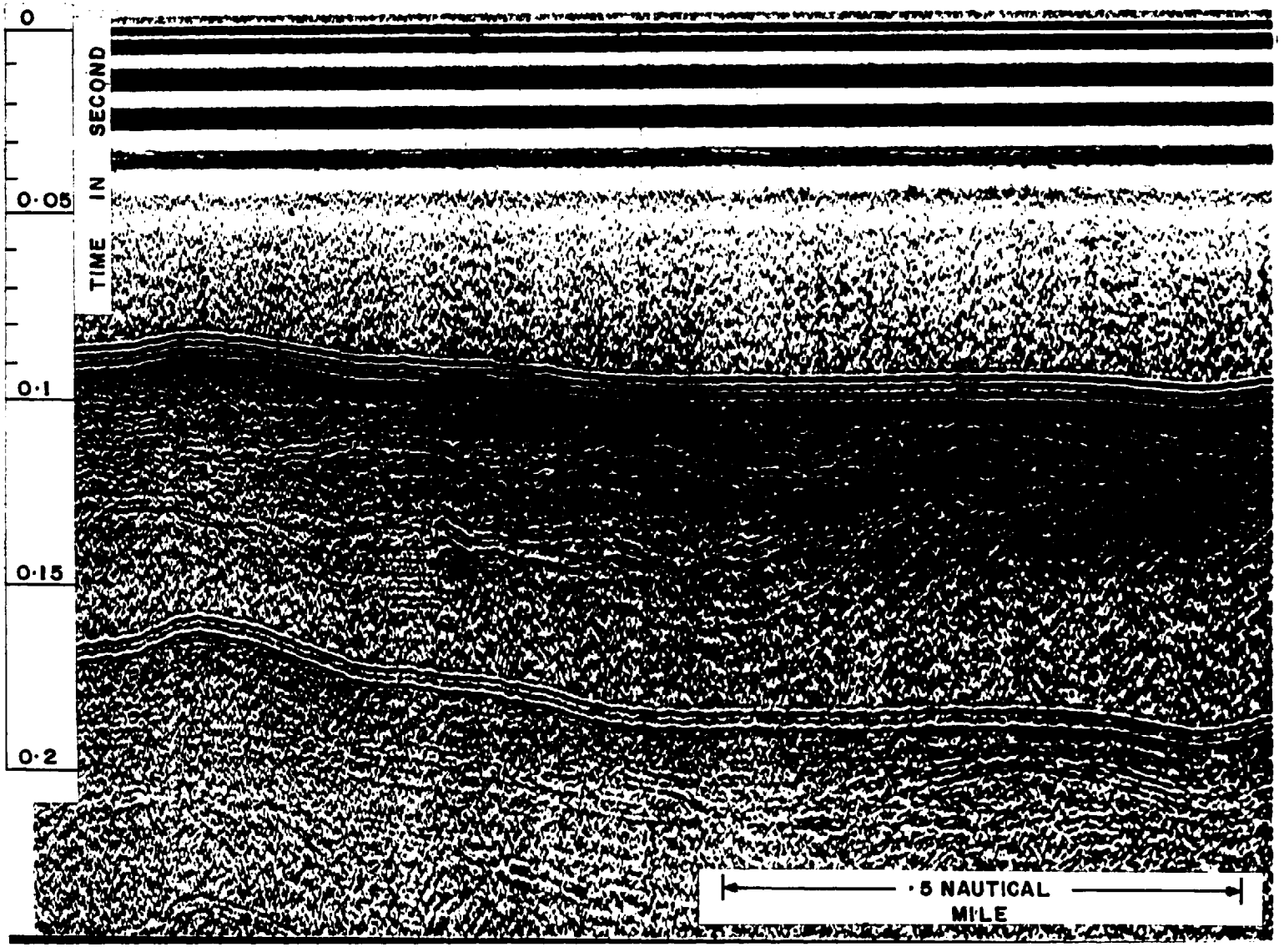

Fig. 5.8. A sub-bottom profile, SW of the Isle of Man

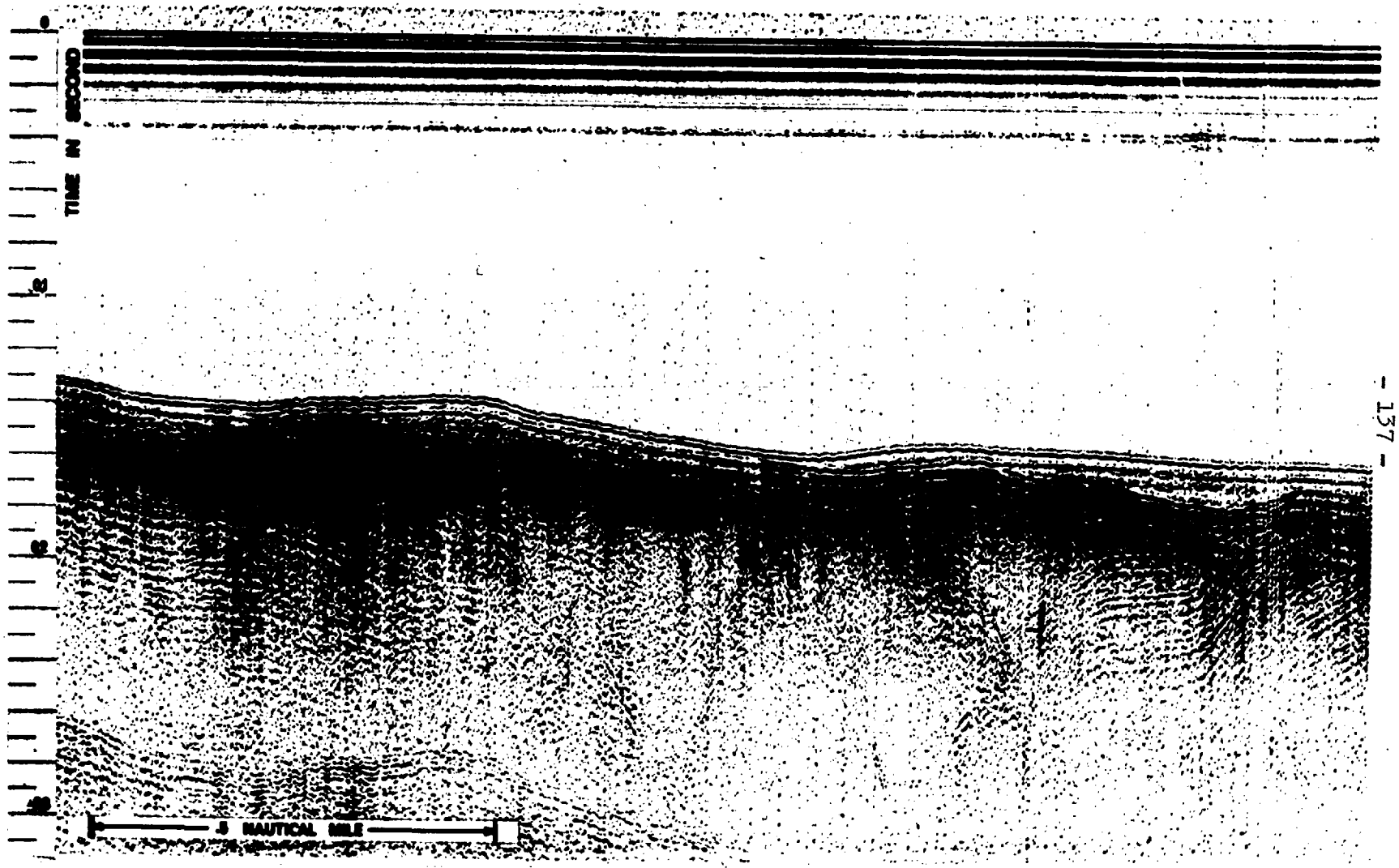

Fig. 5.9. A sub-bottom profile, west of Port Errin, Isle of Man.

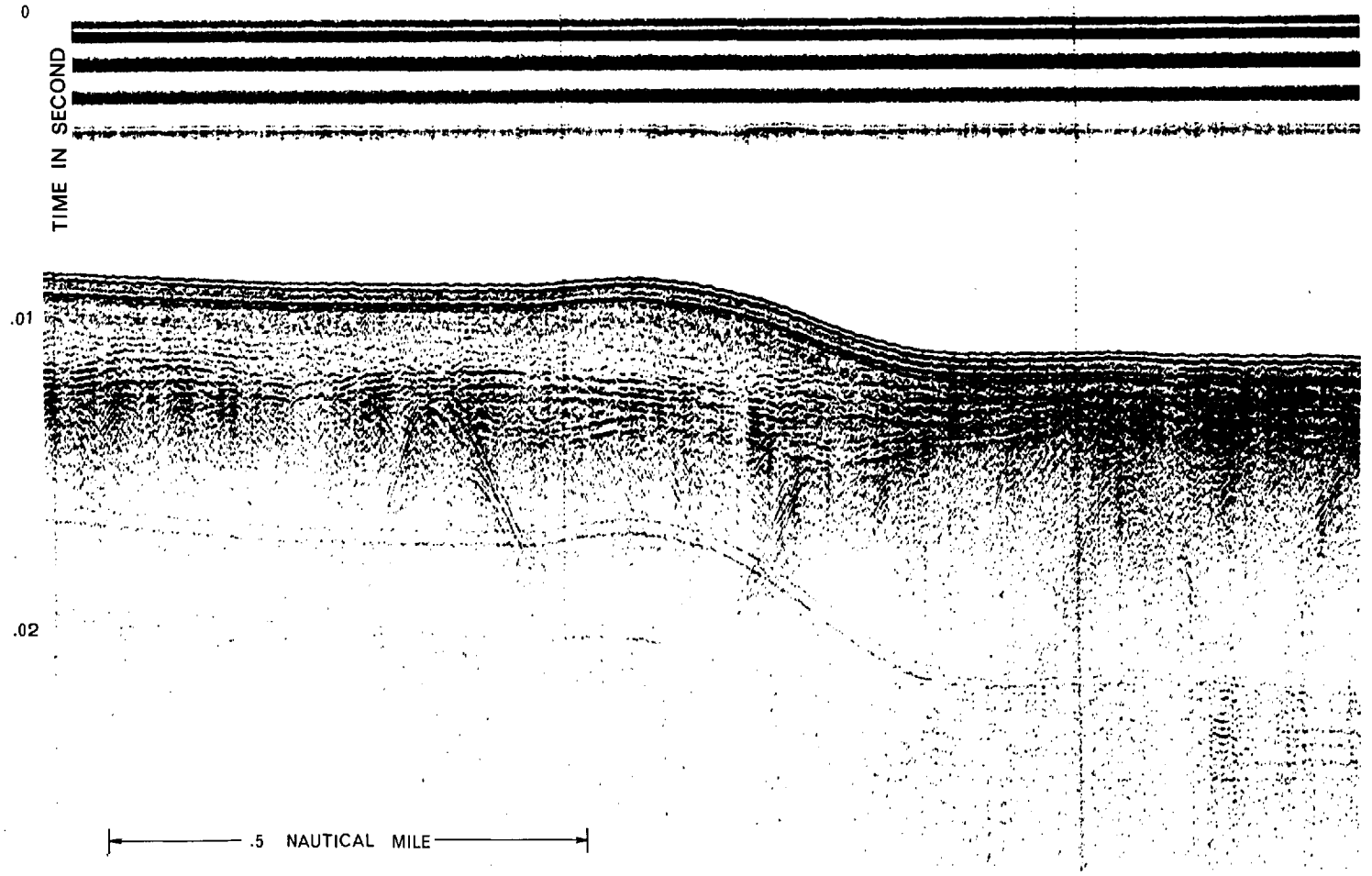

Fig. 5.10. A sub-bottom profile, west of Peel, Isle of Man.

control with zones of homogeneously distributed sediment in layers of varying thickness of a particular type overlying material with a pronounced velocity discontinuity, thus more or less conforming to one of the situations shown in Fig. 2-4 of the simplified models. Further field areas could then be selected where the situation is identical to the above except that the sediment grade is changed.

As mentioned earlier in Section 5.1., most of the sea floor in the Irish Sea consists of Pleistocene boulder-clay, a mixture of sand, mud, shell and gravel with various interstratified patterns upon part of which may rest variable quantities of later sediments. This can hardly be regarded as a suitable area for carrying out research such as this based on a theoretically developed approach, particularly when geological control such as bore-hole data is totally lacking. However, it cannot be entirely ruled out that certain places in the general area might still possess a sub-bottom of good reflecting quality upon which rest a wedge-shaped layer of more or less homogeneous sediment of one grade or another. The problem was that during the present research period, no research vessel was freely available to carry out an extensive and uncertain investigation solely for site assessment.

The boat time available for sub-bottom acoustic measurements was necessarily associated with two other research projects of the Marine Sciences Laboratories and Birmingham University respectively, when vessels were available. From all the acoustic data collected, portions were selected which matched as nearly as possible the idealized assumptions and at places where either the composition of the surface sediment or the layer velocity were known through other workers. In view of the circumstances detailed and the trial nature of both the instrumentation and methods of the research the choice of provisional experimental grounds was extremely restricted.

During the Alpine Sparker surveys west of Holyhead, the newly developed record/reproduce system was still in an instrumental trial stage and hence no tape recordings were made of any of the exploratory profiling traverses in this area. Bottom samples taken in connection with benthic fauna studies indicated too great a variety of bottom material and in addition, clear-cut sub-bottom reflectors were seldom observed except near the sand wave region in this part of the Irish Sea. Therefore it was decided not to re-investigate this region with the record/reproduce system.

The track west of the Isle of Man was surveyed with the record/reproduce system. Based on the profile record obtained 10 acoustic stations and one bottom sample collection station were occupied, but the generally contorted sub-bottom structures discovered and the comparatively thin sediment layer on top deviated greatly from the ideal experimental situation required. Better profiling records with the advantage of some geological control were found later in surveys in Cardigan Bay and indicated that this area might show promise as a suitable experimental area.

However, these profile records indicated that the Cardigan Bay area was not completely able to match the essential requirements of the basic models despite some excellent sub-bottom records showing penetration in the range of 900-1,500 ft. below the sea floor. Places were selected, nevertheless, from the survey records from traverses where prominent sub-bottom reflections were indicated. Consideration was also given to the requirement of a varying first layer depth so that at least three sites with different thicknesses were chosen within a small area where there was an obvious continuation of the prominent sub-bottom structure, and to areas with a second sub-bottom or multiple reflecting sub-bottom horizon. Since all traverses had Decca position fixes recorded at 5-minute intervals

as a standard practice, the geographic coordinates could be readily determined.

The main advantage in analysing data obtained in the Cardigan Bay region is that independent information was available concerning the textural analysis of the superficial sediments as well as the approximate velocities obtained through seismic work in the general area. It is certainly a great pity that the stations occupied eventually proved to be unsatisfactory. The analysis of the acoustic data extracted from actual surveys over four areas only (circled in Fig. 5-6) has rendered this investigation necessarily a rather limited one.

5.6. Acoustic Stations

It was first decided that in order to obtain successive reflections from a very confined portion of a bottom or sub-bottom reflecting surface, the sound source and the receiving element must be maintained at a relatively fixed position for the transmissions. This is preferable because variations in spectral characteristics obtained from a series of successive reflections could then be statistically averaged out without introducing error due to lateral variations of the bottom.

During the reconnaissance survey west of the Isle of Man ten acoustic stations were taken. In the combined survey of Cardigan Bay, eighteen stations were occupied.

5.6.1. Station Procedures

When occupying a station, it would be preferable if the boat could anchor and remain stationary. In practice, this proved to be most difficult and the attempts made were not successful. In the case of the boat "Insula", the size of the boat and its anchoring facilities could not cope with the

situation of anchoring out in the Irish Sea. Even in the case of the ship "Jonrix", the prevalent windy weather and the current pattern in Cardigan Bay during most of the survey period were such that the anchoring operation in any part of the Bay would have been hazardous. Besides, anchoring in the condition encountered would have entailed rapid swinging of the ship. There was also a time factor involved as the ship's time allocated for the acoustic part of the investigation was limited, particularly, after the great reduction of the overall available time due to adverse weather during the period. It was finally decided to occupy the acoustic stations with the ship hove-to.

As both the Sparkarray and the hydrophone were slung over the sides of the boat and maintained by overhead ropes at their respective positions in the water, no changes were needed for taking an acoustic station. In actual practice, in Cardigan Bay, the stations were occupied between surveying traverses whenever the ship was in a position near to the site of interest, thus keeping the time required for station work to a minimum.

When the ship was hove-to at a station, some ten minutes continuous recording was made on the tape recorder. At the same time graphic recording was also maintained to monitor the operation. In any event, the operation of the Mufax recorder was essential for triggering the transmission as well as for providing the 1kcps time reference. While hove-to, the Decca position fixes were recorded every two minutes instead of the usual five for normal survey. This gave a closer check on the ship's drift while at a station. Except for the ship's manœuvering in getting onto a station, the whole station recording operation was not much different from that of the normal survey with this sub-bottom profiling system. Unfortunately, nearly all the stations were occupied during a state of moderate sea.

5.6.2. Station Results

After all these efforts made in preparing and establishing the acoustic stations, the reflection data was not extracted for laboratory analysis, because of the poor results obtained. Some of the adverse effects were immediately obvious even in the field, others were only realized after review and analysis of the data in the laboratory at a later stage. The acoustic stations failed for the following reasons:

1. In moderate sea or, for that matter, in most sea states, a ship when hove-to will tend to roll at a wider angle than when underway. With the over-the-side rig-up arrangements of the Sparkarray and the hydrophone, recording on station resulted in poorer correlation between successive reflections because of the signal coeherence being upset by the variation in the surface reflected pulse as well as the overall path length due to variation in submersion.
2. Precisely relocating a previously recorded Decca position and maintaining a stationary position with reference to the sea floor proved to be extremely difficult for the surveying boat. There were the inherent errors in the Decca Navigator system in the first place and any residual momentum of the boat when it reached the station site could carry it for a considerable distance. Furthermore, wind and current, especially the latter, could have a pronounced influence on the ship's actual movement. Manœuvering of ship's engine could

lessen the drift to a certain extent but it was not easy to control it to a satisfactory degree. As the ship's engine was stopped to cut down the background noise during observation, the drift was not controllable. In the event, the drifts at most of the stations were so large that the station recordings were practically traverses made at slow speed (at times up to 3 knots).

3. There was a steady increase of submersion under the sea surface of both the Sparkarray and the hydrophone independent of the ship's rolling when the boat was drifting as compared to when underway. This varied from 1 to 3 ft., depending on the current and the actual conditions under which the drift took place. This further changed the appearance of the graphic profile when compared with that of a normal survey.

All the above reasons have led to a considerable uncertainty concerning the bottom and sub-bottom reflecting horizon thus recorded. It was doubtful if the records so obtained were directly comparable with those obtained during the reconnaissance for the selection of the sites, particularly in the probable difference of actual positions. After looking through all the station records, it was decided that data for the pulse spectrum analysis should be taken directly from the actual survey recording instead. Fig. 5-11 shows the comparison between a better-than-average station record (b) and the original profile (a) from which the station site (marked with an arrow) was chosen. It must be noted that the vertical scales in (a) and (b) are different, the total vertical length of the former being $\frac{1}{2}$ sec. and of the latter 1 sec. Drifting at the station can be readily seen.

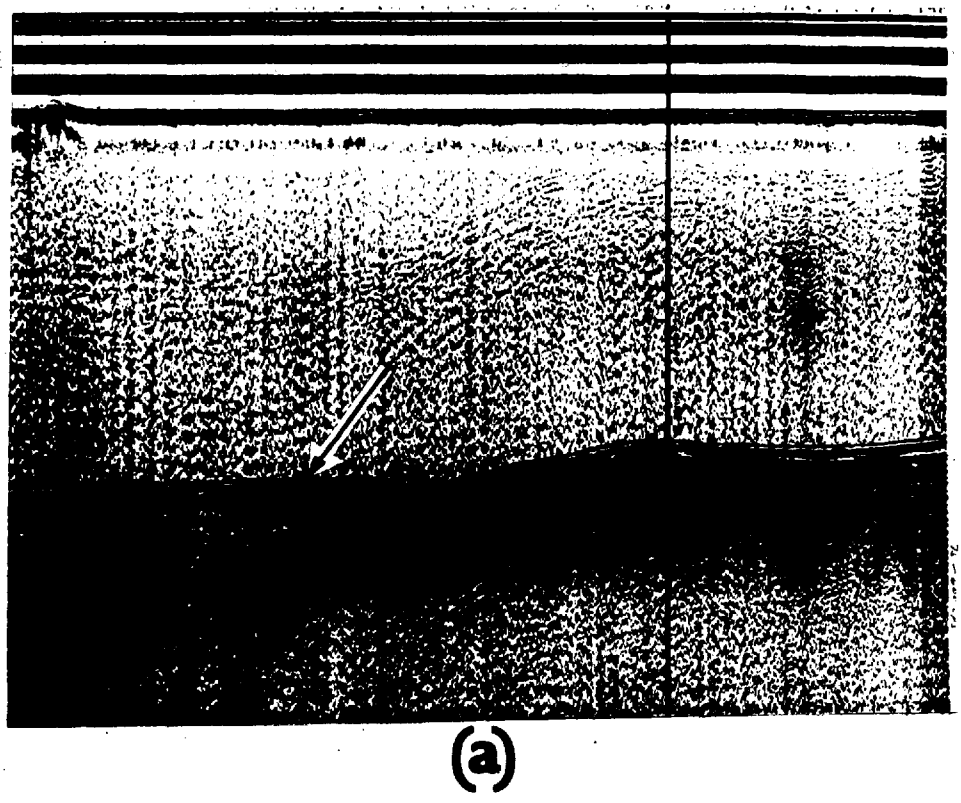

(a)

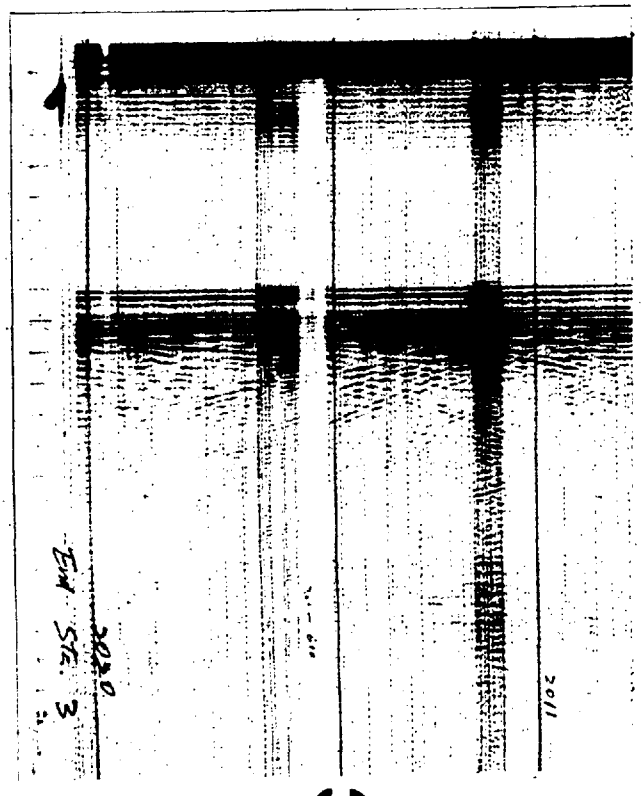

(b)

Fig. 5.11. Comparison between a sub-bottom profile and an acoustic station record.

On the other hand, analysis of data taken from actual survey recording provides the inherent advantage suggested by the proposed method. Because of continued correlation of the reflection data, acoustic interfaces can be picked out and interpreted with positive certainty. It is obviously more convenient in application since no special arrangements are necessary to occupy a station and maintain the boat stationary. Although a special fixed station can provide a quieter platform with reduced ambient noise for the possible recording of the weaker sub-bottom reflections, the difficulties encountered far outweigh this advantage.

5.7. Free-Field Observation of the Spark Pulse

Experiments conducted for the measurements of the direct arrivals were carried out by placing both the transmitting transducer and the receiving hydrophone well below the water surface and at the same time well above the sea bottom in locations with adequate depth of water so that the direct signal could be positively isolated from the surface reflected (or ship's hull-reflected) and bottom-reflected pulse trains thus allowing the measurement of intensity due to direct transmission before the arrival of energy travelling along other paths.

Using the record/reproduce profiling system, recordings were made on magnetic tape over a short period with continuous transmissions in a manner similar to normal surveying. The boat, as a floating platform, was usually left drifting as long as no shallow area was approached.

In the experiments with the Sparkarray as the acoustic source the long transducer frame was suspended vertically with the centre electrode at a depth of about 80 ft. beneath the surface together with the hydrophone with a horizontal separation of some 25 ft. Thus the hydrophone, on a line at right angles to the array would receive a pulse identical with that which

would travel down to the sea bed in the course of a normal survey.

Often during actual surveys, particularly, at night, sparking could not be observed at one or two of the three electrodes. It was decided to investigate the acoustic effect by first firing all three electrodes, then two, and then only one. The candle type electrode not used was effectively sealed at its exposed end by Bostick, a quick-setting water-tight cement. It was therefore necessary to haul up the Sparkarray when the number of firing electrodes was changed. This investigation found an interesting relation between the number of firing electrodes and the corresponding effective pulse characteristics.

Similar experiments were carried out with the adjustable-gap electrode designed earlier. The pulse characteristics of the direct arrivals were recorded over a range of gap-width.

A 1 in. barium titanate ball hydrophone calibrated above 2 kcps and which was loaned by the Admiralty Underwater Weapons Establishment, Portland was frequently used during some of the fixed station work as well as in the direct arrival measurements. However, it did not prove to be very successful, primarily because of the problem of proper matching to the receiving system. One cause might be that this hydrophone was supplied with only 60 ft. of cable. The necessary lengthening of this cable would modify its calibration figures as well as presenting a complex matching possibly requiring underwater preamplification of the received signal. The E. G. & G. hydrophone was therefore used throughout.

The operation of signal isolation from the data tape, its transfer to a tape loop, and its subsequent analysis is discussed in Chapter VI dealing with laboratory work. The results of the analysis discussing all the experimental results is given in Chapter VII.

CHAPTER VI

LABORATORY APPARATUS, PROCEDURES, AND METHODS FOR DATA ANALYSIS

6.1. General

To analyse the various reflected pulses stored in a continuous reflection profiling tape record, it is first of all necessary to extract the various events of interest with precision timing. At the same time, means must be found so that the total useful frequency content of each pulse can be measured. Additional laboratory apparatus must, therefore, be specially designed or acquired while particular procedures and methods geared to the instrumentation system must be developed.

Generally speaking, complex wave forms appear either as continuous signals in a steady state or as transients which may or may not recur. For the rapid and methodical analysis of continuous complex wave forms, the heterodyne receiver with provision for automatic scanning to obtain the spectral distribution of levels with frequency is mostly used. To carry out an analysis of signals of the transient type, such as the various arrivals in a profiling tape record, it is, however, essential that the signal input to the analyser be made repetitive. One way of achieving this is to obtain a tape recording of the signal and joint the ends together. The tape loop thus formed can be replayed and the amplified signal fed to such an analyser of the above type. For short transient data

transcribed and stored in a comparatively long loop, there exists the problem of realising a full spectral result. To obtain a spectrum analysis of such brief acoustic data, it is most essential that the signal be examined at each frequency of interest. However, if a proper relationship between the tape loop-time and the analyser sweep-rate is chosen, the data sample can pass through one heterodyning filter bandwidth for each circulation of the tape loop, resulting in a full-spectrum output just as though the sample were continuously recorded throughout the loop. This basic method was used for all data processing in the present experiments.

Suitable sections of the tape record, selected on the basis of the visual Mufax record, were transferred through a specially developed signal isolation gating unit to a closed loop magnetic tape and continuously presented via a Ferrograph tape recorder, to a heterodyne type sonic spectrum analyser manufactured by Singer Metrics. Except for a digital analysis and the use of a 1/3 octave narrow-band filtering system to check the results of one set of data, this system was used throughout.

6.2. Apparatus

The apparatus used in the laboratory for data analysis consists of the recording equipment of the developed record/reproduce sub-bottom profiling system, some general laboratory equipment, and a few instruments devised or acquired especially for the present work. Two main procedures were followed to obtain the experimental results. These were the isolation of data of interest from a continuous record of magnetic tape and the subsequent extraction of information from

the isolated data.

Fig. 6-1 shows a general view of the equipment used for the analysis. The equipment is numbered in the photograph as follows:

(1) precision 50 cps power supply
(2) Allison variable band-pass filters
(3) Venner electronic counter-timer
(4) Tektronix storage oscilloscope
(5) Dowe white-noise generator
(6) Sola constant voltage transformer
(7) Marconi precision wide range oscillator
(8) Tandberg 2-channel tape recorder
(9) Vortexion power amplifier
(10) Solartron pulse generator
(11) Tektronix time-mark generator
(12) Mufax precision graphic recorder
(13) Singer sonic spectrum analyzer
(14) Avo oscilloscope camera
(15) Ferrograph 2-channel recorder with endless tape loop cassette
(16) signal-gating switch

The Tandberg tape recorder (8), driven by the precision power supply (1), was used solely for play back in the laboratory. The variable band-pass filters (2), the power amplifier (9), and the Mufax recorder (13) were used, just as in the field, for producing the graphic record. The Tektronix storage oscilloscope (4) was employed to observe direct signals as well as for spectral displays. The white-noise generator (5), the time-mark generator (11), and the oscillator (7) were used to facilitate calibrations. A signal-

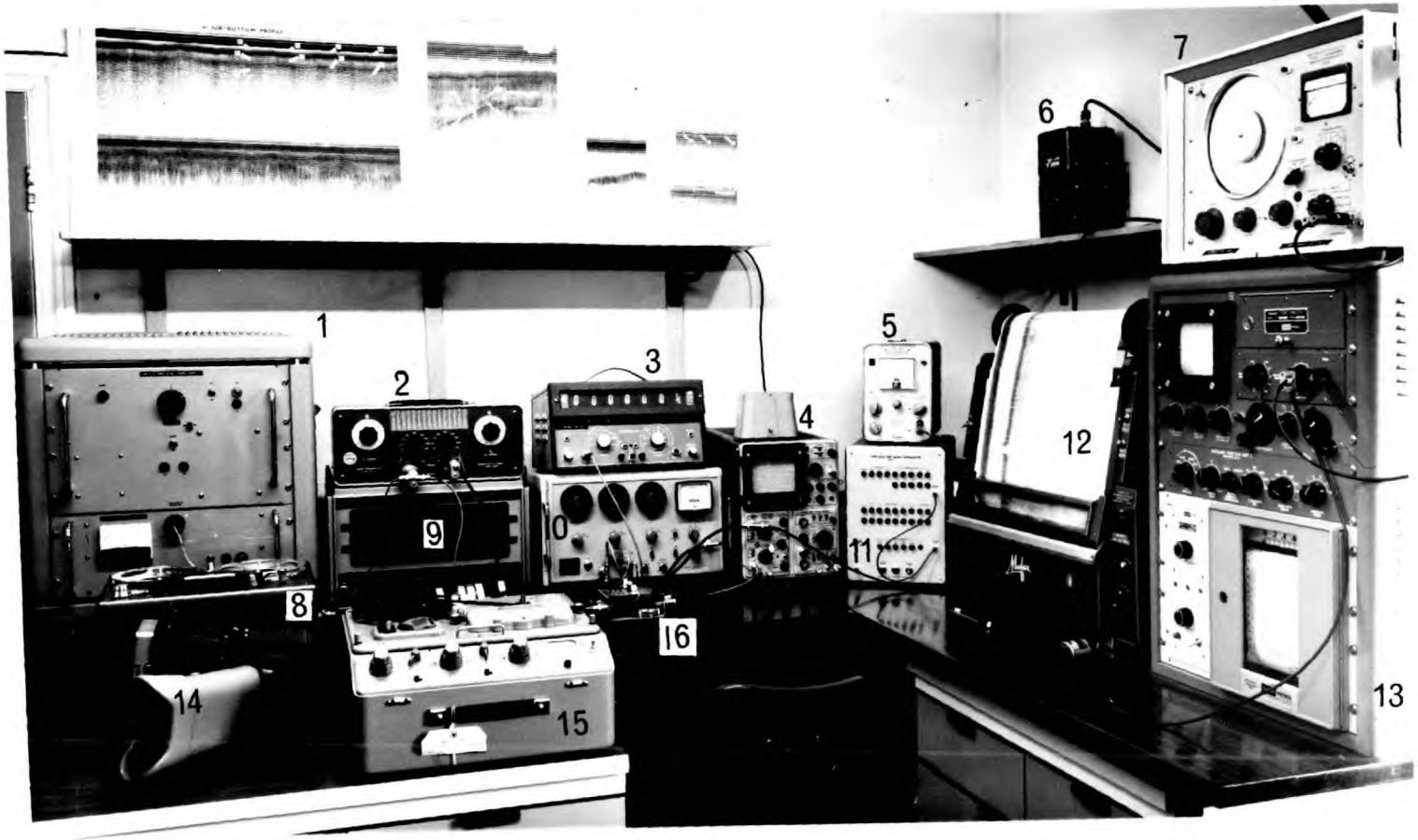

Fig. 6.1. A general view of the laboratory equipment for data analysis.

gating switch (16) was devised for data isolation to be recorded with a second tape recorder (15) on endless tape loops as well as for oscilloscope observation. Tape loop data were fed to a sonic spectrum analyzer (13) with which a constant voltage transformer(6) was used. An Avo camera (14) was used to photograph the cathode-ray tube screen showing the output from either the sonic spectrum analyzer or the storage oscilloscope.

As many of the items used have been described previously in connection with the development of the record/reproduce sub-bottom profiling system (Chapter IV), only those instruments of particular significance in the laboratory process will be mentioned in detail. While the overall functioning of individual equipment will be appreciated more readily in the system analysis procedures (Sections 6.3 & 6.4), some of the constructional and operating principles governing the individual instruments will be introduced first.

6.2.1. Signal-Gating Switch

To examine a specific portion of data continuously recorded on magnetic tape, it is obvious that some means has to be provided for its isolation if the particular phenomenon only is to be treated. For data transcription from tape to tape of signals of a very short duration, such as the acoustic pulses in the present study, a low voltage switching device with accurate duration control is necessary. A gating switch, employing a mercury-wetted reed switch as its main element, together with a precision-controlled pulse generator was developed for this purpose.

The basic reed switch comprises two slender metal reeds hermetically sealed in a glass tube, mounted with an overlap giving a small gap between them. Fig. 6-2(a). The reeds are of ferromagnetic material and when an external magnetic field, either by a permanent magnet or a solenoid coil, is applied; the ends of the reed assume opposite magnetic polarites. If the applied field is strong enough the ends of the reeds are mutually attracted and accelerate into contact. The residual flexibility of the reeds causes them to spring apart when the magnetic field is removed. Due to the low inertia and small initial gap, a very fast make-and-break action is achieved.

The use of suitable contact materials, usually being some form of silver, rhodium, or tungsten, with a filling of inert gas to exclude contaminants, enables a reliable fast, low-voltage switch action to be maintained over wide range of environmental conditions. The mechanical characteristics of the switch determine the magnetising force (generally specified in ampere-turns) required to actuate it.

The simple circuit diagram of the relay-operated signal-gating switch is shown in Fig. 6-2(b). For exciting the coil the square pulse output from the Solartron pulse generator can be utilised. A very useful feature of this pulse generator is the adjustable output pulse-width because the width of the square pulse determines the length of time the contacts of the reed switch remain closed. The 1 megohm resistor on the input side is high enough not to affect the matching of the incoming and outgoing signals between the adjacent equipment. This resistor, together with two others of similar value, also served to distribute and to limit the current from the monitoring battery. The battery switch connects the battery but only after the gate-test switch is closed can the d.c. gate be monitored from the outgoing signal lead.

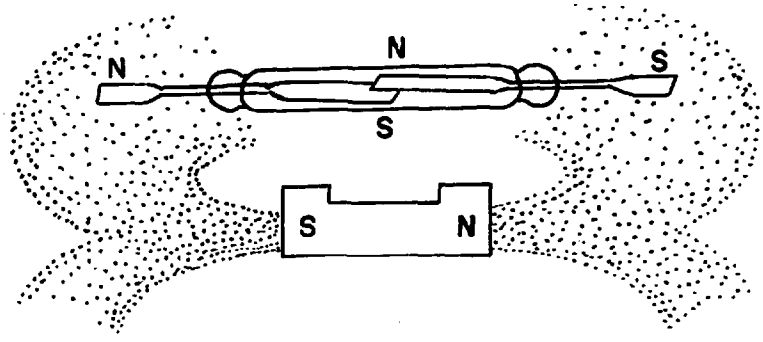

OPERATION PRINCIPLES OF A BASIC REED SWITCH

(a)

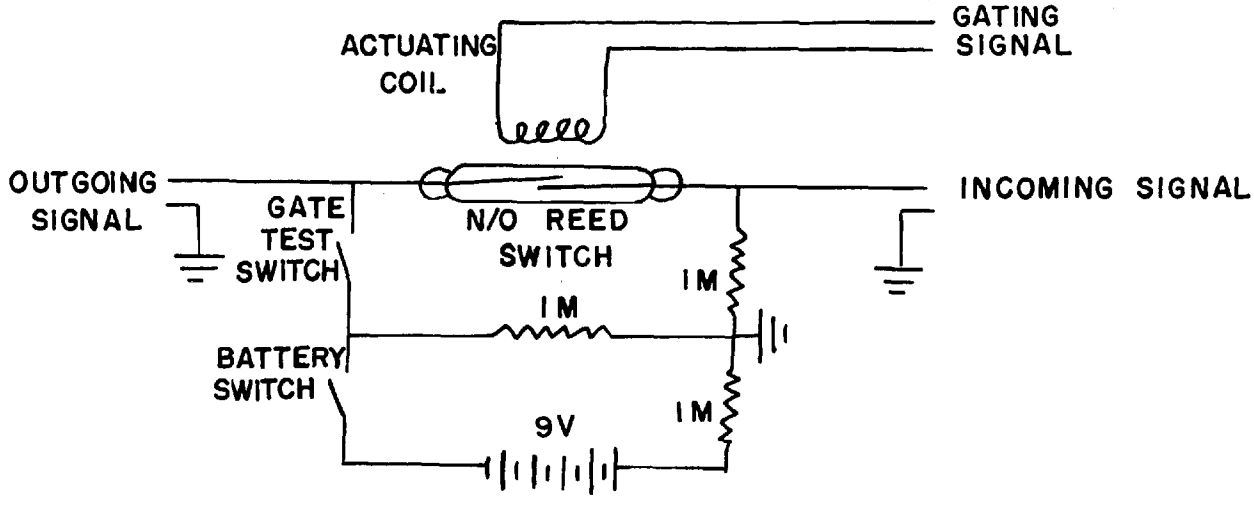

CIRCUIT DIAGRAM OF THE SIGNAL-GATING SWITCH

(b)

FIG. 6.2 ELEMENTS OF THE SIGNAL-GATING SWITCH

First dry reed switch was tested by inserting it into the solenoid coil energized by a suitable pulse from the pulse generator. The actuating time, defined as the time lag between the leading edge of the gating pulse and the actual closing of the ends of the reeds, observed to be about 1 millisecond in this case, gave a satisfactory fast switching action. The dry reed switch used had a measured contact resistance of only 0.1 ohm. However, it was found that after the initial closing of the contacts there always existed for a short period a series of contact bounces lasting from one to two milliseconds regardless of the driving pulse amplitude. This is most undesirable for the gating of signals in the milliseconds range. This adverse effect can be eliminated by the use of a mercury-wetted reed switch instead.

The construction of a mercury-wetted reed switch differs from a dry reed switch in that only one reed is movable. The switch is also hermetically sealed within a capsule in an inert gas which is pressurized to approximately 3-4 atmospheres. The capsule contains an amount of liquid mercury and should be mounted vertically with the moving reed immersed partially in the mercury pool. This lower reed is machined to assist the capillary action. In the particular type used, tilting of the mounting position beyond 30 degrees from vertical will result in a permanent closed contact.

The mercury-wetted switch combines the advantages of a high speed and low contact resistance(less than 50 milliohms) with no contact bounce at all because of the mercury-wetted contact surface. Incorporating this into the signal-gating switching unit proved to be satisfactory after conducting a series of monitoring tests. A photograph of the actual signal-gating switch is shown in Fig. 6-3.

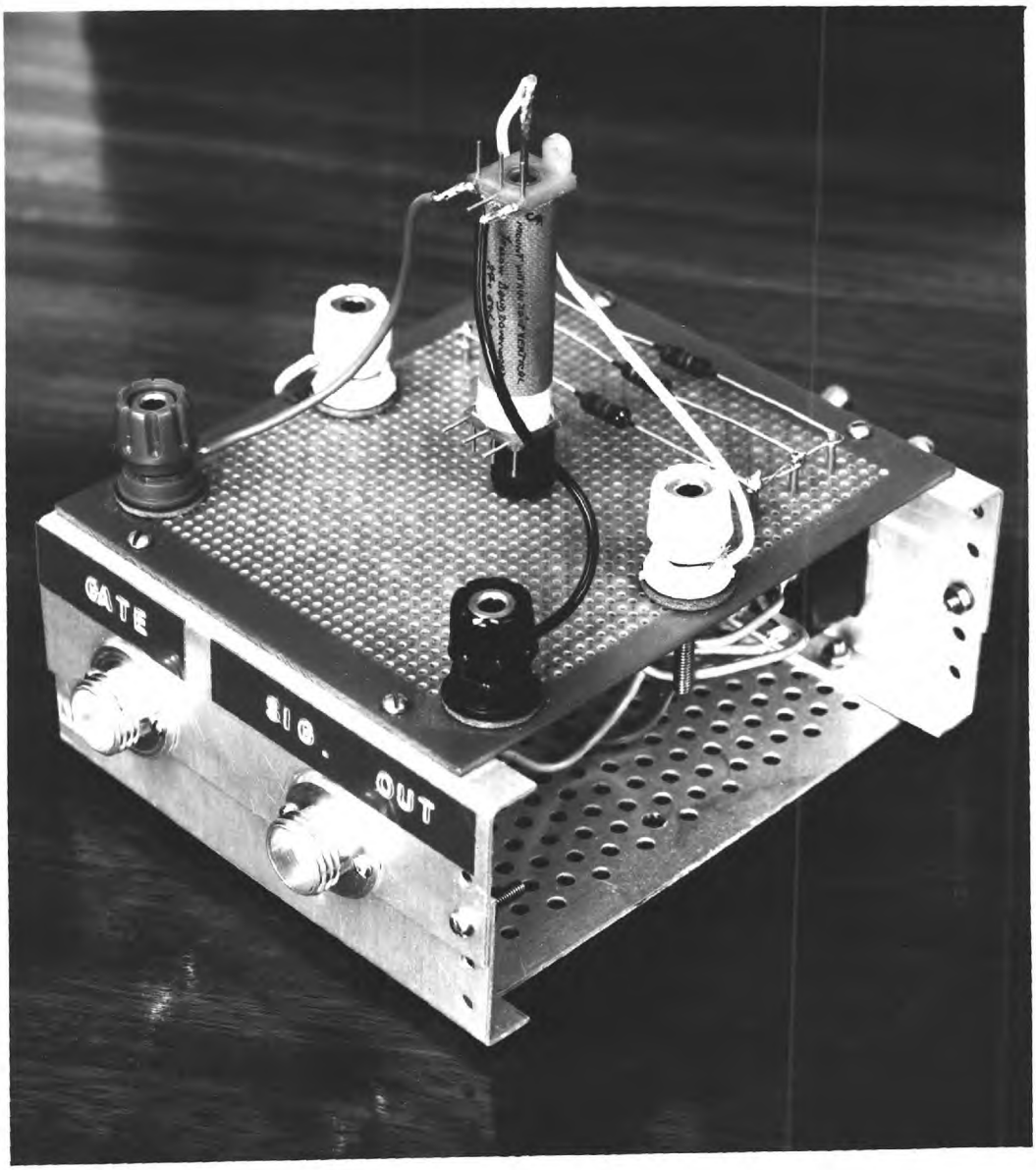

Fig. 6.3. The signal-gating switch assembly.

The monitoring of a gated d.c. voltage of about 14 millisec. duration without external signal is shown in Fig. 6-4(a) in which the upper trace is the monitored gate while the lower is the 1,000 cps reference signal. Such monitoring observation is essential before signal isolation for ensuring proper gate-width control. During actual data transfer the d.c. test part of the circuit was of course always cut off. Fig. 6-4(b) shows the time-expanded closing edge of the same d.c. monitored gate indicating a rise time of less than 0.1 microsec. (the lower trace representing a 1-microsec. time mark), verifying the instantaneous switch closure without any contact bounce. Fig. 6-4(c) shows the opening of the gate trailing off in some 60 microsec. (the lower trace representing a 10-microsec. time mark). This might be explained by the surface tension of the mercury trapped between the closed contacts tending to create a time increasing contact resistance in the breaking of the switch action.

A test was also made of the amount of jittering of this gating switch. Sixty successive switching operations were monitored with a storage oscilloscope in a storage mode. The closing edge of the gate is shown in Fig. 6-4(d) which indicates a total jitter of less than 20 microsec. (the lower trace representing a 10-microsec. time mark). In practice, this gate jitter, as well as the slope of the gate opening, when compared to the gate width used (usually greater than 10 millisec.), produced a negligible effect.

6.2.2. Endless Tape Loop

One way of making a transient signal repetitive is to obtain a tape recording of the signal in an endless loop. The tape loop can

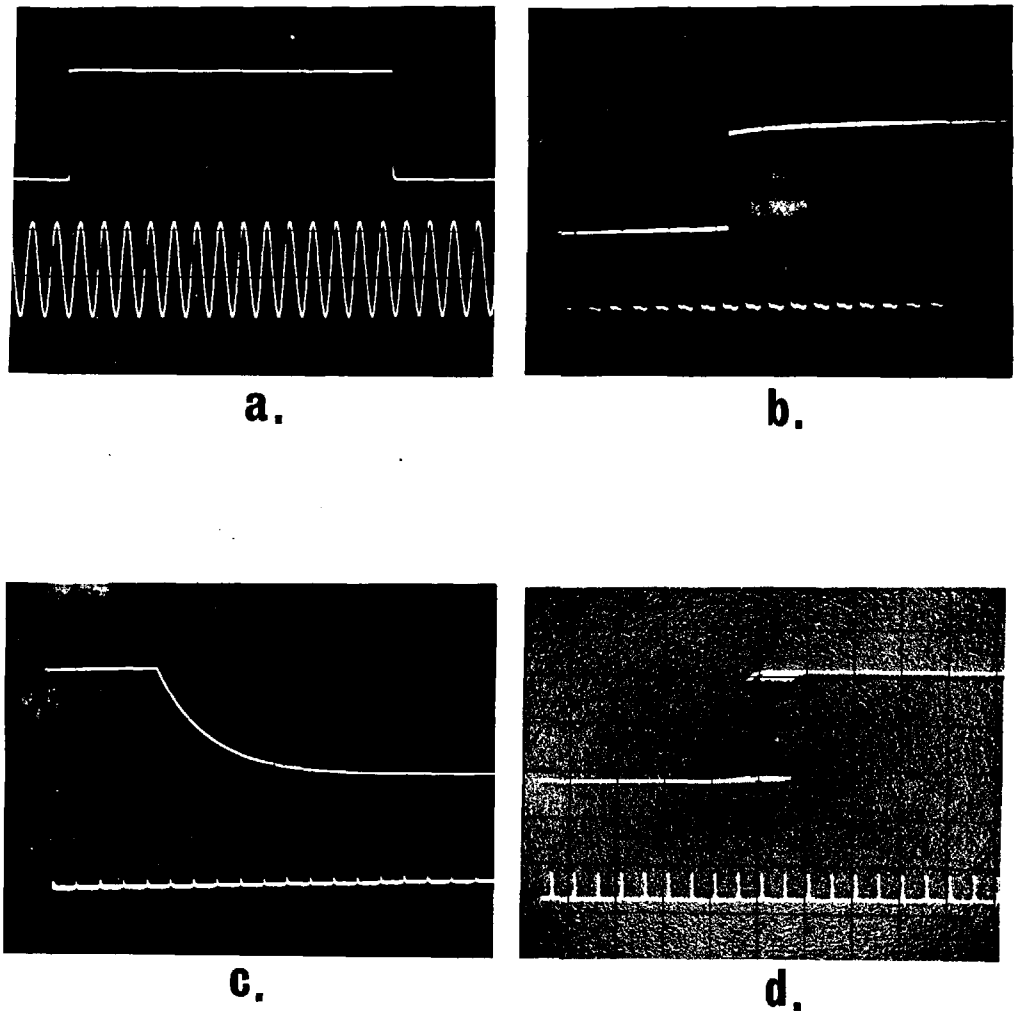

Fig. 6.4. The performance characteristics of the signal-gating switch.

then be replayed and repeatedly fed to a receiver for processing or display. In the present analysis, the duration of the pulses of interest was in the range of a few millisec. up to 20 millisec. The method of cutting the primary tape and joining the ends of a section to form a loop would not be possible in this case. Signal isolation for tape loop storage necessitated the use of a second tape recorder.

A Ferrograph magnetic tape recorder was chosen because it can be readily converted to adapt a standard endless loop cassette attachment. The method of forming the loop drive is by accommodating the length of the slack tape on a single spool, being wound on at the outside of the reel and taken away from the inside as illustrated in Fig. 6-5(a). The spool hub is provided with a series of rollers to ease withdrawal of the tape from the reel and prevent jamming. The whole cassette is metal with an anodised surface as the constant relative movement between layers of tape tends to build up a very high electrostatic charge.

Fig. 6-5(b) shows the endless loop cassette in position on top of the tape deck. In operation the tape was pulled out of the inside of the cassette and by virtue of the inter-turn friction, the whole mass of tape revolved easily on the anodised surface and the rollers, and wound itself again on the outside.

When first run after loading on to the instrument, the winding tension adjusted itself automatically to the correct inter-turn friction and settled down to a constant running speed within a short time, depending on loop length.

The Ferrograph tape recorder used was Model 632 with which two tracks of signal may be recorded or reproduced simultaneously. All through the experiments a speed of 15 inches per second of tape speed

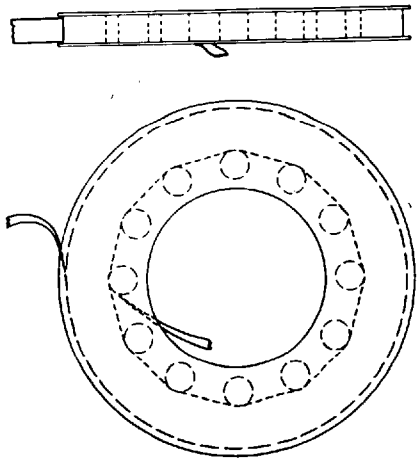

a

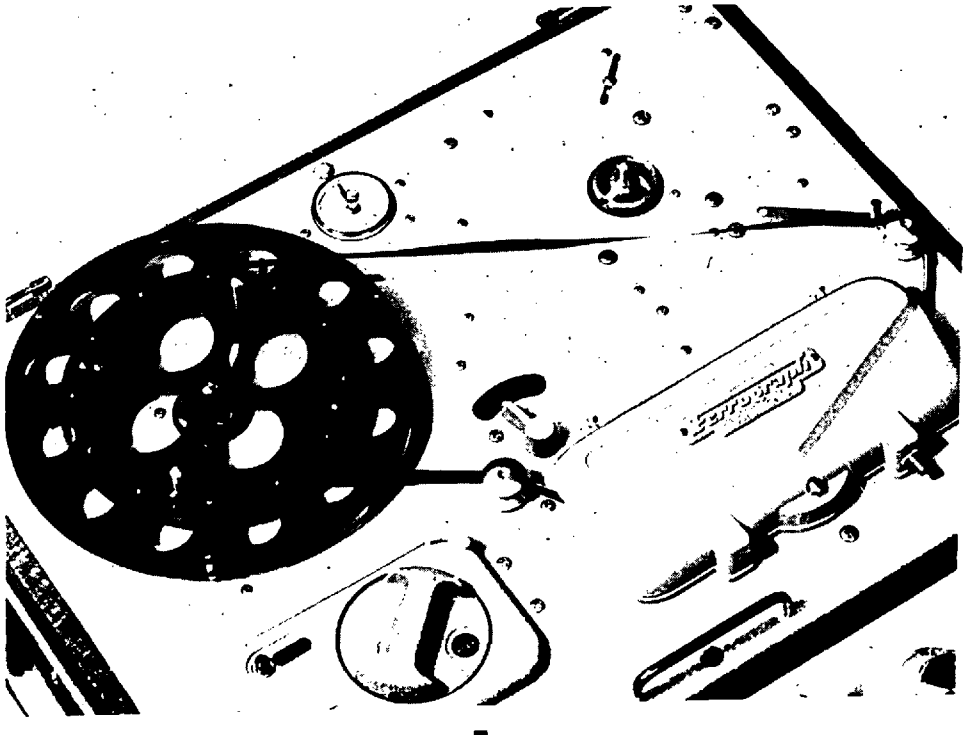

b

Fig. 6.5. The endless tape loop assembly.

was used. At this tape speed the frequency response is 30-18,000 cps . ± 3dB with flutter less than 0.16%. These are the optimised manufacturer's specifications. However, a distortion check was included in the signal transcription procedure.

The use of a short loop can give a higher repetition rate of the stored signal and yet the shortest possible loop will necessarily be limited by the physical arrangement of the tape loop attachment. A steady speed was achieved by using $2\frac{1}{2}$ turns of tape around the central hub of the cassette to maintain a constant tape tension, resulting in a minimum loop time of just over 5 seconds.

A speed check was carried out to ensure that there was no appreciable speed drift with the use of such a tape loop. The exact length of the tape spliced for making the loop was 83.7 inches, the loop time at 15 i.p.s. being 5.58 seconds. This cycling time was difficult to check by an ordinary stop watch but a frequency measurement method was effectively employed instead. After loading the cassette and splicing the tape ends to form the loop, the recorder was turned on to recording mode and was allowed to run. A 10 kcps signal monitored by the Venner counter-timer was then recorded on the loop. When the tape loop was played back to the same counter, tape speed deviation could then be read out straight from the counter indication at 0.1 or 1 second intervals. It was found during a 10 minutes continuous play-back reading that speed drift did not exceed ± 1%. The length and the type of tape chosen were therefore considered acceptable.

The choice of a suitable tape for loop operation also required some experimentation. Sticking and binding which caused erratic tape movement occurred between the turns in the cassette in all

types of new tapes tried except the graphite lubricated tape. Scotch 151 single-side graphite-lubricated tape was finally chosen.

When making the conversion to endless loop operation, the take-up and magazine motors must be disconnected so that they do not revolve. This was done by the installation of an extra switch to control the power lead to the motors for loop operation.

A defluxer was also used from time to time for demagnetizing the record and playback heads for preventing hiss and protecting tapes from cummulative background noise.

6.2.3. Spectrum Analyzer

The heterodyne frequency analyzer was the Panoramic Sonic Analyzer Model LP-1a manufactured by the Singer Metrics Company of America. This scanning heterodyne instrument automatically provides a visual, two-dimensional display of the frequency components of a complex wave in the region of 20-22,500 cps, or in a selected segment of that region. The display appears on the screen of a long-persistence cathode-ray tube as vertical deflections distributed horizontally in order of component frequency. A logarithmic or linear frequency scale may be selected. The height of a given vertical deflection indicated the relative magnitude of its corresponding frequency component and the position along the calibrated horizontal axis indicates its frequency.

Fig. 6-6 is a simplified block diagram showing only the basic stages necessary to illustrate the operation of spectrum analyzers of the heterodyne type. The output of the sweep generator sweeps the local oscillator between two chosen frequency limits. The signal from

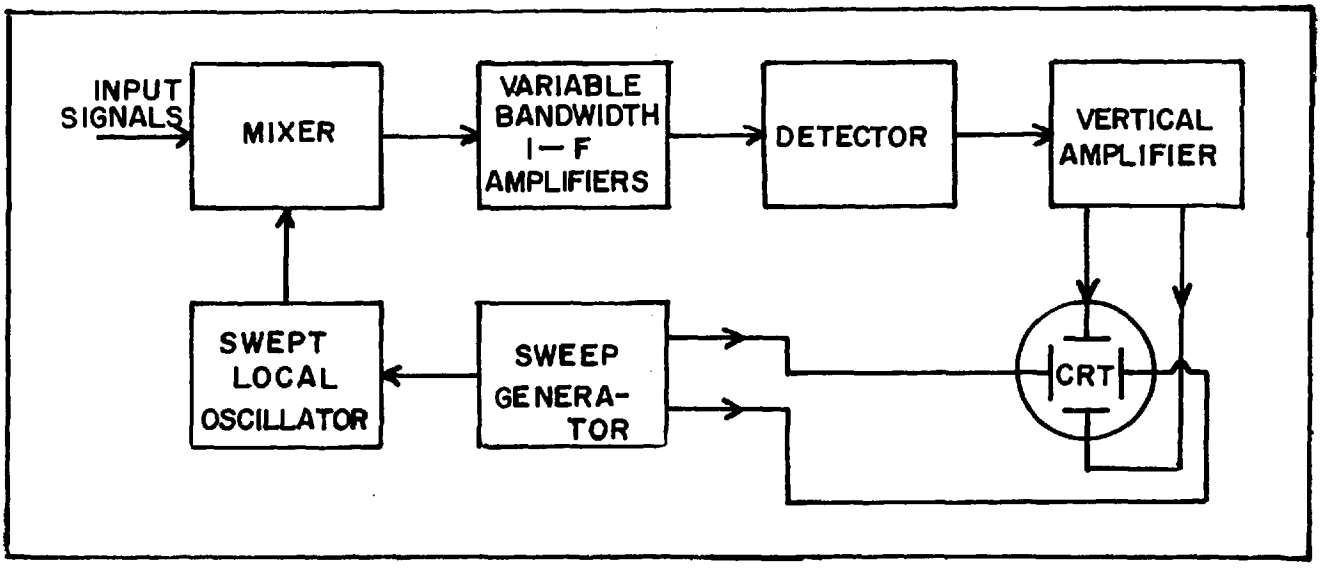

FIG. 6.6 Simplified block diagram, spectrum analyzer.

the swept local oscillator combines with the incoming signals in the mixer stage. The variable bandwidth i-f amplifier is tuned to a given frequency, and will pass only signals of that frequency. When the sum (or the difference, depending on the design considerations) of the oscillator frequency and the incoming signal frequency is equal to the intermediate frequency, an output will appear at the i-f stage. As the swept oscillator moves across its frequency range, it progressively heterodynes in order of frequency with those signals present within the chosen limits to produce the required i-f. After passing the i-f amplifier, the signals are detected and then amplified by the vertical amplifier to provide drive for the vertical plates of the cathode-ray tube beam.

The same wave form that sweeps the local oscillator drives the horizontal plates of the cathode-ray tube, so that the movement of the spot across the cathode-ray tube screen bears a definite relationship to the swept local oscillator frequency. Thus each discrete frequency corresponds to a particular point along the horizontal axis of the cathode-ray tube.

Fig. 6-7 is a block diagram of the Model LP-1a spectrum analyzer which contains many more stages than those illustrated in Fig. 6-6 to perform the specific functions required in actual use. The equipment consists of a calibrated input attenuator, a phase splitter, a swept oscillator, a balanced modulator, variable-selectivity intermediate-frequency amplifiers, a detector, a vertical amplifier, a cathode-ray tube indicator, and associated sweep and selectivity circuits, and power supply.

The mixer stage is a balanced modulator which balances out the oscillator frequency, leaving only the input signal and the sum and

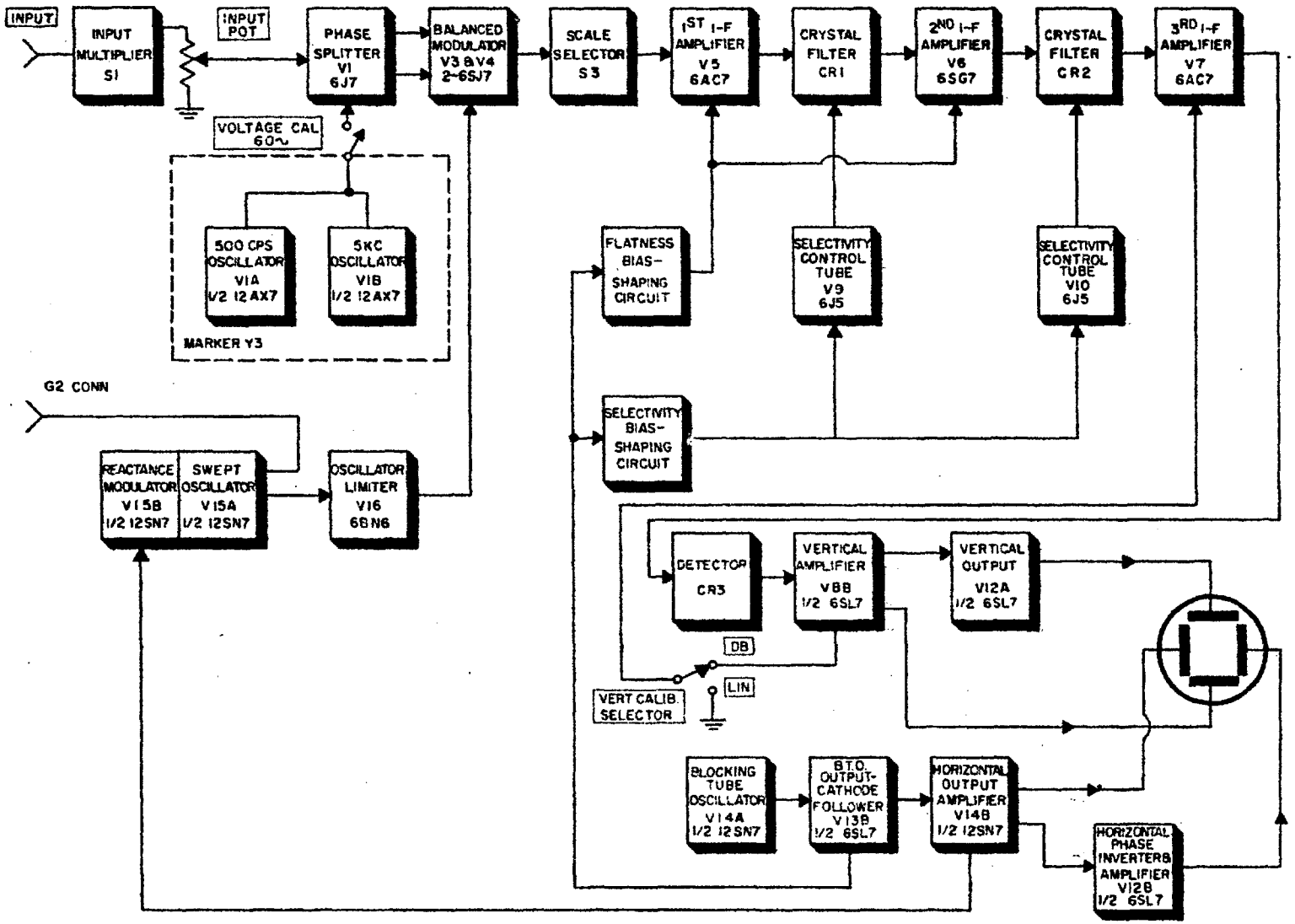

Fig. 6.7. **Block Diagram, Model LP-1a.**

difference frequencies of the input signal and oscillator frequencies. Only when the sum frequency is 100 kc is it passed by the tuned 100 kc intermediate frequency section. The output voltage from the i-f section is detected, amplified, and applied to the vertical deflection plates of the cathode-ray tube. The output voltage of the i-f section is proportional to the amplitude of the sampled portion of the input signal.

Oscillator sweep is achieved by a varying voltage applied to the reactance tube which forms part of the oscillator circuit. A sawtooth generator, which is the source of the varying voltage, also provides the sawtooth voltage for the horizontal sweep of the cathode-ray beam.

The i-f section includes two variable-selectivity crystal filter stages. The selectivity of the instrument is varied by changing the bandwidth of the two crystal filters in a manner which provides approximately optimum resolution at all times. The last i-f stage contains provision for the selection of either a linear or logarithmic mode of amplification.

6.3. Procedures of Signal Isolation

Unlike conventional seismic methods, recording during the continuous reflection profiling operation is, as its name implies, on a continuous basis whether in graphic or magnetic form. As with conventional seismic recordings in which the single trace record is of limited value in interpretation; the continuous profiling reflection method in particular depends critically on the automatic correlation of successive recordings provided by the graphic recorder. In order to be able to single out a certain tape-stored event such as a reflection

event and to transfer it onto a separate tape loop, graphic monitoring is most essential. A special laboratory system was developed to do this.

Fig. 6-8 is a block diagram of the process. The Tandberg tape recorder which originally recorded the signals at sea was used to play back the acoustic data and the 1 kcps as synchonization signals. Use of the same recorder for recording and reproducing should eliminate any signal distortion that might be introduced by change of machine. The constant frequency power supply unit was connected to the Tandberg recorder the same way as in the field. The 1 kcps output from the tape recorder synchonized the drive of the Mufax graphic recorder which, when operating, sent off programmed trigger signals. The Venner counter system was used for counting the number of recording sweeps. Sweep counting is important because when a single particular reflection is to be studied, isolation of the signal has to begin with the identification of the particular sweep. Counting of the recording sweeps can be achieved in two ways. In one case the number of turns of the helix is used and in the other the cycles of the 1 kcps synchonizing signal. In the latter case a sub-multiple may be involved because the helix may rotate several times per second. The Venner counter could be used to measure either the number of recording sweeps directly indicating the sweep count, or indirectly indicating a multiple of the sweep count. The latter was found to be more reliable but both will be described here.

The first method is a straight-forward measurement of the trigger signal from the monitoring Mufax recorder. When the programme switch at the Mufax was set to 1/1 (as was used in all actual field experiments), the rates of the recording sweep, helix

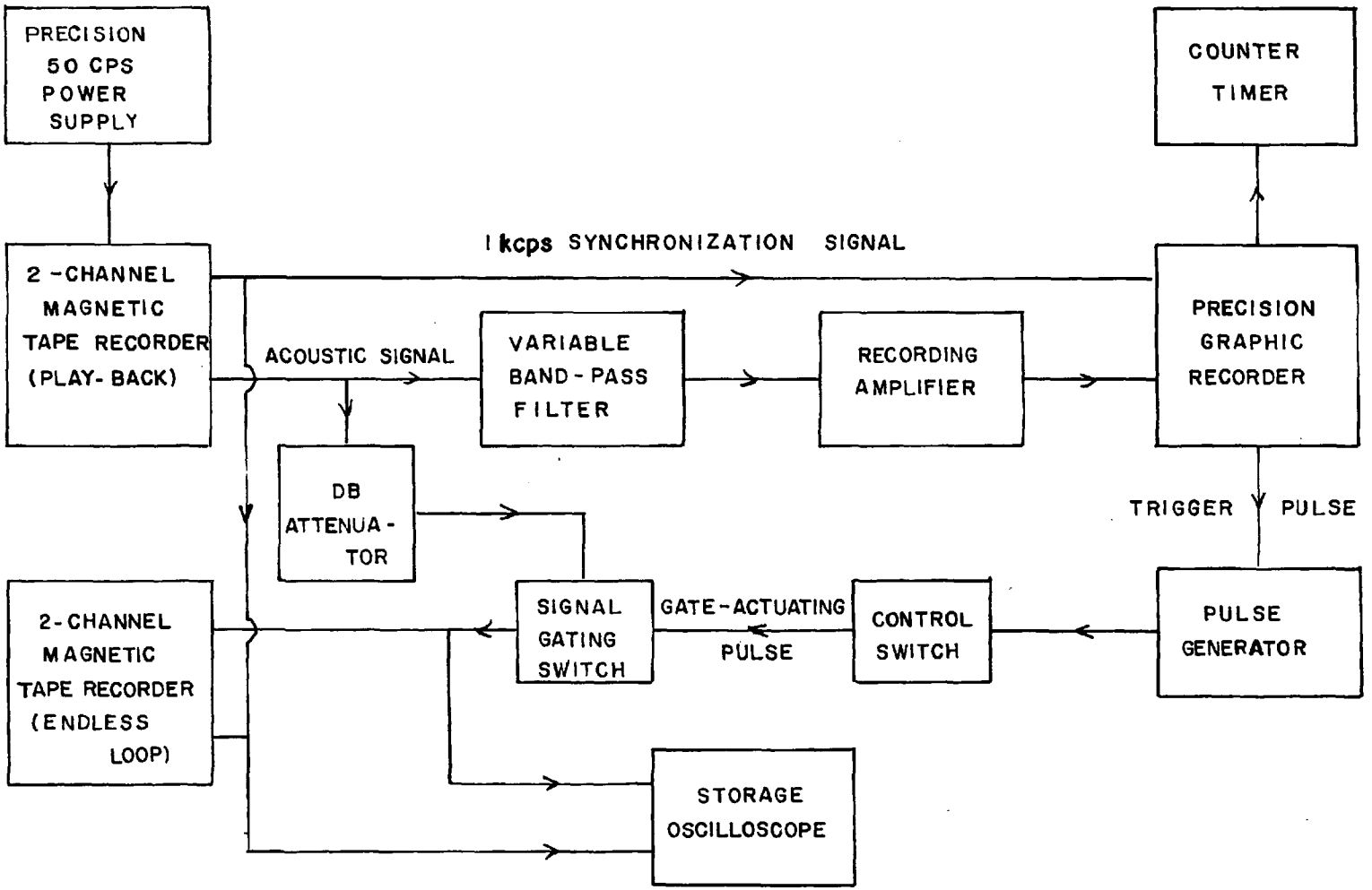

BLOCK DIAGRAM OF SIGNAL ISOLATION PROCESS

FIG. 6.8

revolution, and trigger output were the same. The counter connection to the trigger output will, therefore, indicate directly the number of recording sweeps. However, as spurious triggering could occasionally occur even with the use of a photo-electric trigger system there was a possibility of a miscount. After some trial and observation, this method was eventually abandoned in favour of the other arrangement.

The second method is to utilize the synchronization 1 kcps signal which, when driving the Mufax recorder, has a definite ratio in relation to the revolution of the helix which in turn depends on the speed setting of the recorder. For instance, at the speed setting of one revolution per second, the number of sweeps will be equal to the accumulated reference signal measured in units of kilocycles.

There are three essential requirements for signal isolation in continuous reflection recording using a record/reproduce sub-bottom profiling system, namely,

(i) the location of the particular sweep upon which the event occurs;

(ii) the beginning of isolation or the timing of the opening of the gating switch;

(iii) the end of isolation or the width of the gate.

The counting of the sweep was achieved by connecting the electronic counter-timer to the 1 kcps synchronization signal. The timing of the actuation of the gate is controlled both by a reference signal on the sweep, i.e. the triggering moment, and by the delay setting of the pulse generator which is initiated by the reference signal. As previously mentioned, the gate width of the relay switch was controlled by the pulse width setting of the pulse generator.

When a particular locality, indicated on the graphic record, was chosen for signal analysis, some recognisable feature occurring some two or three minutes in survey time before it was noted on the record. A graphic playback was then made over this spot in order to establish a visual reference on the magnetic tape. This was done by stopping the tape recorder when the selected reference feature began to appear on the monitoring playback profile. A small piece of splicing tape was then fixed to the tape near one of the tape-guiding posts. The approximate number of sweeps from this reference point to the spot of interest could be determined by multiplying the separation between them on the graphic paper by the line density. While it is most important that control of the repetition of a single sweep must be exact, the choice of a particular sweep or reflection among a small group of sweeps at a point of interest is regarded as relatively unimportant. After the reference mark on the data tape was made, the tape was wound back a few minutes ready for replayfor signal isolation and transfer.

The Ferrograph tape recorder was set to its recording position with a tape-loop on. One channel was connected to the Tandberg 1 kcps output, the other to the output from the signal-gating switch. The Venner counter-timer was reset to zero. Counting would only commence after a starting switch had been pressed. The storage oscilloscope was connected to both the signal-gating output and the reproduced 1 kcps, and was set to store one single sweep on the upper portion of the screen for both channels.

The Tandberg tape recorder was then played back so that the Mufax recorder could print out a correlated graphic record. At this stage it was necessary to shift the profile horizontally across

the recorder so that the reflection of interest would be within 0.1 second after either the zero or the middle triggering position. This is because of the limited delay time available from the particular pulse generator used. A time scale, properly calibrated, was marked on the back of the Mufax writing blade, so that the correct delay time for gating was easily found, and adjusted accordingly.

The appearance of the reference mark on the tape during playback could usually be expected by noting the indication of the tape pool revolution counter on the tape deck as a rough guide. At the exact moment when the reference mark passed the reference guide post in the tape deck assembly, the initiation switch at the Venner counter-timer was pressed down to start the counting of the apparent time reproduced in terms of 1 kc for one second, and hence the corresponding number of recording sweeps.

A normally closed micro-switch was connected to the pulse generator's output, shorting out the energising signal to the gating switch coil. This micro-switch served as a transfer control switch which, when pressed, actuated the gating switch.

Gain settings of both the playback and tape-loop recorders were fixed so that a common datum in acoustic level, though arbitrary, applied to a whole set of data in any particular area investigated. Signal strength control for proper recording was accomplished by using an external dB step attenuator. Through monitoring with the recording level meter on the Ferrograph tape deck and the oscilloscope a proper recording level in the signal isolation and transfer processes was readily maintained throughout.

In the process of signal isolation and transfer, the transfer control switch must be left in its normally closed position awaiting

the designated sweep count for the switching action. Since the Ferrograph recorder was self erasing, a few tests were usually conducted before the actual final transfer. No test could be made within a loop time before the designated count, or an unwanted signal would be present in the tape-loop.

At the precise moment when the designated count, say 108,000 cycles, or 108 apparent seconds after counting started, two swift actions of pressing both the control switch and the oscilloscope single sweep reset switch must be performed simultaneously. At the same moment, a single swing of the needle of the recording level meter at the tape-loop recorder could be observed. The tape-loop recorder was then immediately stopped. Erasure of the data in the loop would result should the delay in switching off approach or exceed one loop time. An event marking line could also be made on the monitoring graphic record immediately after the transfer so as to give an approximate position of the sweep in the graphic profile.

The isolated pulse together with the 1 kcps reference signal was recorded in storage mode on the upper part of the screen of the oscilloscope. It was a standard procedure to playback the tape-loop data to the oscilloscope and to store them on the lower half screen, enabling a direct comparison of signals before and after isolation in order to ascertain the success of one transfer before proceeding to the next. The comparison could also serve the useful purpose of observing the degree of signal distortion. Fig. 6-9 shows samples of oscilloscope photographs of such a comparison.

The transfer operation was essentially manual requiring very precise timing for the switch action with regard to the sweep count. In the actual experiments, it happened quite often, especially at the

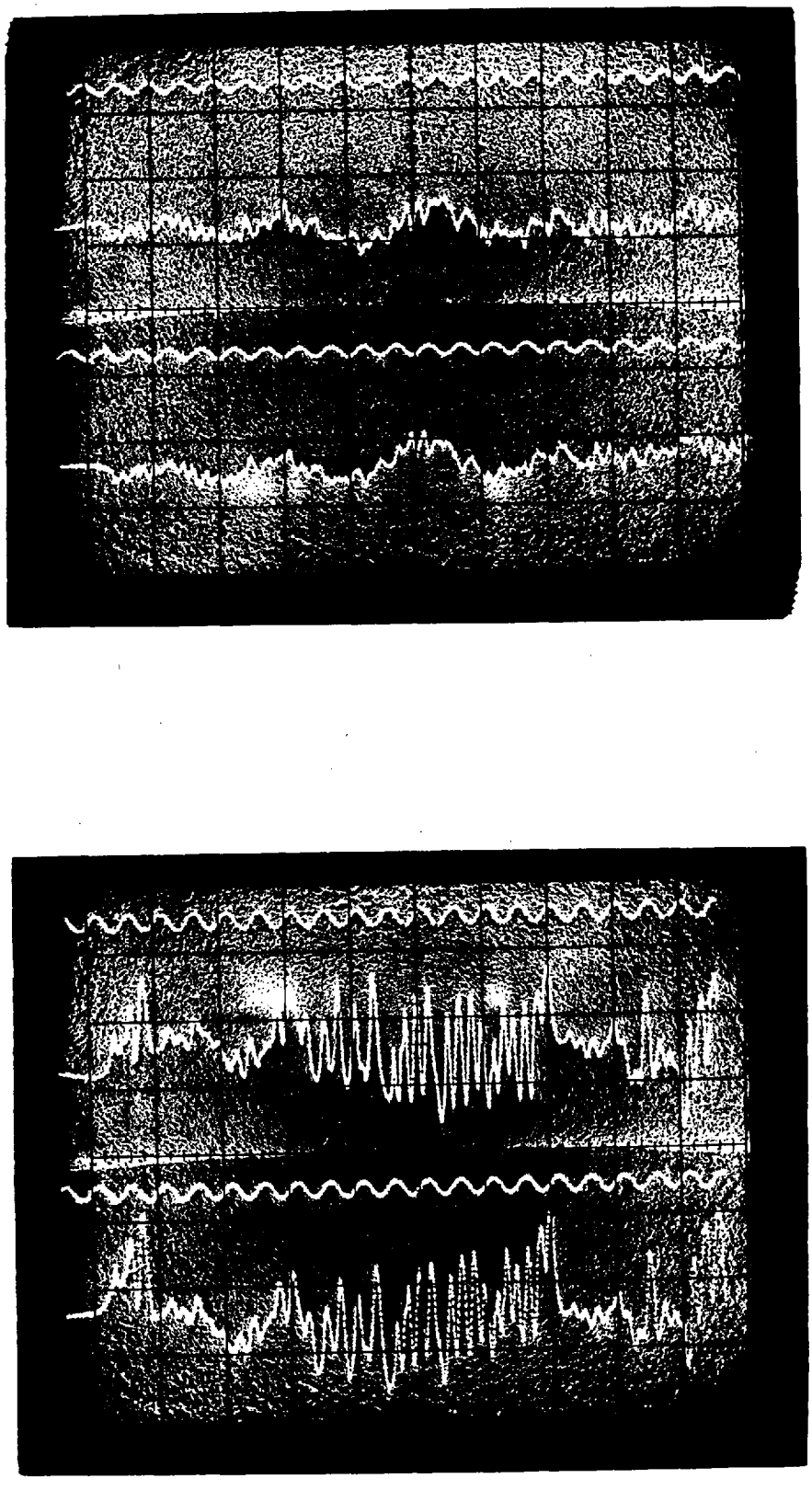

Fig. 6.9. Comparison of signals before and after transcription.

beginning, that either none or two successive pulses were recorded during one transfer switching. This was due to a manual switching action too short or too long to coordinate with the usual $\frac{1}{2}$ second sweep data recording. However, such errors were immediately detected by playing back to the oscilloscope. Nevertheless, some practice and great caution were essential for successful data isolation and transfer.

6.4. Methods of Analysis

The analysis of the pulse data stored in the tape loops was carried out by the spectrum analyzer. Since the output impedance of the Ferrograph tape recorder is 600 ohms, and the input impedance of the analyzer is approximately 250,000 ohms, a 600 ohm/grid impedance matching transformer was used. Care was taken to ensure that the instantaneous peak voltages of signals fed to the input of the spectrum analyzer did not cause amplitude overloading at the input stage for any particular setting. Playback signals were therefore first measured with the oscilloscope for peak level examination before being actually fed into the analyzer.

The playback amplification of the tape loop recorder was fixed at one particular level for any particular set of data in order to maintain the relative attenuation values of the various pulses. This, again, is because all the gain controls on the Ferrograph recorder are not step-calibrated in dB values. The arbitrarily-fixed gain levels were chosen to provide a suitable input level at a common setting for the analyzer to display spectra for all data.

The internal sweep rate for logarithmic frequency scanning is once per second ± 5%. Short pulses of the order of 10-20 millisec. were heterodyned by the analyzer once every 5.58 seconds, the periodic time of the tape loop. Owing to the differential effect, the sampling point on the frequency axis shifted its position when both machines were being continuously operated, resulting in a gradual spectral coverage being built up with time. Difficulty was first encountered in photographing the trace on the screen of the analyzer because of the prolonged exposure time required. The comparatively fast rising pip and the much slower horizontal sweep had different trace brilliancy so that a clear picture with the proper exposure on both could not be obtained.

Instead the Tektronix type 564 storage oscilloscope was used effectively as a slave indicator of the spectral analysis results of which photographs were satisfactorily taken. Connections were made to the spectrum analyzer to lead out the vertical output together with a sweep starting synchronization pulse. However, there was no provision for external horizontal input on this type of storage oscilloscope. With the time sweep of the oscilloscope set to one second per screen width, the use of the synchronization signal from the analyzer for external triggering made the scans in both the oscilloscope and the analyzer started together. It should be noted that this synchronism occurred only every other sweep of the spectrum analyzer because the actual recurring interval in the oscilloscope of the nominally one second sweep was slightly greater than one second. This unfortunately greatly increases the time required for the recording of any specific number of analyzer sweeps. On the other hand the storage feature of the oscilloscope which provides

only a fixed contrast between the trace traversed area and the background of the oscilloscope screen simplifies the photographic procedure.

Calibrations of the spectrum analyzer and the associated oscilloscope for both sensitivity and frequency are necessary for the correct presentation of results. Discrete and non-discrete signal spectra require different calibration methods. There is no simple or direct correlation between sine-wave sensitivity and distributed-spectra sensitivity of a spectrum analyzer. This is because the latter depends upon the response characteristics of the i-f band width while the former does not.

A precision sine-wave signal generator was used to check the discrete frequency calibrations which included both frequency and sensitivity. On frequency calibration, the Venner counter-timer was connected to the output of the signal generator for accurate frequency monitoring. A dB step attenuator was inserted between the signal generator and the spectrum analyzer for sensitivity, or vertical scale, calibration. Sensitivity in dB was measured by feeding a constant amplitude signal to the analyzer and varying the attenuation. The spectrum analyzer provides 500 cps and 5,000 cps calibration marker pips, but the external signal generator was necessary for a detailed frequency calibration. As the final spectral results were taken from the storage oscilloscope display, it was necessary to have both the horizontal and the vertical positions of the graticule calibrated in terms of frequency and relative amplitude.

For non-discrete frequency calibration, a white noise generator (Dawe, type 419c) with calibrated output in the frequency range of 10 cps - 20kcps was used. Since the i-f bandwidth of the analyzer

changes automatically in the logarithmic scan, the noise sensitivity of the equipment also changes. A test was made by feeding into the analyzer a constant amplitude white noise. The presentation was found to decline by 1.2 dB per octave across the spectrum from 20,000 cps to 40 cps in the direction of the scan. This was in accordance with the inherent design characteristics of the equipment as stated by the manufacturer. Accordingly a correction of 1.2 dB per octave, among others, must be made when absolute spectral data are required.

During the signal analysis process, scan synchronization pulses from the spectrum analyzer were also fed to the Venner counter-timer to obtain a scan count. For each pulse on the tape loop analyzed, at least 1,800 scans were made before the resulting spectrum on the oscilloscope screen was photographed. However, the effective heterodyned sweeps appearing in the results were about 1/12 of the total number of scans performed by the analyzer.

CHAPTER VII

EXPERIMENTAL RESULTS

As indicated in the chart of Cardigan Bay (Fig. 5-6), four areas were selected in different parts of the Bay for reflection studies with a view to trying out the attenuation and frequency dependence approach for the identification of marine sediments. The areas are arbitrarily designated (15), (12), (11) and (6) respectively, the number being the number of pulses of interest in the individual areas. Graphic profiles of these areas with arrows pointing out approximately the positions of the reflections involved will be shown in a series of figures to follow, together with the corresponding spectral results of the various isolated pulses, processed by the spectrum analyzer. Also shown in the figures are the corresponding sets of graphs comparing the reflection spectra to indicate relations between various frequencies, their relative spectral levels, and the distances travelled. While the spectral results in their raw forms look rather confusing, the various curves in the graphs give a neater and more systematic presentation though still revealing some peculiarities in the data. In this form the results were more readily appreciated. General features concerning the spectral analysis as a whole will be mentioned in detail when discussing area (15), exemplifying those of other areas investigated.

Together with the spectral analysis of the reflection data, results on the studies of fluctuation of reflections, and the variation of intensity of different spark sources and their pulse characteristics will also be given.

7.1. Area (15)

7.1.1. The Profile

Fig. 7-1 shows the graphic profile of this area reproduced from magnetic tape using 75-600 cps band-pass filtering. The area was chosen because of the presence of a very strong sub-bottom reflection and an interesting sub-bottom structure, the sloping boundary affording a varying first layer depth within a reasonably short distance. In addition, besides two other multiples between sea surface and sea bottom, a second sub-bottom multiple reflection is clearly visible on the record. This should be most useful for differentiating the attenuation effect because of its double penetrations into the sediment. The feature of double penetrations can easily be discerned when referring to other reflections by comparing the slope and boundary characteristics of this reflection with those of the sub-bottom reflection.

7.1.1. The Raw Spectra

The resulting spectra of the various pulses as presented by the spectrum analyzer are shown in Fig. 7-2. The general pattern of the spectra is very erratic in the manner of its frequency distribution. A relative high spectral level between 1 kcps and 5 kcps can be seen to exist in practically all the spectral results. This might be due to the presence of noise and other irregularities, possibly from non-linear effects during recording at the high frequency end of the spectrum, caused by the varying high frequency response of the hydrophone. A free-field voltage sensitivity curve together with some other characteristics of this hydrophone is shown in Fig. 7-3. Moreover, a sharp 1 kcps peak was observed occurring in all the raw spectra. This phenomena could most probably be attributed to the cross-talk effect due to the recording of the 1 kcps reference signal on the

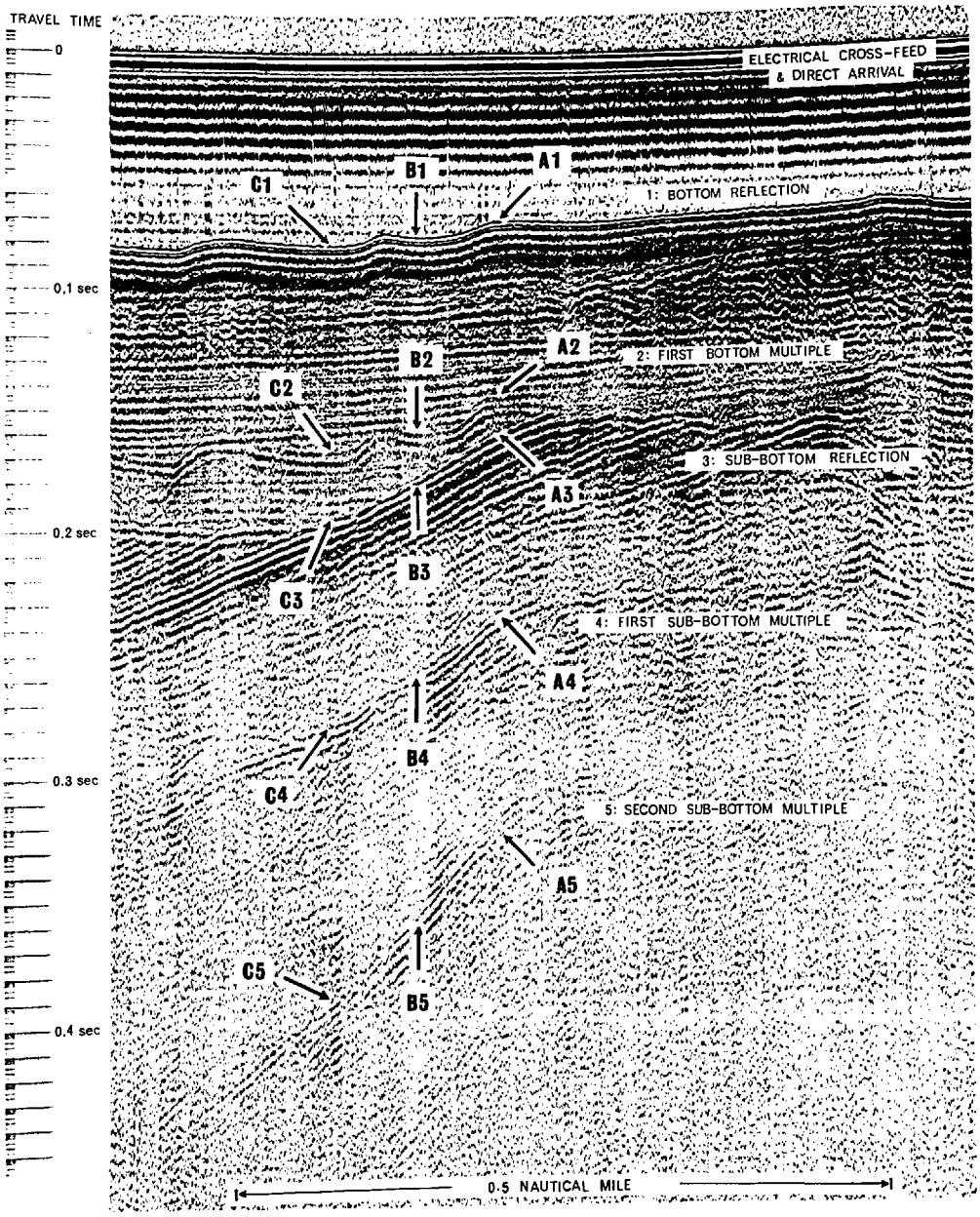

Fig. 7.1. The sub-bottom profile, Area(15).

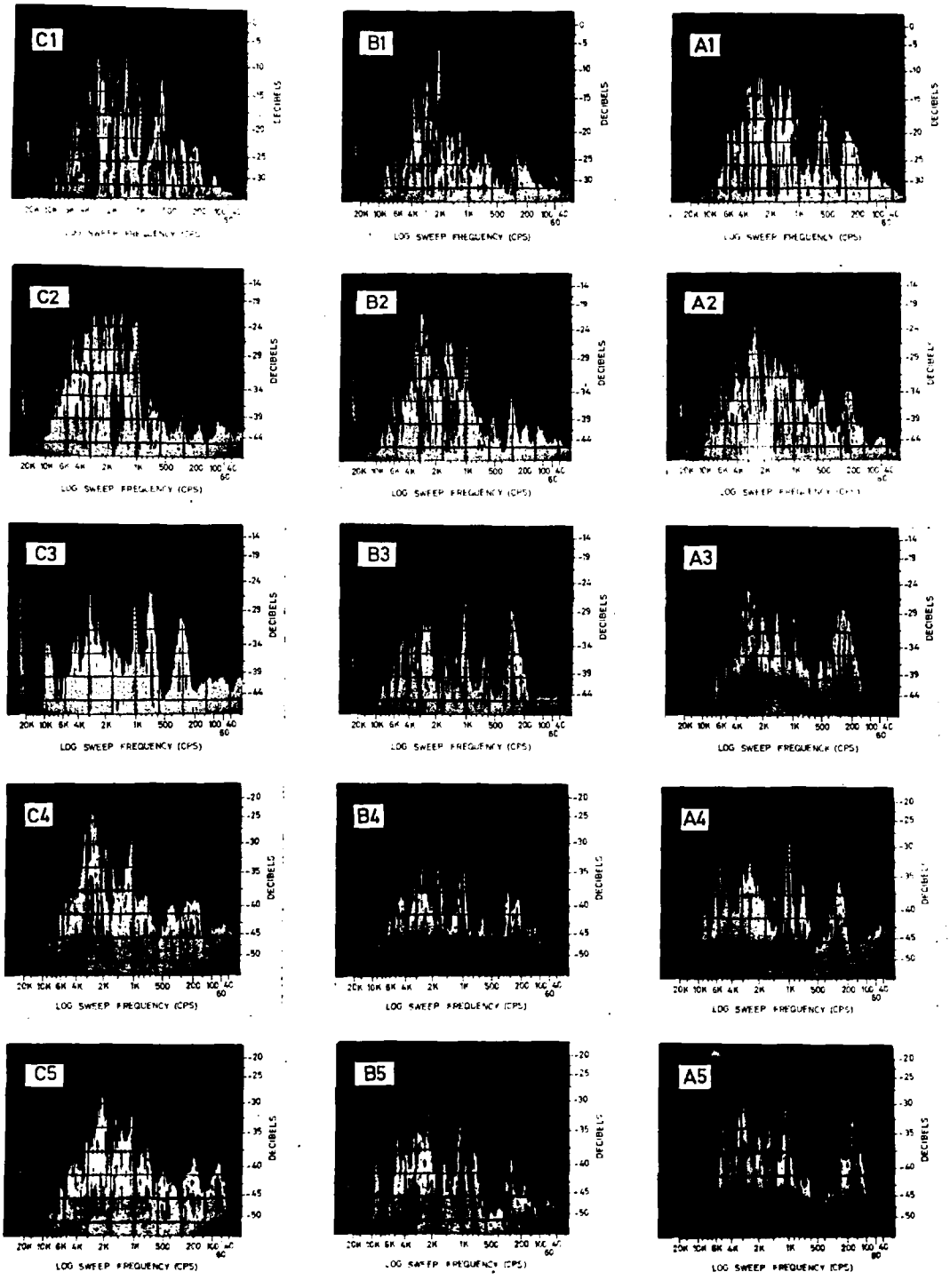

Fig. 7.2. The spectra, Area(15).

Sensitivity (re 1 v/μb)	Frequency Range (c/s)	Resonant Frequency (c/s)	Capacitance (μμf)	Operating Depth (ft)	Beam Pattern	Weight (oz)	Cable (ft)
-90 (min)	10 to 6000	4000 Approx.	4500 ± 15%	60	Spherical	Air 10 Water 6	60.0 +2' -0'

* Free-Field Voltage Sensitivity
(Open circuit voltage at
end of 60 ft. cable)

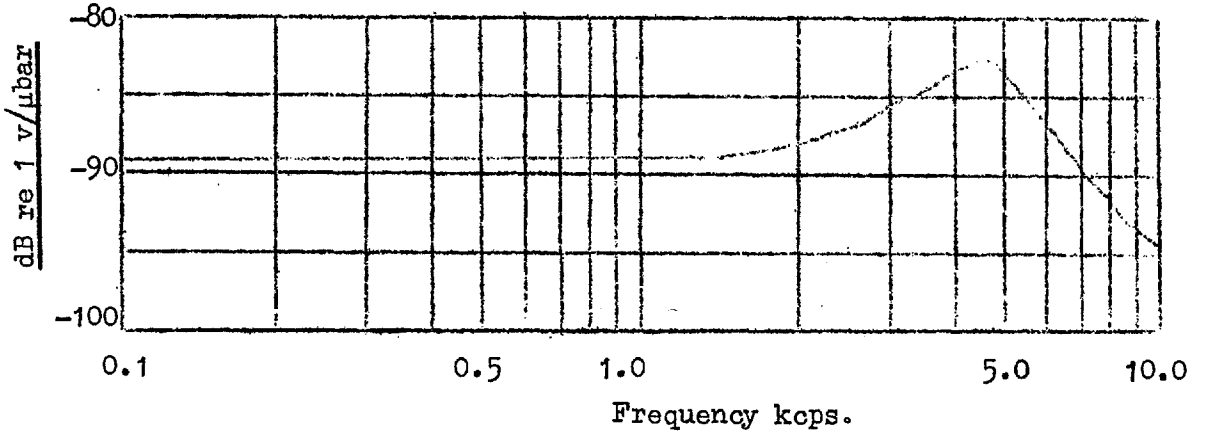

Fig. 7-3 ESSENTIAL CHARACTERISTICS OF THE E.G.& G. 262B ROCKET HYDROPHONE

other track of the data tape. Evidence of this could be found in the fact that the weaker the acoustic signal recorded, the higher the relative level of this peak.

7.1.3. Reflection Spectra Comparison

From data extracted from the raw spectra, 3 sets of curves were drawn each using 6 centre frequencies. A graph of this is shown in Fig. 7-4. Centre frequencies selected are respectively 150, 300, 600, 1,000 and 3,000 cps, the first three being within the most commonly used band-pass filtering range (75-800 cps) in continuous reflection profiling work while the 1 kcps being the possible cross-talk interference during magnetic tape recording of the reference signal. The 3 kcps was selected because it appears to be the representative of the high frequency section, composed of signal and noise band influenced by the rising gain due to the resonance. The presentation of the graph is in relative spectrum level in dB of these centre frequencies versus path length between the principal reflecting interfaces, expressed in time units of millisec. Average values of actual losses are also indicated in the series serving to indicate the trend of total pulse attenuation as a whole. The curve shown by a broken line is the logarithmic curve

$$Y(dB) = M(20 \log_{10} t),$$

M being an arbitrary constant. This indicates the theoretical spreading loss. This is a useful reference for visual evaluation of data as well as for obtaining graphically the spreading loss values between interfaces. Since the reference for all the relative acoustic pressure amplitudes are arbitrarily set and a dB scale was used for plotting it is permissible to shift the logarithmic curves up or down to pass the points of average bottom reflection loss, again arbitrarily fixed as a matter of convenience.

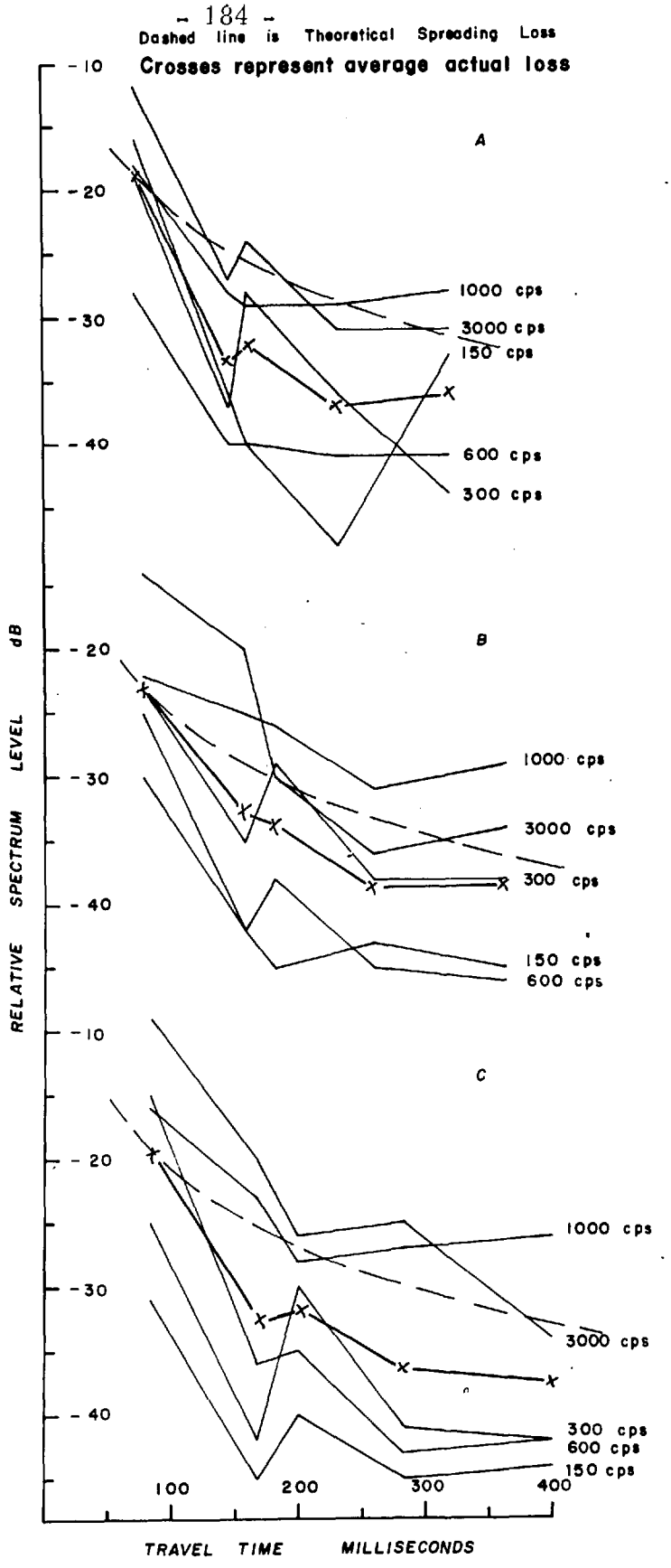

FIG. 7.4 REFLECTION SPECTRA COMPARISON, AREA (15).

Blundell (private communication, 1966) provided the uppermost sediment layer velocity as 5,000 ft/sec from the results obtained with his refraction investigations in Cardigan Bay. This is close to the average sea water velocity in that region thus simplifying the differential travel path calculations. The irregularities of the raw spectral data is such that any discrepancies resulting from the use of the same velocity for both sea water and underlying sediment will be negligible.

7.1.4. Computations of Attenuation and Frequency Dependence

When the sound velocity in sea water and that in the sediment are assumed equal, the equations (2-25, 27, 28) derived for the computation of acoustic attenuation in sediment become simplified. Under such circumstances, both v_1 and v_2 can be replaced by a single value v, leading to

$$E_{bf} = S_f - K_1 - 20 \log_{10} v_1 t_1$$
$$= S_f - K_1 - 20 \log_{10} v - 20 \log t_1 \qquad (7\text{-}1)$$

$$E_{sbf} = S_f - K_2 - 20 \log_{10}(v_1 t_1 + v_2 t_2) - \alpha_f v_2 t_2$$
$$= S_f - K_2 - 20 \log_{10} v - 20 \log_{10}(t_1 + t_2) - \alpha_f v t_2, \qquad (7\text{-}2)$$

and

$$E_{bf} - E_{sbf} = K + 20 \log_{10}(t_1 + t_2) - 20 \log_{10} t_1 + \alpha_f v t_2. \qquad (7\text{-}3)$$

By using two sets of values of t_1 and t_2, the attenuation coefficient at a certain frequency can be very readily obtained, there being no need to find out the value of K. Difference of the actual loss between bottom and sub-bottom reflection $E_{bf} - E_{sbf}$ in dB can be determined with ease from the data givein in Fig. 7-4, and corrected for the differential spreading loss. The computation will be best explained by giving a working example below.

For centre frequency 150 cps, the difference between the losses for the bottom (reflection 1) and the sub-bottom (reflection 3) was found to be

equal to 12 dB in sweep A and 15 dB in sweep B, with values of layer depth expressed in time travelled of 88 and 104 millisec. respectively, while the differential spreading loss, read off the theoretical spreading loss curves, are 7 and 7.5 dB respectively. Using 5 ft/millisec. as the sediment velocity and substituting the various values into the two simultaneous equations:

$$12 = K + 7 + 88 \times 5 \times \alpha_{150} \qquad (7\text{-}4)$$

$$15 = K + 7.5 + 104 \times 5 \times \alpha_{150} \qquad (7\text{-}5)$$

which give $\alpha_{150} = 0.0313$ dB/ft.

In the same manner, using spectral data B_1, B_3 and C_1, C_3, the attenuation value at 600 cps was found to be

$$\alpha_{600} = 0.103 \text{ dB/ft.}$$

From these two attenuation values, the frequency dependence in the form of f^n was computed giving $n = 0.86$. Judging from this figure alone, the sediment composition in this area could possibly consist primarily of sandy silts.

7.1.5. Limitations on the Method

It must be noted that the two attenuation values were determined from different pairs of sweeps, one A and B, and the other B and C, and also from reflection 1 and 3 only, the rest of the data being ignored. This is because of the highly irregular characteristics of the spectral data. In order to obtain rational results, it was necessary to reject all the illogical data which were either theoretically impossible, such as a reflection signal having an actual loss less than the spherical spreading loss or a later sub-bottom reflection having a much stronger relative amplitude.

For all the attenuation and frequency dependence analysis, the frequencies were confined to 150 and 600 cps only. The results of the above sequence of computations should yield fairly reliable estimates of some acoustic constants in this frequency range, but the values at high frequencies could not be used safely to decide on any quantitative features due to the reasons already given. In addition, the usual seismic energy used for sub-bottom profiling work, has its most useful spectrum components approximately in this low frequency range. The higher frequency section, often failed to give any meaningful results. This can actually be observed by visual inspection of the irregular spreading of the various relative spectral levels of 3,000 cps as shown in Fig. 7-4.

7.1.6. Confirmatory Spectrum Analysis

To ensure that the raw spectral results obtained by the heterodyne spectrum analyzer were satisfactory, two other independent spectrum analysis methods were used on a few sample pulses. Data A_1, A_3 and A_5, being convenient reflections from bottom, sub-bottom and double-penetrated sub-bottom, were chosen for such a test. These data were then processed by a narrow band-pass filtering method and a digital harmonic analysis using Fourier series. Corresponding results produced turned out to have fairly good agreements in their general spectral pattern with only some expected deviations.

7.1.6.1. Five Sample Reflection Pulses

It is thought to be of some interest to examine an entire series of reflection pulses of a single sweep as it was recorded in pressure amplitude versus the time domain. Five pulses of sweep A were reproduced from the corresponding tape loops. Judging from the monitoring graphic record, the

length of 18 millisecs. used for each pulse appears to include the beginning and end of the coherent part of the prominent reflection signals. Using delayed time base and section-expanded feature of the storage oscilloscope, the relatively long wave trains of individual pulses were first photographed in sections and later joined together, making use of the event fixing 1 kcps reference signal. The relative recording levels, with arbitrary zero reference, are respectively 0, -18, -8, -24 and -17 dBs from A_1 to A_5. The shapes of the isolated pulses, without any filtering, together with a time reference are shown in Fig. 7-5.

It is interesting to note that visual study of these reflection pulses does not reveal any coherent features between signals. They appear to share very little similarity except the general high-frequency oscillations on part of the traces. In fact, a cross-correlation examination of A_1, A_3 and A_5 using a seismic data processing programme provided by the Atomic Energy Authority failed to produce coherence of any significant degree from 150 cps to 20 kops. The underlying cause might be due to considerable transformation of the acoustic pulses passing through irregularities and stratifications in the path media, resulting in considerable attenuation of the effective low frequencies plus perhaps an appreciable amount of scattering and interference. Hence it is not surprising that no cross correlation was detected because there is too much noise present. The pulses would have to be filtered and re-amplified (pass-band 100-600) to obtain valid cross correlation results. However, despite the apparent lack of coherence between various reflections in a single transmission, it is most probable that adequate coherence of corresponding reflections between consecutive transmissions does exist, at least to the extent of being revealing in the continuous reflection profile using variable density display thus allowing the alignment of the slight drift of the consecutive

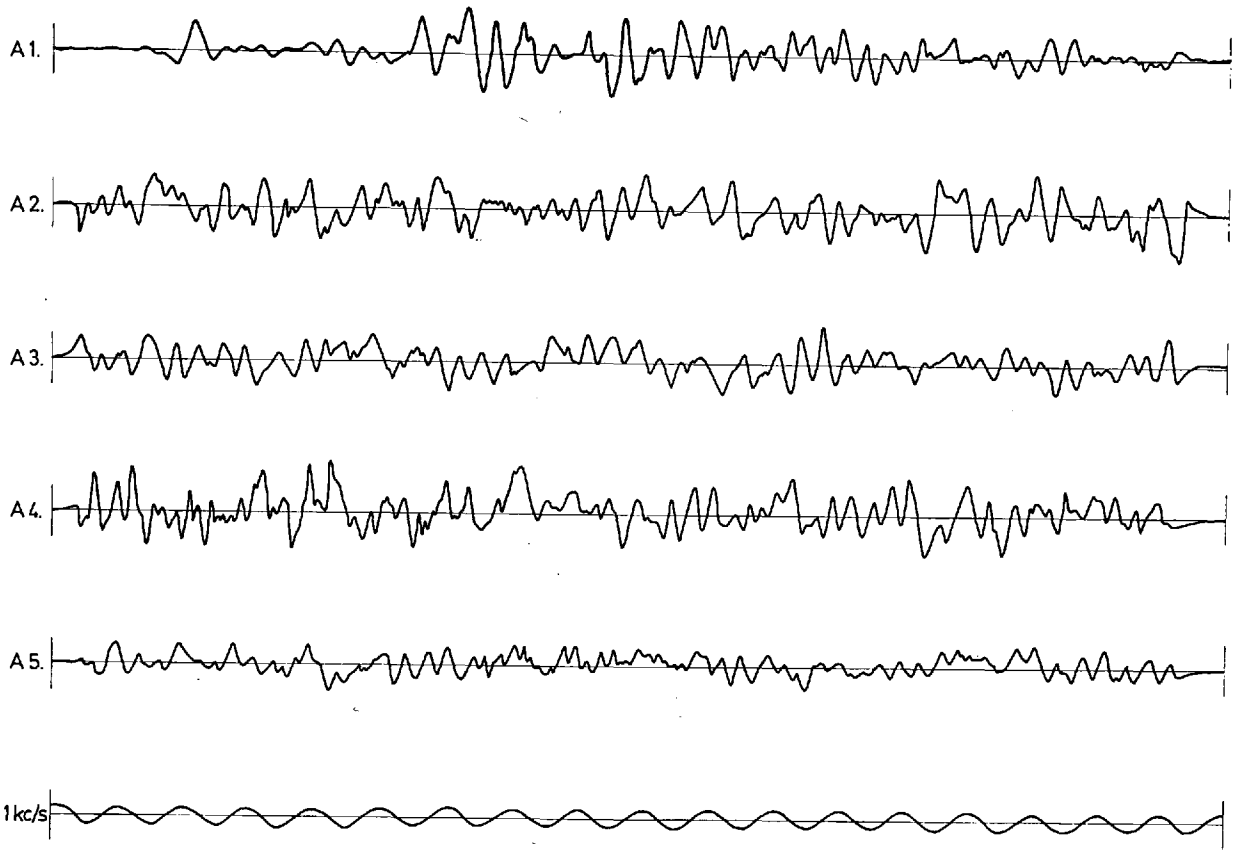

Fig. 7.5. Reflections of Sweep A, Area(15).

pulse peaks without any noticeable effect on profile resolution. This was in fact observed to be the case when consecutively isolated pulses were presented and compared in the storage oscilloscope.

The procedures used to carry out the spectral computations necessitate the use of digitized records. For digitizing in great detail, the pulse trains shown in Fig. 7-5 were projected into a very large piece of graph paper through an epidiascope, obtaining the necessary magnification for convenient replotting and recording of equi-spaced digital values of the amplitude.

7.1.6.2. 1/3 Octave Narrow Band Filtering

The Allison variable filter used in the profiling system was also used for this checking purpose. Test data of A_1, A_3 and A_5 in tape loops were continuously played back to the filter through an input impedance matching transformer. Frequency sampling points from 75 cps onward up to 19,200 cps at 1/3 octave intervals were consecutively chosen and the output peak-to-peak signal values presented on the screen of the storage oscilliscope were read off. Allowing a slight increase in insertion loss, low cutoff and high cutoff sections of the filter were set at the same frequency, the actual passing bandwidth was then approximately $\frac{1}{4}$ octave. To confirm this, a filter calibration test was conducted using a sine-wave oscillator and the oscilloscope. It was observed that the variation of insertion losses at the 1/3 octave points was less than $\pm \frac{1}{2}$ dB from 75 cps to 5 kcps, increasing to $\pm$ 1 dB from 5 kcps to 19 kcps, where the insertion loss began to increase sharply. For comparison purposes this variation in the spectral range of interest was considered negligible, and no correction to the output readings was necessary.

Fig. 7-6 shows the resulting spectra of the three reflection pulses so analysed. Comparison between this set and the corresponding raw spectra shown in Fig. 7-2 indicates a very good overall agreement in their general patterns. The small discrepancies existing in the details of the distribution of spectral level could be due to the different band-averaged effects, the band-pass filter at $\frac{1}{4}$ octave filtering, particularly at the high end, having generally less resolving power than the heterodyne analyzer.

7.1.6.3. Digital Harmonic Analysis

The same set of pulses were also examined by the mathematical method of harmonic analysis. Using the digitized data readily obtained through a very much enlarged projection of the small size traces on graph paper, the analysis involved digital computation by means of the Fourier series formula which is:

$$f(x) = \tfrac{1}{2}a_o + \sum_{n=1}^{\infty} a_n \cos nx + \sum_{n=1}^{\infty} b_n \sin nx$$

$$= \tfrac{1}{2}a_o + \sum_{n=1}^{\infty} \sqrt{a_n^2 + b_n^2} \cos (nx - \phi)$$

where $\tan \phi = b_n/a_n$

$$a_n = 1/2\pi \int_o^{2\pi} f(x) \cos nx \, dx$$

$$b_n = 1/2\pi \int_o^{2\pi} f(x) \sin nx \, dx$$

In order to calculate the Fourier coefficients the facilities of the computing centre of the University of London were employed, using a programme compiled in the EXCHFL language.

To avoid aliasing effect, 1061 equally-spaced data points were taken out of each of the 18 millisec. signal pulses, giving a fundamental frequency of 55.55 cps but enabling harmonic analysis valid up to the 530th order, or 29,442 cps.

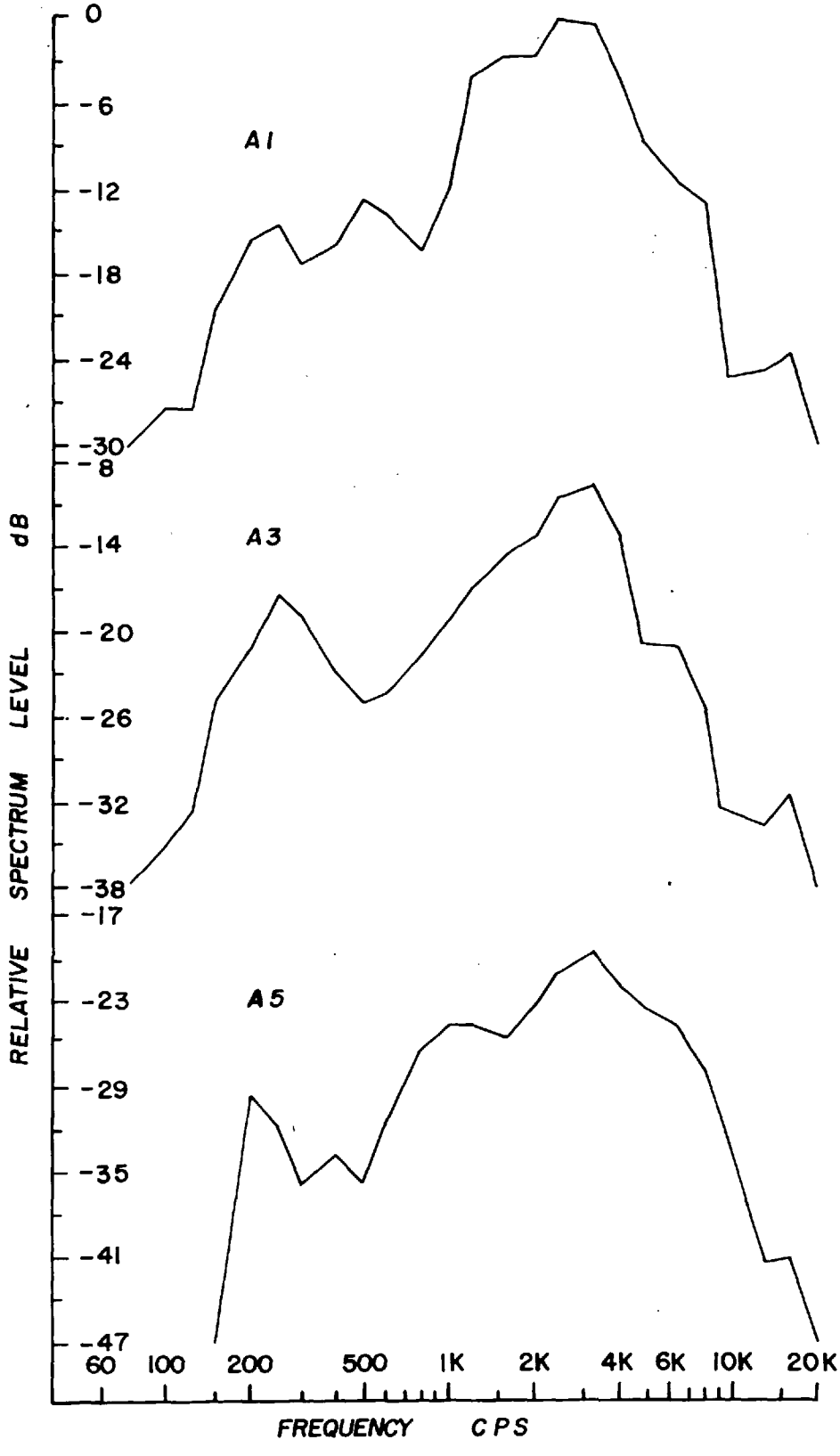

FIG. 7.6 SPECTRUM ANALYSIS, 1/3 OCTAVE BAND-PASS FILTERING AREA (15) A1, A3, A5.

The spectral results so obtained as shown in Fig. 7-7 were found to be different in many respects as compared to those of the heterodying and narrow-band filtering. Comparatively accurate though it may be, but with only a finite length of record available, it was not possible for any harmonic analysis to identify frequency exactly. Spectral estimates so obtained had to be corrected for the noise in the digitization procedure. The neighbouring frequencies with random phases will have effects similar to those of noise in preventing such identification. In particular, the resolution at the low frequency end in the present instance is not satisfactory due to the relatively large fundamental frequency interval, while at the high end, rapid variations appear due to the very close interval when plotted on a log scale. This method has some point by point precision but it lacks the sometimes desirable averaging ability of a heterodyne system which brings the broad frequency band to be studied to a fixed filter, or that of a variable filter which tunes a narrow band-pass filter across a wide frequency range.

It should be noted that scales changes with each spectrum and comparison between spectra by means of the spectral graphs should be made cautiously. In any event, similarity in their general patterns and the major parts of maxima and minima in the relative spectral levels can still be observed.

7.2. Area (12)

7.2.1. The Profile

Area (12) is located not very far from Area (15). Fig. 7-8 is the graphic profile from which several closely spaced intermediate reflecting interfaces can be seen between reflection 1 and 4. Taking into consideration the slightly wider signal-gating window width in order to examine the entire

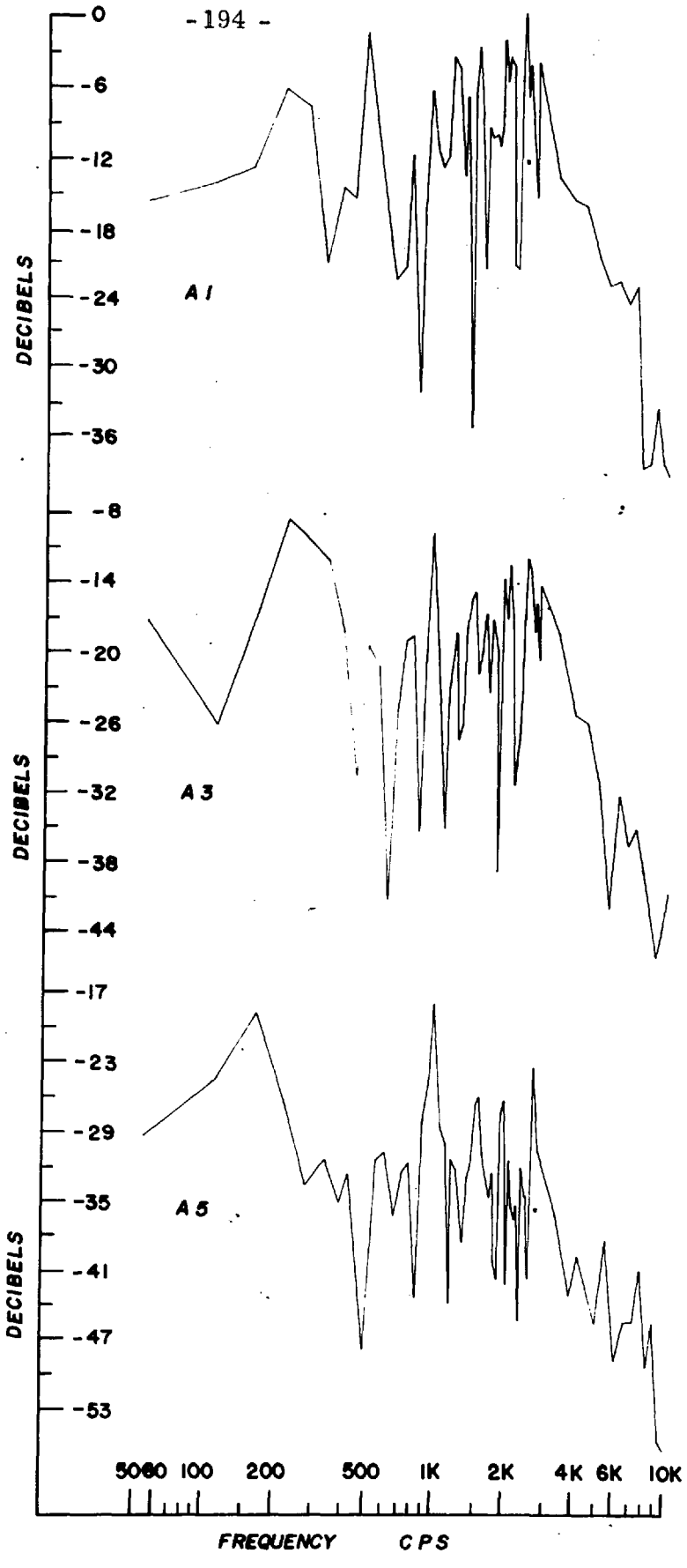

FIG. 7.7 HARMONICS ANALYSIS, AREA (15)-A1, A3 , A5.

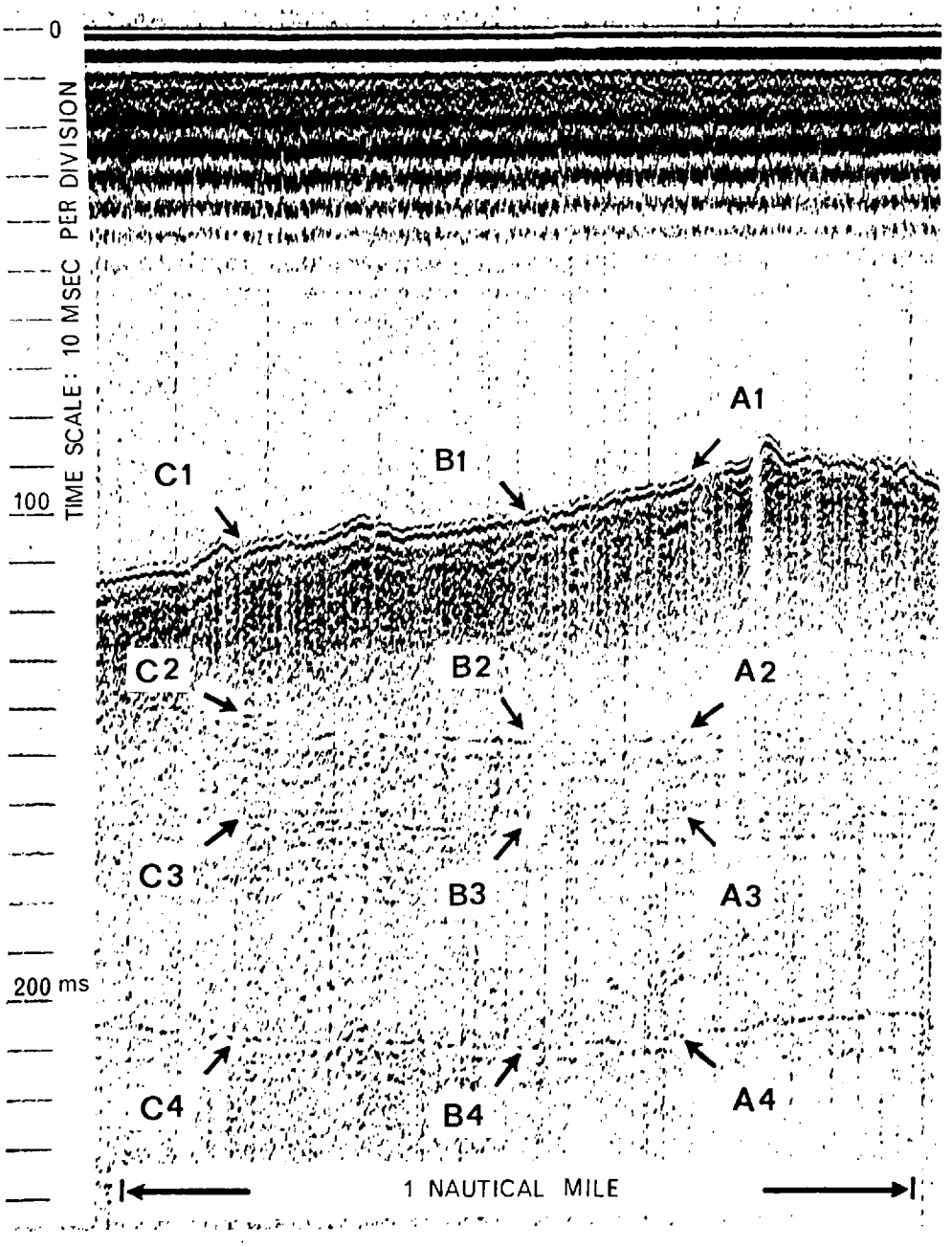

Fig. 7.8. The sub-bottom profile, Area(12).

head and tail of a reflection, only 2 and 3 of the several intermediate interfaces are marked out. In the profile shown, only the first bottom multiple can be vaguely seen. Filtering of the signal for reproducing this profile was again set at a passing band of 75-600 cps. It can be seen that the average water depth in this area is over 250 ft.

7.2.2. The Raw Spectra

Fig. 7-9 shows the corresponding raw spectra to the various pulses of sweep A, B and C indicated as in the preceeding profile. At a glance, all outward characteristics have much in common with those of Area (15) except for the bottom reflection 1, the spectral level below 250 cps being of very low values. As in most other areas, 3 sweeps of reflection pulses were analyzed, any two of which are to provide data of varying layer thickness while the third one supplies alternative data.

7.2.3. Reflection Spectra Comparison and Computed Results

Comparison of reflection spectra in graphical form is shown in Fig. 7-10, in which the data appears to be very irregular. Logical data is particularly difficult to be found for deriving reasonable attenuation results. After many trials, variations of relative spectral level of central frequencies of 150 cps and 600 cps were still used as a basis for calculation but attenuation values were computed using reflection 1 and 2 of A and C for the former while reflection 1 and 4 of B and C for the latter. The computed results were

Attenuations: $\alpha_{150} = 0.0037$ dB/ft.

$\alpha_{600} = 0.0238$ dB/ft.

Band-average: $\alpha_{150\text{-}600} = 0.0138$ dB/ft (0.043 dB/m)

Frequency Dependence $f^{1.33}$

Probable Sediment Composition: Clayey silts.

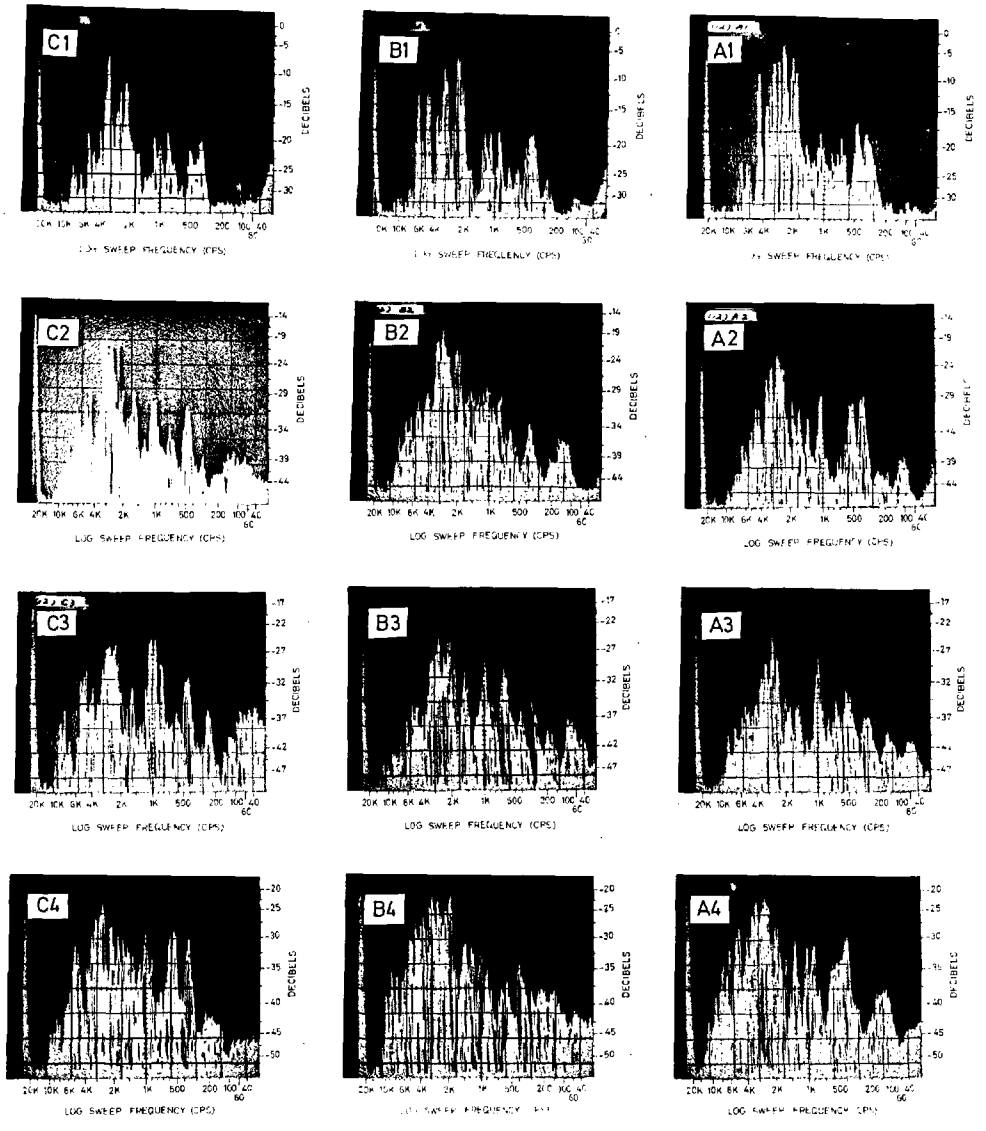

Fig. 7.9. The spectra, Area(12).

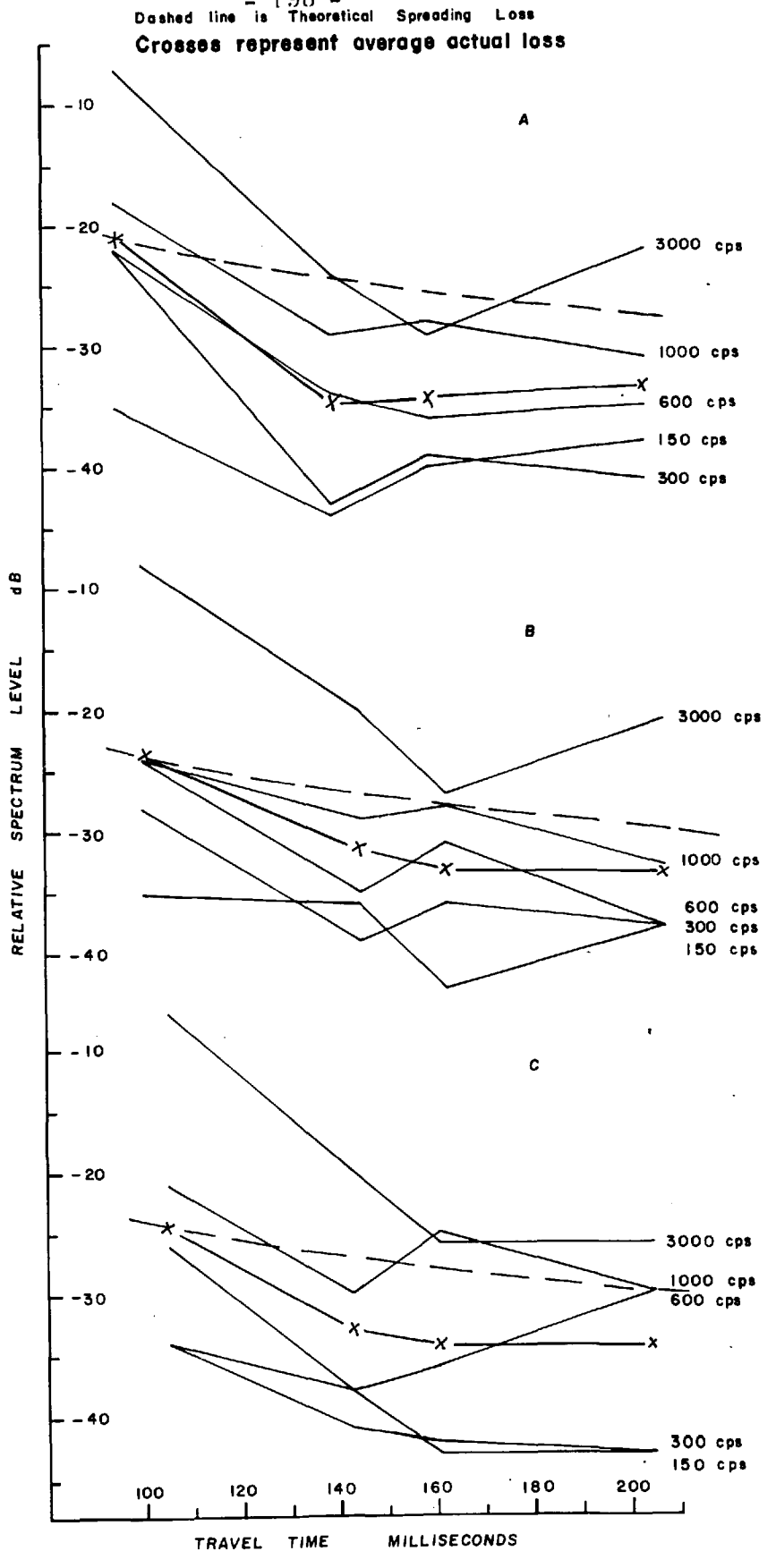

FIG.7.10 REFLECTION SPECTRA COMPARISON, AREA (12).

7.3. Area (11)

7.3.1. The Profile

This is a very interesting area indicating some sort of unconsolidated sediments unconformably overlying a highly stratified geosynclinal sub-strata. In Fig. 7-11, the upper part is a reproduced profile directly from the raw data tape without going through any filtering, using as usual the half-wave rectification for the d. c. graphic printing at the recorder. The bottom and sub-bottom boundaries, as well as deeper structures, can be clearly discerned. The lower part of the figure is the same profile but reproduced through the most commonly used filtering band of 150-600 cps. The ringing effects caused by filtering can be seen most obviously in this instance and, in fact, it has ruined the clarity of the reflection profile, thus concealing vital information otherwise available. Of course the optimum filter setting, including an open one, varies a lot, depending on the geophysical conditions of the area as well as the quality of the raw data collected. This certainly serves as a demonstration of the very great advantage of recording raw acoustic data on magnetic tape.

Four sweeps, A, B, C and D were chosen for analysis in this area. In addition to having varying thickness for the first layer, five reflection pulses were selected from sweep D to see if examination of reflections from deeper structure would yield any correlated information. Unfortunately this proved to be entirely non-conclusive. In this area, as well as Area(6), some bottom sample textural analysis data, diagnostic of very fine sand was kindly provided by Caston (1966). Since this information was strictly confined to the superficial part of the top few inches of the bottom sediment, its relation to the rest of the sediment column of the order of some 100 ft. thick was uncertain, particularly stratification in the top layer can be discerned in the present area.

Fig. 7.11. Area(11).

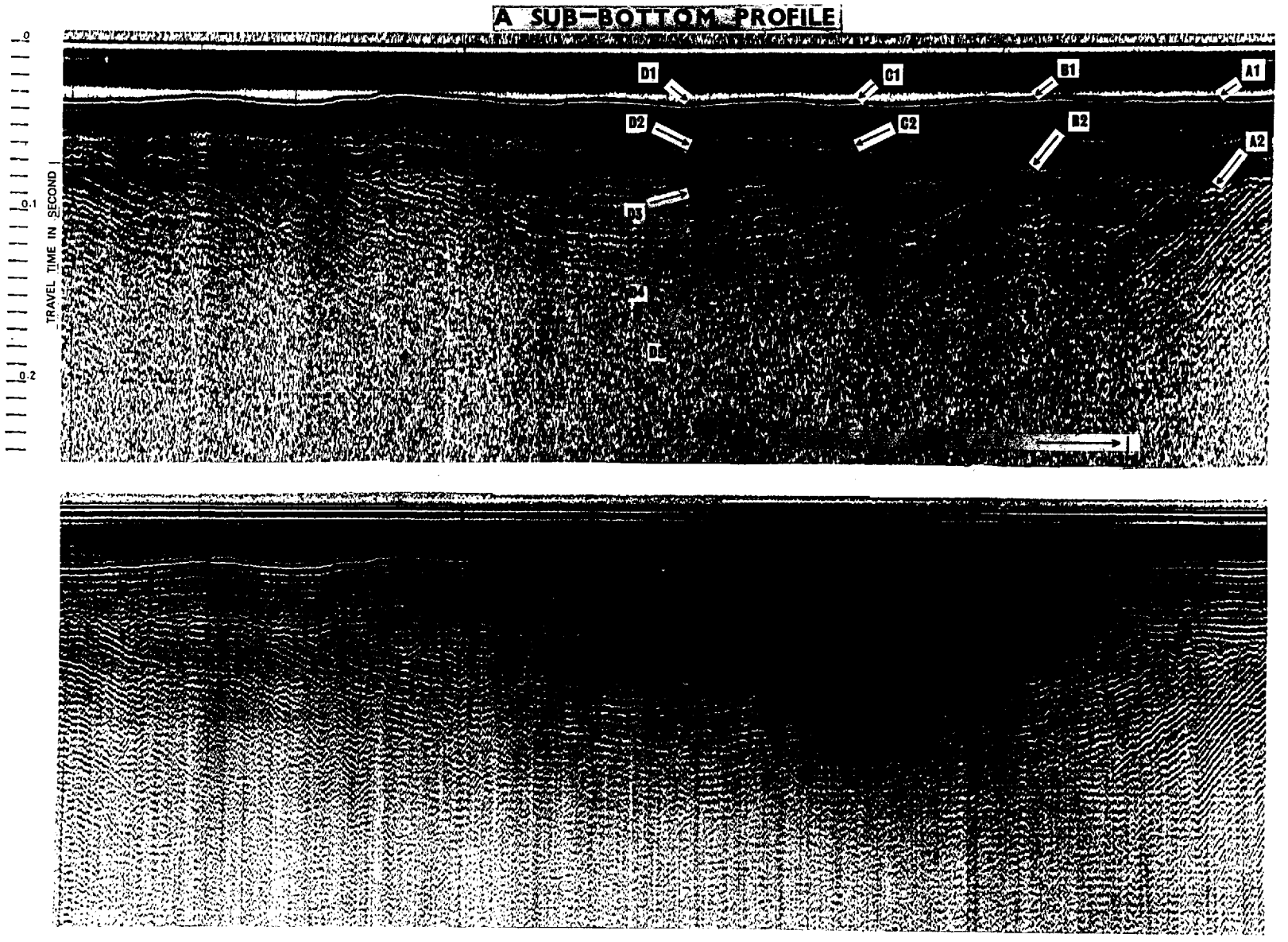

7.3.2. The Raw Spectra

The corresponding spectral results are shown in Fig. 7-12. It can be seen that the low frequency portion (100-400 cps) as compared to the high frequency portion (2-4 kcps) generally becomes more important for reflections from a deeper reflecting interface. This phenomena occurs in data from practically all the four areas investigated. However, this could only serve as rather weak qualitative evidence to support the statement that sedimentary layer and deeper media attenuate the high frequency content more than the low. Quantitative measurements made and analyzed, including the high frequencies, have too often turned out to be too confusing and illogical to be accepted.

7.3.3. Reflection Spectra Comparison and Computed Results.

Relative spectral level comparison of the reflection spectra of this area is shown in Fig. 7-13. Again, the lack of systematic layout of the spectral data curves makes calculation of the attenuation values a highly selective task of choosing only those data that would give acceptable results. Among the reflections, 1 and 2 of sweep B and C, and sweep B and D were used for the calculation of the two sets of attenuation. The values obtained were:

Attenuation: $\alpha_{150} = 0.0025$ dB/ft

$\alpha_{600} = 0.0304$ dB/ft.

Band-average: $\alpha_{150-600} = 0.0165$ dB/ft (0.051 dB/m)

Frequency dependence: $f^{1.79}$

Probable Sediment Composition: Silty Clay.

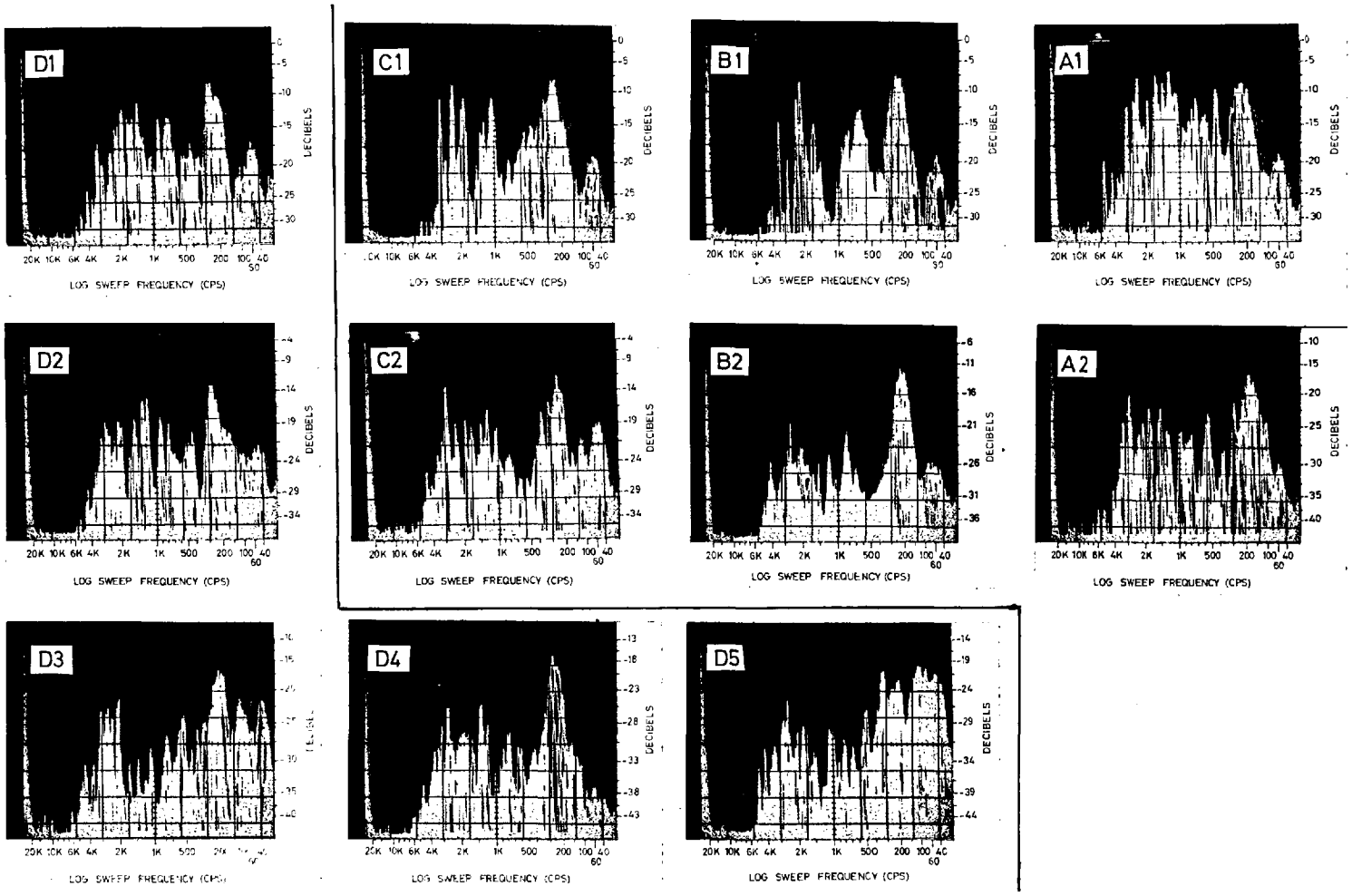

Fig. 7.12. The spectra, Area(11).

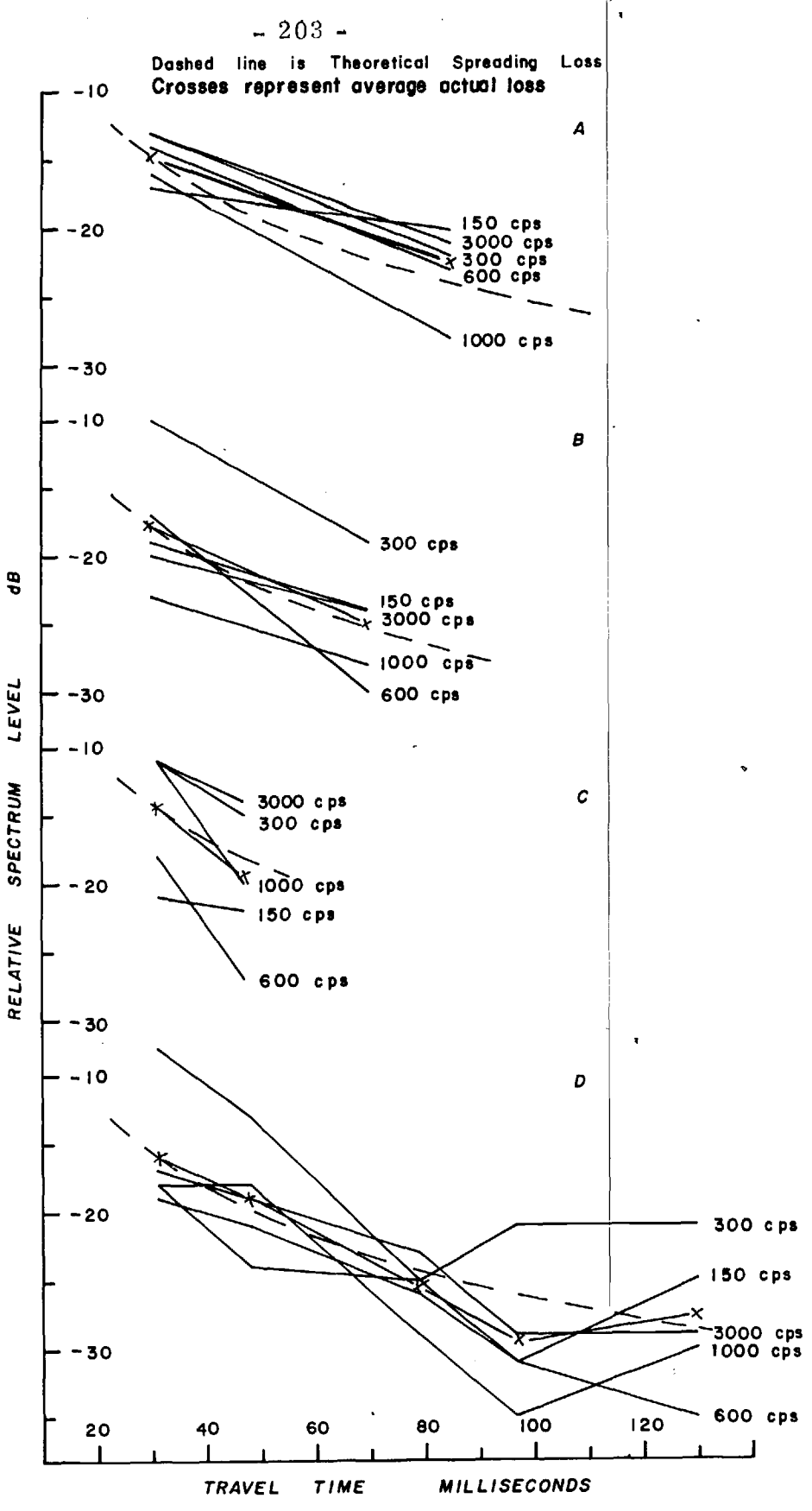

FIG. 7.13 REFLECTION SPECTRA COMPARISON, AREA (11).

7.4. Area (6)

7.4.1. The Profile

A profile near Tremadoc Bay is shown in Fig. 7-14. in which three sweeps of varying layer thickness are indicated. The dipping sub-bottom reflecting boundary lacks good definition but the bottom sediment layer does not show any appreciable intermediate stratifications. Furthermore detailed superficial textural information of the bottom, as mentioned before, is available, showing mainly fine sand particles. The upper part in the figure is a reproduced profile with a band-pass filter (150-600 cps) the ringing effect being still obvious. An unfiltered reproduction of the profile shown in the lower portion of the figure again gives better definition of the main reflections. Water over this area is particularly shallow, being only about 50 ft. However, the fact that no excessive masking reverberations are observed is considered remarkable, probably due to the low reflectivity of the bottom surface material.

7.4.2. The Raw Spectra

Corresponding pulse spectra are shown in Fig. 7-15. As in Area (11), a general relatively high level of the spectral energy occurs at the low frequency end and it is qualitatively apparent that this becomes more important in the sub-bottom reflections. Again this characteristic could be attributed to the frequency dependence though no quantitative results can be systematically drawn.

7.4.3. Reflection Spectra Comparison and Computed Results

The graphs drawn for various spectral levels are shown in Fig. 7-16. Irregular distributions of actual loss with different centre frequencies can still be observed. However, the outlook of the comparisons

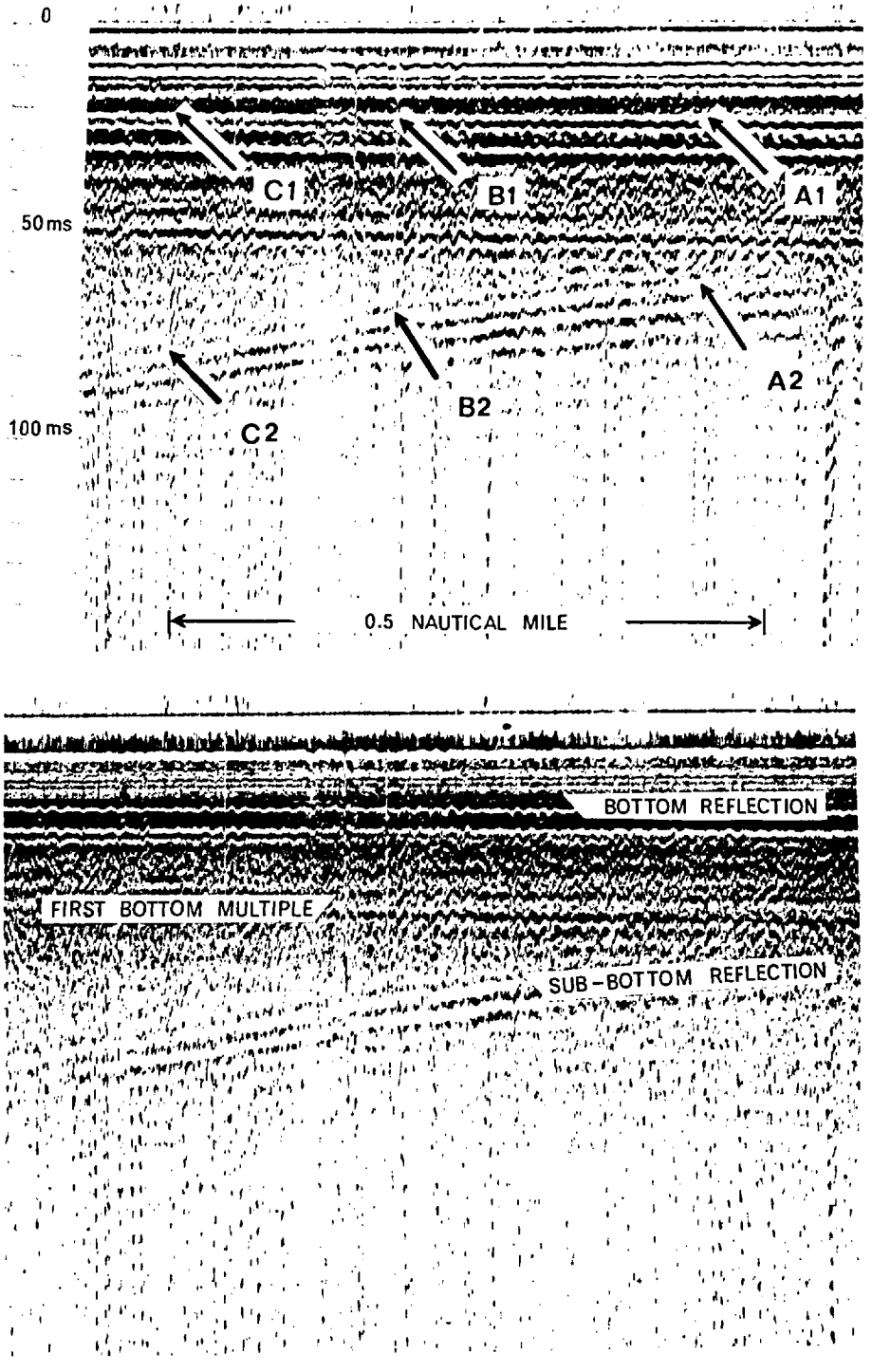

Fig. 7.14. The sub-bottom profile, Area(6)

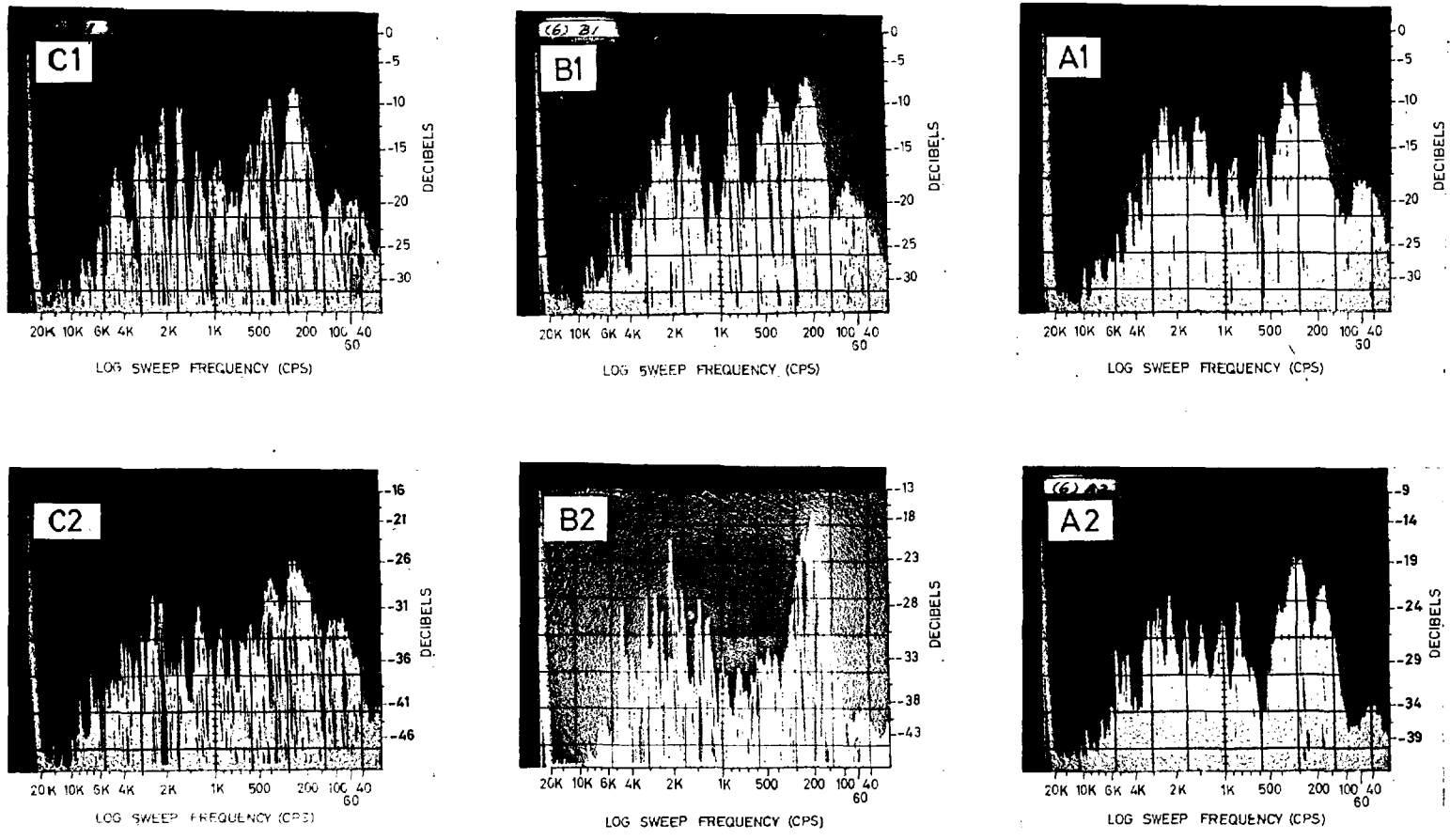

Fig. 7.15. The spectra, Area(6).

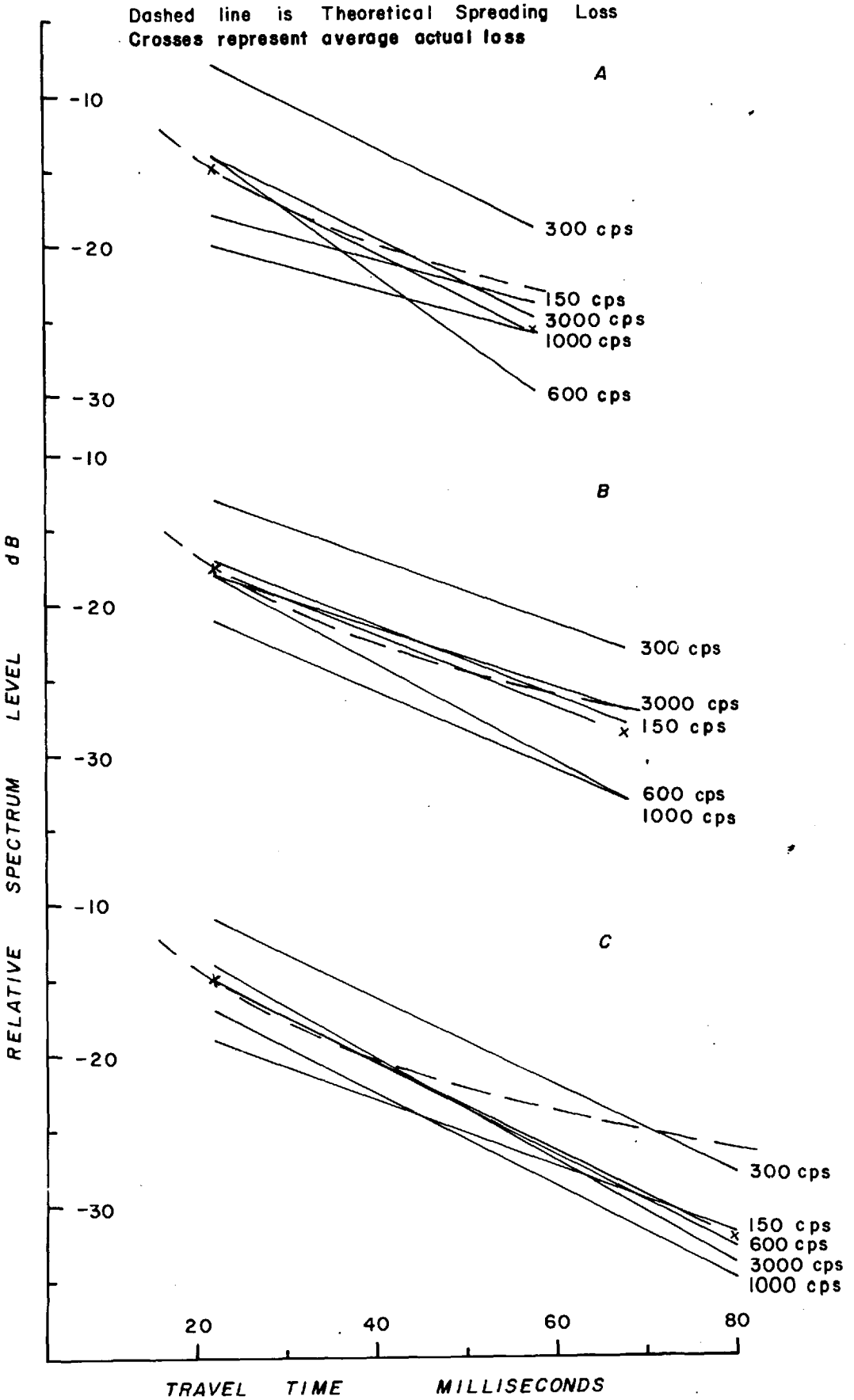

FIG.7.16 REFLECTION SPECTRA COMPARISON, AREA (6).

appears to be less chaotic than in other areas, probably because higher homogeneity of the sediment might indeed exist. The following values of acoustic constants were obtained:

Attenuation = $\alpha_{150} = 0.0083$ dB/ft

$\alpha_{600} = 0.025$ dB/ft

Band-averaged $\alpha_{150\text{-}600} = 0.0167$ dB/ft (0.051 dB/m)

Frequency dependence: $f^{0.78}$

Probable Sediment Composition: Fine Sand

Superficial Textural Analysis: Fine Sand (Caston, 1966)

7.5. Fluctuation of Reflections

From data extracted from the profiling records, it could be observed that the amplitude in successive bottom or sub-bottom reflections at places varies as much as 2 to 1 and in one case a mean variation of 3 dB was obtained. This rapid change in energy level was largely due to the fact that the source and receiver were shallow and the air-water surface was not smooth. For a constant source, fluctuation of signals reflected from a smooth homogeneous reflecting bottom would be zero. In actual practice, fluctuation can be attributed to unstable parameters varying at random such as the waves produced at the air-water surface, the variation of source intensity, together with other random noise superimposed on the signals, and the comparably stable state of the roughness of the reflecting bottom or sub-bottom and its lateral variation. It is therefore logical to believe that by averaging the reflections in groups which are in turn treated statistically it should be possible to produce a moderately indicative relation between signal level fluctuation and bottom or sub-bottom roughness.

7.5.1. Methods

Using the signal-gating switch during playback of the data tape in conjunction with the control and monitoring operation of the Mufax recorder, a series of acoustic events at a certain fixed time interval relative to the transmission were isolated and presented on the screen of the storage oscilloscope. With a slow time sweep, the oscilloscope presentation was either a direct peak-to-peak indication or, after passing through a narrow band filter, an indication of the fluctuation within the bandwidth. Taking account of the desirability of having short geographical translation but adequate size of sample, individual populations usually consisted, on an average number, of twenty pulses.

The fluctuations of the acoustic signal are usually described by their standard deviation and by their distribution law. To express the spread of the amplitude about the mean, it is common practice to give the root mean square of the individual difference from the mean. This result, which is expressed in the same dimensions as the level, is called the standard deviation of the level. The relative standard deviation, v_p, is defined as the ratio of standard deviation and the mean value, p_o, of the acoustic pressure, p,

$$v_p = \frac{(1/n \sum (p-p_0)^2)^{\frac{1}{2}}}{p_o} = \frac{(1/n \sum \Delta p^2)^{\frac{1}{2}}}{p_o}$$

where n is a numeric corresponding to the size of the sample.
The resulting quantity is dimensionless and may be expressed as a percentage. The square of the relative standard deviation is called the relative coefficient of variation. Although this has been employed by other workers it is not used here.

A sample of fluctuation data is shown in Fig. 7-17. Frames a, b and c are signals of surface-reflected arrivals, bottom reflections, and

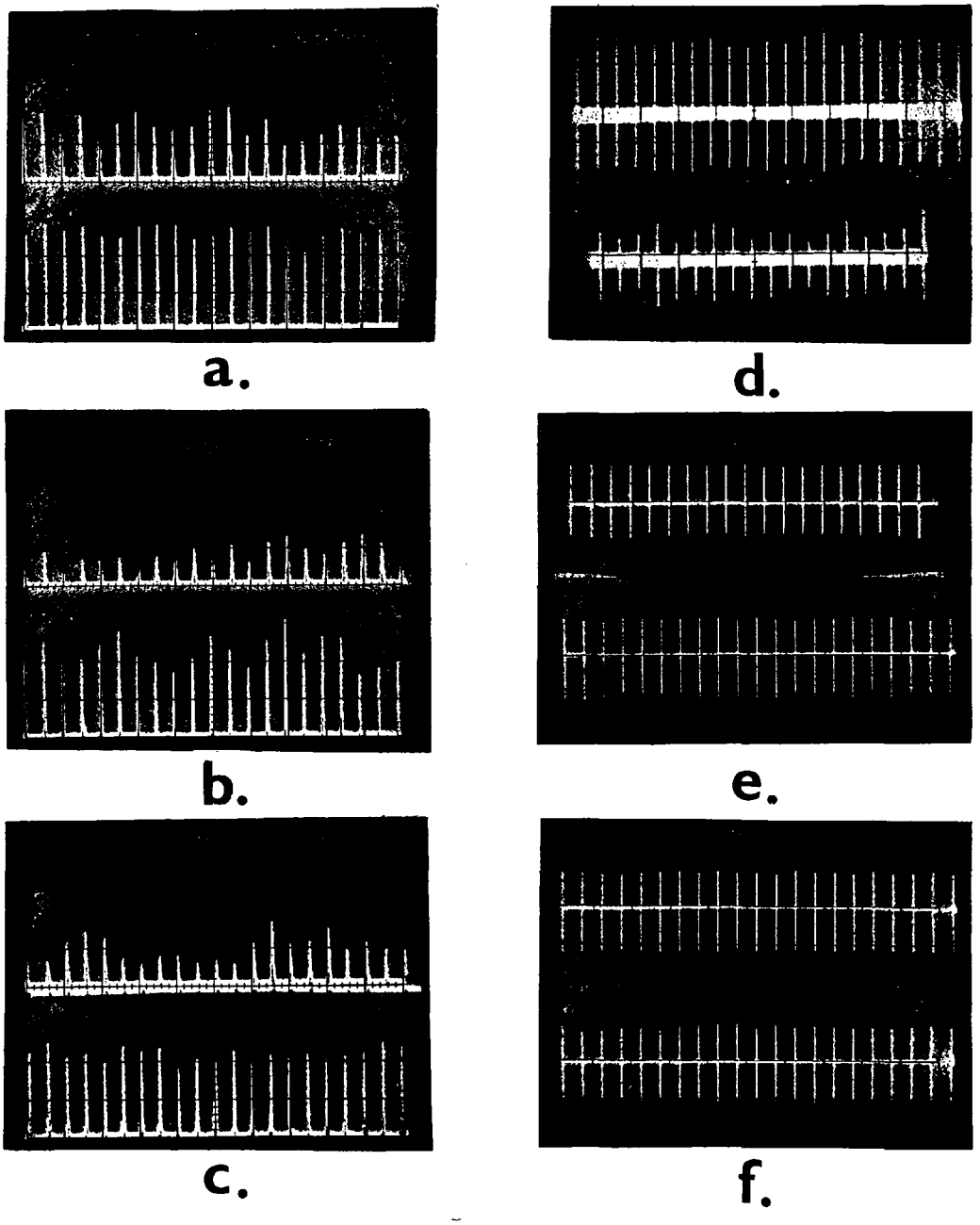

Fig. 7.17. Samples of fluctuation measurements.

sub-bottom reflections respectively in Area (6) around sweep B. The vertical scale is in dB and the centre frequency is 500 cps. The upper traces are the results using a narrow-band (10 cps) filter while the lower traces are using a wide-band (1,000 cps) filter, thus producing different amplitude levels. In frame d, the upper trace shows signals of the direct arrivals from the sparkarray system with all three electrodes operating while the lower trace indicates the results with only one electrode being used. In frames e and f, four series of direct arrivals are shown from the adjustable-gap spark each for a fixed gap-width which increases from top to bottom.

Similar measurements were made of reflection signals collected at Area (15-B) and Area (11-B). Two centre frequencies were used (500 and 5,000 cps) together with a change of sampling bandwidths of 100 cps and 1,000 cps.

7.5.2. Results

In Fig. 7-18, a table lists all the analytical results after the data has been statistically treated and various ratios computed. Some general phenomena of the fluctuations of reflections of broadband sound from bottom and sub-bottom can be summarized as follows: (1) for the same centre frequency, the fluctuations are large for the narrower bandwidth; (2) for a fixed sampling bandwidth, fluctuations are larger for higher centre frequency; (3) the ratio of the fluctuations in the narrow and wide bandwidths at the low frequency is smaller than that at the high frequency; and (4) peak-to-peak measurements produce smaller fluctuations than those of the limited bandwidths.

Reasons for the above statements are self-obvious when the theoretical side of the matter is examined. Fluctuations due to interference

Fig. 7.18 EXPERIMENTAL RESULTS OF SIGNAL FLUCTUATION MEASUREMENTS (Note: $\frac{\text{B.R.}}{\text{S.R.}} = \frac{\text{Bottom Reflections}}{\text{Sub-bottom Reflections}}$)

COLUMN	PULSE DESCRIPTION	CENTRE FREQUENCY CPS	SAMPLING BANDWIDTH CPS	RELATIVE STANDARD DEVIATION %	AVERAGE RELATIVE STANDARD DEVIATION %			RATIO OF R. S. D. %			RATIO OF COLUMN 11 / 5,000/500 %	RATIO OF COLUMN 10 B.R./S.R. %	RATIO OF COLUMN 12 B.R./S.R. %
								B.R./S.R.	CENTRE FREQ. 5,000/500	SAMPLING BANDWIDTH NARROW/WIDE			
1	2	3	4	5	6	7	8	9	10	11	12	13	14
AREA 15(B)	BOTTOM REFLECTION	500	100	19.8	16.1	30.3	23.4	94.7	276	160	244	65	65
			1,000	12.4									
		5,000	100	70.4	44.5					391			
			1,000	18.5									
		P-P	Open	4.6	9.6	9.6							
	SUB-BOTTOM REFLECTION	500	100	12.8	10.3	26.9	24.7		423	167	378		
			1,000	7.7									
		5,000	100	75.2	43.6					631			
			1,000	11.9									
		P-P	Open	20.1	20.1	20.1							
AREA 11(B)	BOTTOM REFLECTION	500	100	9.5	8.2	37.5	26.7	144	815	140	271	293	151
			1,000	6.8									
		5,000	100	105.6	66.8					380			
			1,000	27.9									
		P-P	Open	5.0	5.0	5.0							
	SUB-BOTTOM REFLECTION	500	100	17.0	11.6	21.8	18.6		278	277	179		
			1,000	6.1									
		5,000	100	53.5	32.2					496			
			1,000	10.8									
		P-P	Open	12.0	12.0	12.0							
AREA 6(B)	DIRECT ARRIVAL	SPARKARRAY P-P	1-ELECTRODE	15.7	9.9			108		383		102	
			3-ELECTRODE	4.1									
	SURFACE REFLECTION	500	10	21.6	16					210			
			1,000	10.3									
	BOTTOM REFLECTION	500	10	45.5	30.6					290			
			1,000	15.6									
	SUB-BOTTOM REFLECTION		10	38.5	28.3					285			
			1,000	13.5									

and scattering effects shown in discrete frequency transmission are smoothed out when using the larger receiving bandwidth. The case of peak-to-peak signal reception is the widest bandwidth, or all-pass, reception. At the same time, for a fixed roughness of a reflecting interface, the effects of scattering usually become more pronounced with an increase in the interacting frequency, causing an increase in back scattering.

A most significant feature in the tabulated results is the three mutually confirmatory criteria indices (columes 9, 13 and 14) chosen to indicate the relative roughness of bottom and sub-bottom reflecting interfaces. The comparisons of the average relative standard deviations, the values obtained with high-to-low centre frequency, and the ratios of ratios of narrow-to-wide sampling bandwidths between high and low centre frequencies, each being independent in a sense, agree remarkably in giving comparative indices which, in a way, suggest a method of evaluating the practical possibility of this particular method.

Of the three areas investigated, it is found that area (15), judging from the three indices, has probably a rougher sub-bottom than the first bottom while the reverse might be true in area (11). Area (6) might be regarded as a marginal case where the two boundaries appear to have approximately the same roughness.

It should be pointed out here that despite all the comparative figures listed and the systematic outlook of these fluctuation results, the method used and the tentative conclusions drawn are still essentially qualitative because of the intrinsic complexity in the various interactions between boundary irregularities and the band-limited measurements of fluctuations from a broad-band source. Many more absolute parameters must be known before any quantitative behaviour characteristics can be predicted. Nevertheless, this comparison technique is considered to be

worthwhile in giving relative geophysical information. Appropriate geological control would be needed to have the method become more established.

7.6. Comparison of Variation of Intensity of Source

Data collected from the direct transmission experiments by varying the source parameters was used in the study of the variations of intensity and fluctuations as well as of the pulse form and frequency content. In all such cases, the essential requirement has been to complete the recording of the signal due to transmission over the direct ray path before the arrival of pressure waves which may have been reflected from the surface or the bottom of the sea. This has been, in fact, fulfilled in the field as previously described (Section 5.7). As in the fluctuation measurements of reflection pulses, the storage oscilloscope was again used to present the pressure amplitude. In the present case of studying the variations of intensity and fluctuation of the source, only peak-to-peak values are of interest. These were photographed during replay of the data tape. Various amplitude values are shown in frame d, e and f in Fig. 7-17. A table listing all the pertinent information is shown in Fig. 7-19. A fixed pulse energy level of approximately 1,000 joules and a fixed source-receiver distance were used during the entire field experiments to facilitate direct comparisons.

7.6.1. Tabulated Results

It can be seen most obviously that for the Sparkarray the energy transfer is higher for a larger number of transmitting electrodes. As for the adjustable-gap spark electrode, increasing the gap-width increases the energy transfer but not very markedly. It is also observed that in the case

INDEX DESIGNATED	PHOTOGRAPHIC DATA POSITION	TYPE OF SOURCE	NUMBER OF ELECTRODE OR GAP WIDTH	AVERAGE OF RELATIVE PRESSURE AMPLITUDE (ARBITRARY UNITS)	RELATIVE STANDARD DEVIATION %	RATIO DESCRIPTION	INTENSITY RATIO	ELUCTU-ATION RATIO %
I	(d) Upper	Sparkarray	3-Electrode	26.1	4.1	I/II	1.89	26
II	(d) Lower	Sparkarray	1-Electrode	13.8	15.7	II/II	1.00	100
III	(f) Lower	Open Type Tufnol Ins.	1-Electrode	15.0	4.9	III/II	1.09	31
IV	(e) Upper	Adjustable-Gap	1/8 inch	14.6	4.4	IV/IV	1.00	100
V	(e) Lower	Adjustable-Gap	1/2 inch	15.7	3.2	V/IV	1.08	73
VI	(f) Upper	Adjustable-Gap	1 inch	16.0	2.3	VI/IV	1.10	52

Fig. 7-19

of the Sparkarray, the firing of single electrode causes a greater amplitude fluctuation than firing the whole array (3 electrodes), probably due to the averaging out of the size of bubbles produced under the latter conditions. However, for an enclosed adjustable-gap electrode, increase of the gap-width causes a decrease in the fluctuation level. This might be due to the relative instability produced by the narrow gap-width on the spark pulse. The explanation might lie in the oscillatory electrically-induced bubble formation with impurities in the water playing some role.

From the table it can also be seen that the specially designed open electrode, being tufnol-insulated with an outer earthing ring of 2 in. outside diameter, gave better performance than the Sparkarray candle type electrode, by having a greater energy transfer and less fluctuation. The reason for this can be attributed to the fact that tufnol is a better insulation material than the soft rubber of the Sparkarray candle. Being firmer, although perhaps a little on the brittle side, it will be more stable against burning by arcing.. The best single electrode performance is possessed by the adjustable-gap type which has a better energy transfer than either the candle type or, except at 1/8 in. gap-width, the tufnol-insulated open electrode.

7.7. Acoustic Source - Sparkarray

Great interest is attached to the pulse characteristics and spectral contents produced by a single electrode (the candle type) as well as the various combinations of the number of firing electrodes in a Sparkarray. From data of direct arrivals collected in the field, study of the results, reproduced and processed in the laboratory, has presented conclusive results. It should be remembered that the deep-electrode

deep-hydrophone set-up for direct arrival measurements have associated with them an increase in the hydrostatic pressure when compared with the normal survey arrangement. Slight deviations of behaviour are therefore to be expected at the greater depth. No corrections for this have been made because of the limited scope of the investigations.

7.7.1. Pulse Characteristics

In Fig. 7-20 the upper trace in frame 1 was obtained when all three electrodes of the Sparkarray were operating, the lower trace in the same frame being a 1 kcps reference. Frames 2 and 3 show the acoustic pulses when only two and one electrode respectively was used, all other conditions being essentially the same. Fig. 7-21 shows the corresponding spectra as presented by the spectrum analyzer. In Fig. 7-22 are two tables (A) and (B) listing the essential features both in the time and frequency domains which help indicate their general relation with the number of electrodes used.

From Fig. 7-20 and Table (A) in Fig. 7-22 it can be observed that increasing total pulse length goes with decreasing number of electrode in the transducer array, the energy in the storage bank being unchanged. There appears to be a similar relation in the bubble forming period although one of the results (Frame 2) shows an anomaly.

As electrical energy is converted into acoustic energy through different numbers of electrodes the amount of the total convertible energy, though varying in transfer efficiency to quite an extent, will be roughly divided by the number of electrodes, thus causing the size of the bubble or bubbles created varying inversely with the number of electrodes. It can therefore be observed from the trace in frame 3 of

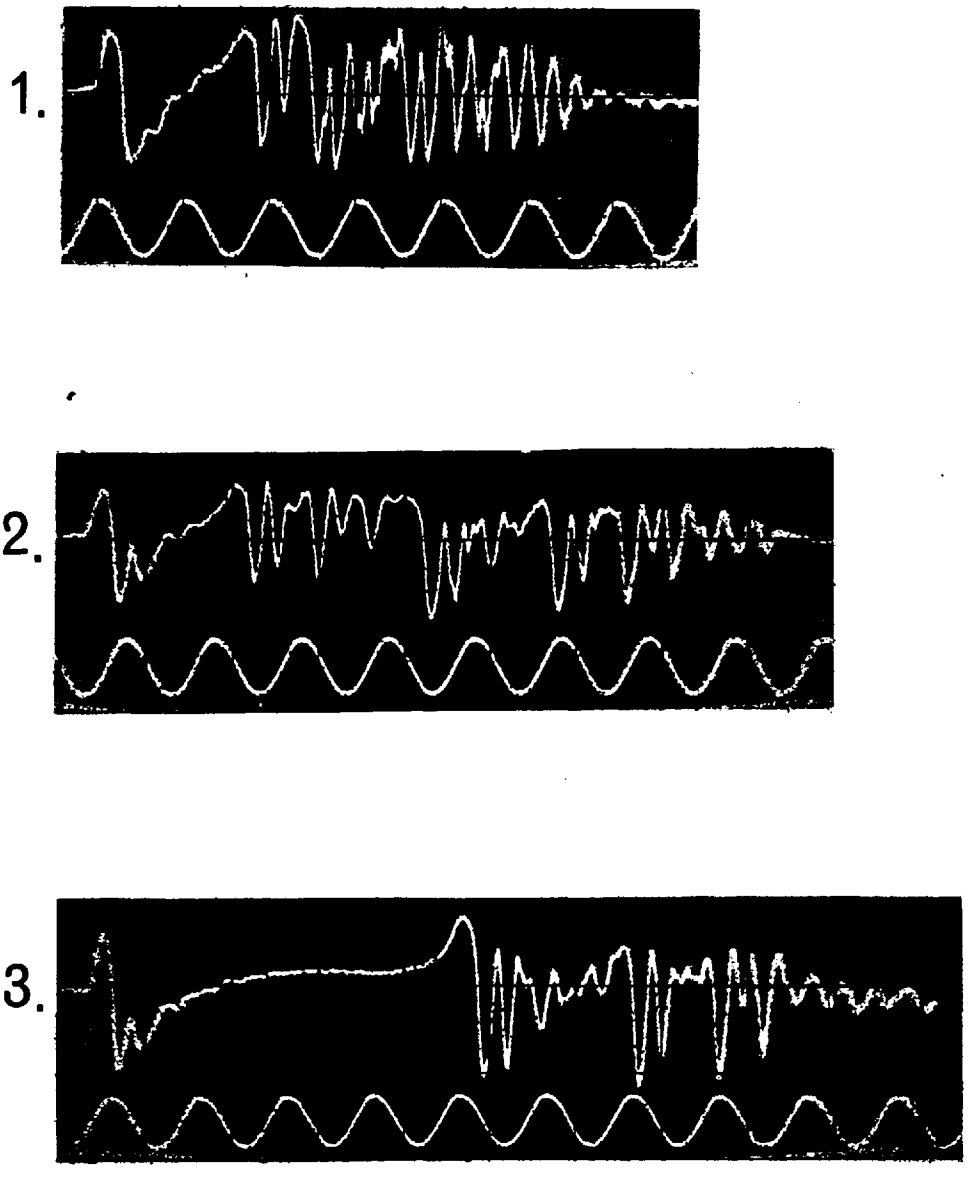

Fig. 7.20. The direct arrivals, the Sparkarray.

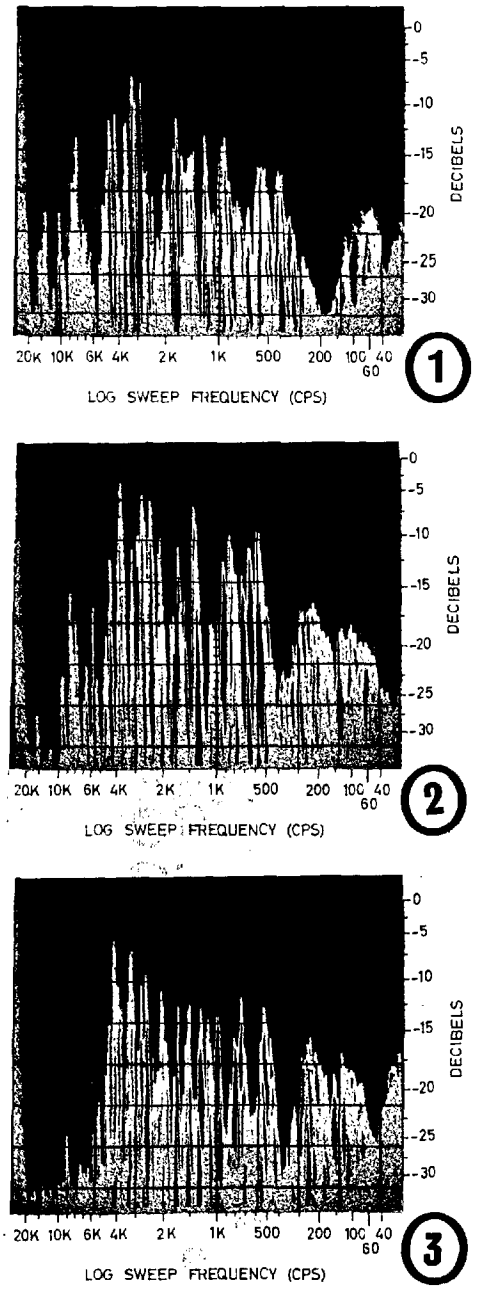

Fig. 7.21. The spectra, the Sparkarray.

TABLE (A) PULSE CHARACTERISTICS

	Pulse 1	Pulse 2	Pulse 3
No. of Firing Electrode	3	2	1
Bubble Forming Period msec	2	1.9	4.6
Total Pulse Length msec	6	8	10

TABLE (B) SPECTRUM ANALYSIS

	Spectrum 1	Spectrum 2	Spectrum 3
No. of Firing Electrode	3	2	1
150 cps (dB)	26	19	19
300 cps (dB)	24	17	17
600 cps (dB)	16	12	15
3,000 cps (dB)	8	6	11
3,000 cps/150 cps	18	13	8
3,000 cps/300 cps	16	11	6
3,000 cps/600 cps	8	6	4
Average Ratio High Freq./Low Freq.	14	10	6

Fig. 7-22 PULSE ANALYSIS OF DIRECT ARRIVALS, SPARKARRAY

Fig. 7-20 that, comparatively, the longest bubble forming period as well as the total pulse length was obtained when one electrode only was used. However, the bubble forming period shown by the trace in frame 2 appears to be slightly less than that of the trace in frame 1 yet the total pulse length of the former is appreciably longer. This could be best explained as due to the uneven formation of the bubbles between the two firing electrodes, creating one large and one small bubble. While the larger bubble extended the total pulse length the earlier beginning of the collapse of the smaller cavity would make the bubble forming period look shorter on the pressure amplitude trace.

7.7.2. Spectrum Analysis

From Fig. 7-21 and Table (B) in Fig. 7-22 the frequency aspect of the characteristics of the acoustic pulses generated by the Sparkarray with varying number of electrodes are systematically presented. An average increase in ratio of high-frequency-to-low-frequency with increasing number of electrodes is characteristically indicated. This again might be attributed to the relation between the size of a bubble and its oscillation. A comparison between table (A) and table (B) in Fig. 7-22 is most interesting. Their mutual correlation appears to be very obvious. It should be noted that the results were derived through only one set of data with rather limited variation in the number of electrodes and under a specific set of conditions. Since the investigation was to seek practical information concerning an existing transducer array, all the correlations should be regarded more qualitatively than quantitatively.

7.8. Acoustic Source - Adjustable-Gap Spark

Among all parameters concerning the performance of the experimentally developed adjustable-gap spark used as an acoustic source, the relationship between the electrode gap-width and the characteristics of the pulse as well as its spectral distribution is of particular interest. The shapes of directly-arrived acoustic pulse and the corresponding spectra obtained with a spectrum analyzer for a range of gap-widths are shown in Fig. 7-23 and Fig. 7-24.

7.8.1. Pulse Characteristics

Fig. 7-23 shows six direct signal pulses isolated and reproduced on the storage oscilliscope screen from magnetic tape. The sinusoidal trace at the bottom of the figure is the 1 kcps reference signal, reproduced to facilitate measurements of pulse length. Trace 1 to trace 5 correspond to electrode gap-widths of 1/8 in., $\frac{1}{4}$ in., $\frac{1}{2}$ in., $\frac{3}{4}$ in. and 1 in. respectively. In all traces except 1, a bubble forming period can be clearly discerned following the initial pressure peak. It ends when the buble starts to collapse. The rarefication peak could usually serve as an evident characteristic of a collapsing cavity. A period of bubble oscillation then follows. In trace 1, the electrode gap-width being set at 1/8 in., the bubble forming period appears to be disrupted by a series of oscillation. This could be due to alternate arcing, with voltage and current reversals, between the closely spaced electrode giving continuously electrical sparking wave fronts during the bubble forming period. On the other hand it might be the effect of a repeatedly formed and recombined central bubble within the narrow gap-width. This presumably would occur only when the gap-width is smaller than a critical distance. Trace 6 was obtained with the use of an open type electrode, having basic dimensions

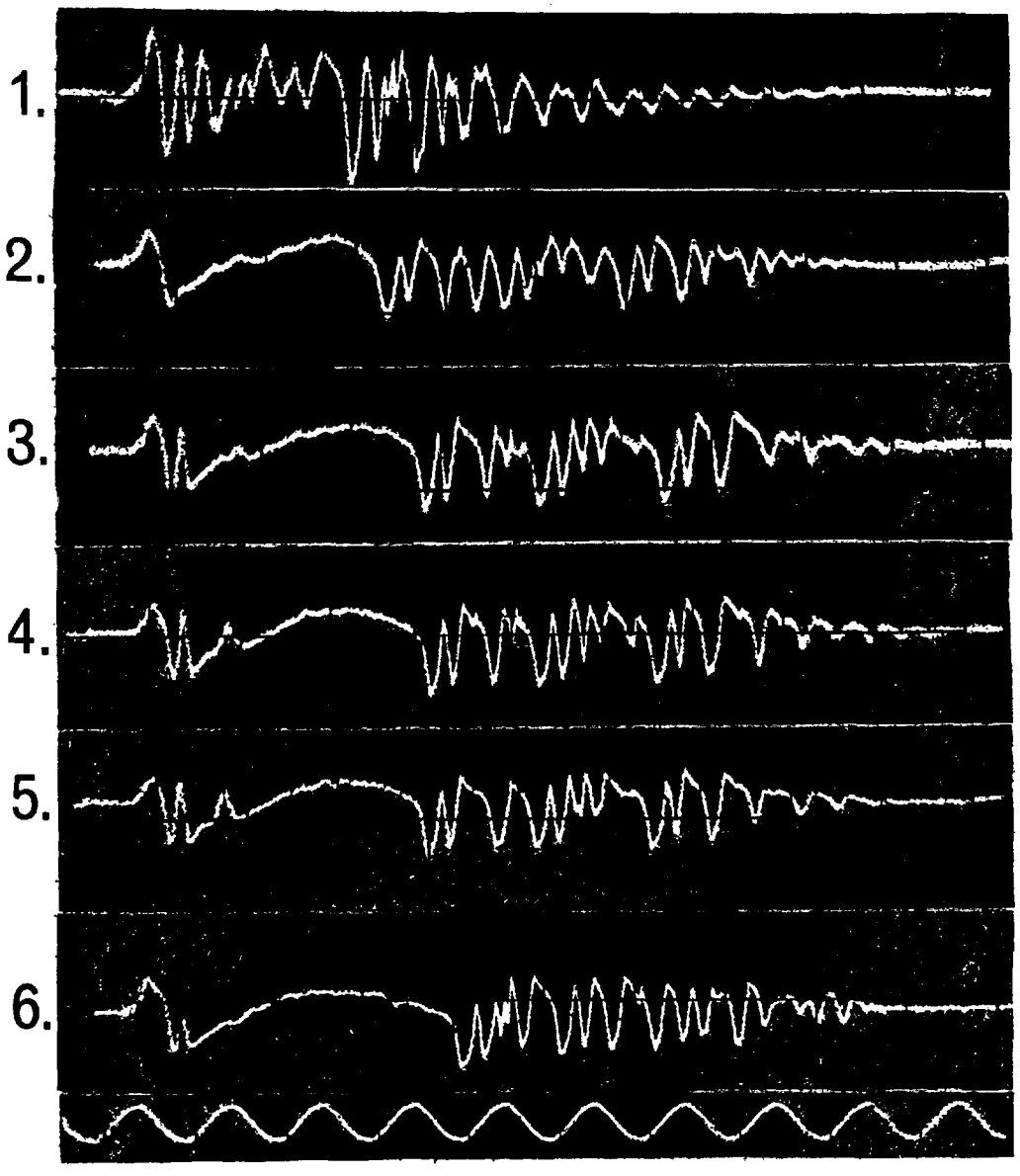

Fig. 7.23. Direct arrivals, adjustable-gap spark.

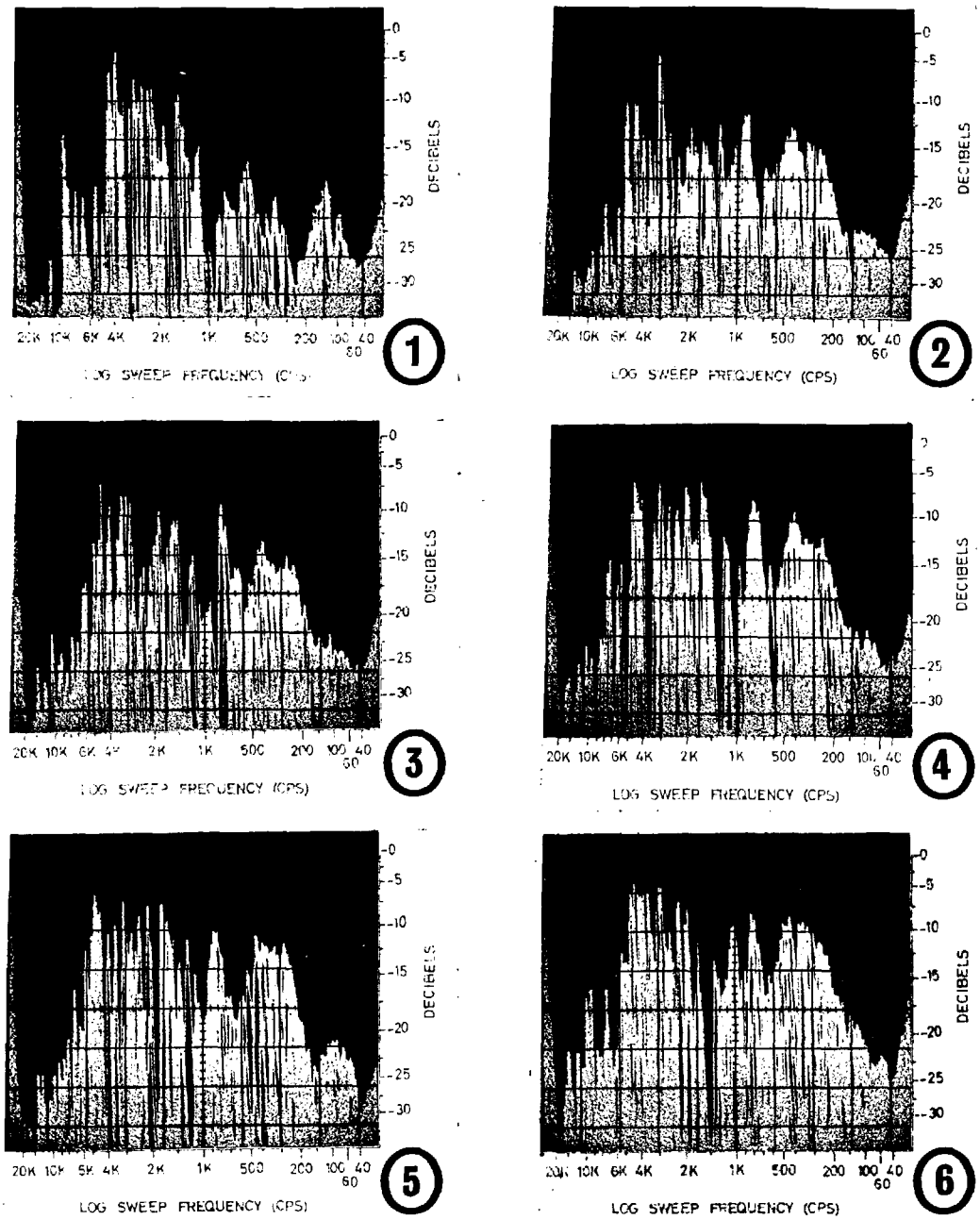

Fig. 7.24. The spectra, the adjustable-gap spark.

similar to the adjustable-gap type used. It must be noted that fluctuations of the spark source and variation in path length of direct transmission during the field experiments have rendered impossible a direct comparison of amplitude of these sample traces. However, comparison of the spectra of individual pulses (shown in Fig. 7-24 with corresponding trace number) gives a rather good indicative frequency-related result. This spectrum analysis will be discussed later in the next section.

Graph (a) in Fig. 7-25 shows the observed relation of total pulse length as well as bubble forming period versus gap-width. The total length of the pulse is taken as the time difference between the beginning of the initial pressure peak and the long tail of bubble oscillations where the amplitude has diminished below 5% of the peak amplitude value. It can be seen that between 1/8 in. and $\frac{1}{2}$ in. gap-width, both bubble forming period and total pulse length increase significantly with the electrode separation. Further increase of the gap-width up to 1 in. does not show a corresponding change, the two curves being almost flat beyond a gap-width of $\frac{1}{2}$ in. This could be explained as caused by the restrictive nature of the physical construction of the four side holes each of diameter 1 in. surrounding the gap. Before the final diameter of the formed bubbles reach 1 in., increased gap-width increases the bubble size. After reaching the diameter of 1 in., further increase in size will only lead to the breaking up of the bubbles when squeezing through the side holes. This is prominently evident by examining trace 6 and graph (a) for which the open type electrode was substituted for the adjustable-gap type, thus removing the major constructional restriction. In fact, in an immersion test of the adjustable-gap spark electrode during field experiments in Cornwall, it was observed that at high energy level and moderate gap-width the central bubble was broken up into four small ones, which were shot out rapidly from the side holes. The sight was quite a fascinating one.

Crosses represent data using open electrode

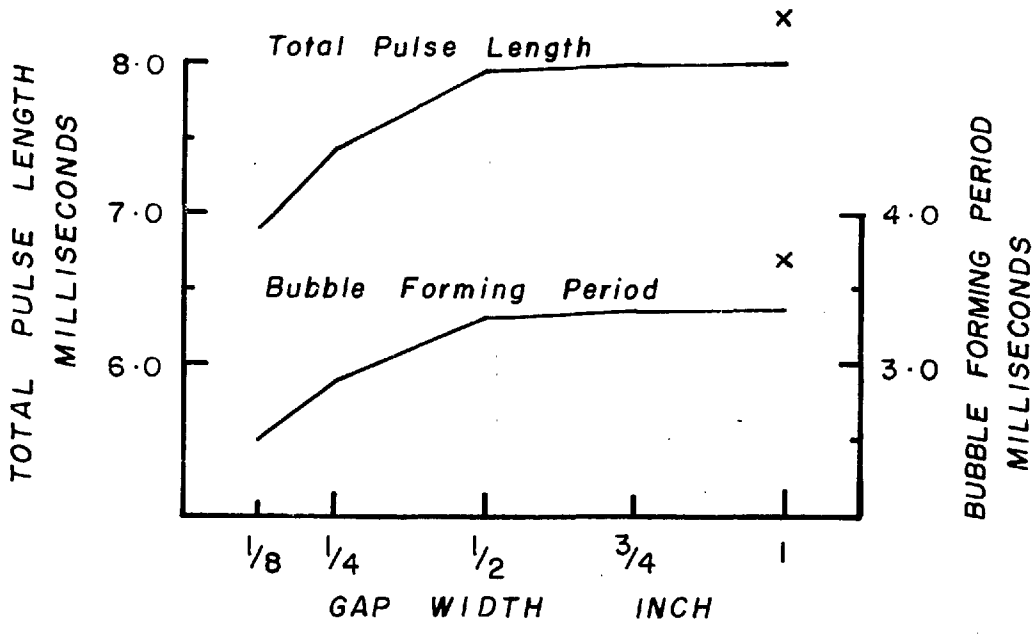

(a)

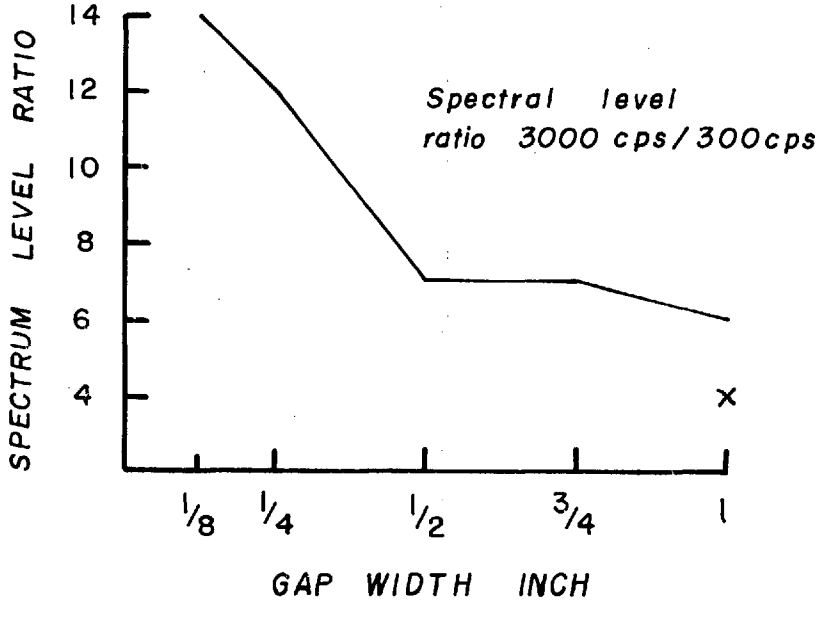

(b)

FIG. 7.25 PULSE ANALYSIS ADJUSTABLE – GAP SPARK .

7.8.2. Spectrum Analysis

Graph (b) in Fig. 7-25 shows the spectral level comparison between the high frequency portion and the low frequency portion of the individual spectra of these six sample pulses. The ratio 3,000 cps to 300 cps was chosen as a proportional criteria because 3,000 cps and 300 cps, though arbitrarily selected, are reasonably representative of the median values of the high frequency portion above 1 kcps and low frequency portion below it. The curve of this ratio in dB versus gap-width indicates an increasingly high proportion of low frequency with increasing gap-width up to $\frac{1}{2}$ in. but the rate flattens off after that.

It appears from comparison of graph (a) and (b) in Fig. 7-25 that the acoustic pulse generated by an underwater spark has its characteristics closely governed by the size of the bubble formed which is in turn determined by the gap-width between the discharging electrodes. The relation between frequency distribution and the size of bubble formed is very obvious again from such a comparison. Again this might be attributed to the varying oscillating frequency versus bubble size as well as the effect of total pulse length upon the fundamental frequency.

In general, with all other parameters constant, the larger the gap-width, the larger will be the bubble formed, the longer the bubble forming period, the longer the total pulse length, and the higher the low-frequency-to-high-frequency ratio in the signal pulse. These relations should hold as long as the forming of the bubble is not restricted in any way. The results so presented can be regarded as quite conclusive since all are theoretically explicable.

CHAPTER VIII

SUMMARY AND CONCLUSIONS

8.1. General Discussions of Results

8.1.1. Transmitting Source

A 1,000 joule energy storage capacitor bank was built and integrated into an original 100 joule commercial sub-bottom profiling system. In association with this, larger electrodes and an adjustable-gap electrode were designed and experimentally tested. It was found that the effectiveness of power-boosting by the parallel connection of an extra capacitor bank would usually be limited by the charging rate and the coordinating speed of the graphic recorder, thus rendering the method less practical unless modifications were extended to the latter as well.

Experimental results have indicated that for a fixed energy level with a multiple electrode system, the larger the number of discharging electrodes (within the physical limitations of the equipment), the higher will be the energy transfer efficiency, the shorter will be the total bubble forming period, and hence the pulse length, and the greater will be the high-frequency-to-low-frequency proportion in the resulting acoustic pulse. With a spark across an adjustable gap, the following phenomena were observed: the smaller the gap-width. the lower will be the energy transfer efficiency, the shorter the bubble forming period, and hence the total pulse length, and the greater will be the high-frequency-to-low-frequency proportion in the acoustic spectrum produced. It is therefore eminently useful as well as practical to incorporate a versatile spark source of variable gap-width and number of electrodes into a multiple source carrier with shipboard remote control. Such a float to embody boomer,

pinger and a special spark source was designed and built but has yet to be put into trial and is awaiting the availability of a properly equipped research vessel.

8.1.2. Receiving Hydrophones

A substantial improvement in the quality of reflection profiles is possible by the use of properly-designed, linear array hydrophone. These provide a directional sensitivity, as well as an enhanced signal-to-noise ratio. However, the total length of the spread of the array must be considered in relation to the distance of the reflecting horizons. Test results using a 10-element array hydrophone have shown that the array was too long for shallow reflection and it caused a lengthening of the received signal, impairing consequently the profile resolution. The best method would be to use a hydrophone array having variable active length. A shipboard control would require that preamplifier be attached to each individual element to prevent any regenerative cross-feed of signal in the cable. A high degree of versatility in both the source and receiver in a profiler or, for that matter any sonar system, is certainly highly desirable.

8.1.3. Development of a New Sub-bottom Profiling System

The modifications to a Mufax fascimile chart receiver for its conversion into a profile recorder whilst retaining its weather-chart receiving function have led to the development of a complex record/reproduce sub-bottom profiling system, having maximum storage energy slightly above 1,000 joules. A very useful synchronization method was developed for reproducing tape-recorded sub-bottom profiles. The performance of the Mufax recorder after the elaborate modifications

proved to be quite satisfactory for working both in the field and in the laboratory.

Instrumentation trials and reconnaissance surveys in the Irish Sea with this sonar system have led to someincidental geological findings supplementing the results of other workers. Amongst these are the dyke-like intrusions off the Isle of Man, the sand waves in the central Irish Sea reported by Harvey, and the state of sedimentation of some areas observed by Belderson with a high-frequency echo-sounder. In connection with the last of these the acoustic characteristics of marine sediments in response to investigations by echo-sounders is fully discussed in Appendix C.

The new sub-bottom profiling system was put to full use in the extensive seismic refraction and reflection surveys in Cardigan Bay in 1965 and were extended further across St. George's Channel in 1966. The combined project was chiefly organized by the Geophysics Section of the University of Birmingham. This collaboration was of great benefit to both sides in that good sub-bottom records showing penetration up to 1,500 ft. were made available to Birmingham to supplement their deeper seismic records while suitable sections were selected from the unfiltered magnetic tape recording for acoustic spectral analysis in the interest of the present research.

8.1.4. Field and Laboratory Procedures

In collecting data for the analysis of sub-bottom reflections, taking records with the ship hove-to was found to have a number of disadvantages compared with recording during normal survey run. This could be attributed mainly to the uncontrollable drift over the sea floor and the excessive roll and pitch of the vessel with the transducers rigged alongside.

In the laboratory, an instrumentation set-up was developed for analyzing the various acoustic signals. In particular the signal-gating switch devised formed a very essential part in the instrumentation system for precision signal isolation and transfer from data tapes. In addition, some features of the modified Mufax recorder were found to be most useful. With the use of this recorder for monitoring and control, precision signal isolation and transfer procedures in processing magnetic tape data have been established which can be regarded as having a considerable technological value.

8.1.5. Results of Spectrum Analysis

The spectral analysis of the various bottom and sub-bottom reflections has turned out some encouraging results. However, as in all geophysical investigations tackling practical problems, there usually exists some data that has not been, and probably cannot be, compared with theory and has led to the introduction of various empirical rules which may involve personal judgement. From the present experimental results a set of values has been obtained for the attenuation and its frequency dependence in sediments in situ in four areas.

The presentation of curves indicating the variations of spectral level at selected centre frequencies from 150 cps to 3,000 cps in relation to path length to and from the principal reflecting interfaces reveals the unpredictable nature of the reflection data. At the same time, within the range 150-600 cps which is characteristic of the useful energy in sub-bottom reflection profiling, values of the effective attenuation coefficient and its frequency dependence were computed. The band-averaged attenuations were found to be in the range 0.014 dB/ft. to 0.067 dB/ft. This range compares very favourably with values found in the same frequency range for the Pierre

Shale (McDonal et al., 1958). However, the range of frequency dependence of the present results which vary from $f^{0.75}$ to $f^{1.79}$ has not been observed in low frequency in situ experiments on sediments or sedimentary rocks in which a linear frequency relationship is more usual. High frequency model experiments and sample measurements generally give a dependence of about $f^{0.5}$ for sand, a linear dependence for silt and something approaching $f^{2.0}$ for clay. Thus the present results in frequency dependence seem to be controlled by the type of superficial sediment.

It is probably purely coincidental that the variations of frequency dependence obtained in the areas investigated compare with those found in the laboratory experiments. However, the attenuation coefficients quoted in the present experiment can rarely represent the coefficients of the superficial loose sediments but more probably that of the consolidated sediment in the lower parts of the sedimentary column.

In the absence of bore-hole controls, the probable type of sediment in layers of thickness up to more than 300 ft. must of necessity be speculative. Despite the fact that bottom superficial textural information available in two areas seems to agree to the diagnosis of the sediment type based on frequency dependency, there is nevertheless a general lack of geological and other evidence to correlate these acoustic attenuation results obtained.

In the present instance, the positive identification of sediment type based on the frequency dependence must necessarily be suspect since the exact nature of the sedimentary column is not known. A greater number of such measurements will need to be carried out over sedimentary layers having a nearer approach to homogeneity than the areas assessed at present. Nevertheless, on the evidence of this small sample, it would seem that conclusions may be drawn and there is some indication that the present approach may lead to a feasible practical method.

8.1.6. Measurements of Intensity Fluctuations

Bottom reflections and sub-bottom reflections depend to a marked degree upon the roughness and the topography of the interfaces. Because the bottom is not perfectly smooth, it causes a considerable amount of random scattering, particularly in the high frequency region. If the bottom and the sub-bottom boundaries are rough, the signal reflected from these interfaces will be partially incoherent, and repeated transmissions will not give the same result as the source and receiver are moved relatively to the bottom because of lateral variations. The signal amplitude will be therefore influenced by the incoherent contributions from individual scattering features. The partition of energy in the coherent and incoherent components of the signal depends on the conditions of the geophysical environment. A similar fluctuation of energy would be observed over a layered bottom with varying thickness of the individual layers, because interference effects will play an important part. It is believed, however, that fluctuations in intensity in sub-bottom profiling are of diagnostic value.

A statistical study of various reflected signals, shows that the observed intensity fluctuations of the reflected signal appear to correlate with the state of roughness of the reflector. The results of investigations in three areas indicate that much of the observed fluctuation is caused by mechanisms at or near the surface, bottom and sub-bottom that scattering due to boundary roughness could be the dominant factor in the signal intensity fluctuations. It appears that for a broad-band sound source, because of the interaction of wave-lengths and the various sizes of interface scatterers, the various values of the relative standard deviation of the fluctuation dispersions based on different centre frequencies and bandwidths could be used as criteria for determining the relative roughness of reflecting

boundaries. A simple rule should be that the rougher the boundary, the greater the change in this figure between high and low frequencies and between narrow and wide bandwidth . samplings. From the statistical results presented, the three areas investigated appear to possess different relative bottom and sub-bottom reflection characteristics. Although no general conclusions should be drawn from these isolated results which are yet to be fully confirmed, it seems a feasible proposition that the study of the range of sound intensity fluctuations by working out various statistical values and indices could lead to a form of identification of the sea-floor material in terms of its relative boundary roughness which in turn may possibly be related to the grain size of the sediment between the bottom and sub-bottom reflections.

8.1.7. Instrumental Limitations

As most data were analyzed on a comparative basis, the extent of errors caused by the instrumentation system behaviour affecting the present results as a whole should be limited. Environmental factors and adverse instrumental performances are usually incorporated into the data collected, and it is difficult to isolate individual effects. Nevertheless, a consideration of some known limitations of the equipment involved will serve to establish a guide for future improvements.

The response of the E. G. &G. hydrophone used throughout the investigations is truly flat below 2 kcps. The calibration curve shows a resonant peak at 4.5 kcps. Hence comparison of the relative spectral level at high frequencies may have included an error due to some variation in the frequency employed. On the other hand, at the low end of the spectrum, low frequency boat noise, flow noise, ambient noise, and electrical cross-feed from the mains throughout the entire recording system may have been

unavoidably included in most of the data collected. The exact extent of the imposition of such low frequency is difficult to determine with any certainty from either the graphic profile through filtering, or the spectral results. In any event, therefore, no spectral presentation of the analysed results should be taken as a true spectral form; but rather only the change in relative spectral level at corresponding frequencies between spectra could be significant.

When the direct recording process is used on magnetic tape to store and reproduce signals, its inability to record very low frequency and its amplitude instability caused by the tape drop-outs are the two major handicaps. In addition, the tape recorders used lacked the precision recording level controls. Sensitivity adjustment at the right recording level, while being not so critical in reproducing graphic profiles, is extremely important in recording the raw signal for frequency analysis. Though precautions have been taken throughout the experiments to guard against making erroneous measurements, it cannot be ruled out that over-saturation or under-level recordings have not, in fact, occurred in some of the samples analysed.

It must be recognised that ultimate distortion of an acoustic pulse when finally reproduced for analysis could sometimes be appreciable. The sequence of going through a hydrophone, a preamplifier and the consecutive stages of recording and reproducing in two direct recording magnetic tape recorders naturally deteriorates the quality of the signal to some extent. The more recording and reproducing stages a signal goes through, the poorer will be its final fidelity, particularly so when the instruments used are not sufficiently refined. This is another factor that must be taken into account when evaluating the present results.

The spectrum analyzer used is a heterodyne type which makes the repeated feeding of a transient signal for spectrum analysis a necessity. The procedures of going through signal isolation and transfer from the original tape to tape-loop, and the subsequent playback to heterodyne a full spectrum are very time-consuming processes which render any statistical treatment of a large amount of tape-loop data rather impractical.

For precision quantitative investigations involving a broad-band source, a Fourier analysis is to be preferred to energy measurements with a broad-band filter, since the latter will average out many interesting effects. However, most of the instrumental limitations of the present method could be removed in a future design so that acoustic information collected would be more accurately presented and more efficiently handled.

8.1.8. Environmental Limitations

Where many factors frequently uncontrollable and unpredictable contribute to the measurements, the agreement between theory and experiment is often marginal. During the present experiments it must be pointed out that the actual geophysical environment encountered was extremely complex and lacked adequate geological control. The greater part of the sea-bed of the Irish Sea is believed to consist of boulder clay (of Pleistocene age) upon which rests variable thicknesses of later sediments which are largely re-worked deposits resulting from boulder-clay erosion. The existence of homogeneity in a sediment can be regarded as a rarity. Among the four areas investigated, some sort of stratification or irregular layering can always be discerned from the graphic record of the reference profile. In fact, a slightly confused pattern of both the

sediment and sub-bottom structures prevails practically over all the traversed regions. However, the trial nature of the present work and the collaboration with other research projects due to the restricted availability of sea-going facilities necessarily dictate the use of accessible experimental areas, allowing very limited assessment for the choice of more ideal sites. All the anomalous conditions could indeed be expected to occur but in the actual cases their importance often exceeded a desirable level.

Despite the fact that each set of pulses spectrally analysed were taken from single transmissions, the chief causes for any discrepancies that may be found in the results arising from this aspect might still be attributed to the fluctuations of reflection amplitude. Due to irregularity of the reflecting boundaries, and the irregular pattern of stratification and layering in the media, the event selected may not be representative. Furthermore, stratification in the media, particularly in the first sediment layer, could form appreciable localized reverberation traps, creating constructive and destructive interferences depending on the layer or sub-layer depth and the wave length concerned. For either any particular discrete frequencies or the frequency spectrum of the pulse as a whole, the total attenuating process in the sediment under such circumstances might be extremely complex. In general, the composite field is a superposition of contributions from a number of energy paths which pass through different media and interact separately with various boundaries. It is the changing interaction of these paths which causes variability.

8.1.9. Validity of the Assumed Model

Since the practical case differs by possibly large and frequent deviations from any ideal model, the present approach might suggest that

any deductions could have little practical value. This is not the case. Ideal conditions usually involve few variables and generally permit these few to be described in simple terms. Having determined the performance to be expected under ideal conditions it is possible to extend the study to include, one by one, the many additional variables associated with anticipated irregularities. The problem of calculating an underwater sound field requires a detailed knowledge of the sea bottom upon sound propagation. Even given the detailed parameters of a particular case, the variability to be expected is such that calculation will be very complex. In addition, the number of data points necessary to allow the situation to be analysed may be very large. Thus, it will often be due to necessity rather than choice that simple approximations are employed. In the statistical analysis the values which emerge are probably representative of the mean influence of all the variations which occur in practice.

It must be admitted that despite the complexity of the experimental ground, the reflection model on which the approach is based is of an over-simplified version assuming homogeneous media and uniform boundary phenomena. However, the three working equations

$$E_{bf} = S_f - K_1 - 20 \log v_1 t_1 \qquad (8\text{-}1)$$

$$E_{sbf} = S_f - K_2 - 20 \log (v_1 t_1 + v_2 t_2) - \alpha_f v_2 t_2 \qquad (8\text{-}2)$$

$$E_{sbf} - E_{bf} = K + 20 \log v_1 t_1 - 20 \log (v_1 t_1 + v_2 t_2) - \alpha_f v_2 t_2 \qquad (8\text{-}3)$$

are firmly based. It is felt that this model is definitely useful in experiments using frequency analysis to obtain sediment attenuation values on smooth and homogeneous bottoms but will have to be modified for rough and stratified areas. Perhaps only a statistical treatment using digital data processing techniques will be capable of resolving the more complicated problems.

The geophysical properties might in the long run be described statistically rather than deterministically.

8.2. Concluding Remarks

8.2.1. Review in General

Through the modifications to an existing commercial sub-bottom profiler, useful knowledge was gained for the subsequent development of a sonar system with better performance much more suitable for continental shelf and slope investigations as well as for conducting the specially designed experiments. Important findings were obtained both in the transmitting and receiving sides of a continuous reflection sub-bottom profiling equipment.

The type of power source used governs to a great extent the available energy and frequency content of the acoustic pulse emitted. A transmitting system having a wide selection of sources together with a variable active length hydrophone array can obtain the maximum amount of information from the area under investigation by the proper choice of combination best suited to the geological conditions. In particular, the underwater spark source can be made to be more versatile by the use of multiple spark or a single spark with an adjustable-gap.

In association with the successful conversion of a weather chart recorder for profiling, a simple synchronization method was devised using an extra recording channel for the synchronization signal. The essence of the method is its general applicability to any profiling system which employs a precision graphic recorder in providing data reproducing facilities from storage magnetic tape at low cost.

A most useful technique was developed to isolate with great accuracy events of interest from sub-bottom profiling data recorded on

magnetic tapes. Isolated acoustic signals can either be examined directly or be further recorded on a tape-loop for repeated playback.

Fluctuation measurements of bottom and sub-bottom reflection data coupled with the use of a statistical treatment have given rise to the practical prospects for a method to determine the relative roughness of bottom and sub-bottom interfaces and, probably, by the scattering characteristics, the grain size of the sediments in between.

In spite of the limitations cited, initial efforts to identifying marine sediment type by using the spectrum analysis approach to give the effective attenuation and frequency dependence have yielded sufficiently encouraging results. It would be very wrong, however, to conclude that the approach of the present research has been carried as far as necessary. It is hoped that these preliminary results of the investigations may give some indications of the feasibility of this particular technique and the difficulties involved.

8.2.2. Future Work on Basis of Present Work

In future effort, the areas in which acoustic data is to be collected, analysed and correlated with the known geological conditions must be chosen to be as ideal as possible in order to establish the method on a satisfactory basis. It is essential for detailed examination of the acquired acoustic data that this is collected in the proximity of established boreholes or associated with sites about to be drilled. Expeditions should therefore be suitably arranged to cover a wide range of conditions, and to make short traverses interpolating and extrapolating the geological controls. In addition to photographing, sampling and coring of the sea bottom, velocity measurements should be made in the sediments themselves and in samples of sea water taken from just above the sea bed.

Even when the sites have been selected with reasonable care it has been found that many factors influence the intensity of the acoustic signal. The application of the method is for the purpose of identifying if possible the nature of sub-bottom sediments as a routine procedure in a standard survey. It is obvious, in general, that the conditions encountered will rarely approximate with ideal situation. Thus it would appear that the most promising extension of this work would be a suitable analysis of all the data taken over a moderately restricted area in order to obtain an average response, with a measure of the fluctuations involved, and to ascertain if this data would allow a reasonable assessment of the nature of the bottom.

The ship-borne acoustic equipment needed will consist primarily of a complex continuous seismic reflection sub-bottom profiling system including a high quality F.M. magnetic tape recorder, a simultaneous multi-filter type spectrum analyzer and a fast digital data acquisition recording equipment. The system should also have a special acoustic source carrier as well as a multi-element hydrophone providing dual facilities for rapidly effecting any desirable change by remote control.

By operating a number of signal-gating switches while profiling, reflections can be isolated in situ and fed directly into a multi-filter spectrum analyzer. The spectral level at various frequency points can then be recorded by a digital data acquisition equipment which, linked to a specially designed shipboard computer, would allow a statistical analysis of the data and the computation of individual and mean values of attenuation, frequency dependence, as well as the relative roughness etc. of the reflecting interfaces. The ultimate goal of research along this line is the development of a system which would enable the direct read-out by a ship underway of a range of the diagnostic properties of marine sediments in situ.

BIBLIOGRAPHY

"Underwater Acoustics Handbook II".

Albers, Vernon M. 1965. ~~"A Textbook of Sound", Bell, London, 610p.~~ Pennsylvania State University Press, Pennsylvania, 356 p.

Arons, A. B. and D. R. Yennie, 1950. "Phase distortion of acoustic pulses obliquely reflected from a medium of higher sound velocity". J. Acoust. Soc. Am., 22: 231-237.

Becken, Bradford A., 1964. "Sonar", pp. 1-93, in Chow, V. T., Editor, "Advances in Hydroscience", Vol. 1., Academic Press, New York and London, 442p.

Beckmann, W. C., A. C. Roberts and B. Luskin, 1959. "Sub-bottom depth recorders". Geophysics, 24: 749-760.

Belderson, R. H., 1964. "Holocene sedimentation in the western half of the Irish Sea". Marine Geology, 2: 147-163.

Bell, T. G., 1964. "Reflection and scattering of sound by the sea bottom". J. Acoust. Soc. Am. 36: 2003.

Biot, M. A., 1956. "Theory of propagation of elastic waves in a fluid-saturated porous solid". J. Acoust. Soc. Am. 28: 168-191.

Blundell, D. J., R. F. King and C. D. V. Wilson, 1964. "Seismic investigations of the rocks beneath the northern part of Cardigan Bay, Wales". Quart. J. Geol. Soc. London, 120: 35-50.

Born, W. T., 1941. "The attenuation constant of earth materials". Geophysics, 6: 132-148.

Bower, R., 1963. "A high-power, low-frequency sonar for sub-bottom profiling". J. Brit. I. R. E., 25: 457-460.

Bruckshaw, J. M., 1956. "Applied geophysics in retrospect and prospect". Inaugural lecture, Imperial College, London, 15 pp.

Caston, V. N. D., 1966. Ph. D. Thesis. University of Wales.

Caulfield, D., 1962. "Predicting sonic pulse shapes of underwater spark discharges". Deep-Sea Res., 9: 339-348.

Cole, B.F., 1965. "Marine sediment attenuation and ocean-bottom reflected sound". J. Acoust. Soc. Am., 37: 291-297.

Eastwood, T., 1963. "British Regional Geology, Northern England". H.M. Stationery Office, London, 72p.

Ewing, John and Roger Zaumere, 1964. "Seismic profiling with a pneumatic sound source". J. Geophys. Res. 69: 4913-4915.

Hampton, L.D., 1966. "Acoustic properties of sediments". D.R.L. Acoustical Report No. 254., Defense Research Laboratory, University of Texas, Austin, Texas.

Harvey, J.G., 1966. "Large sand waves in the Irish Sea". Marine Geology, 4: 49-55.

Hersey, J.B., H.E. Edgerton, S.O. Raymond and G. Hayward, 1961. "Pingers and thumpers advance deep-sea exploration". J. Instrument Soc. Amer., 8: 72-77.

Horton, J.W., 1959. "Fundamentals of Sonar" U.S. Naval Institute, Annapolis, 417p.

Jakosky, J. Jay and John J. Jakosky, Jr., 1952. "Frequency analysis of seismic waves". Geophysics, 17: 721-738.

Jones, N.S., 1951. "The bottom fauna off the south of the Isle of Man". J. Animal Ecol., 20: 132-144.

Kendall, J.M., 1941. "The range of amplitudes in seismic reflection records". Geophysics, 6: 149-157.

Knot, S.T. and J.B. Hersey, 1956. "Interpretation of high-resolution echo-sounding techniques and their use in bathymetry, marine geophysics and biology". Deep-Sea Res., 4: 36-44.

Laughton, A.S., 1957. "Sound propagation in compacted ocean sediments". Geophysics, 22: 233-260.

Lee, M. A., 1965. "A geophysical approach to the geology of south west Cornwall". Ph. D. Thesis, University of London.

Li, W. N. and D. Taylor Smith, 1966a. "Identification of sea bottom sediments by a ship underway". Geophysical Prospecting, 14: 45-47. (Appendix A).

Li, W. N. and D. Taylor Smith, 1966b. "A simple synchronization method for reproducing tape-recorded profiles". Int. Hydro. Rev. 43: 27-31. (Appendix B).

Mackenzie, K. V., 1961. "Bottom reverberation for 530- and 1, 030-cps sound in deep water". J. Acoust. Soc. Am., 33: 1498-1504.

Maranzana F., 1966. "Some experiments on the electric properties of a water spark discharge". D. I. C. Dissertation in preparation, Imperial College, private communication.

Marke, P. A. B., 1965. "The development and use of off-shore mineral exploration techniques". Ph. D. Thesis, University of London.

McCann, C., 1967. Ph. D. Thesis in preparation, University College of North Wales, private communication.

McClure, C. D., H. F. Nelson and W. B. Huckaby, 1958. "Marine sonoprobe system, new tool for geologic mapping". Bull. Amer. Assoc. Petrol. Geol., 42: 701-716.

McDonal, F. J., F. A. Angona, R. L. Mills, R. L. Sengbush, R. G. Van Nostrand and J. E. White 1958. "Attenuation of shear and compressional waves in Pierre Shale". Geophysics 23: 421-439.

Millman, Jacob, 1958. "Vacuum-tube and Semiconductor Electronics". McGraw-Hill, New York, 644p.

Mitchell, G. F., 1960. "The Pleistocene history of the Irish Sea". Advancement of Science, Nov. 1960: 313-325.

Murray, H.W., 1947. "Topography of the Gulf of Marine. Field season of 1940". Bull. Geol. Soc. Amer., 58: 153-196.

Nolle, A.W., W.A. Hoyer, J.F. Mifsud, W.R. Runyan and M.B. Ward, 1963. "Acoustical properties of waterfilled sand" J. Acoust. Soc. Am., 35: 1394-1408.

Officer, C.B., 1955. "A deep-sea seismic reflection profile". Geophysics, 20: 270-282.

Roi, N.A., D.P. Frolov, 1958. "The electro-acoustic efficiency of a spark discharge in water". Doklady Akademii Nauk, 118: 683-686.

Schofield, D., 1961. "Transducers", pp.5-27., in Albers V.M., Editor, "Underwater Acoustics", Plenum Press, New York, 354p.

Shumway, G., 1960. "Sound speed and absorption studies of marine sediments by a resonance method". Geophysics, 25: 451-467, 659-682.

Smith, W. O., 1958. "Recent underwater surveys using low-frequency to locate shallow bedrock". Bull. Geol. Soc. Amer., 69: 69-98.

Stride, A.H., 1963. "Current-swept sea floor near the southern half of Great Britain". Quart. J. Geol. Soc. London, 119: 175-199.

Taylor Smith, D. and W.N. Li., 1966. "Echo-sounding and sea-floor sediments". Marine Geology, 4: 343-364. (Appendix C).

Tolstoy, Ivan and C.S. Clay, 1966. "Ocean Acoustics". McGraw-Hill, New York and London, 293p.

Tucker, D.G., 1961. "Sonar arrays, systems and displays", pp.29-49, in Albers V.M., Editor, "Underwater Acoustics", Plenum Press, New York, 354p.

Wood, A.B., 1955. "A Textbook of Sound". Bell, London, 610p.

Wood, A. B. and D. E. Weston, 1964. "The propagation of sound in mud". Acoustica, 14: 156-162.

Wyllie, M. R. J., G. H. F. Gardner and A. R. Gregory, 1962. "Studies of elastic wave attenuation in porous media". Geophysics 27: 569-589.

ACKNOWLEDGEMENTS

The author is extremely grateful to his supervisor, Prof. J. M. Bruckshaw, for his overall direction of the work, his incessant encouragements and the precious time he spent in the final critical reading of the thesis. The author is greatly indebted to Mr. D. Taylor Smith for his close guidance and continued support throughout the investigation.

Acknowledgement is made to Mr. F. Dewes, Mr. C. McCann and to the members of the Geophysics Section of the University of Birmingham who helped in the field work. Acknowledgement is also made to Prof. Darbyshire and his staff at the Marine Science Laboratories of the University College of North Wales for the collaboration in carrying out this N. E. R. C. sponsored project and in kindly providing various field facilities.

The author wishes to acknowledge the help rendered to him in computer programming from Dr. R. G. Roger, Mr. K. O. Ahmed and Mr. A. Douglas of the U. K. Atomic Energy Authority. Acknowledgement is also made to Mr. F. Maranzana with whom a small part of the study on the underwater spark discharge was conducted as a mutual interest.

The author wishes to thank Dr. S. H. Hall and Mr. C. McCann for their constructive criticism in reading parts of the original manuscript. To the latter the author is particularly indebted for the many valuable discussions all along the course of this research.

The author expresses his sincere appreciation for the frequent encouragements he received from Prof. R. G. Mason.

The author is grateful to Mrs. J. Kelland, Mr. F. Dewes for the preparation of the diagrams, Miss H. Frank for typing the first draft and Miss E. Hawkes and Miss C. Corry for typing the final thesis.

Finally, the author thanks the Ministry of Education, Republic of China, for the award of a two-year scholarship. Thanks are due to the British Petroleum Limited for a Research Busary, awarded through the kind recommendation of Prof. Bruckshaw and which enabled the completion of the present work.

APPENDICES

(Papers Published)

APPENDIX A

"Identification of sea-bottom sediments by a ship underway", reprint from Geophysical Prospecting, Volume XIV, No. 1., 1966.

APPENDIX B

"A simple synchronization method for reproducing tape-recorded profiles", reprint from International Hydrographic Review, Volume VLIII, No. 2., 1966.

APPENDIX C

"Echo-sounding and sea-floor sediments", reprint from Marine Geology, Volume IV, No. 5., 1966.

A

IDENTIFICATION OF SEA-BOTTOM SEDIMENTS BY A SHIP UNDERWAY

BY

W. N. LI and D. TAYLOR SMITH

Reprinted from:

GEOPHYSICAL PROSPECTING, Volume XIV, No.1 , 1966

IDENTIFICATION OF SEA-BOTTOM SEDIMENTS BY A SHIP UNDERWAY*

BY

W. N. LI** and D. TAYLOR SMITH***

ABSTRACT

The authors propose a method of determining the sedimentary composition of the sea-bottom by studying the variation of the frequency contents of the consecutive multiple reflections between bottom and surface of the sea.

As land supplies of sand and gravel gradually become used up, many commercial organisations dealing with this commodity are turning to deposits on the continental shelf. While most of the interested companies examine known sand and gravel banks to locate the material they require, often using the simplest of surveying equipment, some of the larger ones are now prospecting outside these areas with modern sub-bottom acoustic profiling apparatus. Unfortunately, in this context, all that the standard sub-bottom geophysical techniques can provide is an assessment of the thickness and distribution of the sediments with little information concerning the sediment type. In many instances, because of the shallow water depths in the area of the sand-banks, the profiler record is marred by multiple representations of the sea-bottom and sub-bottom as a result of successive reflexions at the sea/air interface.

Multiples of the first reflected pulses are generally regarded as undesirable because of their masking effect on the later weaker arrivals. One method of dealing with the multiples is to remove them by suitable filtering; in one particular form a certain amount of success had been achieved by the use of laser filters. Another technique has been to store the first reflected arrivals on magnetic tape and to feed this back to the record, inverted in phase, at the appropriate time interval to produce cancellation of the multiple. Many other systems are also available to make the later weaker arrivals stand out on the record against the background of the multiple reflexions. Surprisingly, very few attempts have been made to use these multiples as a means of quantitatively measuring the acoustic properties of the sea-floor. There is good reason to

* Manuscript received by the Editor, July, 1965.

** Department of Geophysics, Imperial College, London, England.

*** Marine Science Laboratories, Menai Bridge, Anglesey, North Wales.

believe that the storage of the successive multiples (particularly the sub-bottom multiples), and the subsequent correlation with the original transmitted pulse, will provide a considerable amount of information which could be interpreted in terms of the variation of the various geological media on the sea-floor.

In the case of the first sub-bottom reflexion, the acoustic pulse in travelling through the sea-bottom medium will be duly attenuated according to its various frequency components; the effect is even more marked on the subsequent multiples. If the sea-floor sediment were a mud then this would attenuate a 1 kc/s component by about 0.02 db/foot while a 25 kc/s component would be attenuated by about 0.5 db/foot: the overall effect for (say) 25 feet of sediment would be 1 db and 25 db respectively if no consideration is made of reflexion losses. For a more coarse sediment a vastly different attenuating effect would be produced which for a similar thickness of a certain type (a clayey silt with about 15 % sand-size particles) would be about 2 db and 150 db respectively. The sediment acts, therefore, almost as a low pass filter with its high frequency cut-off position varying between the different sediment grades. Consequently, the analysis and comparison of energy spectra of the source and reflected pulse from a sub-bottom interface can provide some idea of the physical characteristics of the bottom material. The problem in practice, of course, would be to differentiate between the spectral forms of bottom materials whose extinction coefficients were nearly alike. In such cases, comparison of higher order multiples might be more diagnostic; in fact, the higher the order of the successive multiples analysed, the greater would be the differential effect.

Associated with the analysis of energy spectra, comparisons between the various bottom media can be achieved by a direct determination of the magnitude of the bottom losses on reflexion. Under one set of conditions a clayey silt could be expected to have a reflexion loss at normal incidence of about 15db, while a medium-grained sand would have a loss of less than 9db. This effect has been analysed very recently by Breslau (1965) who has performed a considerable number of experiments and analysed them statistically. It has been found that the relationships between bottom loss and sedimentological characteristics agree reasonably well with those postulated theoretically. Undoubtedly, within certain limits, the coarser the material the better will be its reflection characteristics, all other things being equal. (Unfortunately, of course, all things are not necessarily equal: as the sediment becomes coarser acoustic scattering becomes important.) Such variations can be seen easily, in a qualitative manner, on any standard echo-sounding record. However, it does not necessarily follow that the absolute magnitude of the reflexion is directly characteristic of a certain sediment grade, as this technique is fraught

with many problems; in particular the presence of gas derived from organic matter can change the reflexion characteristics of the sea-bottom considerably. Here again the use of multiple reflexions would be of more diagnostic value.

Recent experiments by one of the authors (W.N.L.) has shown that the acoustic source can be chosen to obtain the maximum amount of information from the area under investigation. The conventional spark source can be made to be more versatile by the use of an adjustable spark gap. This used in conjunction with a "Boomer" and a high frequency source (6 kc/s) can provide

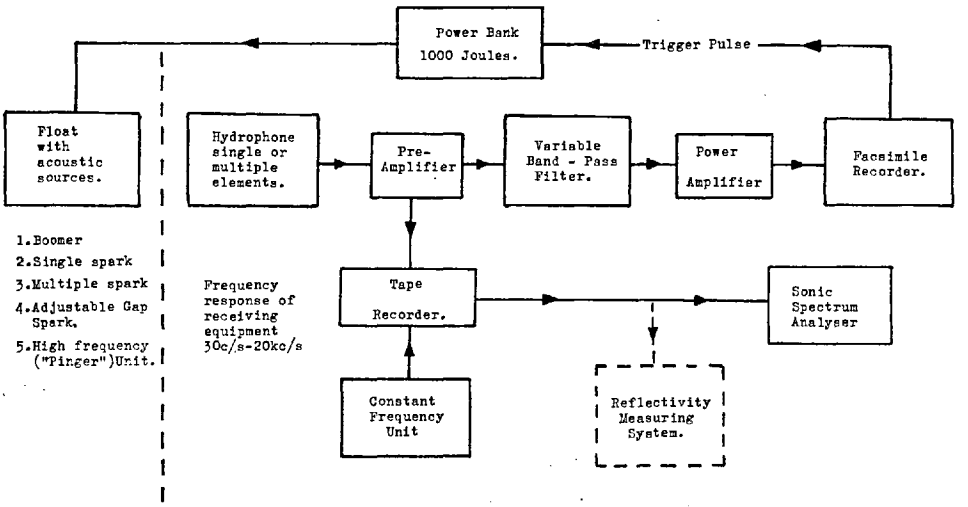

Fig. 1.

considerably more information, of the type needed by the commercial companies, about the characteristics of the sea-floor sediment. All these operations can be made by a ship underway using the general equipment lay-out shown in the block diagram (Fig. 1.) While sea-bottom sampling is necessary to calibrate the equipment, this can be kept to a minimum.

The present collaborative research programme, between the Imperial College and the Marine Science Laboratories, is an attempt to provide a rapid identification of the various sea-bottom media on the basis of their acoustic properties. The programme is financed by a grant-in-aid from the D.S.I.R. awarded to one of the authors (D.T.S.) and Professor J. M. Bruckshaw at the Imperial College.

Reference

Breslau, L., NATO Saclant ASW Research Centre, La Spezia—Private communication, June, 1965.

B

REPRINT
from the

INTERNATIONAL HYDROGRAPHIC REVIEW

Vol. XLIII, N° 2, July 1966

A SIMPLE SYNCHRONISATION METHOD FOR REPRODUCING TAPE-RECORDED PROFILES

by W. N. Li
Department of Geophysics, Imperial College, London
and D. Taylor Smith
Marine Science Laboratories, Menai Bridge, North Wales

ABSTRACT

A simple method has been used to obtain synchronism in the reproduction of tape-recorded continuous reflexion profiling data for graphic display. By use of a 2-channel recording technique a reference signal, from a precision graphic recorder, can be simultaneously recorded with the acoustic data. This reference signal can then be used to govern the speed of the graphic recorder during play-back, totally eliminating any graphic distortion caused by tape speed deviation. The technique can be used with any relatively inexpensive tape recorder and can, consequently, broaden at low cost the scope of any sub-bottom profiling system or, for that matter, any profiling system which employs a precision graphic recorder.

INTRODUCTION

There are many advantages to recording acoustic data, acquired by continous reflexion profiling, on magnetic tape. The fundamental advantage is that the recorded data can be played back and examined under a variety of different processing conditions each adapted to reveal some special feature of the traversed region. A further important advantage is that by means of tape recording, in conjunction with the usual graphic recording, a guarantee can be effected that the acoustic data is continuously collected; this cannot be achieved when the graphic system is used by itself. In addition to all this the tape can either be cleaned after analysis and used again, or it can be stored and, in the event of an advance in interpretation involving new instrumentation, the data can be re-processed with the new technique. These features are familiar to most people.

However, a major difficulty generally encountered in reproducing a tape-recorded signal free from distortion is the presence, in almost all tape recorders, of a certain amount of deviation in tape speed. This is mainly due to the fact that the tape transport mechanism is essentially a friction-controlled device, consisting of a capstan and roller assembly, which is rather sensitive to any slight change of tape tension as well as to environmental conditions. While the use of a precision frequency power supply to drive the capstan motor can eliminate that part of the speed deviation caused by any variation of the shipboard mains frequency, the remaining part of the speed error can only be controlled to a variable extent and is impossible to remove completely. Generally speaking the more expensive the tape recorder the smaller is this speed error. Unfortunately, even with elaborate and costly equipment, a great reduction in tape speed accuracy can usually be expected when the recorder is used for shipboard measurements where mechanical vibrations and a corrosive atmosphere are prevalent.

The effect of speed drift shows itself very obviously when tape-stored correlated data are visually displayed on a graphic recorder. For most tape recorders used professionally an acceptable speed tolerance is about $\pm 0.25\ \%$; the usual flutter accompanying such a speed deviation is negligible for most practical purposes. Such a speed drift, however, would have dire results if it appeared in a play-back of sub-bottom profiling data. With a fixed speed deviation of this kind a horizontal geological structure would appear at a dip of 1/400: for a 1-second graphic sweep the structure would disappear off the edge of the paper in less than 7 minutes. And for the more general case where the tape speed drifts randomly within its tolerance, the reproduced picture would be extremely distorted.

This problem can be solved in a very simple manner with the simplest of tape-recording equipment provided that some synchronising signal can be provided between the normal graphic recorder and the tape recorder, and which is common to both.

CORRECTION TECHNIQUE

Most precision graphic recorders have the common feature that the helix is driven by a gear train which is actuated by a synchronous motor. The speed of the motor is carefully controlled by means of a precision power supply which is itself controlled by a tuning-fork or crystal oscillator. The overall frequency variation in such a system is less than 1 part in 10^5. By recording the tuning-fork, or crystal output simultaneously with the sub-bottom acoustic data, the relative timing of any particular event in the data with respect to the tuning-fork reference signal can be fixed. During play-back, from the tape to the graphic recorder, the stored reference frequency can be used to drive the synchronous motor so locking the motion of the helix to the data being reproduced.

INSTRUMENTATION

A schematic diagram of such a record/reproduce sub-bottom profiling system, as outlined above, is shown in figure 1. A standard Mufax 18-inch chart recorder has been modified such that a photocell assembly gives out programmed trigger pulses. These pulses are used for triggering the acoustic analysis equipment as well as for the normal acoustic transmission control. A fork oscillator provides a 1 kc/s, 0.4 volt peak-to-peak output which is fed to the Channel 1 input of a Tandberg stereo tape recorder at the same time as an acoustic signal is being recorded on Channel 2; the acoustic signal, of course, is recorded also via amplifiers and filters on the Mufax. During play-back the 1 kc/s signal, with its output adjusted to the original voltage level, is fed from the tape recorder to the input stage of the motor drive amplifier. A change-over panel jack, installed at the back of the Mufax recorder, ensures an automatic isolation of the fork oscillator output from the following amplifying stage whenever the reproduced synchronising signal is plugged in.

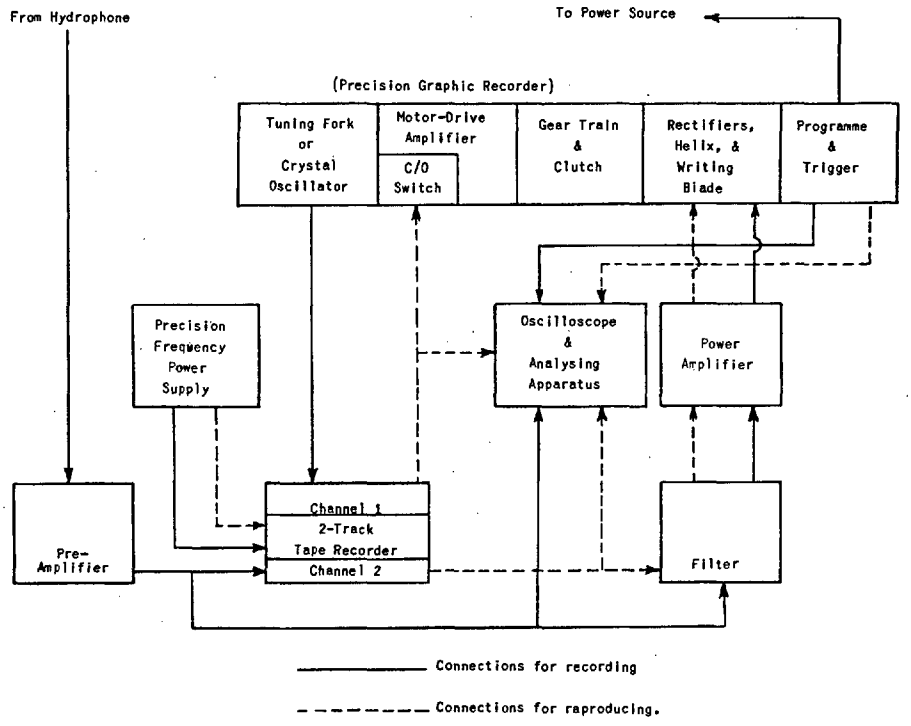

FIG. 1. — Block schematic of a synchronised record/reproduce sub-bottom profiling system.

The 1 kc/s synchronisation signal has a further use : it provides a visual sinusoidal time reference to any data observed on the oscilloscope

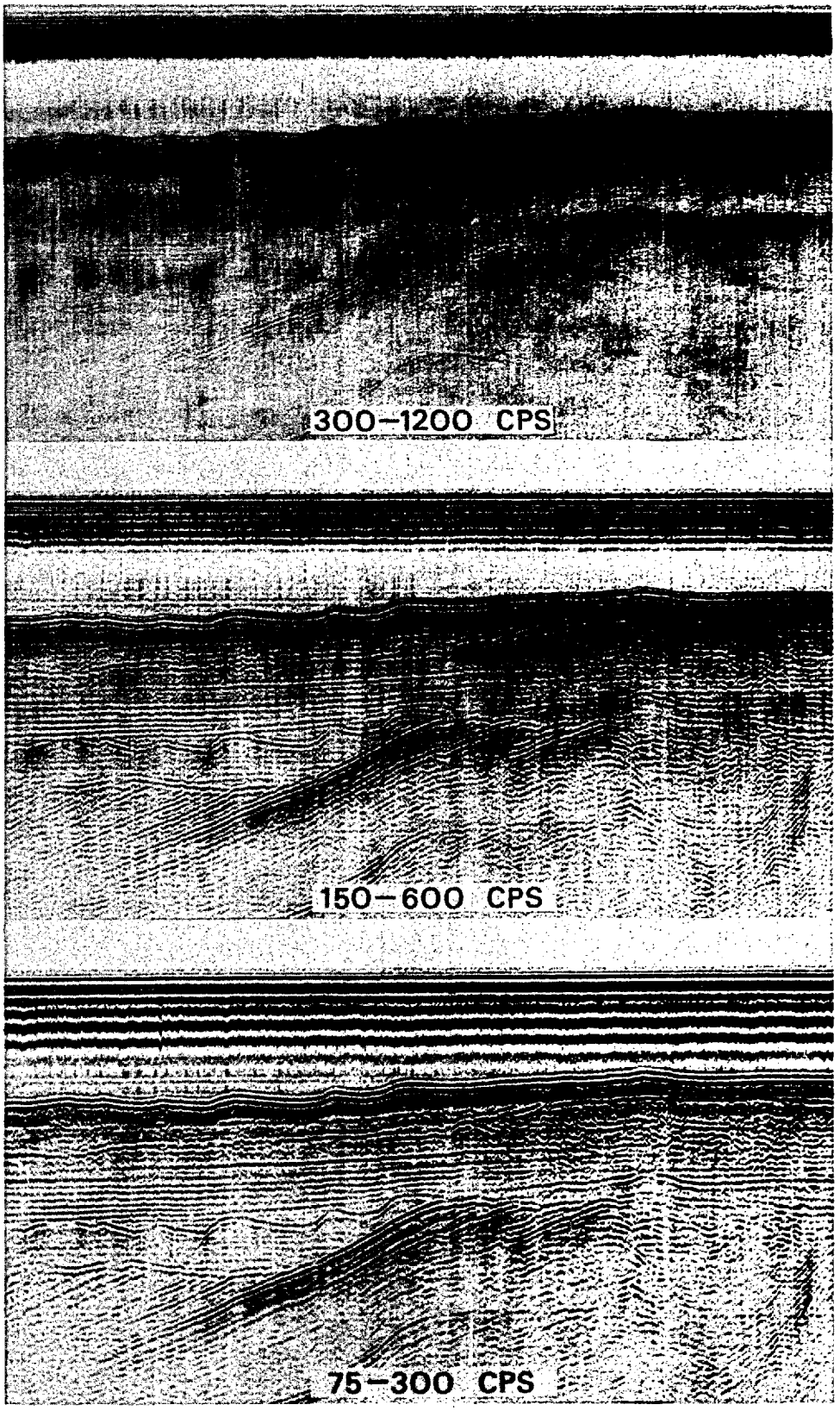

FIG. 2
Reproduced sparker sub-bottom profiles, with different filter settings, via tape recorder play-back.

as well as providing a frequency datum when the acoustic information is examined with a spectrum analyser.

One further point requires mention : as the Tandberg tape recorder is relatively inexpensive, an external precision frequency power supply has been used. To counteract the adverse effects of ship-board conditions, the use of such a unit is desirable in order to maintain the data quality. Most professional tape recorders are supplied with an internal constant frequency source for the capstan motor.

DISCUSSION

Sample records of a section of a sparker traverse synchronously reproduced through three different filter settings are shown in figure 2. Examinations of this kind are necessary for a qualitative interpretation of the record as well as in providing a correlative graphic monitoring during quantitative investigations, such as spectrum analysis, of the various transmitted and reflected pulses.

For the Mufax recorder, the locking-in of such a synchronisation process is effective for all tape speed deviations up to ± 35 %. It must be noted, however, that such synchronisation is not a speed drift control; it is simply a correction for the effects of a speed drift.

This technique can be applied to any continuous data recording system which employs a precision graphic recorder or similar device. Any 2-track tape recorder which has a tolerable flutter can be used without the necessity of purchasing expensive equipment. Full graphic play-back facility can therefore be easily incorporated at low cost into any precision profiling system.

ACKNOWLEDGEMENTS

The authors wish to acknowledge the considerable advice provided by Messrs. D. & C. McCann of the Marine Science Laboratories in the design stages of the modified Mufax recorder. The development and sea trials of this synchronised record/reproduce system is a part of a current collaborative research programme between the Imperial College and the Marine Science Laboratories. Its aim is to provide a rapid indentification of the various sub-bottom media on the basis of their acoustic properties. The project is financed by a grant-in-aid from the Science Research Council awarded to one of the authors (D. Taylor Smith) and Professor J. M. Bruckshaw of the Imperial College.

Marine Geology – Elsevier Publishing Company, Amsterdam – Printed in The Netherlands

ECHO-SOUNDING AND SEA-FLOOR SEDIMENTS[1]

D. TAYLOR SMITH AND W. N. LI

Marine Science Laboratories, Menai Bridge, North Wales (Great Britain)

(Received May 25, 1966)

SUMMARY

The quantity of sound returned to a survey vessel, compared to that sent out by its echosounder, depends on a considerable number of variables. Sediment type by itself is not one of the variables, although this certainly influences the reflection process at the sea-floor; sediment porosity is by far the most important property. This result shows the danger of attempting to identify a bottom sediment, in terms of its type, by the use of an echosounder. The effect is even more complicated when the frequency of the sound signal is considered. It may well be that for a large number of cases the reflected sound has not come from the sea-floor at all but from some lower level.

INTRODUCTION

The echo-sounder has become an essential part of the field equipment of every marine geologist. Apart from providing details of the bathymetry, it is often possible to obtain qualitative information concerning the various media that comprise the sea-floor by a close examination of the echogram. The technique as used by most geologists is relatively simple: it is supposed that, all other things being equal, different rock types and sediments will reflect the sound signal differently such that the received signal amplitude will vary accordingly; the variation in signal amplitude will produce a variation in the density of the trace on the echo-sounding record.

When a change from hard rock to sediments is involved the application of the technique is generally successful. Fig.1. shows an echogram taken over an area where basic igneous rock has been intruded into shales and mudstones. with a flanking of Recent sediments on one side of the intrusion; the intrusion is exposed on the sea floor. A simultaneously-obtained Sparker record is shown beneath the echogram. The change from crystalline rock to sediment is clearly portrayed on the echo-sounding record and can probably be interpreted as such without the use of any other information. GRAINDOR (1959) has extended the technique, by the use of aqualung-fitted geologists,

[1] Marine Science Laboratories Geological Report No. 66-1.

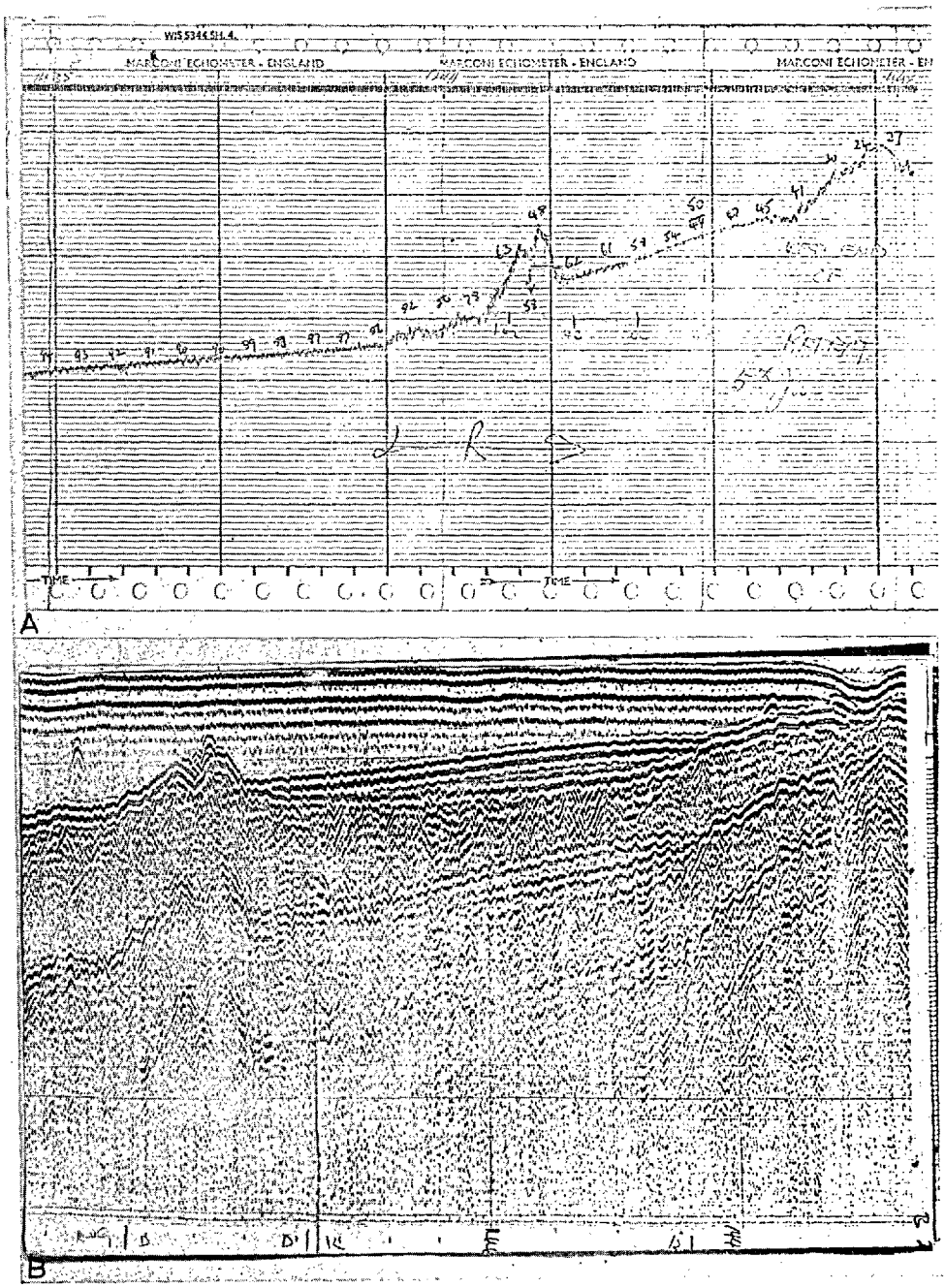

Fig.1. Echogram (A) and sparker record (B) obtained simultaneously over an igneous rock, intruded into sedimentary rocks, with a flanking of Recent sediments (sands) on right-hand side of the intrusion.

to map the Hercynian structures off St. Malo for the French Electricity Authority. The maps he has produced are in almost every way as detailed as those produced by geologists on land.

In some instances the presence of multiple representation of the sea-bottom provides an extra diagnostic criterion: the double bottom is often seen in areas of hard rock but is rarely seen where thick unconsolidated sediments form the bottom medium. Again, some echo-sounders are capable of providing a certain amount of penetration into the bottom medium, and sub-bottom reflections are obtained as well as those obtained from the sea-floor. The Irish Sea work of BELDERSON (1964) provides a good example of this last case. More recently CASTON (1965) has used the oblique version of the echo-sounder (TUCKER and STUBBS 1961) to identify variations in sediment grade (gravel, sand, silt, clay) in Tremadoc Bay, North Wales.

The above-named authors are a few representative examples from the literature where the echo-sounder, or one of its variants, has been used as a means of identifying changes in the sea-bottom geology. They all use the received signal amplitude as the main criterion in the interpretation with some control being effected by bottom sampling. None of them, particularly where sediment studies are concerned, involve themselves with the complex instrumentation of BRESLAU (1965) in order to ensure that the received signal amplitude is of truly diagnostic significance. This appears to be a dangerous position to be in as an examination of the elementary physics of the situation will show.

RECEIVED SIGNAL AMPLITUDE

The amplitude of the echo received, as far as conditions external to be acoustic transducer are concerned, is dependent on:

(*1*) The amplitude of the outgoing signal from the transducer.

(*2*) The path length of the sound signal to and from the reflecting object.

(*3*) The reflecting properties of the sea-floor.

Source signal amplitude

Obviously, the amount of sound energy received at the transducer is dependent on the amount sent out. For most echo-sounders there is no method of verifying that the output energy is a constant for the period of the survey. It is assumed that if the internal electrical power in the echo-sounder is a constant then the output acoustic power is a constant. This is not necessarily true on two counts:

(*a*) Any variation in the supply voltage, which is rarely monitored, will often cause a considerable variation in the internal electrical power supplied to the transducer.

(*b*) Even if the electrical power were a constant, the output acoustic power is dependent also on the relationships existing between the physical properties of the

transducer and those of the surrounding water. While for most surveys at sea this effect is negligible, it can have some importance in areas where a considerable change in water salinity (e.g., off the mouths of large rivers) occurs.

Signal path length

If the path length of the signal to and from the reflecting object is L (for horizontal sea floors, L is twice the depth of water) then the amplitude of the received signal relative to that sent out, is reduced by spherical spreading ($1/L$) and by the attenuation of sound in sea-water (e^{-aL}). Thus on this basis alone, two signals A_1 and A_2 received by reflection paths from the bottom can differ in amplitude as a result of their path lengths without there being any change in the bottom conditions:

$$\frac{A_1}{A_2} = \frac{L_2}{L_1} e^{-a(L_1 - L_2)}$$

assuming that a, the sound attenuation parameter for sea water, is a constant throughout. This relationship assumes some significance in areas of variable submarine topography; it is particularly important in the interpretation of oblique asdic records where the density of the record is often used to provide evidence of lateral changes in sediment type.

Sea-floor reflections

In a similar manner to light waves, acoustic energy is reflected and refracted at any boundary separating two media provided that the media have contrasting properties. The property that is significant is called the *acoustic impedance* Z, this being the product of the velocity of sound c in the medium and the bulk density ρ of the medium. It can be shown that the relationship between the amplitude of the reflected signal to that normally incident at the surface is numerically given by:

$$\frac{A_R}{A_I} = \frac{(Z_2 - Z_1)}{(Z_2 + Z_1)} = \frac{[(Z_2/Z_1) - 1]}{[(Z_2/Z_1) + 1]} = R$$

where Z_1 is the acoustic impedance of water ($\rho_1 c_1$), Z_2 is the acoustic impedance of bottom sediment ($\rho_2 c_2$) and R is the bottom reflectivity.

It is this particular relationship which is used, consciously or unconsciously, in any attempt at the interpretation of an echo-sounding record to indicate the variation of sediment type. It can be seen that what is being measured, all other factors being accounted for, is not so much a variation in the type of sediment but rather a variation in the reflectivity of the bottom which for most cases (but not all) is representative of a variation in sediment acoustic impedance.

It could be argued that acoustic impedance is directly dependent on sediment type. Such an argument is usually based upon the fact that the impedance bears some inverse relationship to porosity: high porosity sediments have a low acoustic

TABLE I

SOME PROPERTIES OF SAND CORRECTED TO MEASUREMENTS AT 20°C

Median diameter (Mdφ)	*Median diameter (mm)*	*Wet density (g/cm^3)*	*Sound velocity (m/sec)*	*Acoustic impedance*[1]	*Porosity (%)*
Medium sands (0–2 phi)					
0.58	0.670	2.08	1,768	3.677	38.3
1.13	0.466	2.05	1,759	3.606	37.9
1.27	0.415	2.05	1,749	3.586	37.6
1.78	0.290	2.03	1,741	3.534	39.7
1.24	0.425	2.02	1,743	3.521	38.3
1.28	0.413	2.00	1,754	3.508	38.7
1.17	0.458	2.00	1,753	3.506	39.4
1.82	0.284	1.99	1,735	3.453	40.2
1.64	0.320	1.995	1,730	3.451	38.8
1.30	0.407	2.00	1,716	3.432	39.3
1.98	0.254	1.99	1,719	3.421	35.7
1.75	0.298	1.99	1,707	3.397	36.2
1.82	0.284	1.99	1,704	3.391	39.1
1.95	0.259	1.96	1,669	3.271	41.7
Fine sands (2–3 phi)					
2.00	0.250	1.94	1,776	3.445	43.2
2.12	0.230	1.996	1,721	3.435	39.7
2.12	0.230	1.99	1,715	3.413	39.9
2.25	0.210	1.98	1,708	3.382	39.7
2.22	0.215	1.96	1,715	3.361	42.2
2.62	0.163	1.89	1,771	3.347	47.9
2.22	0.215	1.97	1,695	3.339	41.4
2.20	0.218	1.95	1,712	3.338	42.4
2.62	0.163	1.88	1,770	3.328	48.2
2.74	0.150	1.98	1,680	3.326	42.7
2.28	0.206	1.92	1,732	3.325	44.5
2.50	0.176	1.96	1,694	3.320	42.9
2.12	0.230	1.93	1,735	3.320	44.0
2.72	0.152	1.98	1,673	3.313	42.7
2.68	0.157	1.97	1,680	3.310	42.6
2.34	0.197	1.96	1,684	3.301	43.1
2.72	0.152	1.96	1,679	3.291	43.2
2.12	0.230	1.95	1,686	3.288	48.1
2.27	0.208	1.95	1,683	3.282	42.4
2.27	0.208	1.94	1.689	3.277	42.9
2.72	0.152	1.96	1,671	3.275	42.6
2.02	0.247	1.95	1,676	3.268	42.6
2.68	0.157	1.95	1,676	3.268	43.2
2.75	0.148	1.92	1,680	3.218	45.4
2.71	0.153	1.92	1,665	3.197	45.8
2.92	0.132	1.82	1,548	2.817	49.3
2.68	0.156	1.80	1,543	2.777	52.6
Very fine sands (3–4 phi)					
3.18	0.110	1.94	1,759	3.412	47.5
3.90	0.067	1.88	1,736	3.264	46.4
3.06	0.120	1.95	1,669	3.255	47.3
3.18	0.110	1.93	1,669	3.221	46.6
3.06	0.120	1.92	1,668	3.203	47.7
3.32	0.10	1.93	1,654	3.192	48.0
3.06	0.120	1.84	1,629	2.997	51.0
3.14	0.114	1.81	1,549	2.804	49.8
3.05	0.121	1.82	1,540	2.790	51.9
3.96	0.064	1.69	1,522	2.572	56.1

[1] Acoustic impedance is measured in 10^5 g/cm^2 sec.

TABLE II

SOME PROPERTIES OF SILT CORRECTED TO MEASUREMENTS MADE AT 20°C

Median diameter (Md φ)	*Median diameter (mm)*	*Wet density (g/cm³)*	*Sound velocity (m/sec)*	*Acoustic impedance*[1]	*Porosity (%)*
Coarse silts (4–5) phi					
4.27	0.052	1.904	1,617	3.079	45.8
4.44	0.046	1.900	1,586	3.013	46.3
4.44	0.046	1.882	1,587	2.987	48.1
4.34	0.050	1.895	1,574	2.983	48.7
4.28	0.051	1.838	1,546	2.842	51.2
4.34	0.050	1.816	1,546	2.808	52.4
4.38	0.048	1.827	1,522	2.781	52.2
4.26	0.052	1.800	1,536	2.765	55.4
4.56	0.046	1.790	1,540	2.757	62.3
4.60	0.041	1.779	1,532	2.725	54.0
4.90	0.033	1.630	1,660	2.706	64.6
4.73	0.038	1.747	1,548	2.704	57.0
4.58	0.042	1.729	1,524	2.635	51.6
4.90	0.033	1.680	1,540	2.587	60.4
4.05	0.060	1.650	1,519	2.506	60.0
4.86	0.034	1.645	1,509	2.482	62.2
4.70	0.039	1.597	1,535	2.451	63.4
4.90	0.033	1.578	1,500	2.367	66.3
4.75	0.037	1.570	1,483	2.328	66.6
Medium and fine silts (5–7 phi)					
5.0	0.0310	1.730	1,515	2.621	55.0
5.8	0.0173	1.670	1,535	2.564	60.4
5.40	0.0240	1.590	1,504	2.391	65.9
5.60	0.0206	1.594	1,495	2.383	65.1
5.22	0.0265	1.590	1,496	2.379	65.6
6.4	0.0114	1.550	1,504	2.331	67.1
6.97	0.008	1.301	1,510	1.965	81.4
6.96	0.0081	1.303	1,478	1.926	81.1
6.90	0.0084	1.289	1,493	1.925	74.5
Very fine silts (7–8 phi)					
7.16	0.0070	1.440	1,598	2.301	71.0
7.98	0.004	1.520	1,506	2.289	71.8
7.98	0.004	1.460	1,552	2.266	73.1
7.20	0.0068	1.450	1,499	2.174	73.0
7.20	0.0068	1.410	1,511	2.131	74.4
7.18	0.0069	1.390	1,513	2.103	79.6
7.10	0.0073	1.400	1,490	2.086	74.8
7.40	0.0058	1.410	1,476	2.081	76.4
7.45	0.0057	1.370	1,517	2 078	77.8
7.60	0.0052	1.369	1,484	2.032	78.3
7.20	0.0068	1.355	1,494	2.024	79.6
7.20	0.0068	1.352	1,493	2.019	78.5
7.26	0.0065	1.348	1,487	2.005	78.2
7.24	0.0066	1.346	1,488	2.003	79.2
7.00	0.0078	1.345	1,493	1.996	78.9
7.10	0.0073	1.334	1,484	1.980	79.9
7.50	0.0055	1.335	1,482	1.979	79.4
7.36	0.0061	1.292	1,484	1.917	85.6

[1] Acoustic impedance is measured in 10^5 g/cm² sec.

TABLE III

SOME PROPERTIES OF VARIOUS CLAYS SMALLER THAN 8 PHI CORRECTED TO MEASUREMENTS MADE AT 20°C

Median diameter (Md φ)	*Median diameter (mm)*	*Wet density (g/cm³)*	*Sound velocity (m/sec)*	*Acoustic impedance*[1]	*Porosity*
Silty clay		1.737	1,515	2.632	58.8
Globigerina ooze		1.590	1,620	2.576	65.5
Terrigenous mud		1.540	1,510	2.325	68.8
Silty clay		1.572	1,472	2.314	68.7
8.96	0.002	1.446	1,599	2.312	68.9
8.96	0.002	1.500	1,523	2.285	70.5
8.38	0.003	1.500	1,520	2.280	74.3
8.38	0.003	1.510	1,489	2.248	80.9
8.05	0.0038	1.485	1,509	2.241	69.4
8.96	0.002	1.450	1,515	2.197	75.6
8.38	0.003	1.410	1,511	2.131	74.6
8.96	0.003	1.390	1,530	2.127	76.8
8.38	0.003	1.330	1,526	2.030	80.1
8.96	0.002	1.310	1,537	2.014	82.3
9.40	0.0015	1.338	1,474	1.972	80.9
8.96	0.002	1.300	1,508	1.960	80.4
8.96	0.002	1.319	1,484	1.957	80.6

[1] Acoustic impedance is measured in 10^5 g/cm² sec.

impedance and conversely. As high porosity occurs with the fine-grained sediments, and low porosity with the coarser types; it is usual to claim that clay is a bad reflector of sound and coarse sand a good reflector. This statement is fair enough in this general context, but the relationship should not be pushed too far so that each particular sediment grade is covered.

Tables I, II and III show data culled from the publications of a number of authors, mainly SHUMWAY (1960), but also HAMILTON (1956), LAUGHTON (1957), and MCCANN (1965). These data have all been corrected to 20°C and generalised curves, relating the variation of acoustic impedance with porosity for different sediment grades, have been drawn (Fig.2). The curves show the usual impedance variation with porosity but, more pertinently, they also show at the mid-way stage (roughly 55% porosity and an impedance of $2.7 \cdot 10^5$ g/cm² sec) that almost any conclusion can be drawn as to sediment type.

It is incidental to this discussion, but nevertheless relevant, to plot the acoustic impedance of an average quantity of sea water (S 35‰, σ_t 24.8) at 20°C on the same graph. When the sediment impedance approaches this value very little sound reflection from the bottom will occur, and most of the energy will be transmitted into the lower material to be reflected at a deeper level. This feature is of some importance as the reflected pulse analysed at the surface may indeed not have come from the bottom at all but from some distance below it; in fact, if the frequency of the acoustic pulse is also considered this effect can provide considerable distortion of the analysis.

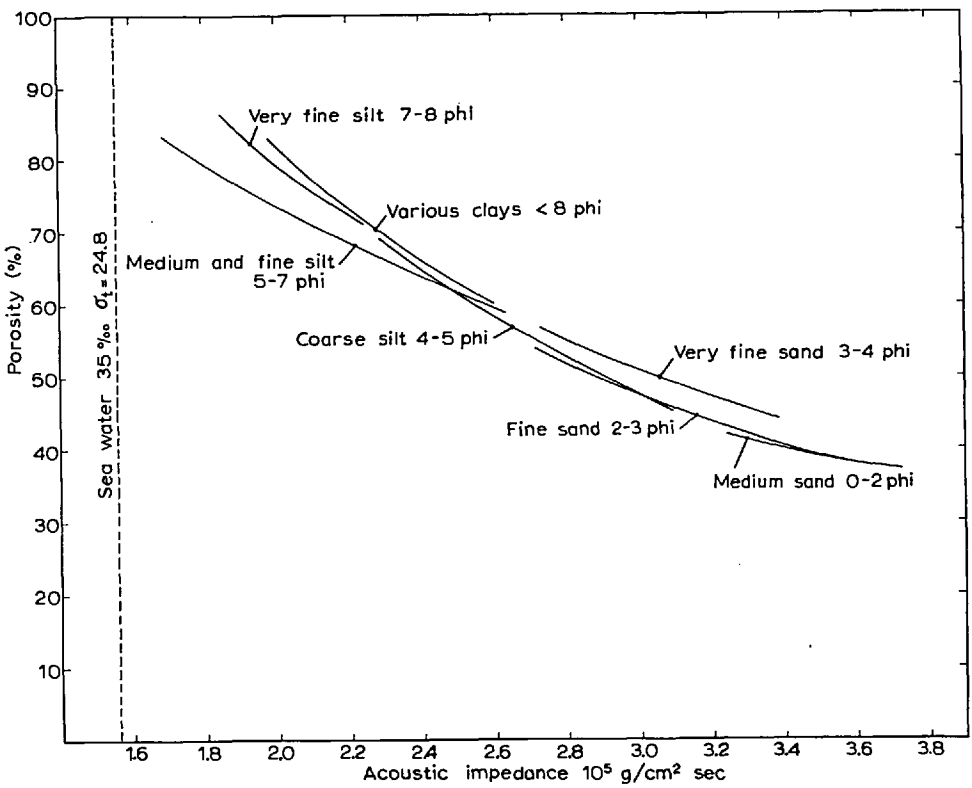

Fig.2. Variation of acoustic impedance with porosity for different sediment grades.

THE EFFECT OF FREQUENCY

All the data, presented in the tables, were obtained at widely different frequencies (20 kc/sec to 1 mega c/sec) and no correction for frequency has been made. Acoustic impedance increases slightly with frequency and strictly speaking some correction for this variation should be made.

COLE (1965) has considered in some detail the reflection process at the sea floor in terms of frequency. He shows that the ratio of incident energy to reflected energy increases with frequency and that at the higher frequencies very little energy is in fact returned back to the surface. His measured curves compare extremely favourably with those calculated by considering the whole process as being related to a three-layer situation (that is, water, bottom sediment, sub-bottom sediment). The overall effect can only be explained by regarding the first sediment layer to be acoustically transparent at very low frequencies, any loss of energy being dependent on the lower interface. At the higher frequencies attenuation in the bottom sediment becomes increasingly important such that at very high frequencies little sound reaches the lower interface and the reflection from the sea bottom is now no longer negligible.

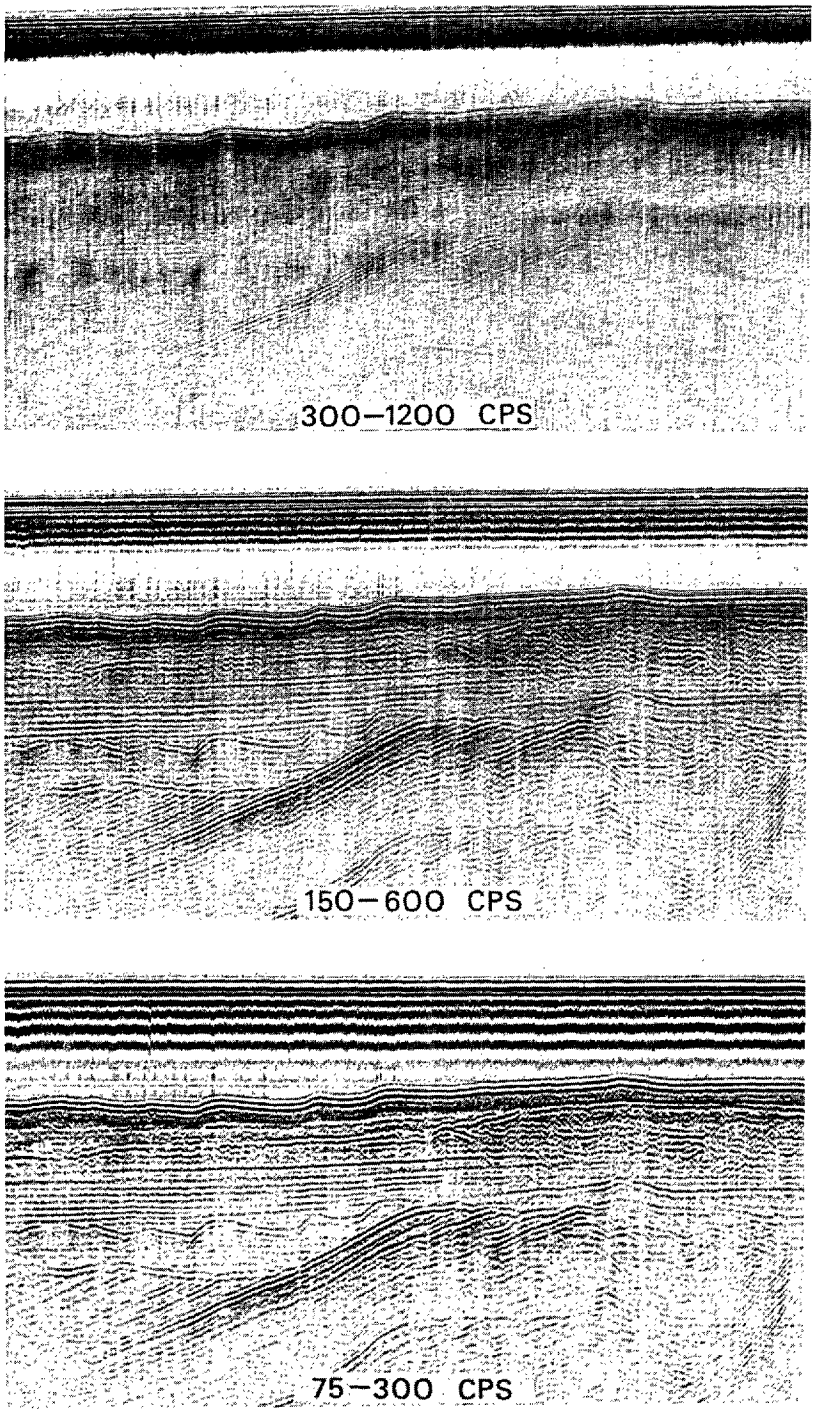

Fig.3. Tape play-back of a broad-band sub-bottom profiler record filtered at various frequency bands.

While his analysis was made at angles of incidence very much away from the normal, and he chose a linear frequency dependence for the attenuation, his results show the complexities inherent in the reflection system. When it is realised that different sediment types have different attenuations (generally, sand greater than clay) and different frequency dependences (roughly, sand $f^{0.5}$, silt f, and clay f^2), the danger of making generalised interpretations on the basis of standard echo-sounding records becomes immediately apparent.

Frequency can also have another effect. Using a high-frequency echo-sounder in sediment surveys sometimes leads to erroneous conclusions in areas where the acoustic impedance variation is not very great. Any sub-bottom boundary exhibiting very little change in impedance across it can often be ignored by the high-frequency sound. The effect is of two parts: the first concerns the weakening of the signal due to the sediment sound attenuation at high frequencies, and the second to the impedance contrast being so low that most of the sound is transmitted rather than reflected. The final result is that the signal to noise ratio of the received sound is so small that no recognisable pattern is indicated on the record. This effect can be seen in Fig.3 where a tape play-back of a record, obtained with a broad frequency-band sub-bottom profiler, is filtered at different frequency bands, the high frequency signal being unable to define clearly the sediment layering over the deeper structure. An example of what may well be a wrong conclusion of this sort is that provided by BELDERSON (1964). On the basis of a lack of intermediate reflections between the bottom and a strong sub-bottom reflection, Belderson concludes that the Holocene sedimentation in the Irish Sea shows no internal stratification. This may not in fact be the case. From the authors' limited observations in roughly the same area as Belderson, layering of a fashion does occur but this is not discernible at high frequencies. The portion of the record shown in Fig.4 was taken in almost the same locality as Belderson's Fig.4 and 5, again using a broad-band signal and filtering at two different frequency levels. In all fairness to him it should be pointed out that his interpretation is based not only on the echograms, but also on core information: the cores generally show an absence of stratification. However, the longest core collected was ca. 2 m and the mud thickness in this particular area can be up to 33 m. There is therefore no conclusive proof that stratification does not indeed exist.

CONCLUSIONS

At the present level of knowledge concerning the acoustic properties of sediments, three general conclusions arise:

(*1*) The reflecting properties depend on the acoustic impedance of the sediment (density $\times$ velocity).

(*2*) The acoustic impedance is roughly related to the sediment type, but more closely correlates with the porosity.

(*3*) It appears that except at high frequencies, the reflected signal may not be

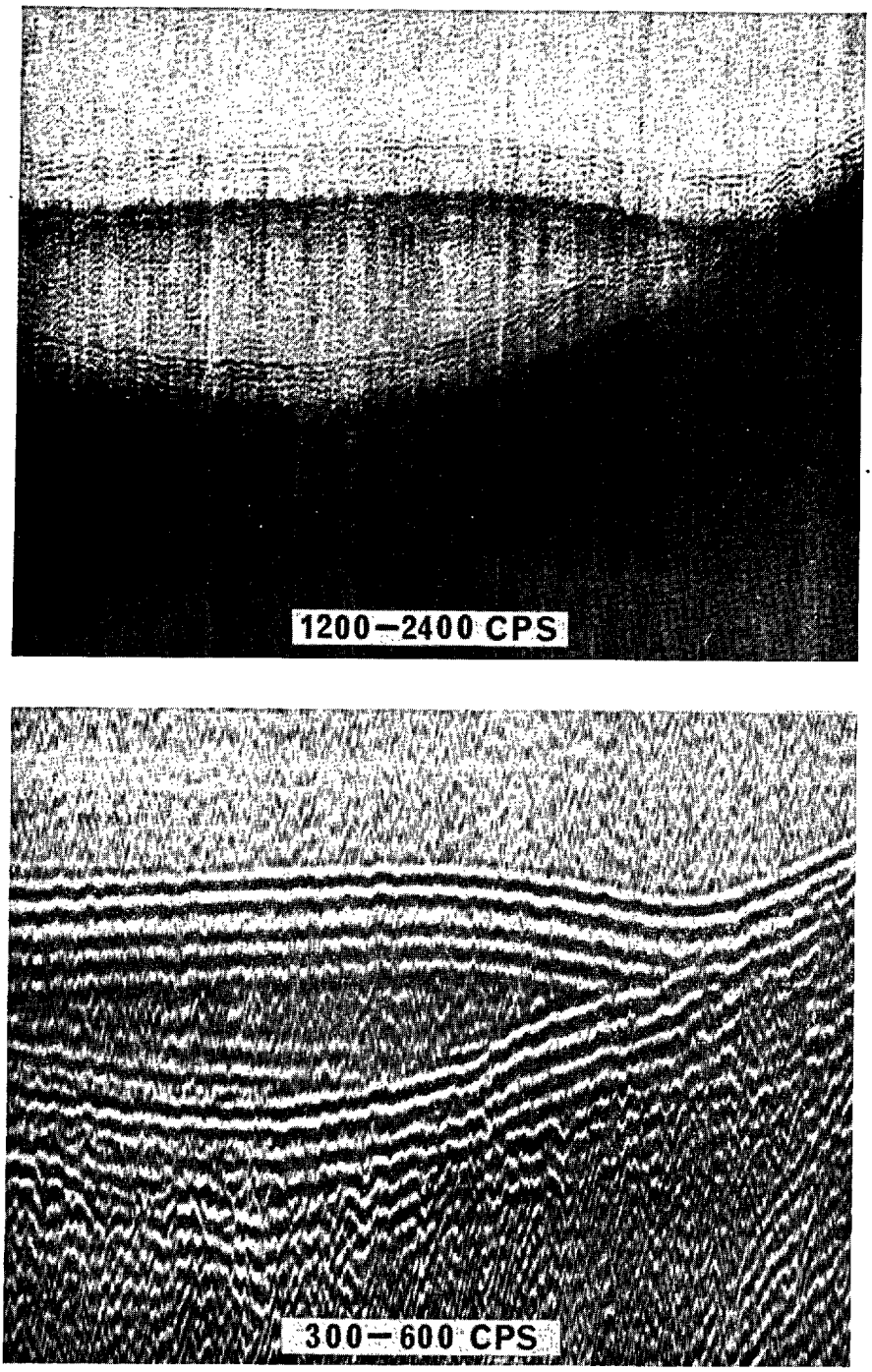

Fig.4. Tape play-back of a broad-band sub-bottom profiler record, obtained west of the Isle of Man, filtered at two frequency levels.

entirely a result of reflection from the sea floor but from an interface below it. The signal may therefore bear an extremely complex, and possibly indeterminate, relationship to sediment type.

While the standard echo-sounder offers a simple tool for the sedimentologist to use, and can sometimes provide him with a wealth of data impossible to obtain as simply by other means, the interpretation of its records should be made with care. Any conclusion as to the presence or absence of a certain sediment type, or to the presence or absence of certain sediment structures, should only be made in the light of confirmatory evidence. It is possible that the echo-sounding record does provide the information necessary to identify the sediment but this information is not immediately obvious. The feature is even further complicated in some areas by the presence of gas derived from organic matter at the sea-bottom. It may well be, as the authors have pointed out elsewhere (LI and TAYLOR SMITH, 1966), that some form of frequency analysis of the bottom and sub-bottom reflections will provide the information required.

REFERENCES

BELDERSON, R. H., 1964. Holocene sedimentation in the western half of the Irish Sea. *Marine Geol.*, 2 : 147–163.

BRESLAU, L., 1965. Classification of sea-floor sediments with a ship-borne acoustical system. *Symp. "Le Petrole et La Mer", Monaco*, 132 : 11 pp.

CASTON, V. N. D., 1965. Oblique asdic equipment in use in Cardigan Bay. *Irish Sea Symp., Dublin*, 27 pp.

COLE, B. F., 1965. Marine sediment attenuation and ocean-bottom reflected sound. *J. Acoust. Soc. Am.*, 37 : 291–297.

GRAINDOR, M. J., 1959. Une méthode de geologie sous-marine. *Rev. Géographie Phys. Géol. Dynamique*, 2 : 29–34.

HAMILTON, E. L., 1956. Acoustic and other physical properties of shallow-water sediments off San Diego. *J. Acoust. Soc. Am.*, 28 : 1–15.

LAUGHTON, A. S., 1957. Sound propagation in compacted ocean sediments. *Geophysics*, 22 : 233–260.

LI, W. N. and TAYLOR SMITH, D., 1966. Identification of sea-bottom sediments by a ship underway. *Geophys. Prospecting*, 14 (1) : 45–47.

MCCANN, D. M., 1965. Measurement of sound velocity and attenuation in North Atlantic core samples. Progress report II. *Marine Sci. Lab. Geol. Report.*, 65-4 : 30 pp.

SHUMWAY, G., 1960. Sound speed and absorption studies of marine sediments by a resonance method. *Geophysics*, 25 : 451–467, 659–682.

TUCKER, M. J. and STUBBS, A. R., 1961. Narrow-beam echo-ranger for fishery and geological investigations. *Brit. J. Appl. Phys.*, 12 : 103–110.